**Response to reviewers' comments on the paper "Anthropogenic Secondary Organic Aerosols Contribute Substantially to Air Pollution Mortality"**

We would like to thank the reviewers for their time and for their useful comments that have helped to improve and clarify our paper. For ease, comments from reviewers are in black, responses in blue, and new text added to paper in **bold blue**.

***Reviewer #1***

1.0 This manuscript leverages an impressive breadth and diversity of data to shed light on a critical public health and environmental policy question: how many premature deaths can be avoided annually with reductions in emissions of organic compounds that humans have direct control over? The methods and approaches that are developed are generally sound, although far from perfect, for this kind of high-level endeavor. My main issue with the paper in its current form are the confusing organization and presentation of ideas, some slight misplaced focus on particular organic aerosol model updates, and the decision to ignore solid fuel burning in the model formulation. These and other issues below should be addressed before publication.

We thank the reviewer for the overall positive review and the detailed input. We have replied to all the specific points below.

General Comments:

1.1 I think the main ideas in the paper are quite compelling: a) reconstruct measured SOA from in situ campaigns using correlations with likely predictors, b) incrementally improve a streamlined parameterization for SOA prediction (SIMPLE), c) integrate the SIMPLE predictions into a full-science CTM prediction of PM2.5 and use satellite data to further refine the predictions, d) feed those predictions to a premature death parameterization to quantify human health impact, and e) investigate key sensitivities. I would reorganize the entire paper so that the methods, results and discussion each flow in that order. Currently, the introduction gives little clue about how the pieces will fit together or the goals of the paper, beyond showing that ASOA is important. Much of (b) above is discussed inappropriately in the current results section 4. Manuscript sections 3, 4, and 5 contain quite a lot of methods discussion that should be moved out to section 2. For example, equations rarely belong in a results section. I could even suggest that most of section 2.2 and 2.4 be moved to SI. The details of the chemical mechanism used in 2.4 are a bit irrelevant once the SOA/R_BTEX enhancement ratio is confirmed for use in SIMPLE. If the mechanism were more sophisticated (e.g. HOM formation, carbon-conserving fragmentation to lower MW products, oligomerization, etc) then I think there would be more cause for focusing on it, but the schemes used here are relatively close to the SIMPLE approach in terms of one-way generation of SOA.

Perhaps some confusion arises from the fact that the paper has two sets of major results. The explanation of the parameters controlling the variability of ASOA at major locations is an important result by itself. The application of state-of-the-art methods (that apply the improved quantification of ASOA) to provide the first realistic estimate of the mortality associated specifically with ASOA is a second important result. Perhaps they could have been reported in two separate papers, but we decided to report them together. Therefore the structure of the paper does make sense, because (a) and (d) are both key results, and (b) and (c) are needed to connect those results.

We have nevertheless made an effort to streamline the structure of the paper to reduce possible confusion for some readers. We have added more discussion in the introduction to better frame the uncertainty in ASOA production impacting both models and the ability to apportion emissions to reduce premature mortality. We have both expanded the methods section (e.g., moving some sections, such as 4.1, into methods) and moved some methods into the SI (those that seemed less important for understanding the entirety of the study, e.g., Error Analysis, Box Model, and GEOS-Chem Description). Further, we have expanded the discussion in Sect. 4 concerning the discussion of implementation and improvement of the SIMPLE model compared to what is currently used in GEOS-Chem.

The text added is:

In introduction:

**"The main method to estimate premature mortality with $PM_{2.5}$ is to use measured $PM_{2.5}$ from ground observations along with derived $PM_{2.5}$ from satellites to fill in missing ground-based observations (van Donkelaar et al., 2015, 2016). To go from total $PM_{2.5}$ to species-dependent and even sector-dependent associated premature mortality from $PM_{2.5}$, chemical transport models (CTMs) are used to predict the fractional contribution of species and/or sector (e.g., Lelieveld et al., 2015; van Donkelaar et al., 2015, 2016; Silva et al., 2016). However, though CTMs may get total $PM_{2.5}$ or even total species, e.g., organic aerosol (OA), correct, the model may be getting the values right for the wrong reason (e.g., de Gouw and Jimenez, 2009; Woody et al., 2016; Murphy et al., 2017; Baker et al., 2018; Hodzic et al., 2020). This is especially important for OA in urban areas, where models have a longstanding issue under predicting secondary OA (SOA) with some instances of over predicting primary OA (POA) (de Gouw and Jimenez, 2009; Dzepina et al., 2009; Hodzic et al., 2010; Woody et al., 2016; Zhao et al., 2016a; Janssen et al., 2017; Jathar et al., 2017). Further, this bias has even been observed for highly aged aerosols in remote regions (Hodzic et al., 2020). As has been found in prior studies for urban areas (e.g., Zhang et al., 2007; Kondo et al., 2008; Jimenez et al., 2009; DeCarlo et al., 2010; Hayes et al., 2013; Freney et al., 2014; Hu et al., 2016; Nault et al., 2018; Schroder et al., 2018) and highlighted here (Fig. 1), a substantial fraction of the observed submicron PM is OA, and a substantial fraction of the OA is composed of SOA (approximately a factor of 2 to 3 higher than POA).**

**Thus, to better understand the sources and apportionment of $PM_{2.5}$ that contributes to premature mortality, CTMs must improve their prediction of SOA versus POA, as the sources of SOA precursors and POA can be different.**

**However, understanding the gas-phase precursors of photochemically-produced anthropogenic SOA (ASOA, defined as the photochemically-produced SOA formed from the photooxidation of anthropogenic volatile organic compounds (AVOC) (de Gouw et al., 2005; DeCarlo et al., 2010)) quantitatively is challenging (Hallquist et al., 2009). Note, for the rest of the paper, unless explicitly stated otherwise, ASOA refers to SOA produced from the photooxidation of AVOCs, as there are potentially other relevant paths for the production of SOA in urban environments (e.g., Petit et al., 2014; Kodros et al., 2018, 2020; Stavroulas et al., 2019). Though the enhancement of ASOA is largest in large cities, these precursors and production of ASOA should be important in any location impacted by anthropogenic emissions (e.g., Fig. 1). ASOA comprises a wide range of condensable products generated by numerous chemical reactions involving AVOC precursors (Hallquist et al., 2009; Hayes et al., 2015; Shrivastava et al., 2017). The number of AVOC precursors, as well as the role of "non-traditional" AVOC precursors, along with the condensable products and chemical reactions, compound to lead to differences in the observed versus predicted ASOA for various urban environments (e.g., de Gouw and Jimenez, 2009; Dzepina et al., 2009; Hodzic et al., 2010; Woody et al., 2016; Janssen et al., 2017; Jathar et al., 2017; McDonald et al., 2018). One solution to improve the prediction in CTMs is to use a simplified model, where lumped ASOA precursors react, non-reversibly, at a given rate constant, to produce ASOA (Hodzic and Jimenez, 2011; Hayes et al., 2015; Pai et al., 2020). This simplified model has been found to reproduce the observed ASOA from some urban areas (Hodzic and Jimenez, 2011; Hayes et al., 2015) but has issues in other urban areas (Pai et al., 2020). This may stem from the simplified model being parameterized to two urban areas (Hodzic and Jimenez, 2011; Hayes et al., 2015). These inconsistencies impact the model predicted fractional contribution of ASOA to total $PM_{2.5}$ and thus the ability to understand the source attribution to $PM_{2.5}$ and premature deaths."**

Other updates for the introduction can be found in other specific comments (e.g., R1.6, R1.7, R1.8, and R1.9).

For Sect. 3.1, added information can be found in R1.3, and for Sect. 3.2, added information can be found in R1.2.

In Sect. 4, about the SIMPLE model improvements, the following has been added:

**"The "improved" SIMPLE shows higher ASOA compared to the default VBS GEOS-Chem (Fig. 6a,b). In areas strongly impacted by urban emissions (e.g., Europe, East Asia, India, east and west coast US, and regions impacted by Santiago, Chile, Buenos Aires, Argentina, Sao Paulo, Brazil, Durban and Cape Town, South Africa, and Melbourne and Sydney, Australia), the "improved" SIMPLE model predicts up to 14 μg $m^{-3}$ more ASOA, or ~30 to 60 times more ASOA than the default scheme (Fig. 6c,d). As shown in Fig. 1, during intensive measurements, the ASOA composed 17-39% of $PM_1$, with an average**

**contribution of ~25%. The default ASOA scheme in GEOS-Chem greatly underestimates the fractional contribution of ASOA to total $PM_{2.5}$ (<2%; Fig. 6e). The "improved" SIMPLE model greatly improves the predicted fractional contribution, showing that ASOA in the urban regions ranges from 15-30%, with an average of ~15% for the grid cells corresponding to the urban areas investigated here (Fig. 6f). Thus, the "improved" SIMPLE predicts the fractional contribution of ASOA to total $PM_{2.5}$ far more realistically, compared to observations. As discussed in Sect. 2.3 and Eq. 11, having the model accurately predict the fractional contribution of ASOA to the total PM is very important, as the total $PM_{2.5}$ is derived from satellite-based estimates (van Donkelaar et al., 2015), and the model fractions are then applied to those total $PM_{2.5}$ estimates. The ability for the "improved" SIMPLE model to better represent the ASOA composition provides confidence attributing the ASOA contribution to premature mortality."**

The figures that have been added to the paper to accompany the text above are:

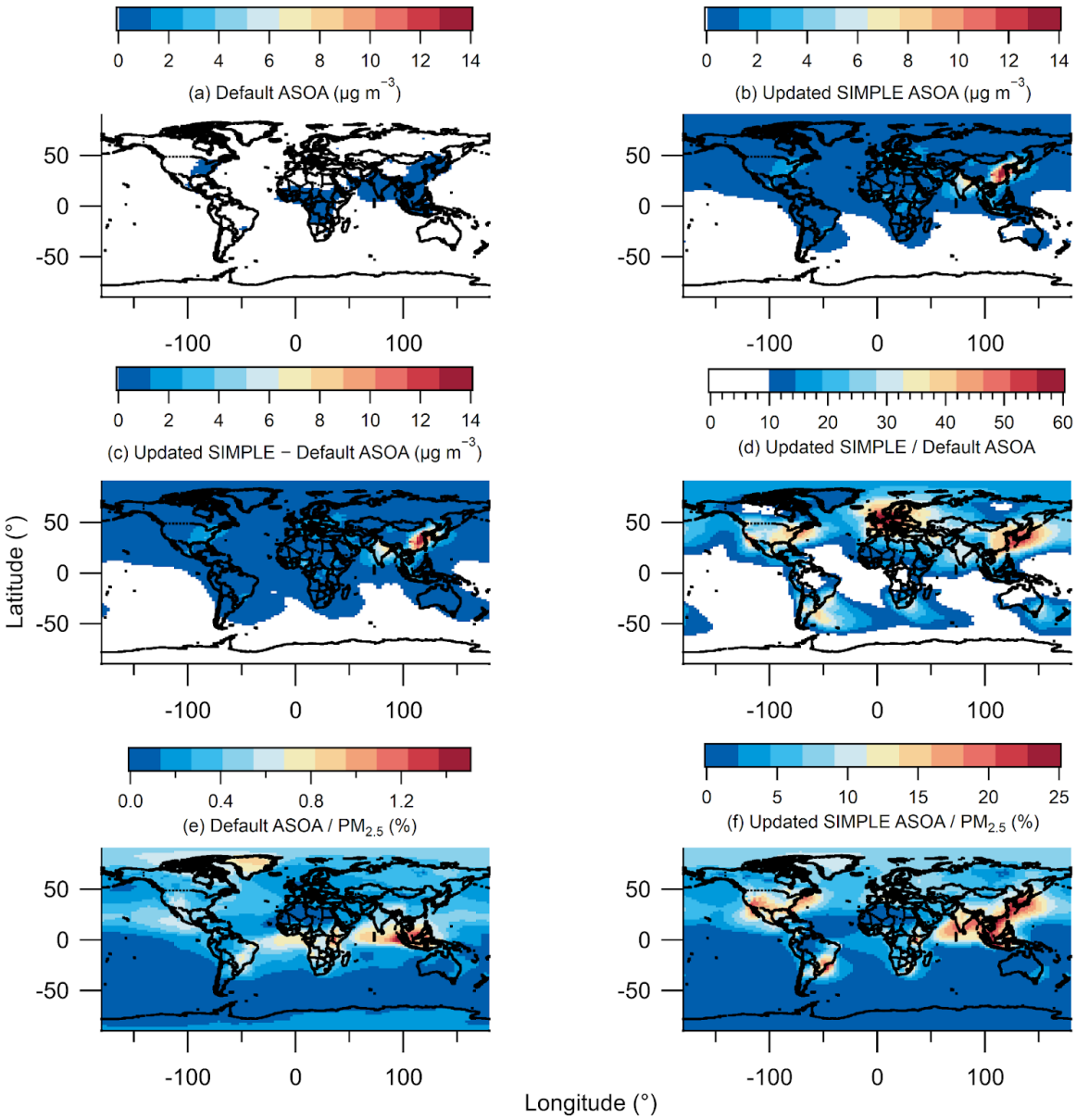


**Figure 6. (a) Annual average modeled ASOA using the default VBS. (b) Annual average modeled ASOA using the updated SIMPLE model. (c) Difference between annual average modeled updated SIMPLE and default VBS. (d) Ratio between annual average modeled updated SIMPLE and default VBS. (e) Percent contribution of annual average modeled ASOA using default VBS to total modelled $PM_{2.5}$. (f) Percent contribution of annual average modeled ASOA using updated SIMPLE to total modelled $PM_{2.5}$.**

Finally, added text for Sect. 5 can be found in R1.3.

1.2 The authors repeatedly compare their updated approach including semivolatile POA to previous efforts to assess ASOA impacts on human health using nonvolatile POA assumptions.

The implication here is that treating POA as semivolatile might be as important to getting ASOA correct as the dramatic increase in ASOA precursors. But one look at Fig. 6 shows that in most cases it's the way BTEX, IVOCs and Other Aromatics are treated (emissions, SOA yields, aging) that is really driving the ASOA formation. So while I think the update to semivolatile POA is a good one and it gives room for greater ASOA production, I think the authors focus on it too much in this study (see specific comment #3 below and lines 574-581 for examples that should be addressed). Instead there should be much more focus in the budget section on how the parameters have chosen for their VCP emissions and SOA chemistry scheme are driving larger IVOC and VOC contributions and how confident they are in those parameters. For the SIMPLE and GEOS-Chem sections, the key sensitivity is the SOA/R_BTEX ratio (see specific comment #7) and there should be more discussion on its impact. Also, the SIMPLE rate constant k is parameterized from the CalNex data, correct? Why was that not revisited and optimized for performance among all the measurement campaigns?

Perhaps there is some misunderstanding of Fig. 6 from the ACPD submission. So first, we would like to clarify Fig. 6. In Fig. 6, the two panels are not two different ways the VOCs are treated, but two different ways to apportion the same VOCs: on the left by type of species, on the right by the source of the species.

We have added the following text at the beginning of Sect. 3.2 to clarify this point:

**"To investigate the correlation between ASOA and $R_{BTEX}$, a box model using the emission ratios from BTEX (Table S5), other aromatics (Table S8), IVOCs (Sect. S1), and SVOCs (Sect. S1) was run for five urban areas: New York City, 2002, Los Angeles, Beijing, London, and New York City, 2015 (see Sect. S1 and S3 for more information). The differences in the results shown in Fig. 4 are due to differences in the emissions for each city."**

We believe the point made in lines 573 - 575 is very important, as many models may get the total OA approximately correct while getting SOA vs POA incorrect (e.g., Hodzic et al., 2020). This in turn can mean that focus of emission controls may be misplaced on reducing POA while neglecting the emissions that lead to the observed ASOA concentrations (e.g., IVOCs from traditional and non-traditional sources). Though POA and IVOC emissions may sometimes originate from similar sources, e.g., diesel (Zhao et al., 2014), the IVOCs will also be emitted from sources that do not include POA, e.g., VCPs (McDonald et al., 2018).

We agree that more emphasis by the community on VCP and IVOC emissions and their SOA production is important. The present paper can also be viewed as a follow-up study to McDonald et al. (2018) that shows the applicability of VCP emissions outside the United States.

Further, we have added the following text to further address these points:

First, about SVOCs:

**"Note, the emissions investigated here ignore any oxygenated VOC emissions not associated with IVOCs and SVOCs due to the challenge in estimating the emission ratios for these compounds (de Gouw et al., 2018). Further, SVOC emission ratios are estimated from the average POA observed by the AMS during the specific campaign and scaled by profiles in literature for a given average temperature and average OA (Robinson et al., 2007; Worton et al., 2014; Lu et al., 2018). As most of the campaigns had an average OA between 1 and 10 μg $m^{-3}$ and temperature of ~298 K, this led to the majority of the estimated emitted SVOC gases in the highest SVOC bin. However, this does not lead to SVOCs dominating the predicted ASOA due to taking into account the fragmentation and overall yield from the photooxidation of SVOC to ASOA."**

We agree the key parameter is SOA/$R_{BTEX}$, and the purpose of Sect. 3.2 is to explore this ratio. As shown in Fig. 6 of the original manuscript, assuming a constant ratio for SOA/$R_{BTEX}$ (the slope from Fig. 5), we are able to explain most of the observed ASOA with the box model and emission inventories. We have added the following text to clarify this point:

**"This investigation shows that the bottom-up calculated ASOA agrees with observed top-down ASOA within 15%. As highlighted above, this ratio is explained by the co-emissions of IVOCs with BTEX from traditional sources (diesel, gasoline, and other fossil fuel emissions) and VCPs (Fig. 5) along with similar rate constants for these ASOA precursors (Table S12). Thus, the ASOA/$R_{BTEX}$ ratio obtained from Fig. 2 results in accurate predictions of ASOA for the urban areas evaluated here, and this value can be used to better estimate ASOA with chemical transport models (Sect. 4)."**

The rate constant of the SIMPLE model, as stated in Line 513 - 520 in the original manuscript, was originally parameterized to the observations from both Mexico City and Los Angeles. It is also generally consistent with observations of ASOA formation with a time scale of 1 day in other studies (e.g., de Gouw et al., 2005; DeCarlo et al., 2010; Nault et al., 2018; Schroder et al., 2018).

The following has been added to the text to also reflect this point:

**"This rate constant is also consistent with observed ASOA formation time scale of ~1 day that has been observed across numerous studies (e.g., de Gouw et al., 2005; DeCarlo et al., 2010; Hayes et al., 2013; Nault et al., 2018; Schroder et al., 2018)."**

1.3 The authors spend some time in the discussion addressing the fact that solid fuel combustion emissions are missing from this study. I'm still very concerned that much of the global results they show are corrupted by this emission, not just in southern Asia and Africa. Large regions of Northern/Western Europe and North America will also be affected by residential wood fuel burning, especially in the winter. The authors should at least justify their omission of solid fuels for the measurement campaigns citing tracer analyses, for example. To address global comparisons, can you add a reference to SOA/CO ratios for wood combustion and comment on their similarity or difference from what has gone into SIMPLE for this study?

This is not quite correct. Unfortunately, we did not emphasize enough that two studies used to constrain the ΔSOA/ΔCO vs $R_{BTEX}$/ΔCO slope shown in Fig. 5a, and thus constrains the updated SIMPLE model, are from campaigns that include large contributions from solid fuel combustion. These include a wintertime campaign in the Northeast US (Schroder et al., 2018) and a late winter, early spring campaign in China (Hu et al., 2013). Both of these studies were strongly impacted by solid fuel combustion, as highlighted in Table S9 in the "Other POA" category (for NYC as we do not have reliable emissions inventory for the observations from Hu et al. (2013)).

Importantly, as we discuss with the updated analysis on the influence of any one point for the slope shown in Fig. 5a (see response to R1.12), the data from these two studies are very close to the slope and do not influence the results. Thus, within the limitations of the available datasets, solid fuels are included and do not result in deviations for the parameterization derived in this study. Clearly it is useful to investigate this point further using data from future campaigns, as we are not aware of any other past campaigns with complete enough data to perform these analyses.

We have added the following text to the revised paper to explain this point in more detail:

**"An important aspect of this study is that most of these observations occurred during spring and summer, when solid fuel emissions are expected to be lower (e.g., Chafe et al., 2015; Lam et al., 2017; Hu et al., 2020). Further, the most important observations used here are during the afternoon, investigating specifically the photochemically produced ASOA. These results here might partially miss any ASOA produced through nighttime aqueous chemistry or oxidation by nitrate radical (Kodros et al., 2020). However, two of the studies included in our analysis, Chinese Outflow (CAPTAIN, 2011) and New York City (WINTER, 2015), occurred in late winter/early spring, when solid fuel emissions were important (Hu et al., 2013; Schroder et al., 2018). We find that these observations lie within the uncertainty in the slope between ASOA and $R_{BTEX}$ (Fig. 2a). Their photochemically produced ASOA observed under strong impact from solid fuel emissions shows similar behavior as the ASOA observed during spring and summer time. Thus, given the limited datasets currently available, photochemically produced ASOA is expected to follow the relationship shown in Fig. 2a and is expected to also follow this relationship for regions**

**impacted by solid fuel burning. Future comprehensive studies in regions strongly impacted by solid fuel burning are needed to further investigate photochemical ASOA production under those conditions."**

In addition, we have also added the following text to section 5 to address the potential uncertainties:

**"Solid fuels are used for residential heating and cooking, which impact the outdoor air quality as well (Hu et al., 2013, 2016; Lacey et al., 2017; Stewart et al., 2020), and which also lead to SOA (Heringa et al., 2011). As discussed in Sect. 3.1, though the majority of the studies evaluated here occurred in spring to summer time, when solid fuel emissions are decreased, two studies occurred during the winter/early spring time, where solid fuel emissions were important (Hu et al., 2013; Schroder et al., 2018). These studies still follow the same relationship between ASOA and $R_{BTEX}$ as the studies that focused on spring/summer time photochemistry. Thus, the limited datasets available indicate that photochemically produced ASOA from solid fuels follow a similar relationship to that from other ASOA sources.**

**Also, solid fuel sources are included in the inventories used in our modeling. For the HTaP emission inventory used here (Janssens-Maenhout et al., 2015), small-scale combustion, which includes heating and cooking (e.g., solid-fuel use), is included in the residential emission sector. Both CO and BTEX are included in this source, and can account for a large fraction of the total emissions where solid-fuel use may be important (Fig. S15). Thus, as CO and BTEX are used in the updated SIMPLE model, and campaigns that observed solid-fuel emissions fall within the trend for all urban areas, the solid-fuel contribution to photochemically-produced ASOA is accounted for (as accurately as allowed by current datasets) in the estimation of ASOA for the attribution to premature mortality.**

**Note that recent work has observed potential nighttime aqueous chemistry and/or oxidation by nitrate radical from solid fuel emissions to produce ASOA (Kodros et al., 2020). Thus, missing this source of ASOA may lead to an underestimation of total ASOA versus the photochemically-produced ASOA we discuss here, leading to a potential underestimation in the attribution of ASOA to premature mortality. From the studies that investigated "night-time aging" of solid-fuel emissions to form SOA, we predict that the total ASOA may be underestimated by 1 to 3 μg $m^{-3}$ (Kodros et al., 2020). This potential underestimation, though, is less than the current underestimation in ASOA in GEOS-Chem (default versus "Updated" SIMPLE)."**

Have also added the following figure in SI to go with the text above:

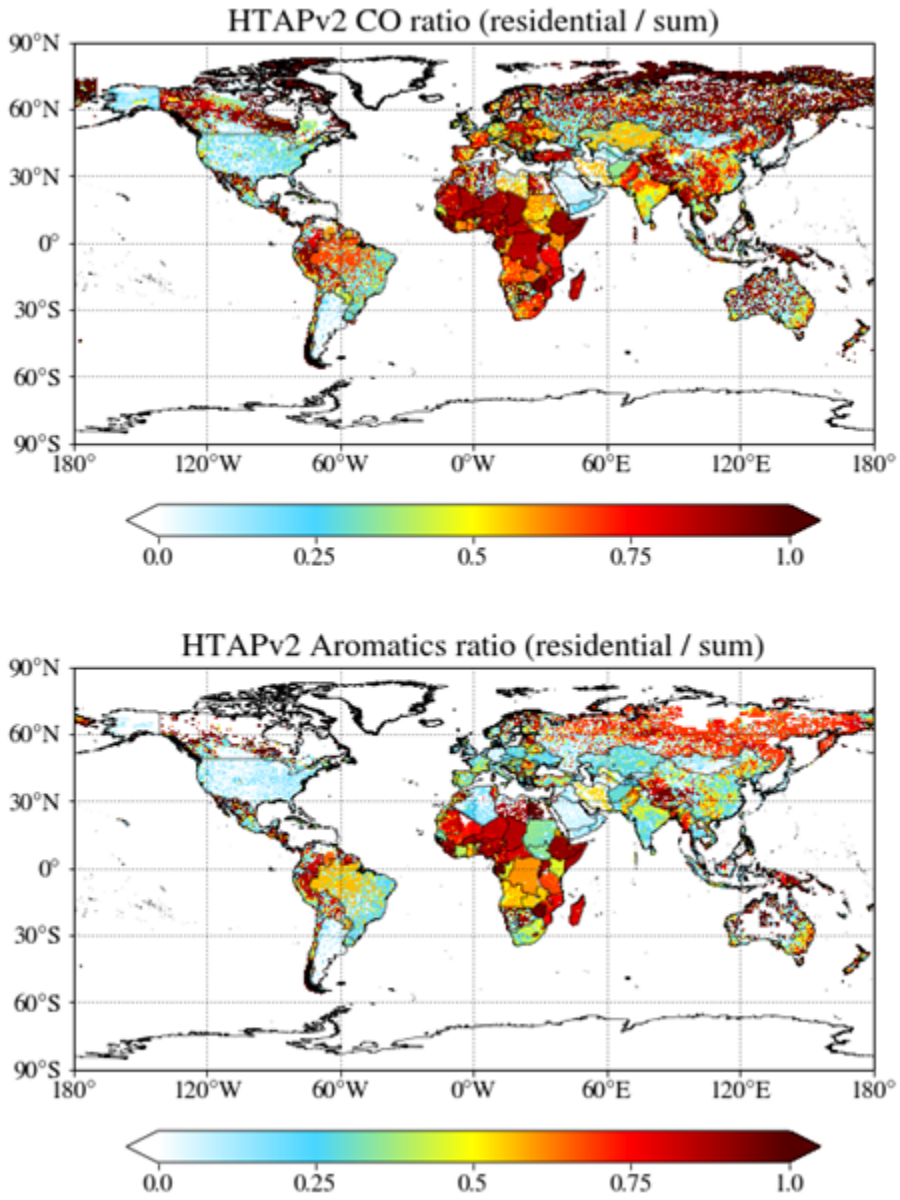


**Figure S15. (top) Fractional contribution of CO emissions from residential sources to total emission sources from HTAP. (bottom) Fractional contribution of BTEX emissions from residential sources to total emission sources from HTAP. Residential sources include small-scale combustion, such as heating and cooking, which may include solid-fuel emissions.**

1.4. Why does SIMPLE model now rely on BTEX alone? It seems to be doing better overall than when it just relied on CO, but why not use more than one variable with BTEX to develop a multilinear fit for the SOAP emissions? For example, Seoul is likely a problematic point in the SOA vs. BTEX regression (see specific comment #7). It's driving down the ratio and thus probably leading to under-representing impacts in the Northeast US and LA. Taken together,

Figs. 3 and 4 suggest that in Seoul there are SOA sources associated with CO emissions that are not as highly associated with BTEX. Using too many independent variables would surely end up overfitting, but why not add 1 or 2 key variables (like CO and POA) since you have a good idea that the relative contributions of sources (e.g. vehicles, VCPs, and solid fuel use) vary from city to city?

As we discuss in response to 1.12, Seoul is not driving the relationship and thus is not a problematic point.

Also, there is perhaps some confusion. The updated version of SIMPLE does not rely on BTEX alone, but rather on both BTEX and CO emissions (e.g., eq. 7 in the ACPD version) as well as OH concentrations within the model. This is an improvement from the original SIMPLE model, in which the parameterization only depended on CO and the model OH fields.

We do not see a reason for a more complex parameterization, since the available data are well-fit with the updated parameterization proposed in the paper. Of course more complex parameterizations could be devised, but they would be underconstrained by the observations. Indeed, Fig. 2 in the ACPD version shows that BTEX is co-emitted in both "traditional" and "non-traditional" sources (fossil fuel versus VCP), and both these sources account for the majority of the predicted ASOA (Fig. 6 of ACPD version). Finally, most emission inventories have BTEX, providing a more straightforward method to implement this parameterization into chemical transport models.

We have added the following text to address this point:

**"The $R_{aromatics}/\Delta CO$ allows a dynamic calculation of the E(VOC)/E(CO) = SOA/ΔCO. Hodzic and Jimenez (2011) and Hayes et al. (2015) used a constant value of 0.069 g $g^{-1}$, which worked well for the two cities investigated, but does not for the expanded dataset studied here. Thus, both the aromatic emissions and CO emissions are used in this study to better represent the variable emissions of ASOA precursors (Fig. S5)."**

The following figure has been added to address the comment as well:

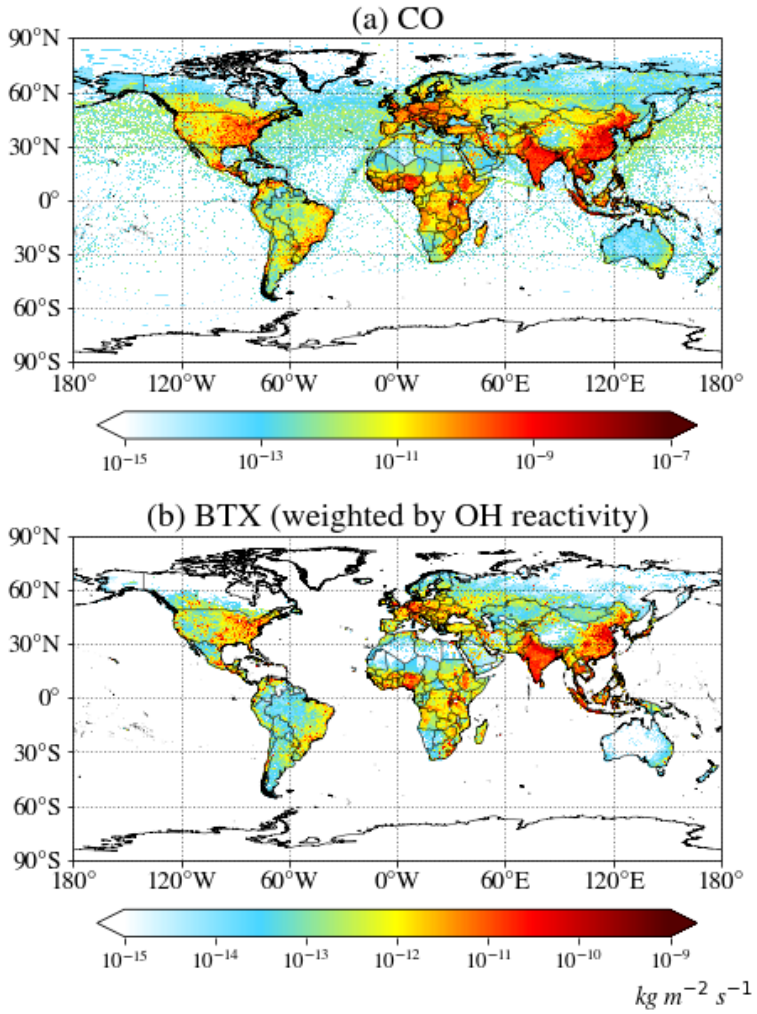


**Figure S5. (a) Annually average CO emissions from HTAP. (b) Annually average benzene, toluene, and xylenes (BTX) emissions, weighted by their OH reaction rate**

**(** $E_{weight} = N \frac{\sum_i E_i k_{OH,i}}{\sum_i k_{OH,i}}$, $i = B, T, X$ **; N=3).**

1.5. Line 455-457: The observation about SVOCs is difficult to believe based on existing NMOG and POA profiles in literature. I have yet to see a volatility profile for any source where the SVOC accounted for half of the total ASOA precursor, let alone 88%. Is there something unexpected going on with the CO normalization of POA vs. VOCs here? I confess this one catches me completely by surprise, and likewise the large influence of SVOCs in Fig. 3 looks strange as well. The authors have made an emphatic case for the dominant and growing role of VCPs. Wouldn't these be overwhelmingly VOCs and IVOCs? Cooking emissions are used to explain this to some degree, but if the Robinson et al. (2007) profile is used for cooking

emissions, I would expect a lot more 10^3 and 10^4 C* compounds. Regardless, SVOC should probably be included on Fig. 2 as a separate series like BTEX and IVOC. And I recommend adding more description about how SVOC smission ratios are derived.

There are multiple prior publications, where ASOA formed from SVOCs were accounted for by several tens of percent of the total SOA (e.g., Dzepina et al., 2009; Ma et al., 2017). As stated in that section "Beijing has the highest contribution of SVOCs to ASOA precursors due to the use of solid fuels and cooking emissions (Hu et al., 2016)." Thus these results are not so surprising. They are correct and are based on the detailed inventories reported here.

We have moved Fig. 3 from the main paper to the SI, as it is not a finding but more a tool that was used to estimate ASOA. Part of the reason is that for the emissions with C* greater than $10^6$ µg $m^{-3}$ only include the VOCs reported in the SI, as the campaigns used here either had missing oxygenated VOCs and/or the challenge of estimating oxygenated VOC emission ratios (e.g., de Gouw et al., 2018; McDonald et al., 2018). Not including OVOCs may lead to an underestimation of the emission ratios at high volatility.

We have added the following text to the SI to describe how the SVOC emission profile was determined:

**"To estimate the SVOC mass concentration in equilibrium with the POA (Table S9) in each bin, the POA mass concentration is first multiplied by the fraction of POA measured in each bin from literature. This yields the concentration of POA for that specific volatility bin. Then the total POA + SVOC concentration for that bin is obtained divided by the amount of material found in the particle phase for that bin for the average temperature (~298 K) and OA mass concentration (~10 µg $m^{-3}$). Then, the gas-phase SVOC concentration is calculated by multiplying the total concentration by the gas-phase fraction. Thus, e.g., SVOC in the C* = 100 µg $m^{-3}$ bin, ~91% of the SVOC mass will be found in the gas-phase."**

Specific Comments:

1.6 Line 95-98: These generalities about IVOCs and SVOCs are perhaps useful for an introduction for those who may be unfamiliar but based on more current understanding of emissions sampling and speciation, they may be more confusing than helpful. Lu et al. (2018) show in their Fig. 1 that most of the IVOC would have missed the filters for the vehicles they studied, but much of the SVOC is expected to be captured by the filters. Even more SVOC would presumably be captured for stationary sources at conditions relevant for "condensable particulate matter" measurements (i.e. low dilution, cooled temperatures); see Morino et al. (2018). As for IVOCs, VBS profiles for biomass burning sources like those in May et al. (2013)

show that IVOCs are probably included in many if not most PM emission factors measured for those sources if the emissions are not diluted enough. The authors here are not focused on wildfires, but certainly cooking/residential wood-burning PM emission factors may include these IVOCs. Admittedly, the problem is even more complicated by the fact that many countries report wood-burning PM emission factors at high temperature conditions, so they may not actually be capturing the IVOCs. Still, it's highly uncertain to what extent they are already measured. I urge the authors to update their discussion of these classes of compounds to better reflect some of the nuances we now understand better.

We have removed that line and have expanded the discussion of S/IVOCs in the introduction to read:

**"Many of these prior studies generally investigated AVOC with high volatility, where volatility here is defined as the saturation concentration, C*, in µg $m^{-3}$ (de Gouw et al., 2005; Volkamer et al., 2006; Dzepina et al., 2009; Freney et al., 2014; Woody et al., 2016). More recent studies have identified lower volatility compounds in transportation-related emissions (e.g., Zhao et al., 2014, 2016b; Lu et al., 2018). These compounds have been broadly identified as intermediate-volatile organic compounds (IVOCs) and semi-volatile organic compounds (SVOCs). IVOCs have a C* generally of $10^3$ to $10^6$ µg $m^{-3}$ while SVOCs have a C* generally of 1 to $10^2$ µg $m^{-3}$. Due to their lower volatility and functional groups, these classes of compounds generally form ASOA more efficiently than traditional, higher volatile AVOCs; however, S/IVOCs have also been more difficult to measure (e.g., Zhao et al., 2014; Pagonis et al., 2017; Deming et al., 2018). IVOCs generally have been the more difficult of the two classes to measure and identify as these compounds cannot be collected onto filters to be sampled off-line (Lu et al., 2018) and generally show up as unresolved complex mixture for in-situ measurements using gas-chromatography (GC) (Zhao et al., 2014). SVOCs, on the other hand, can be more readily collected onto filters and sampled off-line due to their lower volatility (Lu et al., 2018). Another potential issue has been an under-estimation of the S/IVOC aerosol production, as well as an under-estimation in the contribution of photochemically produced S/IVOC from photooxidized "traditional" VOCs, due to partitioning of these low volatile compounds to chamber walls and tubing (Krechmer et al., 2016; Ye et al., 2016; Liu et al., 2019). Accounting for this under-estimation increases the predicted ASOA (Ma et al., 2017). The inclusion of these classes of compounds have led to improvement in some urban SOA budget closure; however, many studies still have indicated a general short-fall in ASOA budget even when including these compounds from transportation-related emissions. (Dzepina et al., 2009; Tsimpidi et al., 2010; Hayes et al., 2015; Cappa et al., 2016; Ma et al., 2017; McDonald et al., 2018)."**

1.7 Line 99-118: I encourage the authors to add residential wood burning/cookstoves to their list, and possibly also the recent work on asphalt emissions (Khare et al., 2020).

We have added the following:

**". . . as well as cooking emissions (Hayes et al., 2015), asphalt emissions (Khare et al., 2020), and solid fuel emissions from residential wood burning and/or cookstoves (e.g., Hu et al., 2013, 2020; Schroder et al., 2018). . ."**

1.8 Line 119-132: I think the authors get somewhat stuck on the SVOC portion of the ASOA problem in this paragraph and would do well to keep the broad focus on both IVOC-SOA and SVOC-SOA they have been introducing so far. For one thing, I'm not sure how important revising the (terrible) assumption of POA nonvolatility is for connecting urban PM to health impacts in the context of annual mean guidelines. Of course it's important to know how much of the PM started as an SVOC vapor for the purposes of control. But meanwhile, if we think that a portion of the SOA mass was emitted in the particle phase and then evaporated, oxidized and recondensed after dilution, then how does updating our conceptual picture to consider that portion volatile necessarily help us control it better - we could still control it with particulate filters. To me, the important reasons to update the conceptual model form nonvolatile POA to semivolatile are to 1) better track composition of the OA because maybe it has different toxicity or efficiencies for losses as it is oxidized, 2) sensitivity to temperature and concentration swings might have an impact on urban scale versus suburban or rural exposure or diurnal timing of concentration peaks and thus impacts on human exposure. Adding in the SVOC and IVOC vapors helps us achieve a total mass balance on the amount of carbon with potential to make SOA and this is really a separate point. In short, the authors could make it more clear in this paragraph, at least qualitatively, which sources of uncertainty they are most concerned about in previous estimations of PM mortality. Is it a) poor traditional POA models, b) undersampled SVOC and IVOC emissions from known sources, c) underestimated yields (i.e. vapor wall-losses, etc), d) missing or unacknowledged sources of vapor precursors or e) something else. Right now, it seems like (a) is their chief concern.

We have addressed some of these concerns ((b) and (c)) in response to 1.6. We have softened this section to be less focused on SVOC, and instead the under estimation of SOA most likely due to IVOC and "non-traditional" sources. We have changed it to clarify:

**"Due to the uncertainty on the emissions of ASOA precursors and on the amount of ASOA formed from them, the number of premature deaths associated with urban organic emissions is largely unknown. Since numerous studies have shown the importance of VCPs and other non-traditional VOC emission sources, efforts have been made to try to improve the representation and emissions of VCPs (Seltzer et al., 2021), which can reduce the**

**uncertainty in ASOA precursors and the associated premature deaths estimations. Currently, most studies have not included ASOA realistically (e.g., Lelieveld et al., 2015; Silva et al., 2016; Ridley et al., 2018) in source apportionment of the premature deaths associated with long-term exposure of $PM_{2.5}$. These models represented total OA as non-volatile POA and "traditional" ASOA precursors (transportation-based VOCs), which largely under-predict ASOA (Ensberg et al., 2014; Hayes et al., 2015; Nault et al., 2018; Schroder et al., 2018) while over-predicting POA (e.g., Hodzic et al., 2010; Zhao et al., 2016a; Jathar et al., 2017). This does not reflect the current understanding that POA is volatile and contributes to ASOA mass concentration (e.g., Grieshop et al., 2009; Lu et al., 2018). Though the models are estimating total OA correctly (Ridley et al., 2018; Hodzic et al., 2020; Pai et al., 2020), the attribution of premature deaths to POA instead of SOA formed from "traditional" and "non-traditional" sources, including IVOCs from both sources, could lead to regulations that may not target the emissions that would reduce OA in urban areas. As $PM_1$ and SOA mass are highest in urban areas (Fig. 1), also shown in Jimenez et al. (2009), it is necessary to quantify the amount and identify the sources of ASOA to target future emission standards that will optimally improve air quality and the associated health impacts. As these emissions are from human activities, they will contribute to SOA mass outside urban regions and to potential health impacts outside urban regions as well."'**

1.9 Line 141: A complete introduction or general description of the modeling approach is needed to begin the methods section. Before the authors get into the extreme details (e.g. how data were averaged), we reader would do well to learn what the basic idea of the study is going to be (i.e. parameterize ASOA in cities using campaign data, replace ASOA in GEOS-Chem with these results, plug new PM2.5 into relative risk and premature death parameterizations, assess the impact, and explore some key sensitivities). For example, on line 142, I'm not sure what 'values' are being discussed, how they are measured, or how they will be used.

We have added the following to introduce everything discussed in Sect. 2:

**"Here, we introduce the ambient observations from various campaigns used to constrain ASOA production (Sect. 2.1), description of the simplified model used in CTMs to better predict ASOA (Sect. 2.2), and description of how premature mortality was estimated for this study (Sect. 2.3). In the SI, the following can be found: description of the emissions used to calculate the ASOA budget for five different locations (Sect. S1), description of how the ASOA budget was calculated for the five different locations (Sect. S2), description of the CTM (GEOS-Chem) used in this study (Sect. S3 - S4), and error analysis for the observations (Sect. S5)."**

1.10 Figures are introduced out of order in the methods section.

We have removed reference to figures in Sect. 3 to instead be references to the sections themselves.

1.11 It looks to me like the emission ratio in Tables S5-S8 that were calculated with Eq. 3 are in most (though not all) cases well outside the range of measured emission ratios from other campaigns. For example, o-xylene in Table S5 is all as high or higher than the maximum observations, propene in Table S7 as well. The values for London in Table S8 are either below the minimum observed or above the maximum, depending on the species. Are these predictions expected by the authors? Can they be explained by variations among cities? I recommend calculating and reporting the performance of the Eq. 3 model in reproducing the observed values in Table S5-S8. Also, what values of t were used to calculate the emission ratios in Eq. 3? I assume many values used and then all averaged together? Or were the values for each daily averaged and then a campaign average derived from that? What is the spread in the intermediate emission ratio values? I think this paragraph (lines 150-161) could be written more clearly to better describe the multiple levels of averaging and error analysis taking place here.

Prior studies have shown very large variability across different cities for the same compound, e.g., Bon et al. (2011) showed an order of magnitude difference in ethane emission ratios across three different studies and a factor of ~20 difference in propane across three different studies. Further, as shown in Bon et al. (2011) and Apel et al. (2010) and highlighted in the table made below, there can be large differences, especially for the alkanes, for the same location, depending on how the emission ratio was determined. Thus, there can be large variability across cities as well as potential uncertainty, which is most prominent for the longer lived compounds that minimally contribute to ASOA production.

We have added the following text in the SI to discuss and clarify this point:

**"A further potential source of uncertainty in this analysis is the calculated VOC emission ratios for the studies that did not have ratios published previously (Houston 2000, London, Houston 2013, and Seoul). To investigate how well Eq. 3 does in estimating the VOC emission ratios, a comparison of the estimated VOC emission ratios versus previously published ratios for two different cities, Mexico City (Apel et al., 2010; Bon et al., 2011) and Los Angeles (de Gouw et al., 2017) was made (Table S10). Also, for Mexico City, two locations, an urban and a suburban site, were compared both against each other (Apel et al., 2010; Bon et al., 2011) and the calculated values from Eq. 3.**

**First, as shown in Table S10, even for the same location (suburban Mexico City), different values in the emission ratio, especially for the alkanes, can be observed, by as much as a factor of 7. This can be partially explained by differences in how the emission ratios were**

**determined. For both Apel et al. (2010) and Bon et al. (2011), the authors took the slope of VOCs versus CO and used different regression techniques and different time periods. Comparing their technique with ours, we generally estimate VOC emission ratios within 50% of the reported values, and the estimation improves for shorter lived compounds (e.g., aromatics). However, de Gouw et al. (2017) more carefully took chemistry into consideration for any potential losses of the VOCs prior to observation to determine emission ratios, similar to this study. We believe the comparison with de Gouw et al. (2017) provides a more useful comparison in the method presented here. We find, at most, a 30% difference in the emission ratios, with an average difference of 4±15% for all compounds. Thus, from this analysis, we conclude that (1) there is large variability in VOC emission ratios across urban areas around the world, which has been highlighted in other studies (Warneke et al., 2007), and (2) the method that considers losses of VOCs is the more accurate procedure to estimate VOC emissions and leads to the best reproducibility across studies and lowest uncertainty (< 30%, ~4% on average).”**

The following table has been added to the SI:

**Table S10. Comparison of estimated VOC emission ratios from two studies from Mexico City (Apel et al., 2010; Bon et al., 2011), one study from Los Angeles (de Gouw et al., 2017), and this study.**

| VOC Ratio | Apel et al. (2010) Downtown MC | This Study | Apel et al. (2010) Suburbs MC | Bon et al. (2011) Outskirt MC | This Study | de Gouw et al. (2017) LA | This Study |
|---|---|---|---|---|---|---|---|
| Ethane | 7.4 | 8.2 | 3.0 | 21.5 | 8.2 | 16.5 | 18.9 |
| Propane | 41.5 | 36.9 | 49.3 | 61.7 | 38.4 | 13.4 | 14.0 |
| n-Butane | 15.1 | 14.9 | 15.3 | 21.7 | 14.1 | 5.0 | 5.7 |
| i-Butane | 4.8 | 4.8 | 5.3 | 7.2 | 4.9 | 3.2 | 3.5 |
| n-Pentane | 2.1 | 2.9 | 2.1 | 2.5 | 2.1 | 3.4 | 3.4 |
| i-Pentane | 2.7 | 3.6 | 3.2 | 3.3 | 3.1 | 8.7 | 7.8 |
| n-Hexane | 1.5 | 1.9 | 1.3 | 1.5 | 1.2 | 1.4 | 1.7 |
| Ethene | 8.4 | 6.1 | 7.9 | 7.0 | 7.1 | 11.2 | 9.6 |
| Propene | 2.6 | 1.3 | 2.9 | 3.0 | 1.6 | 4.1 | 3.9 |
| Benzene | 0.9 | 1.0 | 1.2 | 1.2 | 1.3 | 1.3 | 1.4 |
| Toluene | 7.5 | 9.2 | 5.2 | 4.2 | 4.1 | 3.4 | 3.0 |

| | | | | | | | |
|---|---|---|---|---|---|---|---|
| **Ethylbenzene** | **0.9** | **0.8** | **0.4** | **4.3*** | **0.4** | **0.6** | **0.6** |
| **m+p-Xylene** | **1.1** | **0.7** | **0.5** | **No Data** | **0.4** | **2.1** | **1.9** |
| **o-Xylene** | **0.4** | **0.2** | **0.2** | **No Data** | **0.2** | **0.8** | **0.7** |
| **Trimethylbenzenes** | **No Data** | **No Data** | **No Data** | **No Data** | **No Data** | **1.6** | **1.1** |
| **Ethyltoluenes** | **No Data** | **No Data** | **No Data** | **No Data** | **No Data** | **0.6** | **0.4** |
| **Propylbenzene** | **No Data** | **No Data** | **No Data** | **No Data** | **No Data** | **0.1** | **0.1** |

*In Bon et al. (2011), they reported the sum of C8 aromatics, which is the sum of ethylbenzene and xylenes

1.12 Lines 181-188: I appreciate the spirit of the leave-one-out sensitivity study and the results presented in Table S10. However, I do not think it accomplishes what the authors intended, which is to justify the regressed slope of 24.8. The reference to 95% confidence intervals seems misleading, perhaps because a clear null hypothesis is not stated. I'm not sure I've seen confidence intervals used to prove two slopes are statistically similar before, but I'd be interested to learn if the authors can show their work. A conventional leave-one-out would calculate the error in predicting the removed point and then average the errors across all trials. I'm not sure how knowing this error statistic would be helpful either though, except to perhaps compare among similar leave-one-out analyses for the other slopes in Fig. 5. In my opinion, a better analysis would involve an assessment of the degree to which the Seoul data point is influencing the slope parameter. For example, the Cook's distance is commonly used in regression approaches to flag highly influential data points. If the point is determined to be influential, then the authors need to discuss what impact the change in slope from 24.8 to 34.0 has on the conclusion of the paper.

The equation we had used to investigate statistical difference in slopes was:

$$t = \frac{b_1 - b_2}{\sqrt{s_{b_1}^2 + s_{b_2}^2}}$$

Where $b_i$ is the slope and $s_i$ is the standard deviation about the slope.

In addition, we have also conducted the Cook's distance test, of which we were not aware. We appreciate the reviewer bringing this statistical tool to our knowledge. We have found that the T-test, Cook's distance test, and the difference in fits test all show that the one point from Seoul is not an outlier. We have added the following table and text to the paper:

**Table S11. Statistical analysis of the data used in Fig. 2 to determine if any point is influencing the slope, using the T-test, Cook's Distance test, and Difference in Fits test. For**

**the T-test, the point is influential if the t value is < 0.05 while for the Cook's Distance and Difference in Fits test, the point is influential if the value is > 1.**

| Campaign | T-test | Cook's Distance | Difference in Fits |
|---|---|---|---|
| NE US Ship | 0.63 | 0.06 | -0.29 |
| NE US Aircraft | 0.12 | 0.27 | 0.73 |
| Mexico City | 0.39 | 0.06 | 0.33 |
| Los Angeles | 0.32 | 0.08 | 0.38 |
| Changdao Island, China | 0.41 | 0.09 | -0.38 |
| Beijing | 0.42 | 0.06 | -0.32 |
| London | 0.31 | 0.13 | -0.48 |
| NYC | 0.90 | 0.00 | -0.05 |
| Seoul | 0.99 | 0.00 | 0.01 |

We have updated the text to say:

**"Statistical analysis for the influence of the data from Seoul on the figure was conducted, including a T-test, Cook's Distance test, and Difference in Fits test (Table S11). All three statistical tests show that the data from Seoul (and all the data in general) is not overly influencing the reported slope."**

1.13 The SIMPLE model relies on having an accurate BTEX field for input. So how consistent were the HTAPv2 emission inputs with each of the measurement campaigns, allowing the expected deviations for year to year trends?

We have added the following text in the SI:

**"Analysis of the HTAP emissions, compared to other emission inventories, generally showed the highest correlation with observations ($R^2$ = 0.54), versus the other inventories (CEDS $R^2$ = 0.26, MACCity $R^2$ = 0.00, and RETROv2 $R^2$ = 0.04), leading to the selection of this emission inventory."**

1.14 Why not add a supplemental figure showing the average spatial distribution of CO and R_btex emissions so readers can get a sense for which is driving the SIMPLE predictions in the

various countries? I recommend at least plotting this as country average, if not both country averages and grid cells.

Please see response to comment 1.4.

1.15 Consider adding to the conclusions the ASOA-associated premature death estimates you are most confident in.

We respectfully disagree on this point, as prior studies have discussed $PM_{2.5}$-associated premature death estimates with less investigation into how well the models predicted the composition of the total $PM_{2.5}$ while still attributing premature deaths to different sources (e.g., Lelieveld et al., 2015; Silva et al., 2016; Ridley et al., 2018).

Minor comments:

1.16 Line 60: Rewrite "anthropogenic reactivity of specific organic compounds" to "reactivity of specific anthropogenic volatile organic compounds"?

Completed.

1.17 Line 66: "results in up to . . ."

Completed.

1.18 Line 67: "extrapolation" of what data specifically? Is it more informative to say "extrapolation from regions where detailed emission inventory data are available to other regions where uncertainties in emissions are larger."?

We have updated the line to say:

**"A limitation of this study is the extrapolation from cities with detailed studies and regions where detailed emission inventories are available to other regions where uncertainties in emissions are larger."**

1.19 Line 68: I agree that comprehensive air quality campaigns are certainly helpful and possibly necessary, but it seems that robust national-scale institutions (government, academic, or private) are absolutely necessary to accurately catalogue emission factors and activity data to the level required to reduce the uncertainties discussed in this manuscript. Perhaps this sentence could be broadened to something like: "In addition to further development of institutional air quality management infrastructure, comprehensive air quality campaigns . . ."

We have updated the line to say:

**"In addition to further development of institutional air quality management infrastructure, . . ."**

1.20 Lines 104 - 106: Suggest rewriting: "Biogenic SOA (BSOA) in urban areas typically results from advection of regional background concentrations rather than processing of locally emitted biogenic VOCs."

Updated to this.

1.21 Lines 116 - 118: Seltzer et al. (2021) is currently finalizing discussion in ACPD and presents a detailed VCP emission inventory for the U.S. Based on this the authors may want to update this sentence to include that step forward, but it's their choice.

We have added the following to address this:

**"Since numerous studies have shown the importance of VCPs and other non-typical VOC emission sources, efforts have been made to try to improve the representation and emissions of VCPs (Seltzer et al., 2021), which can reduce the uncertainty in ASOA precursors and the associated premature deaths estimation."**

1.22 Line 119: "uncertainty on the (burden of -or- emissions of) ASOA precursors. . ."

Updated the text to say:

**". . . uncertainty on the emissions of ASOA precursors . . ."**

1.23 Eq. 3: Recommend adding an exp subscript to [OH] here to make it clear that it is calculated from Eq. 2.

Updated.

1.24 Table S10. Please indicate which slope is being shown here (delta_SOA/R_BTEX)

We have removed this Table due to response 1.12 and have replaced it with the table shown there.

1.25 Line 201: Many of the BTEX values are modeled with equation 3 right? Please make this clear.

For the IVOCs used in this analysis, only 1 city had BTEX was calculated with Eq. 3 (London) while the rest of the BTEX are used from studies (NE USA, LA, Beijing, and NYC).

We have added the following to clarify:

**"The IVOC:BTEX emission ratio from inventories are multiplied with the observed BTEX, either the reported value from studies (NE US aircraft (Warneke et al., 2007), Los Angeles (de Gouw et al., 2017), Beijing (Wang et al., 2014), and New York City (Warneke et al., 2007)) or estimated from Eq. 3 (London), . . ."**

1.26 Line 213: C* range is not consistent with how IVOCs are usually defined.

We have updated the values to $10^3 < C^* < 10^6$ μg $m^{-3}$.

1.27 Line 209 - 210: Based on the reference, it appears the authors are specifically referring to underestimation of IVOCs in the ambient. Please make that more clear in the sentence.

We have rephrased the sentences to clarify this point:

**"Additionally, we rely on inventories for estimating atmospheric abundances of IVOCs because it has been challenging to measure the full range of IVOC precursors that are emitted into urban air due to many of the IVOCs from VCPs being oxygenated VOCs. These compounds are challenging to measure using traditional instrumentation (e.g., gas chromatography-mass spectrometry), leading to potential underestimation of the IVOC emission ratios (Zhao et al., 2014, 2017; Lu et al., 2018)."**

1.28 Line 214 - 216: It's unclear to me how the IVOCs and unspeciated SOA precursors relate to each other here. Are the authors saying they used SOA yields from Jather et al. (2014) to define the IVOC SOA yields uniformly for all C* bins? Please clarify. For example, a clearer way of making that point might be, "SOA yields from IVOC oxidation were parameterized with data from n-tridecane for gasoline engines and n-pentadecane for diesel engines (Jathar et al., 2014)."

We have updated to the text to say:

**"The ASOA yields and rate constants for IVOC oxidation were parameterized with data from n-tridecane and n-pentadecane for gasoline and diesel emissions, respectively (Jathar**

**et al., 2014), and for VCPs, the yields and rate constants for IVOC oxidation were parameterized with data from n-tetradecane (McDonald et al., 2018).”**

1.29 Lines 216 - 218: Should VOCs be IVOCs here? Again, aren't all the IVOCs in this study unspeciated? If so, why make the distinction?

We have added the I before the VOCs here. Also, we made the distinction for unspeciated specifically for VCPs as the IVOCs are unspeciated; however, BTEX, which can be in VCPs (Fig. 2), is speciated.

1.30 Line 224: Why was the Huffman et al. (2009) distribution not used for the cooking VBS distribution?

To be consistent with Ma et al. (2017), we used the same profiles as those authors used in their analysis.

We have added the following to clarify:

**“These profiles were selected to be consistent with Ma et al. (2017).”**

1.31 Table S9: What is the HOA and Other POA mass normalized to? Shouldn't these also be normalized to CO, or is POA a separate variable in the inventories? POA is never mentioned in the SI in the discussion of the inventory development.

We have updated the table to include the CO term; thus, the units are $\mu g\ sm^{-3}\ ppmv^{-1}$. As described in line 217 - 218, the SVOC emission ratios were estimated relative to the POA mass concentrations.

1.32 SI Line 70: The emission ratios are small, or the range is small?

The range is small and has been updated.

1.33 Lines 250 - 273: Is the TSI parameterization with the Ma parameterization or are they different cases that are explored? It seems like Ma et al. (2017) is used for IVOC SOA yields instead of Jather et al. (2014). There are a lot of parameterizations, precursors classes and products in this model approach. I strongly recommend adding a table(s) explicitly specifying all of the SOA yields and the corresponding precursors used in this study.

No, the TSI parameterization was not used, but the “WOR + ROB + MA” case from Ma et al. (2017). We have added the following table, from Ma et al. (2017), as the compounds used and their rate constants were already included:

**Table 13. Parameters for VOC, IVOC, and SVOC aerosol yields. The yields are taken from Ma et al. (2017).**

| Compound | Stoichiometric SOA yield High-NOx, 298 K (μg $m^{-3}$) | | | | |
|---|---|---|---|---|---|
| | 0.1 | 1 | 10 | 100 | 1000 |
| Benzene | N/A | 0.276 | 0.002 | 0.431 | 0.202 |
| Toluene | | | | | |
| Ethyltoluene | | | | | |
| Propylbenzenes | | | | | |
| Xylenes | N/A | 0.310 | 0.000 | 0.420 | 0.209 |
| Trimethylbenzenes | | | | | |
| IVOC C* = 6 | 0.007 | 0.090 | 0.206 | 0.350 | 0.00 |
| IVOC C* = 5 | 0.0498 | 0.0814 | 0.456 | 0.278 | 0.00 |
| IVOC C* = 4 | 0.053 | 0.103 | 0.464 | 0.266 | 0.00 |
| IVOC C* = 3 | 0.064 | 0.0914 | 0.562 | 0.209 | 0.00 |
| HOA C* = 2 | N/A | N/A | 0.28 | N/A | N/A |
| HOA C* = 1 | N/A | 0.18 | N/A | N/A | N/A |
| HOA C* = 0 | 0.12 | N/A | N/A | N/A | N/A |
| COA C* = 2 | N/A | N/A | 0.1881 | N/A | N/A |
| COA C* = 1 | N/A | 0.1188 | N/A | N/A | N/A |
| COA C* = 0 | 0.0594 | N/A | N/A | N/A | N/A |

We have also updated the rate constant table to include the rate constants for IVOCs and SVOCs.

1.34 Line 273: Recommend rephrasing “increase in mass of 0.99” to “change in mass of 0.99” or “decrease in mass of 1%”.

We have updated the text to say:

**“. . . a decrease in mass of 1%. . .”**

1.35 Line 276 - 281: This opening sentence is overly dense and meandering. What is the point of the appositive, “for ASOA apportionment (Fig. 1)”? It seems redundant. Should the second “apportionment” be “attribution”? The last portion of the sentence, after the GEOS-Chem reference should be broken off into its own sentence.

We have changed this text to say:

**“The model used in this study is GEOS-Chem v12.0.0 (Bey et al., 2001; The International GEOS-Chem User Community, 2018). This model is used for the following calculations: (1) ASOA apportionment (Fig. 1), (2) apportionment of ASOA to total PM2.5 for premature mortality calculations (Sect. 5), and (3) sensitivity analysis for ASOA production and emissions on premature mortality calculations. GEOS-Chem is operated at 2°×2.5° horizontal resolution.”**

1.36 Line 335: Recommend presenting Eq. 4 as the summation of premature deaths among all considered causes.

We disagree, as this is how the equation is typically presented in epidemiology papers (e.g., Burnett et al., 2018), and we stated in line 333 that the equation varies according to both the particular disease category and geographic region. The combination of these two dependencies would make writing the summation harder to understand.

***Reviewer #2***

2.0 The study represents an attempt to estimate the premature mortality linked to Anthropogenic Secondary Organic Aerosols. Using 11 urban areas on three continents and specific volatile organic compounds emission ratios were estimated and a budget for ASOA is attempted. With the studied dataset the SIMPLE parameterization for ASOA in the GEOS-Chem model is updated to reproduce observed ASOA. Finally an attribution of ASOA PM2.5 premature deaths is attempted.

General comment:

2.1 My greatest concern for the specific study is the overall omission of solid fuel combustion in all calculations, both for ASOA production (emissions and subsequent processing/oxidation/ageing) as well as its contribution to premature mortality. Not only biomass burning for heating purposes but also forest forest, burning of crops etc. This leads to

unaccounted emissions from urban areas such as Europe/US during winter from household heating but also from forested areas such as the Amazon, Canada, Siberia, Southeast Asia.

The purpose of this paper was to investigate the role of photochemically produced anthropogenic SOA. We provide further discussion and clarification of this point in response to 1.3.

We have also added the following line in the introduction to clarify this point:

**"Note, for the rest of the paper, unless explicitly stated otherwise, ASOA refers to SOA produced from the photooxidation of AVOCs, as there are potentially other relevant paths for the production of SOA in urban environments (e.g., Petit et al., 2014; Kodros et al., 2018, 2020; Stavroulas et al., 2019)."**

Specific Comments:

2.2 Line 110 - 114: Isn't solid fuel combustion/biomass burning aged SOA considered as ASOA? According to Kodros et al. (2020) in active fire regions bbOOA increases by more than 50-60% from fast oxidation processes even in the dark. Significant contribution of primary BBOA oxidation to the oxygenated OA have also been identified in large urban centers such as Paris (2014) and Athens (2019).

We have added the following:

**". . . and solid fuel emissions from residential wood burning and/or cookstoves (e.g., Hu et al., 2013, 2020; Schroder et al., 2018), . . ."**

Further, as discussed in R1.3, we further emphasize two studies that did have important impacts from solid fuel emissions. The results for these studies fall within the trend of the photochemically-produced ASOA.

However, we do not have the ability to potentially constrain or include "dark-aging" of bbOA into bbOOA. Thus, as we noted in R1.3, we suggest that the ASOA concentrations in this study may be an underestimate for this reason.

2.3 Line 119 - 132: Isn't the current study also under-predicting ASO by ignoring bbOOA? Furthermore, there is also the additive effect of the different pollutants when considering premature mortality. For example, Kodros et al. (2018) estimate joint exposure from household solid fuel use and ambient PM2.5 pollution and find 18% more deaths than by separating household and ambient mortality calculations. Which shows that solid fuel combustions is important for mortality as well, not only for ASOA calculations.

The Kodros et al. (2018) study investigated indoor and outdoor exposure; whereas, the purpose of this study is to only investigate the role of exposure to outdoor $PM_{2.5}$. We agree that this source of indoor pollution (among others, e.g., HOMEChem and other references) could be important additional sources of $PM_{2.5}$ exposures, and thus contributors to premature mortality, Kodros et al.

(2018)

acknowledged a large source of uncertainty associated with the indoor estimation of solid-fuel use and thus associated premature mortality.

To clarify this point, we have added the following:

**"Though there are potentially other important exposure pathways to PM that may increase premature mortality, such as exposure to solid-fuel emissions indoors (e.g., Kodros et al., 2018), the focus of this paper is on exposure to outdoor ASOA and its associated impacts to premature mortality."**

2.4 Fig.5a and Line 174-180, Fig. 6 and line 423-428: Authors only mention the uncertainties in x- and y-axis values. Does really by removing just one point increases the slope that much? The y-axis has an upper value of 140 compared to x-axis of 6! Why only 25% of the observed ASOA be associated with BTEX? What about the rest? Isn't this a solid proof that solid fuel combustion (BBOA) should definitely be taken into account?

See response to comment 1.12 concerning a more robust statistical analysis to determine if any one point could be driving the slope or not.

We have updated the text (see R1.3) to reflect that we have two studies (Chinese Outflow 2011 and New York City 2015) that had major impacts of solid fuel emissions (coal combustion for Chinese Outflow and biomass burning from New York City). As discussed in response to 1.12, these two points are not outliers and do not individually overly influence the slope; thus, the update we propose here for the SIMPLE model that is used in GEOS-Chem appears to capture and not underestimate the *photochemical* ASOA production from those sources as well. See response to 1.3 for updated text and clarification on this point.

In regards to the 25% of observed ASOA being explained by BTEX, as stated on pg 18, lines 410 - 413 in the original manuscript:

"However, BTEX alone cannot account for much of the ASOA formation (see budget closure discussion below), and instead, BTEX may be better thought of as both partial contributors and also as indicators for the co-emissions of other (unmeasured) organic precursors that are also efficient at forming ASOA."

BTEX only explaining 25±6% of the observed ASOA is not shocking, as has been highlighted in prior studies (e.g., Dzepina et al., 2009; Ensberg et al., 2014; Hayes et al., 2015; Ma et al., 2017; Nault et al., 2018), which led to the McDonald et al. (2018) study and the importance for the finding of VCPs potentially explaining a large fraction of the missing *photochemically* produced ASOA. To further clarify this point, we have added the following:

**"BTEX only explaining 25% of the observed ASOA is similar to prior studies that have done budget analysis of precursor gases and observed SOA (e.g., Dzepina et al., 2009; Ensberg et al., 2014; Hayes et al., 2015; Ma et al., 2017; Nault et al., 2018)."**

As explained throughout Section 3.2 and with Fig. 6, the remaining budget of the observed *photochemically* produced ASOA is explained by other aromatic compounds, IVOCs, and SVOCs. This is the important finding, as we have expanded the work from McDonald et al. (2018) to show the importance of IVOCs and VCPs in the production of *photochemically* produced ASOA. Specifically, we find (pg 21, line 464 of original submission) 85±12% of the observed ASOA for the five different cities to be explained by BTEX, aromatic compounds, IVOCs, and SVOCs.

2.5 Section 2.5.2 Once more, by not including solid fuel combustion in ASOA all the respective chemistry and oxidation is missing, losing 50-60% of SOA from fast oxidation of BBOA, even in the dark (NO3 radicals) (Kodros et al., 2020).

As explained in response to comments 1.3 and 2.4, solid fuel combustion is included in both the experimental studies and the model. We do not have a way to include the dark oxidation of BBOA, and we have acknowledged that this may lead to an underestimate of the concentrations and thus the health effects of ASOA (see response to R1.3).

2.6 Line 578 - 579: How is the "model constrained to atmospheric observations for a more accurate contribution of SOA" when an important source of ASOA such as solid fuel combustion is omitted?

As summarized in response comments 1.3, 2.4, and 2.5, this is a misunderstanding. Solid fuel combustion is included. We have updated this text to say:

**"Using a model constrained to day-time atmospheric observations (Fig. 2 and Fig. 4, see Sect. 4) leads to more accurate estimation of the contribution of photochemically-produced ASOA to $PM_{2.5}$ associated premature mortality that has not been possible in prior studies."**

Technical corrections:

2.7 Fig. 7 & 8: USOA? Should it be ASOA?

Updated:

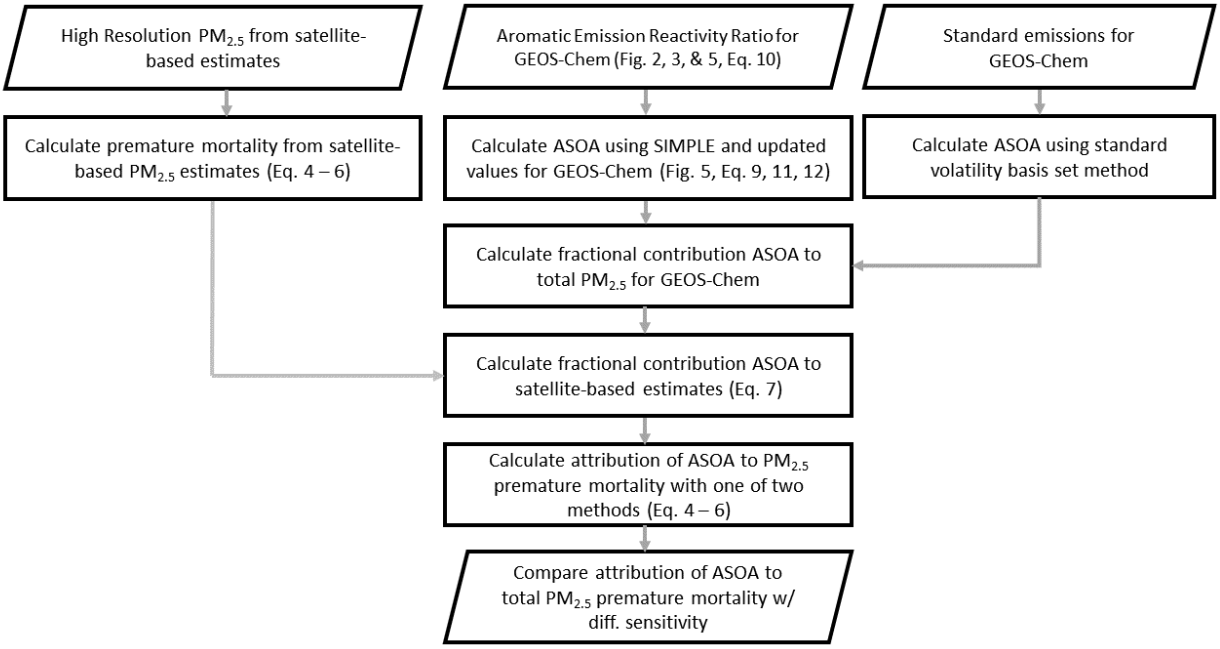


**Figure 7. Flowchart describing how observed ASOA production was used to calculate ASOA in GEOS-Chem, and how the satellite-based $PM_{2.5}$ estimates and GEOS-Chem $PM_{2.5}$ speciation was used to estimate the premature mortality and attribution of premature mortality by ASOA. See Sect. 2 for further information about the details in the figure. SIMPLE is described in Eq. 9 and by Hodzic and Jimenez (2011) and Hayes et al. (2015). The one of two methods mentioned include either the Integrated Exposure-Response (IER) (Burnett et al., 2014) with Global Burden of Disease (GBD) dataset (IHME, 2016) or the new Global Exposure Mortality Model (GEMM) (Burnett et al., 2018) methods. For both IER and GEMM, the marginal method (Silva et al., 2016) or attributable fraction method (Anenberg et al., 2019) are used.**

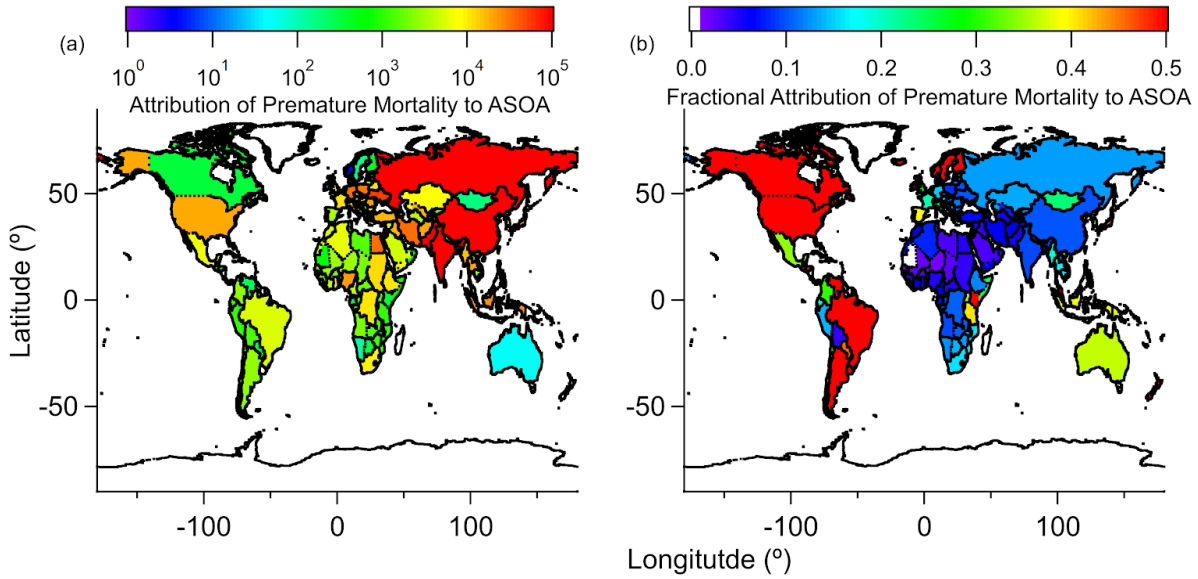


**Figure 8. Five-year average (a) estimated reduction in $PM_{2.5}$-associated premature deaths, by country, upon removing ASOA from total $PM_{2.5}$, and (b) fractional reduction (reduction $PM_{2.5}$ premature deaths / total $PM_{2.5}$ premature deaths) in $PM_{2.5}$-associated premature deaths, by country, upon removing ASOA from GEOS-Chem. The IER methods are used here. See Fig. S9 and Fig. S12 for results using GEMM. See Fig. S10 for 10×10 km$^2$ area results in comparison with country-level results.**

We also noticed an error in the labels in Fig. 6 and have updated and include the update below:

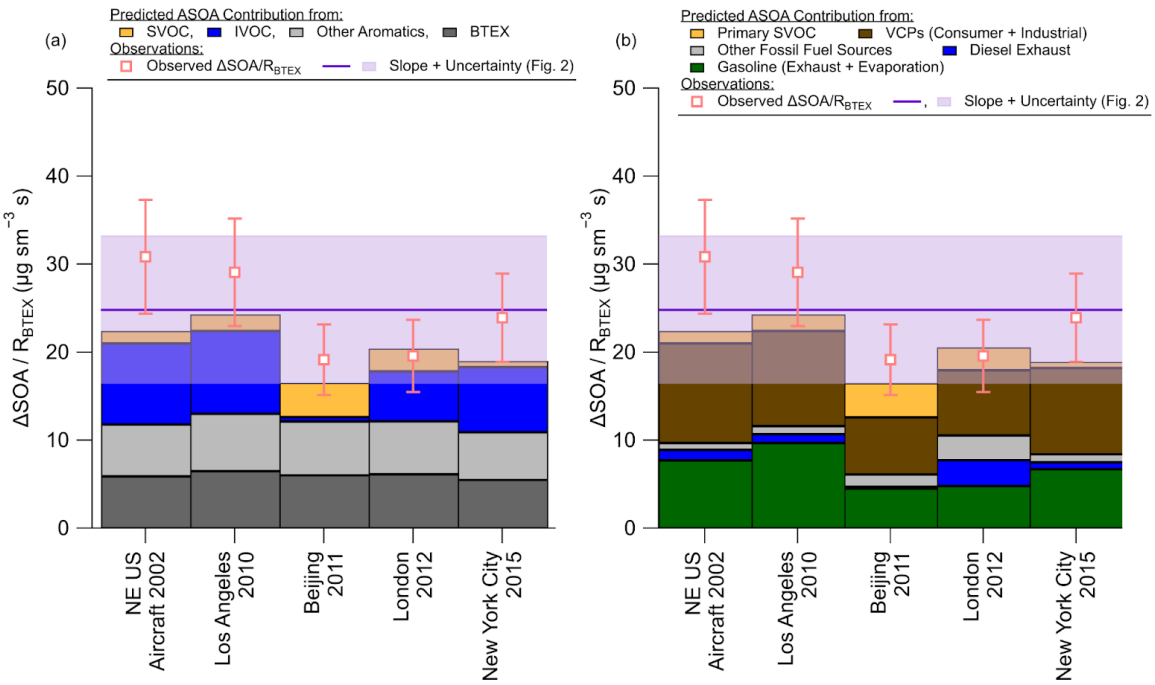

**Figure 4. (a) Budget analysis for the contribution of the observed ΔSOA/$R_{BTEX}$ (Fig. 25) for cities with known emissions inventories for different volatility classes (see SI and Fig. 2 and Fig. S6). (b) Same as (a), but for sources of emissions. For (a) and (b), SVOC is the contribution from both vehicle and other (cooking, etc.) sources. See Sect. 2 and SI for information about the emissions, ASOA precursor contribution, error analysis, and discussion about sensitivity of emission inventory IVOC/BTEX ratios for different cities and years in the US.**

**References**

Anenberg, S., Miller, J., Henze, D. and Minjares, R.: A global snapshot of the air pollution-related health impacts of transportation sector emissions in 2010 and 2015, ICCT, Climate & Clean Air Coalition., 2019.

Apel, E. C., Emmons, L. K., Karl, T., Flocke, F., Hills, a. J., Madronich, S., Lee-Taylor, J., Fried, A., Weibring, P., Walega, J., Richter, D., Tie, X., Mauldin, L., Campos, T., Weinheimer, A., Knapp, D., Sive, B., Kleinman, L., Springston, S., Zaveri, R., Ortega, J., Voss, P., Blake, D., Baker, A., Warneke, C., Welsh-Bon, D., de Gouw, J., Zheng, J., Zhang, R., Rudolph, J., Junkermann, W. and Riemer, D. D.: Chemical evolution of volatile organic compounds in the outflow of the Mexico City Metropolitan area, Atmos. Chem. Phys., 10(5), 2353–2375, 2010.

Baker, K. R., Woody, M. C., Valin, L., Szykman, J., Yates, E. L., Iraci, L. T., Choi, H. D., Soja, A. J., Koplitz, S. N., Zhou, L., Campuzano-Jost, P., Jimenez, J. L. and Hair, J. W.: Photochemical model evaluation of 2013 California wild fire air quality impacts using surface, aircraft, and satellite data, Sci. Total Environ., 637-638, 1137–1149, 2018.

Bey, I., Jacob, D. J., Yantosca, R. M., Logan, J. A., Field, B. D., Fiore, A. M., Li, Q., Liu, H. Y., Mickley, L. J. and Schultz, M. G.: Global modeling of tropospheric chemistry with assimilated meteorology: Model description and evaluation, J. Geophys. Res. D: Atmos., 106(D19), 23073–23095, 2001.

Bon, D. M., Ulbrich, I. M., de Gouw, J. A., Warneke, C., Kuster, W. C., Alexander, M. L., Baker, A., Beyersdorf, A. J., Blake, D., Fall, R., Jimenez, J. L., Herndon, S. C., Huey, L. G., Knighton, W. B., Ortega, J., Springston, S. and Vargas, O.: Measurements of volatile organic compounds at a suburban ground site (T1) in Mexico City during the MILAGRO 2006 campaign: measurement comparison, emission ratios, and source attribution, Atmos. Chem. Phys., 11(6), 2399–2421, 2011.

Burnett, R., Chen, H., Szyszkowicz, M., Fann, N., Hubbell, B., Pope, C. A., Apte, J. S., Brauer, M., Cohen, A., Weichenthal, S., Coggins, J., Di, Q., Brunekreef, B., Frostad, J., Lim, S. S., Kan, H., Walker, K. D., Thurston, G. D., Hayes, R. B., Lim, C. C., Turner, M. C., Jerrett, M., Krewski, D., Gapstur, S. M., Diver, W. R., Ostro, B., Goldberg, D., Crouse, D. L., Martin, R. V., Peters, P., Pinault, L., Tjepkema, M., van Donkelaar, A., Villeneuve, P. J., Miller, A. B., Yin, P., Zhou, M., Wang, L., Janssen, N. A. H., Marra, M., Atkinson, R. W., Tsang, H., Quoc Thach, T., Cannon, J. B., Allen, R. T., Hart, J. E., Laden, F., Cesaroni, G., Forastiere, F., Weinmayr, G., Jaensch, A., Nagel, G., Concin, H. and Spadaro, J. V.: Global estimates of mortality associated with long-term exposure to outdoor fine particulate matter, Proc. Natl. Acad. Sci. U. S. A., 115(38), 9592–9597, 2018.

Burnett, R. T., Pope, C. A., Ezzati, M., Olives, C., Lim, S. S., Mehta, S., Shin, H. H., Singh, G., Hubbell, B., Brauer, M., Anderson, H. R., Smith, K. R., Balmes, J. R., Bruce, N. G., Kan, H., Laden, F., Prüss-Ustün, A., Turner, M. C., Gapstur, S. M., Diver, W. R. and Cohen, A.: An integrated risk function for estimating the global burden of disease attributable to ambient fine particulate matter exposure, Environ. Health Perspect., 122(4), 397–403, 2014.

Cappa, C. D., Jathar, S. H., Kleeman, M. J., Docherty, K. S., Jimenez, J. L., Seinfeld, J. H. and

Wexler, A. S.: Simulating secondary organic aerosol in a regional air quality model using the statistical oxidation model - Part 2: Assessing the influence of vapor wall losses, Atmos. Chem. Phys., 16(5), 3041–3059, 2016.

Chafe, Z., Brauer, M., Heroux, M.-E., Klimont, Z., Lanki, T., Salonen, R. O. and Smith, K. R.: Residential heating with wood and coal: Health impacts and policy options in Europe and North America, WHO/UNECE LRTAP., 2015.

DeCarlo, P. F., Ulbrich, I. M., Crounse, J., de Foy, B., Dunlea, E. J., Aiken, A. C., Knapp, D., Weinheimer, A. J., Campos, T., Wennberg, P. O. and Jimenez, J. L.: Investigation of the sources and processing of organic aerosol over the Central Mexican Plateau from aircraft measurements during MILAGRO, Atmos. Chem. Phys., 10(12), 5257–5280, 2010.

Deming, B., Pagonis, D., Liu, X., Talukdar, R. K., Roberts, J. M., Veres, P. R., Krechmer, J. E., de Gouw, J. A., Jimenez, J. L. and Zieman, P. J.: Measurements of Delays of Gas-Phase Compounds in a Wide Variety of Tubing Materials due to Gas-Wall Partitioning, Atmos. Meas. Tech., In Prep., 2018.

van Donkelaar, A., Martin, R. V., Brauer, M. and Boys, B. L.: Use of Satellite Observations for Long-Term Exposure Assessment of Global Concentrations of Fine Particulate Matter, Environ. Health Perspect., 123(2), 135–143, 2015.

van Donkelaar, A., Martin, R. V., Brauer, M., Hsu, N. C., Kahn, R. A., Levy, R. C., Lyapustin, A., Sayer, A. M. and Winker, D. M.: Global Estimates of Fine Particulate Matter using a Combined Geophysical-Statistical Method with Information from Satellites, Models, and Monitors, Environ. Sci. Technol., 50(7), 3762–3772, 2016.

Dzepina, K., Volkamer, R. M., Madronich, S., Tulet, P., Ulbrich, I. M., Zhang, Q., Cappa, C. D., Ziemann, P. J. and Jimenez, J. L.: Evaluation of recently-proposed secondary organic aerosol models for a case study in Mexico City, Atmos. Chem. Phys., 9(15), 5681–5709, 2009.

Ensberg, J. J., Hayes, P. L., Jimenez, J. L., Gilman, J. B., Kuster, W. C., de Gouw, J. A., Holloway, J. S., Gordon, T. D., Jathar, S., Robinson, A. L. and Seinfeld, J. H.: Emission factor ratios, SOA mass yields, and the impact of vehicular emissions on SOA formation, Atmos. Chem. Phys., 14(5), 2383–2397, 2014.

Freney, E. J., Sellegri, K., Canonaco, F., Colomb, A., Borbon, A., Michoud, V., Crumeyrolle, S., Amarouche, N., Bourianne, T., Gomes, L., Prevot, A. S. H., Beekmann, M. and Schwarzenböeck, A.: Characterizing the impact of urban emissions on regional aerosol particles: Airborne measurements during the MEGAPOLI experiment, Atmos. Chem. Phys., 14(3), 1397–1412, 2014.

de Gouw, J. A. and Jimenez, J. L.: Organic Aerosols in the Earth's Atmosphere, Environ. Sci. Technol., 43(20), 7614–7618, 2009.

de Gouw, J. A., Middlebrook, A. M., Warneke, C., Goldan, P. D., Kuster, W. C., Roberts, J. M., Fehsenfeld, F. C., Worsnop, D. R., Canagaratna, M. R., Pszenny, A. A. P., Keene, W. C., Marchewka, M., Bertman, S. B. and Bates, T. S.: Budget of organic carbon in a polluted

atmosphere: Results from the New England Air Quality Study in 2002, J. Geophys. Res. D: Atmos., 110(16), 1–22, 2005.

de Gouw, J. A., Gilman, J. B., Kim, S.-W., Lerner, B. M., Isaacman-VanWertz, G., McDonald, B. C., Warneke, C., Kuster, W. C., Lefer, B. L., Griffith, S. M., Dusanter, S., Stevens, P. S. and Stutz, J.: Chemistry of Volatile Organic Compounds in the Los Angeles basin: Nighttime Removal of Alkenes and Determination of Emission Ratios, J. Geophys. Res.: Atmos., 122(21), 11,843–11,861, 2017.

de Gouw, J. A., Gilman, J. B., Kim, S.-W., Alvarez, S. L., Dusanter, S., Graus, M., Griffith, S. M., Isaacman-VanWertz, G., Kuster, W. C., Lefer, B. L., Lerner, B. M., McDonald, B. C., Rappenglück, B., Roberts, J. M., Stevens, P. S., Stutz, J., Thalman, R., Veres, P. R., Volkamer, R., Warneke, C., Washenfelder, R. A. and Young, C. J.: Chemistry of volatile organic compounds in the Los Angeles basin: Formation of oxygenated compounds and determination of emission ratios, J. Geophys. Res., 123(4), 2298–2319, 2018.

Grieshop, A. P., Logue, J. M., Donahue, N. M. and Robinson, A. L.: Laboratory investigation of photochemical oxidation of organic aerosol from wood fires 1: measurement and simulation of organic aerosol evolution, Atmos. Chem. Phys., 9(4), 1263–1277, 2009.

Hallquist, M., Wenger, J. C., Baltensperger, U., Rudich, Y., Simpson, D., Claeys, M., Dommen, J., Donahue, N. M., George, C., Goldstein, A. H., Hamilton, J. F., Herrmann, H., Hoffmann, T., Iinuma, Y., Jang, M., Jenkin, M. E., Jimenez, J. L., Kiendler-Scharr, A., Maenhaut, W., McFiggans, G., Mentel, T. F., Monod, A., Prévôt, A. S. H., Seinfeld, J. H., Surratt, J. D., Szmigielski, R. and Wildt, J.: The formation, properties and impact of secondary organic aerosol: current and emerging issues, Atmos. Chem. Phys., 9(14), 5155–5236, 2009.

Hayes, P. L., Ortega, A. M., Cubison, M. J., Froyd, K. D., Zhao, Y., Cliff, S. S., Hu, W. W., Toohey, D. W., Flynn, J. H., Lefer, B. L., Grossberg, N., Alvarez, S., Rappenglück, B., Taylor, J. W., Allan, J. D., Holloway, J. S., Gilman, J. B., Kuster, W. C., de Gouw, J. A., Massoli, P., Zhang, X., Liu, J., Weber, R. J., Corrigan, A. L., Russell, L. M., Isaacman, G., Worton, D. R., Kreisberg, N. M., Goldstein, A. H., Thalman, R., Waxman, E. M., Volkamer, R., Lin, Y. H., Surratt, J. D., Kleindienst, T. E., Offenberg, J. H., Dusanter, S., Griffith, S., Stevens, P. S., Brioude, J., Angevine, W. M. and Jimenez, J. L.: Organic aerosol composition and sources in Pasadena, California, during the 2010 CalNex campaign, J. Geophys. Res. D: Atmos., 118(16), 9233–9257, 2013.

Hayes, P. L., Carlton, A. G., Baker, K. R., Ahmadov, R., Washenfelder, R. A., Alvarez, S., Rappenglück, B., Gilman, J. B., Kuster, W. C., de Gouw, J. A., Zotter, P., Prévôt, A. S. H., Szidat, S., Kleindienst, T. E., Ma, P. K. and Jimenez, J. L.: Modeling the formation and aging of secondary organic aerosols in Los Angeles during CalNex 2010, Atmos. Chem. Phys., 15(10), 5773–5801, 2015.

Heringa, M. F., DeCarlo, P. F., Chirico, R., Tritscher, T., Dommen, J., Weingartner, E., Richter, R., Wehrle, G., Prévôt, A. S. H. and Baltensperger, U.: Investigations of primary and secondary particulate matter of different wood combustion appliances with a high-resolution time-of-flight aerosol mass spectrometer, Atmos. Chem. Phys., 11(12), 5945–5957, 2011.

Hodzic, A. and Jimenez, J. L.: Modeling anthropogenically controlled secondary organic aerosols in a megacity: A simplified framework for global and climate models, Geosci. Model Dev., 4(4), 901–917, 2011.

Hodzic, A., Jimenez, J. L., Madronich, S., Canagaratna, M. R., DeCarlo, P. F., Kleinman, L. and Fast, J.: Modeling organic aerosols in a megacity: potential contribution of semi-volatile and intermediate volatility primary organic compounds to secondary organic aerosol formation, Atmos. Chem. Phys., 10(12), 5491–5514, 2010.

Hodzic, A., Campuzano-Jost, P., Bian, H., Chin, M., Colarco, P. R., Day, D. A., Froyd, K. D., Heinold, B., Jo, D. S., Katich, J. M., Kodros, J. K., Nault, B. A., Pierce, J. R., Ray, E., Schacht, J., Schill, G. P., Schroder, J. C., Schwarz, J. P., Sueper, D. T., Tegen, I., Tilmes, S., Tsigaridis, K., Yu, P. and Jimenez, J. L.: Characterization of Organic Aerosol across the Global Remote Troposphere: A comparison of ATom measurements and global chemistry models, Atmos. Chem. Phys., 20(8), 4607–4635, 2020.

Hu, W., Hu, M., Hu, W., Jimenez, J. L., Yuan, B., Chen, W., Wang, M., Wu, Y., Chen, C., Wang, Z., Peng, J., Zeng, L. and Shao, M.: Chemical composition, sources, and aging process of submicron aerosols in Beijing: Contrast between summer and winter, J. Geophys. Res. D: Atmos., 121(4), 1955–1977, 2016.

Hu, W., Downward, G., Wong, J. Y. Y., Reiss, B., Rothman, N., Portengen, L., Li, J., Jones, R. R., Huang, Y., Yang, K., Chen, Y., Xu, J., He, J., Bassig, B., Seow, W. J., Hosgood, H. D., Zhang, L., Wu, G., Wei, F., Vermeulen, R. and Lan, Q.: Characterization of outdoor air pollution from solid fuel combustion in Xuanwei and Fuyuan, a rural region of China, Sci. Rep., 10(1), 11335, 2020.

Hu, W. W., Hu, M., Yuan, B., Jimenez, J. L., Tang, Q., Peng, J. F., Hu, W., Shao, M., Wang, M., Zeng, L. M., Wu, Y. S., Gong, Z. H., Huang, X. F. and He, L. Y.: Insights on organic aerosol aging and the influence of coal combustion at a regional receptor site of central eastern China, Atmos. Chem. Phys., 13(19), 10095–10112, 2013.

IHME: Global Burden of Disease Study 2015 (GBD 2015) Data Resources, GHDx [online] Available from: http://ghdx.healthdata.org/gbd-2015 (Accessed 2019), 2016.

Janssen, R. H. H., Tsimpidi, A. P., Karydis, V. A., Pozzer, A., Lelieveld, J., Crippa, M., Prévôt, A. S. H., Ait-Helal, W., Borbon, A., Sauvage, S. and Locoge, N.: Influence of local production and vertical transport on the organic aerosol budget over Paris, J. Geophys. Res. D: Atmos., 122(15), 8276–8296, 2017.

Janssens-Maenhout, G., Crippa, M., Guizzardi, D., Dentener, F., Muntean, M., Pouliot, G., Keating, T., Zhang, Q., Kurokawa, J., Wankmüller, R., Denier van der Gon, H., Kuenen, J. J. P., Klimont, Z., Frost, G., Darras, S., Koffi, B. and Li, M.: HTAP_v2.2: a mosaic of regional and global emission grid maps for 2008 and 2010 to study hemispheric transport of air pollution, Atmos. Chem. Phys., 15(19), 11411–11432, 2015.

Jathar, S. H., Gordon, T. D., Hennigan, C. J., Pye, H. O. T., Pouliot, G., Adams, P. J., Donahue, N. M. and Robinson, A. L.: Unspeciated organic emissions from combustion sources and their

influence on the secondary organic aerosol budget in the United States, Proc. Natl. Acad. Sci. U. S. A., 111(29), 10473–10478, 2014.

Jathar, S. H., Woody, M., Pye, H. O. T., Baker, K. R. and Robinson, A. L.: Chemical transport model simulations of organic aerosol in southern California: model evaluation and gasoline and diesel source contributions, Atmos. Chem. Phys., 17(6), 4305–4318, 2017.

Jimenez, J. L., Canagaratna, M. R., Donahue, N. M., Prevot, A. S. H., Zhang, Q., Kroll, J. H., DeCarlo, P. F., Allan, J. D., Coe, H., Ng, N. L., Aiken, A. C., Docherty, K. S., Ulbrich, I. M., Grieshop, A. P., Robinson, A. L., Duplissy, J., Smith, J. D., Wilson, K. R., Lanz, V. A., Hueglin, C., Sun, Y. L., Tian, J., Laaksonen, A., Raatikainen, T., Rautiainen, J., Vaattovaara, P., Ehn, M., Kulmala, M., Tomlinson, J. M., Collins, D. R., Cubison, M. J., Dunlea, E. J., Huffman, J. A., Onasch, T. B., Alfarra, M. R., Williams, P. I., Bower, K., Kondo, Y., Schneider, J., Drewnick, F., Borrmann, S., Weimer, S., Demerjian, K., Salcedo, D., Cottrell, L., Griffin, R., Takami, A., Miyoshi, T., Hatakeyama, S., Shimono, A., Sun, J. Y., Zhang, Y. M., Dzepina, K., Kimmel, J. R., Sueper, D., Jayne, J. T., Herndon, S. C., Trimborn, A. M., Williams, L. R., Wood, E. C., Middlebrook, A. M., Kolb, C. E., Baltensperger, U. and Worsnop, D. R.: Evolution of organic aerosols in the atmosphere, Science, 326(5959), 1525–1529, 2009.

Khare, P., Machesky, J., Soto, R., He, M., Presto, A. A. and Gentner, D. R.: Asphalt-related emissions are a major missing nontraditional source of secondary organic aerosol precursors, Sci Adv, 6(36), doi:10.1126/sciadv.abb9785, 2020.

Kodros, J. K., Carter, E., Brauer, M., Volckens, J., Bilsback, K. R., L'Orange, C., Johnson, M. and Pierce, J. R.: Quantifying the Contribution to Uncertainty in Mortality Attributed to Household, Ambient, and Joint Exposure to PM2.5 From Residential Solid Fuel Use, Geohealth, 2(1), 25–39, 2018.

Kodros, J. K., Papanastasiou, D. K., Paglione, M., Masiol, M., Squizzato, S., Florou, K., Skyllakou, K., Kaltsonoudis, C., Nenes, A. and Pandis, S. N.: Rapid dark aging of biomass burning as an overlooked source of oxidized organic aerosol, Proc. Natl. Acad. Sci. U. S. A., 117(52), 33028–33033, 2020.

Kondo, Y., Morino, Y., Fukuda, M., Kanaya, Y., Miyazaki, Y., Takegawa, N., Tanimoto, H., McKenzie, R., Johnston, P., Blake, D. R., Murayama, T. and Koike, M.: Formation and transport of oxidized reactive nitrogen, ozone, and secondary organic aerosol in Tokyo, J. Geophys. Res. D: Atmos., 113(D21), D21310, 2008.

Krechmer, J. E., Pagonis, D., Ziemann, P. J. and Jimenez, J. L.: Quantification of Gas-Wall Partitioning in Teflon Environmental Chambers Using Rapid Bursts of Low-Volatility Oxidized Species Generated in Situ, Environ. Sci. Technol., 50(11), 5757–5765, 2016.

Lacey, F. G., Henze, D. K., Lee, C. J., van Donkelaar, A. and Martin, R. V.: Transient climate and ambient health impacts due to national solid fuel cookstove emissions, Proc. Natl. Acad. Sci. U. S. A., 114(6), 1269–1274, 2017.

Lam, N. L., Upadhyay, B., Maharjan, S., Jagoe, K., Weyant, C. L., Thompson, R., Uprety, S., Johnson, M. A. and Bond, T. C.: Seasonal fuel consumption, stoves, and end-uses in rural

households of the far-western development region of Nepal, Environ. Res. Lett., 12(12), 125011, 2017.

Lelieveld, J., Evans, J. S., Fnais, M., Giannadaki, D. and Pozzer, A.: The contribution of outdoor air pollution sources to premature mortality on a global scale, Nature, 525(7569), 367–371, 2015.

Liu, X., Deming, B., Pagonis, D., Day, D. A., Palm, B. B., Talukdar, R., Roberts, J. M., Veres, P. R., Krechmer, J. E., Thornton, J. A., de Gouw, J. A., Ziemann, P. J. and Jimenez, J. L.: Effects of gas–wall interactions on measurements of semivolatile compounds and small polar molecules, , doi:10.5194/amt-12-3137-2019, 2019.

Lu, Q., Zhao, Y. and Robinson, A. L.: Comprehensive organic emission profiles for gasoline, diesel, and gas-turbine engines including intermediate and semi-volatile organic compound emissions, Atmos. Chem. Phys., 18, 17637–17654, 2018.

Ma, P. K., Zhao, Y., Robinson, A. L., Worton, D. R., Goldstein, A. H., Ortega, A. M., Jimenez, J. L., Zotter, P., Prévôt, A. S. H., Szidat, S. and Hayes, P. L.: Evaluating the impact of new observational constraints on P-S/IVOC emissions, multi-generation oxidation, and chamber wall losses on SOA modeling for Los Angeles, CA, Atmos. Chem. Phys., 17(15), 9237–9259, 2017.

May, A. A., Levin, E. J. T., Hennigan, C. J., Riipinen, I., Lee, T., Collett, J. L., Jimenez, J. L., Kreidenweis, S. M. and Robinson, A. L.: Gas-particle partitioning of primary organic aerosol emissions: 3. Biomass burning, J. Geophys. Res. D: Atmos., 118(19), 11,327–11,338, 2013.

McDonald, B. C., de Gouw, J. A., Gilman, J. B., Jathar, S. H., Akherati, A., Cappa, C. D., Jimenez, J. L., Lee-Taylor, J., Hayes, P. L., McKeen, S. A., Cui, Y. Y., Kim, S.-W., Gentner, D. R., Isaacman-VanWertz, G., Goldstein, A. H., Harley, R. A., Frost, G. J., Roberts, J. M., Ryerson, T. B. and Trainer, M.: Volatile chemical products emerging as largest petrochemical source of urban organic emissions, Science, 359(6377), 760–764, 2018.

Morino, Y., Chatani, S., Tanabe, K., Fujitani, Y., Morikawa, T., Takahashi, K., Sato, K. and Sugata, S.: Contributions of Condensable Particulate Matter to Atmospheric Organic Aerosol over Japan, Environ. Sci. Technol., 52(15), 8456–8466, 2018.

Murphy, B. N., Woody, M. C., Jimenez, J. L., Carlton, A. M. G., Hayes, P. L., Liu, S., Ng, N. L., Russell, L. M., Setyan, A., Xu, L., Young, J., Zaveri, R. A., Zhang, Q. and Pye, H. O. T.: Semivolatile POA and parameterized total combustion SOA in CMAQv5.2: impacts on source strength and partitioning, Atmos. Chem. Phys., 17(18), 11107–11133, 2017.

Nault, B. A., Campuzano-Jost, P., Day, D. A., Schroder, J. C., Anderson, B., Beyersdorf, A. J., Blake, D. R., Brune, W. H., Choi, Y., Corr, C. A., de Gouw, J. A., Dibb, J., DiGangi, J. P., Diskin, G. S., Fried, A., Huey, L. G., Kim, M. J., Knote, C. J., Lamb, K. D., Lee, T., Park, T., Pusede, S. E., Scheuer, E., Thornhill, K. L., Woo, J.-H. and Jimenez, J. L.: Secondary Organic Aerosol Production from Local Emissions Dominates the Organic Aerosol Budget over Seoul, South Korea, during KORUS-AQ, Atmos. Chem. Phys., 18, 17769–17800, 2018.

Pagonis, D., Krechmer, J. E., de Gouw, J., Jimenez, J. L. and Ziemann, P. J.: Effects of Gas-Wall Partitioning in Teflon Tubing and Instrumentation on Time-Resolved Measurements of

Gas-Phase Organic Compounds, Atmospheric Measurement Techniques Discussions, 1–19, 2017.

Pai, S. J., Heald, C. L., Pierce, J. R., Farina, S. C., Marais, E. A., Jimenez, J. L., Campuzano-Jost, P., Nault, B. A., Middlebrook, A. M., Coe, H., Shilling, J. E., Bahreini, R., Dingle, J. H. and Vu, K.: An evaluation of global organic aerosol schemes using airborne observations, Atmos. Chem. Phys., 20(5), 2637–2665, 2020.

Petit, J.-E., Favez, O., Sciare, J., Canonaco, F., Croteau, P., Močnik, G., Jayne, J., Worsnop, D. and Leoz-Garziandia, E.: Submicron aerosol source apportionment of wintertime pollution in Paris, France by double positive matrix factorization ($PMF^2$) using an aerosol chemical speciation monitor (ACSM) and a multi-wavelength Aethalometer, Atmos. Chem. Phys., 14(24), 13773–13787, 2014.

Ridley, D. A., Heald, C. L., Ridley, K. J. and Kroll, J. H.: Causes and consequences of decreasing atmospheric organic aerosol in the United States, Proc. Natl. Acad. Sci. U. S. A., 115(2), 290–295, 2018.

Robinson, A. L., Donahue, N. M., Shrivastava, M. K., Weitkamp, E. A., Sage, A. M., Grieshop, A. P., Lane, T. E., Pierce, J. R. and Pandis, S. N.: Rethinking Organic Aerosols: Semivolatile Emissions and Photochemical Aging, Science, 315(5816), 1259–1262, 2007.

Schroder, J. C., Campuzano-Jost, P., Day, D. A., Shah, V., Larson, K., Sommers, J. M., Sullivan, A. P., Campos, T., Reeves, J. M., Hills, A., Hornbrook, R. S., Blake, N. J., Scheuer, E., Guo, H., Fibiger, D. L., McDuffie, E. E., Hayes, P. L., Weber, R. J., Dibb, J. E., Apel, E. C., Jaeglé, L., Brown, S. S., Thronton, J. A. and Jimenez, J. L.: Sources and Secondary Production of Organic Aerosols in the Northeastern US during WINTER, J. Geophys. Res. D: Atmos., doi:10.1029/2018JD028475, 2018.

Seltzer, K. M., Pennington, E., Rao, V., Murphy, B. N., Strum, M., Isaacs, K. K. and Pye, H. O. T.: Reactive organic carbon emissions from volatile chemical products, Atmos. Chem. Phys., 21, 5079–5100, 2021.

Shrivastava, M., Cappa, C. D., Fan, J., Goldstein, A. H., Guenther, A. B., Jimenez, J. L., Kuang, C., Laskin, A., Martin, S. T., Ng, N. L., Petaja, T., Pierce, J. R., Rasch, P. J., Roldin, P., Seinfeld, J. H., Shilling, J., Smith, J. N., Thornton, J. A., Volkamer, R., Wang, J., Worsnop, D. R., Zaveri, R. A., Zelenyuk, A. and Zhang, Q.: Recent advances in understanding secondary organic aerosol: Implications for global climate forcing, Rev. Geophys., 55(2), 509–559, 2017.

Silva, R. A., Adelman, Z., Fry, M. M. and West, J. J.: The Impact of Individual Anthropogenic Emissions Sectors on the Global Burden of Human Mortality due to Ambient Air Pollution, Environ. Health Perspect., 124(11), 1776–1784, 2016.

Stavroulas, I., Bougiatioti, A., Grivas, G., Paraskevopoulou, D., Tsagkaraki, M., Zarmpas, P., Liakakou, E., Gerasopoulos, E. and Mihalopoulos, N.: Sources and processes that control the submicron organic aerosol composition in an urban Mediterranean environment (Athens): a high temporal-resolution chemical composition measurement study, Atmos. Chem. Phys., 19(2), 901–919, 2019.

Stewart, G. J., Nelson, B. S., Acton, W. J. F., Vaughan, A. R., Farren, N. J., Hopkins, J. R., Ward, M. W., Swift, S. J., Arya, R., Mondal, A., Jangirh, R., Ahlawat, S., Yadav, L., Sharma, S. K., Yunus, S. S. M., Hewitt, C. N., Nemitz, E., Mullinger, N., Gadi, R., Sahu, L. K., Tripathi, N., Rickard, A. R., Lee, J. D., Mandal, T. K. and Hamilton, J. F.: Emissions of intermediate-volatility and semi-volatile organic compounds from domestic fuels used in Delhi, India, Atmos. Chem. Phys. Discuss., doi:10.5194/acp-2020-860, 2020.

The International GEOS-Chem User Community: geoschem/geos-chem: GEOS-Chem 12.0.0 release, , doi:10.5281/ZENODO.1343547, 2018.

Tsimpidi, A. P., Karydis, V. A., Zavala, M., Lei, W., Molina, L., Ulbrich, I. M., Jimenez, J. L. and Pandis, S. N.: Evaluation of the volatility basis-set approach for the simulation of organic aerosol formation in the Mexico City metropolitan area, Atmos. Chem. Phys., 10(2), 525–546, 2010.

Volkamer, R., Jimenez, J. L., San Martini, F., Dzepina, K., Zhang, Q., Salcedo, D., Molina, L. T., Worsnop, D. R. and Molina, M. J.: Secondary organic aerosol formation from anthropogenic air pollution: Rapid and higher than expected, Geophys. Res. Lett., 33(17), L17811, 2006.

Wang, M., Shao, M., Chen, W., Yuan, B., Lu, S., Zhang, Q., Zeng, L. and Wang, Q.: A temporally and spatially resolved validation of emission inventories by measurements of ambient volatile organic compounds in Beijing, China, Atmos. Chem. Phys., 14(12), 5871–5891, 2014.

Warneke, C., McKeen, S. A., de Gouw, J. A., Goldan, P. D., Kuster, W. C., Holloway, J. S., Williams, E. J., Lerner, B. M., Parrish, D. D., Trainer, M., Fehsenfeld, F. C., Kato, S., Atlas, E. L., Baker, A. and Blake, D. R.: Determination of urban volatile organic compound emission ratios and comparison with an emissions database, J. Geophys. Res. D: Atmos., 112(D10), doi:10.1029/2006JD007930, 2007.

Woody, M. C., Baker, K. R., Hayes, P. L., Jimenez, J. L., Koo, B. and Pye, H. O. T.: Understanding sources of organic aerosol during CalNex-2010 using the CMAQ-VBS, Atmos. Chem. Phys., 16(6), 4081–4100, 2016.

Worton, D. R., Isaacman, G., Gentner, D. R., Dallmann, T. R., Chan, A. W. H., Ruehl, C., Kirchstetter, T. W., Wilson, K. R., Harley, R. A. and Goldstein, A. H.: Lubricating Oil Dominates Primary Organic Aerosol Emissions from Motor Vehicles, Environ. Sci. Technol., 48(7), 3698–3706, 2014.

Ye, P., Ding, X., Hakala, J., Hofbauer, V., Robinson, E. S. and Donahue, N. M.: Vapor wall loss of semi-volatile organic compounds in a Teflon chamber, Aerosol Sci. Technol., 50(8), 822–834, 2016.

Zhang, Q., Jimenez, J. L., Canagaratna, M. R., Allan, J. D., Coe, H., Ulbrich, I., Alfarra, M. R., Takami, A., Middlebrook, A. M., Sun, Y. L., Dzepina, K., Dunlea, E., Docherty, K., DeCarlo, P. F., Salcedo, D., Onasch, T., Jayne, J. T., Miyoshi, T., Shimono, A., Hatakeyama, S., Takegawa, N., Kondo, Y., Schneider, J., Drewnick, F., Borrmann, S., Weimer, S., Demerjian, K., Williams, P., Bower, K., Bahreini, R., Cottrell, L., Griffin, R. J., Rautiainen, J., Sun, J. Y., Zhang, Y. M. and Worsnop, D. R.: Ubiquity and dominance of oxygenated species in organic aerosols in anthropogenically-influenced Northern Hemisphere midlatitudes, Geophys. Res. Lett., 34(13),

L13801, 2007.

Zhao, B., Wang, S., Donahue, N. M., Jathar, S. H., Huang, X., Wu, W., Hao, J. and Robinson, A. L.: Quantifying the effect of organic aerosol aging and intermediate-volatility emissions on regional-scale aerosol pollution in China, Sci. Rep., 6, 28815, 2016a.

Zhao, Y., Hennigan, C. J., May, A. A., Daniel, S., Gouw, J. A. D., Gilman, J. B., Kuster, W. C. and Robinson, A. L.: Intermediate-Volatility Organic Compounds: A Large Source of Secondary Organic Aerosol, Environ. Sci. Technol, 48(23), 13743–13750, 2014.

Zhao, Y., Nguyen, N. T., Presto, A. A., Hennigan, C. J., May, A. A. and Robinson, A. L.: Intermediate Volatility Organic Compound Emissions from On-Road Gasoline Vehicles and Small Off-Road Gasoline Engines, Environ. Sci. Technol., 50(8), 4554–4563, 2016b.

Zhao, Y., Saleh, R., Saliba, G., Presto, A. A., Gordon, T. D., Drozd, G. T., Goldstein, A. H., Donahue, N. M. and Robinson, A. L.: Reducing secondary organic aerosol formation from gasoline vehicle exhaust, Proc. Natl. Acad. Sci. U. S. A., 114(27), 6984–6989, 2017.

# Anthropogenic Secondary Organic Aerosols Contribute Substantially to Air Pollution Mortality

Benjamin A. Nault[1,2,*], Duseong S. Jo[1,2], Brian C. McDonald[2,3], Pedro Campuzano-Jost[1,2], Douglas A. Day[1,2], Weiwei Hu[1,2,**], Jason C. Schroder[1,2,***], James Allan[4,5], Donald R. Blake[6], Manjula R. Canagaratna[7], Hugh Coe[5], Matthew M. Coggon[2,3], Peter F. DeCarlo[8], Glenn S. Diskin[9], Rachel Dunmore[10], Frank Flocke[11], Alan Fried[12], Jessica B. Gilman[3], Georgios Gkatzelis[2,3,****], Jacqui F. Hamilton[10], Thomas F. Hanisco[13], Patrick L. Hayes[14], Daven K. Henze[15], Alma Hodzic[11,16], James Hopkins[10,17], Min Hu[18], L. Greggory Huey[19], B. Thomas Jobson[20], William C. Kuster[3,*****], Alastair Lewis[10,17], Meng Li[2,3], Jin Liao[13,21], M. Omar Nawaz[15], Ilana B. Pollack[22], Jeffrey Peischl[2,3], Bernhard Rappenglück[23], Claire E. Reeves[24], Dirk Richter[12], James M. Roberts[3], Thomas B. Ryerson[3,******], Min Shao[25], Jacob M. Sommers[14,26], James Walega[12], Carsten Warneke[2,3], Petter Weibring[12], Glenn M. Wolfe[13,27], Dominique E. Young[5,*******], Bin Yuan[25], Qiang Zhang[28], Joost A. de Gouw[1,2], and Jose L. Jimenez[1,2,+]

1. Department of Chemistry, University of Colorado, Boulder, Boulder, CO, USA
2. Cooperative Institute for Research in Environmental Sciences, Boulder, Colorado, USA
3. Chemical Sciences Division, NOAA Earth System Research Laboratory, Boulder, CO
4. National Centre for Atmospheric Sciences, School of Earth and Environmental Sciences, University of Manchester, Manchester, UK
5. Centre of Atmospheric Science, School of Earth and Environmental Sciences, University of Manchester, Manchester, UK
6. Department of Chemistry, University of California, Irvine, Irvine, CA, USA
7. Center for Aerosol and Cloud Chemistry, Aerodyne Research Inc., Billerica, MA, USA
8. Department of Environmental Health Engineering, Johns Hopkins University, Baltimore, MD, USA
9. NASA Langley Research Center, Hampton, Virginia, USA
10. Wolfson Atmospheric Chemistry Laboratories, Department of Chemistry, University of York, York, UK
11. Atmospheric Chemistry Observations and Modeling Laboratory, National Center for Atmospheric Research, Boulder, CO, USA
12. Institute of Arctic and Alpine Research, University of Colorado, Boulder, CO, USA
13. Atmospheric Chemistry and Dynamic Laboratory, NASA Goddard Space Flight Center, Greenbelt, MD, USA
14. Department of Chemistry, Université de Montréal, Montréal, QC, Canada
15. Department of Mechanical Engineering, University of Colorado, Boulder, Boulder, CO, USA
16. Laboratoires d'Aréologie, Université de Toulouse, CNRS, UPS, Toulouse, France
17. National Centre for Atmospheric Sciences, Department of Chemistry, University of York, York, UK
18. State Key Joint Laboratory of Environmental Simulation and Pollution Control, College of Environmental Sciences and Engineering, Peking University, Beijing, China
19. School of Earth and Atmospheric Sciences, Georgia Institute of Technology, Atlanta, Georgia, USA
20. Laboratory for Atmospheric Research, Department of Civil and Environmental Engineering, Washington State University, Pullman, WA, USA
21. Universities Space Research Association, GESTAR, Columbia, MD, USA
22. Department of Atmospheric Science, Colorado State University, Fort Collins, CO, USA
23. Department of Earth and Atmospheric Science, University of Houston, Houston, TX, USA
24. Centre for Ocean and Atmospheric Sciences, School of Environmental Sciences, University of East Anglia, Norwich, UK
25. Institute for Environmental and Climate Research, Jinan University, Guangzhou, China
26. Air Quality Research Division, Environment and Climate Change Canada, Toronto, Ontario, Canada
27. Joint Center for Earth Systems Technology, University of Maryland, Baltimore County, Baltimore, MD, USA
28. Ministry of Education Key Laboratory for Earth System Modeling, Department of Earth System Science, Tsinghua University, Beijing, China

*Now at Center for Aerosol and Cloud Chemistry, Aerodyne Research Inc., Billerica, MA, USA

**Now at State Key Laboratory at Organic Geochemistry, Guangzhou Institute of Geochemistry, Chinese Academy of Sciences, Guangzhou, China

***Now at Colorado Department of Public Health and Environment, Denver, CO, USA

****Now at Forschungszentrum Juelich GmbH, IEK-8, Juelich, Germany

*****Has retired and worked on this manuscript as an unaffiliated co-author.

******Now at Scientific Aviation, Boulder, CO, USA

53 *******Now at Air Quality Research Center, University of California, Davis, CA, USA
54
55 +Corresponding author: Jose L. Jimenez (jose.jimenez@colorado.edu)
56

**Abstract**

Anthropogenic secondary organic aerosol (ASOA), formed from anthropogenic emissions of organic compounds, constitutes a substantial fraction of the mass of submicron aerosol in populated areas around the world and contributes to poor air quality and premature mortality. However, the precursor sources of ASOA are poorly understood, and there are large uncertainties in the health benefits that might accrue from reducing anthropogenic organic emissions. We show that the production of ASOA in 11 urban areas on three continents is strongly correlated with the ~~anthropogenic~~ reactivity of specific anthropogenic volatile organic compounds. The differences in ASOA production across different cities can be explained by differences in the emissions of aromatics and intermediate- and semi-volatile organic compounds, indicating the importance of controlling these ASOA precursors. With an improved modeling representation of ASOA driven by the observations, we attribute 340,000 $PM_{2.5}$ premature deaths per year to ASOA, which is over an order of magnitude higher than prior studies. A sensitivity case with a more recently proposed model for attributing mortality to $PM_{2.5}$ (the Global Exposure Mortality Model) results in up~~up~~ to 900,000 deaths. A limitation of this study is the extrapolation from cities with detailed studies and regions where detailed emission inventories are available to other~~from~~ regions ~~with detailed data to others where data is not available~~ where uncertainties in emissions are larger. In addition to further development of institutional air quality management infrastructure, c~~C~~omprehensive air quality campaigns in the countries in South and Central America, Africa, South Asia, and the Middle East are needed for further progress in this area.

## 1. Introduction

Poor air quality is one of the leading causes of premature mortality worldwide (Cohen et al., 2017; Landrigan et al., 2018). Roughly 95% of the world's population live in areas where $PM_{2.5}$ (fine particulate matter with diameter smaller than 2.5 μm) exceeds the World Health Organization's 10 μg $m^{-3}$ annual average guideline (Shaddick et al., 2018). This is especially true for urban areas, where high population density is co-located with increased emissions of $PM_{2.5}$ and its gas-phase precursors from human activities. It is estimated that $PM_{2.5}$ leads to 3 to 4 million premature deaths per year, higher than the deaths associated with other air pollutants (Cohen et al., 2017). More recent analysis using concentration-response relationships derived from studies of populations exposure to high levels of ambient $PM_{2.5}$ suggest the global premature death burden could be up to twice this value (Burnett et al., 2018).

The main method to estimate premature mortality with $PM_{2.5}$ is to use measured $PM_{2.5}$ from ground observations along with derived $PM_{2.5}$ from satellites to fill in missing ground-based observations (van Donkelaar et al. 2015; van Donkelaar et al. 2016). To go from total $PM_{2.5}$ to species-dependent and even sector-dependent associated premature mortality from $PM_{2.5}$, chemical transport models (CTMs) are used to predict the fractional contribution of species and/or sector (e.g., (van Donkelaar et al. 2015; Silva et al. 2016; Lelieveld et al. 2015; van Donkelaar et al. 2016). However, though CTMs may get total $PM_{2.5}$ or even total species, e.g., organic aerosol (OA), correct, the model may be getting the values right for the wrong reason (e.g., de Gouw and Jimenez, 2009; Woody et al., 2016; Murphy et al., 2017; Baker et al., 2018; Hodzic et al., 2020). This is especially important for OA in urban areas, where models have a longstanding issue under predicting secondary OA (SOA) with some instances of over predicting

primary OA (POA) (de Gouw and Jimenez, 2009; Dzepina et al., 2009; Hodzic et al., 2010; Woody et al., 2016; Zhao et al., 2016a; Janssen et al., 2017; Jathar et al., 2017). Further, this bias has even been observed for highly aged aerosols in remote regions (Hodzic et al., 2020). As has been found in prior studies for urban areas (e.g., Zhang et al., 2007; Kondo et al., 2008; Jimenez et al., 2009; DeCarlo et al., 2010; Hayes et al., 2013; Freney et al., 2014; Hu et al., 2016; Nault et al., 2018; Schroder et al., 2018) and highlighted here (Fig. 1), a substantial fraction of the observed submicron PM is OA, and a substantial fraction of the OA is composed of SOA (approximately a factor of 2 to 3 higher than POA). Thus, to better understand the sources and apportionment of $PM_{2.5}$ that contributes to premature mortality, CTMs must improve their prediction of SOA versus POA, as the sources of SOA precursors and POA can be different.

~~The average measured chemical composition of submicron PM ($PM_1$, which typically comprises most of $PM_{2.5}$ (Wang et al., 2015)) for various megacities, urban areas, and outflow regions around the world is shown in Fig. 1. A substantial fraction of urban $PM_1$ is organic aerosol (OA), which is composed of primary OA (POA, organic compounds emitted directly in the particle phase) and secondary OA (SOA, formed from chemical reactions of precursor organic gases). SOA is typically a factor of 2 to 3 higher than POA for these locations.~~

However, ~~U~~understanding the gas-phase precursors of photochemically-produced anthropogenic SOA (ASOA, defined as the photochemically-produced SOA formed from the photoxidation of anthropogenic volatile organic compounds (AVOC) (de Gouw et al., 2005; DeCarlo et al., 2010)) quantitatively is challenging (Hallquist et al., 2009). Note, for the rest of the paper, unless explicitly stated otherwise, ASOA refers to SOA produced from the photoxidation of AVOCs, as there are potentially other relevant paths for the production of SOA

in urban environments (e.g., (Petit et al. 2014; Kodros et al. 2020; Kodros et al. 2018; Stavroulas et al. 2019)). Though the enhancement of ASOA is largest in large cities, these precursors and production of ASOA should be important in any location impacted by anthropogenic emissions (e.g., Fig. 1). ASOA comprises a wide range of condensable products generated by numerous chemical reactions involving AVOC precursors (Hallquist et al., 2009; Hayes et al., 2015; Shrivastava et al., 2017). The number of AVOC precursors, as well as the role of "non-traditional" AVOC precursors, along with the condensable products and chemical reactions, compound to lead to differences in the observed versus predicted ASOA for various urban environments (e.g., (de Gouw and Jimenez 2009; Dzepina et al. 2009; Hodzic et al. 2010; Woody et al. 2016; Janssen et al. 2017; Jathar et al. 2017; McDonald et al. 2018)). One solution to improve the prediction in CTMs is to use a simplified model, where lumped ASOA precursors react, non-reversibly, at a given rate constant, to produce ASOA (Hodzic and Jimenez 2011; Hayes et al. 2015; Pai et al. 2020). This simplified model has been found to reproduce the observed ASOA from some urban areas (Hodzic and Jimenez 2011; Hayes et al. 2015) but issues in other urban areas (Pai et al. 2020). This may stem from the simplified model being parameterized to two urban areas (Hodzic and Jimenez 2011; Hayes et al. 2015). These inconsistencies impact the model predicted fractional contribution of ASOA to total $PM_{2.5}$ and thus the ability to understand the source attribution to $PM_{2.5}$ and premature deaths. ~~These condensable products include intermediate volatile organic compounds (IVOCS, less volatile than traditional VOCs and often not measured or considered (Robinson et al., 2007; Hayes et al., 2015)) and semi volatile organic compounds (SVOCs, less volatile than IVOC and similarly not measured or considered).~~

The main categories of gas-phase precursors that dominate ASOA have been the subject of intensive research. The debate on what dominates can in turn impact the understanding of what precursors to regulate to reduce ASOA, to improve air quality, and to reduce premature mortality associated with ASOA. Transportation-related emissions (e.g., tailpipe, evaporation, refueling) were assumed to be the major precursors of ASOA, which was supported by field studies (Parrish et al., 2009; Gentner et al., 2012; Warneke et al., 2012; Pollack et al., 2013). Yet, budget closure of observed ASOA mass concentrations could not be achieved with transportation-related VOCs (Ensberg et al., 2014). The contribution of urban-emitted biogenic precursors to SOA in urban areas is typically small. ~~, and rather, the contribution of b~~Biogenic SOA (BSOA) in urban areas ~~is~~ typically results from ~~dominated by regionally advected~~ advection of regional background concentrations rather than processing of locally emitted biogenic VOCs~~SOA background~~ (e.g., Hodzic et al., 2009, 2010a; Hayes et al., 2013; Janssen et al., 2017). BSOA is thought to dominate globally (Hallquist et al., 2009), but as shown in Fig. 1, the contribution of BSOA (1% to 20%) to urban concentrations, while often substantial, is typically smaller than that of ASOA (17% to 39%) (see Sect. S3.1~~2~~).

Many of these prior studies generally investigated AVOC with high volatility, where volatility here is defined as the saturation concentration, C*, in μg $m^{-3}$ (de Gouw et al., 2005; Volkamer et al., 2006; Dzepina et al., 2009; Freney et al., 2014; Woody et al., 2016). More recent studies have identified lower volatility compounds in transportation-related emissions (e.g., Zhao et al., 2014, 2016b; Lu et al., 2018). These compounds have been broadly identified as intermediate-volatile organic compounds (IVOCs) and semi-volatile organic compounds (SVOCs). IVOCs have a C* generally of $10^3$ to $10^6$ μg $m^{-3}$ while SVOCs have a C* generally of

1 to $10^2$ μg $m^{-3}$. Due to their lower volatility and functional groups, these classes of compounds generally form ASOA more efficiently than traditional, higher volatile AVOCs; however, S/IVOCs have also been more difficult to measure (e.g., Zhao et al., 2014; Pagonis et al., 2017; Deming et al., 2018). IVOCs generally have been the more difficult of the two classes to measure and identify as these compounds cannot be collected onto filters to be sampled off-line (Lu et al., 2018) and generally show up as unresolved complex mixture for in-situ measurements using gas-chromatography (GC) (Zhao et al., 2014). SVOCs, on the other hand, can be more readily collected onto filters and sampled off-line due to their lower volatility (Lu et al., 2018). Another potential issue has been an under-estimation of the S/IVOC aerosol production, as well as an under-estimation in the contribution of photochemically produced S/IVOC from photooxidized "traditional" VOCs, due to partitioning of these low volatile compounds to chamber walls and tubing (Krechmer et al., 2016; Ye et al., 2016; Liu et al., 2019). Accounting for this under-estimation increases the predicted ASOA (Ma et al. 2017). The inclusion of these classes of compounds have led to improvement in some urban SOA budget closure; however, many studies still have indicated a general short-fall in ASOA budget even when including these compounds from transportation-related emissions. (Dzepina et al., 2009; Tsimpidi et al., 2010; Hayes et al., 2015; Cappa et al., 2016; Ma et al., 2017; McDonald et al., 2018).

Recent studies have indicated that emissions from volatile chemical products (VCPs), defined as pesticides, coatings, inks, adhesives, personal care products, and cleaning agents (McDonald et al., 2018), as well as cooking emissions (Hayes et al., 2015), asphalt emissions (Khare et al., 2020), and solid fuel emissions from residential wood burning and/or cookstoves (e.g., Hu et al., 2013, 2020; Schroder et al., 2018), are important. While total amounts of ASOA

187 precursors released in cities have dramatically declined (largely due to three-way catalytic
188 converters in cars (Warneke et al., 2012; Pollack et al., 2013; Zhao et al., 2017; Khare and
189 Gentner, 2018)), VCPs have not declined as quickly (Khare and Gentner, 2018; McDonald et al.,
190 2018). Besides a few cities in the US (Coggon et al., 2018; Khare and Gentner, 2018; McDonald
191 et al., 2018), extensive VCP emission quantification has not yet been published.

192 Due to the uncertainty on the emissions of ASOA precursors and on the amount of
193 ASOA formed from them, the number of premature deaths associated with urban organic
194 emissions is largely unknown. Since numerous studies have shown the importance of VCPs and
195 other non-traditional VOC emission sources, efforts have been made to try to improve the
196 representation and emissions of VCPs (Seltzer et al. 2020), which can reduce the uncertainty in
197 ASOA precursors and the associated premature deaths estimations. Currently, most studies have
198 not included ASOA realistically (e.g., Lelieveld et al., 2015; Silva et al., 2016; Ridley et al.,
199 2018) in source apportionment calculations of the premature deaths associated with long-term
200 exposure of $PM_{2.5}$. These models represented total OA as non-volatile POA and "traditional"
201 ASOA precursors (transportation-based VOCs), which largely under-predict ASOA (Ensberg et
202 al., 2014; Hayes et al., 2015; Nault et al., 2018; Schroder et al., 2018) while over-redicting POA
203 (e.g., (Hodzic et al. 2010; Zhao et al. 2016; Jathar et al. 2017). ~~given that the~~ This does not
204 reflect the current understanding ~~is~~ that POA is volatile and contributes to ASOA mass
205 concentration (e.g., Grieshop et al., 2009; Lu et al., 2018). Though the models are estimating
206 total OA correctly (Ridley et al. 2018; Hodzic et al. 2020; Pai et al. 2020), the attribution of
207 premature deaths to POA instead of SOA formed from "traditional" and "non-traditional"
208 sources, including IVOCs from both sources, could lead to regulations that may not target the

emissions that would reduce OA in urban areas. As $PM_1$ and SOA mass are highest in urban areas (Fig. 1), also shown in Jimenez et al. (2009), it is necessary to quantify the amount and identify the sources of ASOA to target future emission standards that will optimally improve air quality and the associated health impacts. As these emissions are from human activities, they will contribute to SOA mass outside urban regions and to potential health impacts outside urban regions as well. Though there are potentially other important exposure pathways to PM that may increase premature mortality, such as exposure to solid-fuel emissions indoors (e.g., Kodros et al., 2018), the focus of this paper is on exposure to outdoor ASOA and its associated impacts to premature mortality.

Here, we investigate the factors that control ASOA using 11 major urban, including megacities, field studies (Fig. 1 and Table 1). The empirical relationships and numerical models are then used to quantify the attribution of premature mortality to ASOA around the world, using the observations to improve the modeled representation of ASOA. The results provide insight into the importance of ASOA to global premature mortality due to $PM_{2.5}$ and further understanding of the~~understanding the~~ precursors and sources of ASOA in urban regions.

## 2. Methods

Here, we introduce the ambient observations from various campaigns used to constrain ASOA production (Sect. 2.1), description of the simplified model used in CTMs to better predict ASOA (Sect. 2.2), and description of how premature mortality was estimated for this study (Sect. 2.3). In the SI, the following can be found: description of the emissions used to calculate the ASOA budget for five different locations (Sect. S1), description of how the ASOA budget was

calculated for the five different locations (Sect. S2), description of the CTM (GEOS-Chem) used in this study (Sect. S3 - S4), and error analysis for the observations (Sect. S5).

### 2.1 Ambient Observations

For values not previously reported in the literature (Table S4), observations taken between 11:00 – 16:00 local time were used to determine the slopes of SOA versus formaldehyde (HCHO) (Fig. S12), peroxy acetyl nitrate (PAN) (Fig. S23), and $O_x$ ($O_x = O_3 + NO_2$) (Fig. S34). For CalNex, there was an approximate 48% difference between the two HCHO measurements (Fig. S41). Therefore, the average between the two measurements were used in this study, similar to what has been done in other studies for other gas-phase species (Bertram et al., 2007). All linear fits, unless otherwise noted, use the orthogonal distance regression fitting method (ODR).

For values in Table S4 through Table S8 not previously reported in the literature, the following procedure was applied to determine the emissions ratios, similar to the methods of Nault et al. (2018). An OH exposure ($OH_{exp} = [OH] \times \Delta t$), which is also the photochemical age (PA), was estimated by using the ratio of $NO_x/NO_y$ (Eq. 1) or the ratio of m+p-xylene/ethylbenzene (Eq. 2). For the m+p-xylene/ethylbenzene, the emission ratio (Table S5) was determined by determining the average ratio during minimal photochemistry, similar to prior studies (de Gouw et al., 2017). This was done for only one study, TexAQS 2000. This method could be applied in that case as it was a ground campaign that operated both day and night; therefore, a ratio at night could be determined when there was minimal loss of both VOCs. The average emission ratio for the other VOCs was determined using Eq. 3 after the

$OH_{exp}$ was calculated in Eq. 1 or Eq. 2. The rate constants used for determining $OH_{exp}$ and emission ratios are found in Table S121.

$$OH_{exp} = [\mathrm{OH}] \times t = \ln\left(\frac{\left(\frac{[\mathrm{NO_x}]}{[\mathrm{NO_y}]}\right)}{k_{\mathrm{OH+NO_2}}}\right) \quad \text{Eq. 1}$$

$$OH_{exp} = [\mathrm{OH}] \times t = -\frac{1}{k_{m+p-xylene} - k_{ethylbenzene}} \times \ln\left(\frac{[\mathrm{m+p-xylene}]_t}{[ethylbenzene]_t} - \frac{[m+p-xylene]_0}{[ethylbenzene]_0}\right) \quad \text{Eq. 2}$$

$$\frac{[\mathrm{VOC(i)}]}{[\mathrm{CO}]}(0) = -\frac{[\mathrm{VOC(i)}]}{[\mathrm{CO}]}(t) \times \left(1 - \frac{1}{exp\left(-k_i \times [\mathrm{OH}]_{exp} \times t\right)}\right) \times k_i + \frac{[\mathrm{VOC(i)}]}{[\mathrm{CO}]}(t) \times k_i \quad \text{Eq. 3}$$

## 2.2 Updates to the SIMPLE Model

With the combination of the new dataset, which expands across urban areas on three continents, the SIMPLE parameterization for ASOA (Hodzic and Jimenez, 2011) is updated in the standard GEOS-Chem model to reproduce observed ASOA in Fig. 2a. The parameterization operates as represented by Eq. 4.

$$\mathrm{Emissions} \rightarrow \mathrm{SOAP} \xrightarrow{k \times [\mathrm{OH}]} \mathrm{ASOA} \quad \text{Eq. 4}$$

SOAP represents the lumped precursors of ASOA, k is the reaction rate coefficient with OH ($1.25\times10^{-11}$ $cm^3$ $molecules^{-1}$ $s^{-1}$), and [OH] is the OH concentration in molecules $cm^{-3}$. This rate constant is also consistent with observed ASOA formation time scale of ~1 day that has been observed across numerous studies (e.g., de Gouw et al., 2005; DeCarlo et al., 2010; Hayes et al., 2013; Nault et al., 2018; Schroder et al., 2018).

SOAP emissions were calculated based on the relationship between ΔSOA/ΔCO and $R_{aromatics}$/ΔCO in Fig. 2a. First, we calculated $R_{aromatics}$/ΔCO (Eq. 5) for each grid cell and time step as follows:

$$\frac{R_{aromatics}}{\Delta CO} = \frac{E_B \times k_B + E_T \times k_T + E_X \times k_X}{E_{CO}} \quad \text{Eq. 5}$$

Where E and k stand for the emission rate and reaction rate coefficient with OH, respectively, for benzene (B), toluene (T), and xylenes (X). Ethylbenzene was not included in this calculation because its emission was not available in HTAPv2 emission inventory. However, ethylbenzene contributed a minor fraction of the mixing ratio (~ 7%, Table S5) and reactivity (~6%) of the total BTEX across the campaigns. Reaction rate constants used in this study were $1.22\times10^{-12}$, $5.63\times10^{-12}$, and $1.72\times10^{-11}$ $cm^3$ $molec.^{-1}$ $s^{-1}$ for benzene, toluene, and xylene, respectively (Atkinson and Arey, 2003; Atkinson et al., 2006). The $R_{aromatics}$/ΔCO allows a dynamic calculation of the E(VOC)/E(CO) = SOA/ΔCO. Hodzic and Jimenez (2011) and Hayes et al. (2015) used a constant value of 0.069 g $g^{-1}$, which worked well for the two cities investigated, but not for the expanded dataset studied here. Thus, both the aromatic emissions and CO emissions are used in this study to better represent the variable emissions of ASOA precursors (Fig. S5).

Second, $E_{SOAP}/E_{CO}$ can be obtained from the result of Eq. 6, using slope and intercept in Fig. 2a, with a correction factor (F) to consider additional SOA production after 0.5 PA equivalent days, since Fig. 2a shows the comparison at 0.5 PA equivalent days.

$$\frac{E_{SOAP}}{E_{CO}} = \left( Slope \times \frac{R_{Aromatics}}{\Delta CO} + Intercept \right) \times F \quad \text{Eq. 6}$$

Where slope is 24.8 and intercept is –1.7 from Fig. 2a. F (Eq. 7) can be calculated as follows:

$$F = \frac{ASOA_{t=\infty}}{ASOA_{t=0.5d}} = \frac{SOAP_{t=0}}{SOAP_{t=0} \times (1 - exp(-k \times \Delta t \times [OH]))}, \Delta t = 43200\ s \quad \text{Eq. 7}$$

F was calculated as 1.8 by using [OH] = $1.5 \times 10^6$ molecules $cm^{-3}$, which was used in the definition of 0.5 PA equivalent days for Fig. 2a.

Finally, $E_{SOAP}$ can be computed by multiplying CO emissions ($E_{CO}$) for every grid point and time step in GEOS-Chem by the $E_{SOAP}/E_{CO}$ ratio.

¶

**2.2 Error Analysis of Observations**¶

The errors that will be discussed here are in reference to Fig. 5 and Fig. 6 and Table S4 either come from the 1σ uncertainty in the slopes (the SOA versus $O_x$, HCHO, or PAN values) or propagation of uncertainty in observations. For SOA, we estimate the 1σ uncertainty of ~15%, which is lower than the typical 1σ uncertainty of the AMS (Bahreini et al., 2009) due to the careful calibrations and excellent intercomparisons in the various campaigns (see Table 1 for references for the AMS comparisons). For ΔCO, the largest uncertainty is associated with the CO background (Hayes et al., 2013; Nault et al., 2018), and is estimated to be ~10% at 0.5 photochemical equivalent days (Hayes et al., 2013). The uncertainty in the emission ratios is ~10% (Wang et al., 2014; de Gouw et al., 2017); though, it may be higher for the values calculated here (see above) due to the uncertainty in CO background, rate constants, and photochemical age. Therefore, for Fig. 5a, the uncertainty in the y-values is 18% and the uncertainty in the x-values is 10%. For Fig. 6, the uncertainty in the measurement is 21%.¶

Another potential source of uncertainty may stem from the fit of the data in Fig. 5a, as the data point from Seoul (KORUS-AQ) could be impacting the fit due to the difference in its value compared to the other locations. A sensitivity analysis, where one study was removed and a new fit was derived, was conducted to determine the impact of any one study on the fit reported in Fig. 5a (see Table S10). We find that though removing the Seoul data point increases the slope, the value is still within the uncertainty and statistically significant at the 95% confidence interval. Thus, the data from Seoul does not change the results and conclusions reported in this study.¶

**2.3 Emission Inventories for Various Urban Areas around the World**¶

All BTEX (benzene, toluene, ethylbenze, and xylenes) and non-BTEX aromatic emissions are shown in Table S5 (BTEX) or Table S8 (non-BTEX aromatics) and are described above. The emission ratios are derived from ambient measurements utilizing photochemical aging techniques (Nault et al., 2018).¶

Details of the emission inventories for cities in the US, for Beijing, and for London/UK used here to estimate the IVOC:BTEX emission ratio (Fig. 2) and thus the IVOC emissions can be found in SI Sect. 1 through 3. Briefly, emissions for the US are based on McDonald et al. (2018), for China on the Multi-resolution Emission Inventory for China (MEIC) (Zhang et al., 2009; Zheng et al., 2014, 2018; Liu et al., 2015; Li et al., 2017, 2019), and for the UK on the National Atmospheric Emissions Inventory (NAEI) (EMEP/EEA, 2016). The IVOC:BTEX emission ratio from inventories are multiplied with the observed BTEX measured in urban air to estimate IVOCs emitted in each region (Table S5), including North America, Europe, and Asia.

This ensures IVOC emissions used in our calculations properly reflect differences in mixtures of emission sources (e.g., mobile sources versus VCPs) that vary by continent for each field campaign. Additionally, we rely on inventories for estimating atmospheric abundances of IVOCs because it has been challenging to measure the full range of IVOC precursors that are emitted into urban air (Zhao et al., 2014, 2017; Lu et al., 2018). In particular, many of the IVOCs emitted from VCPs are oxygenated, which are challenging to measure using traditional gas chromatography-mass spectrometry (GC-MS) techniques. Oxygenated IVOCs may not elute completely through a non-polar column, and are likely underestimated (Zhao et al., 2014). The bottom-up IVOC:BTEX ratios for the US, Beijing, and UK are described in greater detail in SI Sect. S1 through S3. IVOC emissions are classified based on their vapor pressure (effective saturation concentration: $0.3 < C^* < 3 \times 10^6$ μg $m^{-3}$), with the vapor pressure estimated by the SIMPOL.1 model (Pankow and Asher, 2008). Unspeciated mass has been suggested as important SOA precursors from gasoline and diesel engines, and parameterized by n-tridecane and n-pentadecane, respectively (Jathar et al., 2014). For VCPs, the volatility distribution of VOCs is in-between that of gasoline and diesel fuel. Therefore, n-tetradecane was suggested as a surrogate for unspeciated mass of VCPs by McDonald et al. (2018).¶

Similar to IVOCs, the ability to measure the full range of SVOCs emitted into urban air is challenging. Therefore, we estimate SVOC emission ratios relative to POA mass concentrations (Table S9), as described by Ma et al. (2017). For the hydrocarbon-like portion, we used the volatility distribution from Worton et al. (2014) to estimate SVOC, as this is associated with fossil fuel emissions from transportation (Zhang et al., 2005). For the other POA, we used the

volatility distribution from Robinson et al. (2007), as this POA is typically cooking primary aerosol.¶

Fig. 3 shows the calculated emission ratio versus saturation concentration (c*) for the cities with emission inventories. The saturation concentration for SVOC was determined as part of the estimation procedure discussed above. For IVOC, the emission ratios for the different sources (gasoline, diesel, other fossil fuel sources, and VCP emissions) were split into the volatility bins, as in McDonald et al. (2018). Finally, for BTEX and non-BTEX aromatics, and other VOC emission ratios (see Fig. 3 for references for the other VOC emission ratios), CRC (Rumble, 2019) or SIMPOL.1 (Pankow and Asher, 2008) (for estimating vapor pressures not in CRC) was used to estimate the saturation concentrations.¶

**2.4 ASOA Budget Analysis of Ambient Observations**¶

To calculate the ASOA budget, we used the observed BTEX (Table S5) and non-BTEX aromatic (Table S8) emission ratios, the emission inventories for IVOC (see above), and estimated SVOCs from the primary OA emissions (see above). The methods to calculate ASOA from emissions have been described in detail elsewhere (Hayes et al., 2015; Ma et al., 2017; Schroder et al., 2018), and are briefly described here. All calculations described were conducted with the KinSim v4.02 chemical kinetics simulator (Peng and Jimenez, 2019) within Igor Pro 7 (Lake Oswego, Oregon), and are summarized in Fig. S5. A typical average particle diameter for urban environments of ~200 nm (Seinfeld and Pandis, 2006) is used to estimate the condensational sink term for the partitioning of gas-to-particle, although condensation is always fast compared to the experiment timescales. Further, we assume an average 250 g $mol^{-1}$ molar

mass for OA and an average SOA density of 1.4 g $cm^{-3}$ (Vaden et al., 2011; Kuwata et al., 2012). Finally, all models are initialized with the campaign specific OA background (typically ~2 μg $sm^{-3}$) and POA (Table S9) for partitioning of gases to the particle phase, and ran at the average temperature for the campaign.¶

For the modeled VOCs (BTEX and non-BTEX aromatics), each species undergoes temperature-dependent OH oxidation (Table S11), forming four SVOCs that partition between gas- and particle-phase, using updated SOA yields that account for wall loss (Ma et al., 2017). For IVOCs, the emission weighted SOA yields and rate constants from the "Zhao" option (Zhao et al., 2014) of Ma et al. (2017) are used, and the products are apportioned into three SVOC bins and one low-volatility organic compound (LVOC) bin (Fig. S5). Finally, SVOCs undergo photooxidation at a rate of $4\times10^{-11}$ $cm^3$ $molecules^{-1}$ $s^{-1}$ (Dzepina et al., 2009; Hodzic et al., 2010b; Tsimpidi et al., 2010; Hodzic and Jimenez, 2011; Hayes et al., 2015; Ma et al., 2017; Schroder et al., 2018), producing one product per oxidation step, with yields from Robinson et al. (2007) for cooking and other SVOCs and yields from Worton et al. (2014) for fossil fuel related SVOCs, as recommended by Ma et al. (2017). The products from SVOC and IVOC oxidation are allowed to further oxidize, as highlighted in Fig. S5 and described in prior studies (Hayes et al., 2015; Ma et al., 2017; Schroder et al., 2018). Generally, each product reacts at a rate of $4\times10^{-11}$ $cm^3$ $molecules^{-1}$ $s^{-1}$ to produce some product at one volatility bin lower, adding one oxygen to the compound for each oxidation (Dzepina et al., 2009; Tsimpidi et al., 2010; Hodzic and Jimenez, 2011; Hayes et al., 2015; Ma et al., 2017; Schroder et al., 2018). An update includes fragmentation for a fraction of the molecules that are oxidized, as described in Schroder et al. (2018) and Koo et al. (2014). As shown in Fig. S5, fragmentation of the compound occurs as it is

oxidized and goes down one volatility bin. For further oxidation of SVOCs from the oxidation of primary IVOCs, one oxygen is added and 0.25 carbon is removed per step, leading to an increase in mass of 1.03 (instead of 1.07) per oxidation step (Koo et al., 2014; Schroder et al., 2018). For further oxidation of products from primary SVOC emissions, one oxygen is added and 0.5 carbon is removed per step, leading to an increase in mass of 0.99 (instead of 1.07) per oxidation step (Koo et al., 2014; Nault et al., 2018).¶

**2.5 GEOS-Chem Modeling¶**

The model used in this study, for ASOA apportionment (Fig. 1), for apportionment of ASOA to total PM2.5 for premature mortality calculations (Worldwide Premature Deaths Due to ASOA), and for sensitivity analysis for ASOA production and emissions on premature mortality calculations, is the GEOS-Chem v12.0.0 global chemical transport model (Bey et al., 2001; The International GEOS-Chem User Community, 2018) to calculate global concentrations of $PM_{2.5}$ and ASOA at 2°×2.5° horizontal resolution. Goddard Earth Observing System – Forward Processing (GEOS-FP) assimilated data from the NASA Global Modeling and Assimilation Office (GMAO) were used for input meteorological fields. The model was run for 2013 to 2018 to take into account interannual variability of meteorological impacts onto $PM_{2.5}$ (therefore, averaging $PM_{2.5}$ over variations in meteorology). However, the HTAPv2 emission inventory, which was used for anthropogenic emissions (Janssens-Maenhout et al., 2015), was kept constant for the 5 years. GEOS-Chem simulates gas and aerosol chemistry with ~700 chemical reactions. GEOS-Chem calculates the following $PM_{2.5}$ species: sulfate, ammonium, nitrate (Park et al., 2006); black carbon and POA (Park et al., 2005); SOA (Pye and Seinfeld, 2010; Marais et al.,

2016); sea salt (accumulation mode only (Jaeglé et al., 2011)); and, dust (Duncan Fairlie et al., 2007).¶

¶

**2.5.1 Biogenic SOA** ¶

For monoterpene and sesquiterpene SOAs, we used the default complex SOA scheme (without semi-volatile POA) using the two-product model framework (Pye and Seinfeld, 2010). This scheme calculates initial oxidation of VOCs with OH, $O_3$, and $NO_3$, and resulting products are assigned to four different gas-phase semi-volatile species (TSOA0–3) based on volatilities ($c^*$ = 0.1, 1, 10, 100 μg $m^{-3}$). Aerosol and gas species fractions are calculated online using the partitioning theory, and all are removed by dry and wet deposition processes. ¶

For isoprene SOA, we used the explicit isoprene chemistry developed by Marais et al. (2016). All the isoprene-derived gas-phase products, including isoprene peroxy radical, ISOPOOH, IEPOX, glyoxal, and methylglyoxal, are explicitly simulated. Irreversible heterogeneous uptake of precursors to aqueous aerosols are further calculated using online aerosol pH and surface area. ¶

GEOS-Chem was used to estimate the relative fractions of the measured SOA in our studies between anthropogenic and biogenic (isoprene and monoterpene) sources (Fig. 1). Extensive research has been conducted to evaluate and improve the models performance in predicting BSOA, as summarized in Table S3. Though these evaluations mainly occurred in the southeast US, a recent study has also included more global observations to compare with GEOS-Chem (Pai et al., 2020). Generally, GEOS-Chem appears to overestimate biogenically derived SOA; however, the model predicted SOA is typically within the uncertainty of the AMS

(Table S3). The overestimation, though, would suggest that the fraction of urban SOA may be under-predicted by this method, whereas the BSOA may be over-predicted. Therefore, in urban regions, the amount of SOA from biogenic sources may be lower, especially after the rapid SOA enhancements (within 12 to 24 equivalent photochemical hours that have been observed around the world (Nault et al., 2018)). Typically the BSOA is present as a regional background and subtracted for the analyses used in this work, which focus on strong urban plumes on top of that background (Hayes et al., 2013, 2015). ¶

¶

**2.5.2 Default GEOS-Chem Sensitivity to ASOA Simulations**¶

For the sensitivity calculation using the "traditional" ASOA precursors, we used the two-product model framework (Pye and Seinfeld, 2010). Benzene, toluene, and xylene are oxidized with OH and converted to peroxy radicals. These peroxy radicals react with $HO_2$ or NO, resulting in non-volatile ASOA ($HO_2$ pathway, ASOAN species in GEOS-Chem) or semi-volatile ASOA tracers (NO pathway, ASOA1-3 in GEOS-Chem). As is the case for monoterpene and sesquiterpene SOA above, GEOS-Chem calculates online partitioning and dry/wet deposition processes for semi-volatile ASOA tracers. Other conditions including mortality calculation are kept the same as the base simulation above.¶

## 2.36 Estimation of Premature Mortality Attribution

Premature deaths were calculated for five disease categories: ischemic heart disease (IHD), stroke, chronic obstructive pulmonary disease (COPD), acute lower respiratory illness

(ALRI), and lung cancer (LC). We calculated premature mortality for the population aged more than 30 years, using Eq. 84.

$$Premature\ Death = Pop \times y_0 \times \frac{RR - 1}{RR} \quad \text{Eq. 84}$$

Mortality rate, $y_0$, varies according to the particular disease category and geographic region, which is available from Global Burden of Disease (GBD) Study 2015 database (IHME, 2016). Population (Pop) was obtained from Columbia University Center for International Earth Science Information Network (CIESIN) for 2010 (CIESIN, 2017). Relative risk, RR, can be calculated as shown in Eq. 95.

$$RR = 1 + \alpha \times \left(1 - exp\left(\beta \times \left(PM_{2.5} - PM_{2.5,Threshold}\right)^{\rho}\right)\right) \quad \text{Eq. 95}$$

α, β, and ρ values depend on disease category and are calculated from Burnett et al. (2014) (see Table S142 and associated file). If the $PM_{2.5}$ concentrations are below the $PM_{2.5}$ threshold value (Table S142), premature deaths were computed as zero. However, there could be some health impacts at concentrations below the $PM_{2.5}$ threshold values (Krewski et al., 2009); following the methods of the GBD studies, these can be viewed as lower bounds on estimates of premature deaths.

We performed an additional sensitivity analysis using the Global Exposure Mortality Model (GEMM) (Burnett et al., 2018). For the GEMM analysis, we also used age stratified population data from GWPv3. Premature death is calculated the same as shown in Eq. 84; however, the relative risk differs. For the GEMM model, the relative risk can be calculated as shown in Eq. 106.

$$RR = exp(\theta \times \lambda) \text{ with } \lambda = \frac{\log\left(1 + \frac{z}{\alpha}\right)}{\left(1 + \exp\left(\frac{(\hat{\mu} - z)}{\pi}\right)\right)} \quad \text{Eq. 106}$$

Here $z$ = max(0,$PM_{2.5}$-$PM_{2.5,Threshold}$); θ, π, $\hat{\mu}$, α, and $PM_{2.5,Threshold}$ depends on disease category and are from Burnett et al. (2018). Similar to the Eq. 95, if the concentrations are below the threshold (2.4 μg $m^{-3}$, Burnett et al. (2018)), then premature deaths are computed as zero; however, the GEMM has a lower threshold than the GBD method.

For GBD, we do not consider age-specific mortality rates or risks. For GEMM, we calculate age-specific health impacts with age-specific parameters in the exposure response function (Table S153). We combine the age-specific results of the exposure-response function with age distributed population data from GPW (CIESIN, 2017) and a national mortality rate across all ages to assess age-specific mortality.

We calculated total premature deaths using annual average total $PM_{2.5}$ concentrations derived from satellite-based estimates at the resolution of 0.1°×0.1° from van Donkelaar et al. (2016) . Application of the remote-sensing based $PM_{2.5}$ at the 0.1°×0.1° resolution rather than direct use of the GEOS-Chem model concentrations at the 2°×2.5° resolution helps reduce uncertainties in the quantification of $PM_{2.5}$ exposure inherent in coarser estimates (Punger and West, 2013). We also calculated deaths by subtracting from this amount the total annual average ASOA concentrations derived from GEOS-Chem (Fig. S119). To reduce uncertainties related to spatial gradients and total concentration magnitudes in our GEOS-Chem simulations of $PM_{2.5}$, our modeled ASOA was calculated as the fraction of ASOA to total $PM_{2.5}$ in GEOS-Chem, multiplied by the satellite-based PM2.5 concentrations (Eq. 117).

$$ASOA_{sat} = (ASOA_{mod}/PM_{2.5,mod}) \times PM_{2.5,sat}$$

Eq. 11~~7~~

Finally, this process for estimating $PM_{2.5}$ health impacts considers only $PM_{2.5}$ mass concentration and does not distinguish toxicity by composition, consistent with the current US EPA position expressed in Sacks et al. (2019).

## 3. Observations of ASOA Production across Three Continents

### 3.1 Observational Constraints of ASOA Production across Three Continents

Measurements during intensive field campaigns in large urban areas better constrain concentrations and atmospheric formation of ASOA because the scale of ASOA enhancement is large compared to SOA from a regional~~from regional~~ background. Generally, ASOA increased with the amount of urban precursor VOCs and with atmospheric PA (de Gouw et al., 2005; de Gouw and Jimenez, 2009; DeCarlo et al., 2010; Hayes et al., 2013; Nault et al., 2018; Schroder et al., 2018; Shah et al., 2018). In addition, ASOA correlates strongly with gas-phase secondary photochemical species, including $O_x$, HCHO, and PAN (Herndon et al., 2008; Wood et al., 2010; Hayes et al., 2013; Zhang et al., 2015; Nault et al., 2018; Liao et al., 2019) (Table S4; Fig. S1~~2~~ to Fig. S3~~4~~), which are indicators of photochemical processing of emissions.

However, as initially discussed by Nault et al. (2018) and shown in Fig. 3~~4~~~~,~~ there is large variability in these various metrics across the urban areas evaluated here. To the best of the authors' knowledge, this variability has not been explored and its physical meaning has not been interpreted. As shown in Fig. 3~~4~~, though, the trends in ΔSOA/ΔCO are similar to the trends in the slopes of SOA versus $O_x$, PAN, or HCHO. For example, Seoul is the highest for nearly all

metrics, and is approximately a factor of 6 higher than the urban area, Houston, that generally showed the lowest photochemical metrics. This suggests that the variability is related to a physical factor, including emissions and chemistry.

The VOC concentration, together with how quickly the emitted VOCs react ($\Sigma k_i \times [VOC]_i$, i.e., the hydroxyl radical, or OH, reactivity of VOCs), where k is the OH rate coefficient for each VOC, are a determining parameter for ASOA formation over urban spatial scales (Eq. 128). ASOA formation is normalized here to the excess CO mixing ratio (ΔCO) to account for the effects of meteorology, dilution, and non-urban background levels, and allow for easier comparison between different studies:

$$\frac{\Delta \mathrm{ASOA}}{\Delta \mathrm{CO}} \propto [\mathrm{OH}] \times \Delta t \times \left( \sum_i k_i \times \left[ \frac{\mathrm{VOC}}{\mathrm{CO}} \right]_i \times \mathrm{Y_i} \right)$$

Eq. 128

where Y is the aerosol yield for each compound (mass of SOA formed per unit mass of precursor reacted), and [OH]×Δt is the PA.

BTEX are one group of known ASOA precursors (Gentner et al., 2012; Hayes et al., 2013), and their emission ratio (to CO) was determined for all campaigns (Table S5). BTEX can thus provide insight into ASOA production. Fig. 25a shows that the variation in ASOA (at PA = 0.5 equivalent days) is highly correlated with the emission reactivity ratio of BTEX ($R_{BTEX}$, $\sum_i [VOC/CO]_i$) across all the studies. However, BTEX alone cannot account for much of the ASOA formation (see budget closure discussion below), and instead, BTEX may be better thought of as both partial contributors and also as indicators for the co-emission of other (unmeasured) organic precursors that are also efficient at forming ASOA.

$O_x$, PAN, and HCHO are produced from the oxidation of a much wider set of VOC precursors (including small alkenes, which do not appreciably produce SOA when oxidized). These alkenes have similar reaction rate constants with OH as the most reactive BTEX compounds (Table S12~~1~~); however, their emissions and concentration can be higher than BTEX (Table S7). Thus, alkenes would dominate $R_{Total}$, leading to $O_x$, HCHO, and PAN being produced more rapidly than ASOA (Fig. 2~~5~~b–d). When $R_{BTEX}$ becomes more important for $R_{Total}$, the emitted VOCs are more efficient in producing ASOA. Thus, the ratio of ASOA to gas-phase photochemical products shows a strong correlation with $R_{BTEX}/R_{Total}$ (Fig. 2~~5~~b–d).

An important aspect of this study is that most of these observations occurred during spring and summer, when solid fuel emissions are expected to be lower (e.g., Chafe et al., 2015; Lam et al., 2017; Hu et al., 2020). Further, the most important observations used here are during the afternoon, investigating specifically the photochemically produced ASOA. These results here might partially miss any ASOA produced through nighttime aqueous chemistry or oxidation by nitrate radical (Kodros et al., 2020). However, two of the studies included in our analysis, Chinese Outflow (CAPTAIN, 2011) and New York City (WINTER, 2015), occurred in late winter/early spring, when solid fuel emissions were important (Hu et al., 2013; Schroder et al., 2018). We find that these observations lie within the uncertainty in the slope between ASOA and $R_{BTEX}$ (Fig. 2a). Their photochemically produced ASOA observed under strong impact from solid fuel emissions shows similar behavior as the ASOA observed during spring and summer time. Thus, given the limited datasets currently available, photochemically produced ASOA is expected to follow the relationship shown in Fig. 2a and is expected to also follow this relationship for regions impacted by solid fuel burning. Future comprehensive studies in regions

strongly impacted by solid fuel burning are needed to further investigate photochemical ASOA production under those conditions.

### 3.2 Budget Closure of ASOA for 4 Urban Areas on 3 Continents Indicates Reasonable Understanding of ASOA Sources

To investigate the correlation between ASOA and $R_{BTEX}$, a box model using the emission ratios from BTEX (Table S5), other aromatics (Table S8), IVOCs (Sect. S1), and SVOCs (Sect. S1) was run for five urban areas: New York City, 2002, Los Angeles, Beijing, London, and New York City, 2015 (see Sect. S1 and S3 for more information). The differences in the results shown in Fig. 4 are due to differences in the emissions for each city. We show that BTEX alone cannot explain the observed ASOA budget for urban areas around the world. Fig. ~~4~~6a shows that approximately 25±6% of the observed ASOA originates from the photooxidation of BTEX. ~~Therefore, other precursors must account for most of the ASOA produced.~~ BTEX only explaining 25% of the observed ASOA is similar to prior studies that have done budget analysis of precursor gases and observed SOA (e.g., Dzepina et al., 2009; Ensberg et al., 2014; Hayes et al., 2015; Ma et al., 2017; Nault et al., 2018). Therefore, other precursors must account for most of the ASOA produced.

Because alkanes, alkenes, and oxygenated compounds with carbon numbers less than 6 are not significant ASOA precursors, we focus on emissions and sources of BTEX, other mono-aromatics, IVOCs, and SVOCs. These three classes of VOCs, aromatics, IVOCs, and SVOCs, have been suggested to be significant ASOA precursors in urban atmospheres (Robinson et al., 2007; Hayes et al., 2015; Ma et al., 2017; McDonald et al., 2018; Nault et al.,

593 2018; Schroder et al., 2018; Shah et al., 2018), originating from both fossil fuel and VCP
594 emissions.

595 Using the best available emission inventories from cities on three continents
596 (EMEP/EEA, 2016; McDonald et al., 2018; Li et al., 2019) and observations, we quantify the
597 emissions of BTEX, other mono-aromatics, IVOCs, and SVOCs for both fossil fuel (e.g.,
598 gasoline, diesel, kerosene, etc.), VCPs (e.g., coatings, inks, adhesives, personal care products,
599 and cleaning agents), and cooking sources (Fig. 52 ~~and Fig. 3~~). This builds off the work of
600 McDonald et al. (2018) for urban regions on three different continents.

601 Note, the emissions investigated here ignore any oxygenated VOC emissions not
602 associated with IVOCs and SVOCs due to the challenge in estimating the emission ratios for
603 these compounds (de Gouw et al. 2018). Further, SVOC emission ratios are estimated from the
604 average POA observed by the AMS during the specific campaign and scaled by profiles in
605 literature for a given average temperature and average OA (Robinson et al., 2007; Worton et al.,
606 2014; Lu et al., 2018). As most of the campaigns had an average OA between 1 and 10 μg $m^{-3}$
607 and temperature of ~298 K, this led to the majority of the estimated emitted SVOC gases in the
608 highest SVOC bin. However, as discussed later, this does not lead to SVOCs dominating the
609 predicted ASOA due to taking into account the fragmentation and overall yield from the
610 photooxidation of SVOC to ASOA.

611 Combining these inventories and observations for the various locations provide the
612 following insights about the potential ASOA precursors not easily measured or quantified in
613 urban environments (e.g., Zhao et al., 2014; Lu et al., 2018): (1) aromatics from fossil fuel
614 accounts for 14-40% (mean 22%) of the total BTEX and IVOC emissions for the five urban

areas investigated in-depth (Fig. 52), agreeing with prior studies that have shown that the observed ASOA cannot be reconciled by the observations or emission inventory of aromatics from fossil fuels (e.g., Ensberg et al., 2014; Hayes et al., 2015). (2) BTEX from both fossil fuels and VCPs account for 25-95% (mean 43%) of BTEX and IVOC emissions (Fig. 52). China has the lowest contribution of IVOCs, potentially due to differences in chemical make-up of the solvents used daily (Li et al., 2019), but more research is needed to investigate the differences in IVOCs:BTEX from Beijing versus US and UK emission inventories. Nonetheless, this shows the importance of IVOCs for both emissions and ASOA precursors. (3) IVOCs are generally equal to, if not greater than, the emissions of BTEX in 4 of the 5 urban areas investigated here (Fig. 52). (4) Overall, VCPs account for a large fraction of the BTEX and IVOC emissions for all five cities. (5) Finally, SVOCs account for 27-88% (mean 53%) of VOCs generally considered ASOA precursors (VOCs with volatility saturation concentrations $\leq 10^7$ μg $m^{-3}$) (Fig. S63). Beijing has the highest contribution of SVOCs to ASOA precursors due to the use of solid fuels and cooking emissions (Hu et al., 2016). Also, this indicates the large contribution of a class of VOCs difficult to measure (Robinson et al., 2007) that are an important ASOA precursor (e.g., Hayes et al., 2015), showing further emphasis should be placed in quantifying the emissions of this class of compounds.

These results provide an ability to further investigate the mass balance of predicted and observed ASOA for these urban locations (Fig. 46). The inclusion of IVOCs, other aromatics not including BTEX, and SVOCs leads to the ability to explain, on average, 85±12% of the observed ASOA for these urban locations around the world (Fig. 46a). Further, VCP contribution to

ASOA is important for all these urban locations, accounting for~~accounting or~~, on average, 37±3% of the observed ASOA (Fig. 4~~6~~b).

This bottom-up mass budget analysis provides important insights to further explain the correlation observed in Fig. 2~~5~~. First, IVOCs are generally co-emitted from similar sources as BTEX for the urban areas investigated in-depth (Fig. 5~~2~~). The oxidation of these co-emitted species leads to the ASOA production observed across the urban areas around the world. Second, S/IVOCs generally have similar rate constants as toluene and xylenes ($\geq 1\times10^{-11}$ $cm^3$ $molec.^{-1}$ $s^{-1}$) (Zhao et al., 2014, 2017), the compounds that contribute the most to $R_{BTEX}$, explaining the rapid ASOA production that has been observed in various studies (de Gouw and Jimenez, 2009; DeCarlo et al., 2010; Hayes et al., 2013; Hu et al., 2013, 2016; Nault et al., 2018; Schroder et al., 2018) and correlation (Fig. 2~~5~~). Finally, the contribution of VCPs and fossil fuel sources to ASOA is similar across the cities, expanding upon and further supporting the conclusion of McDonald et al. (2018) in the importance of identifying and understanding VCP emissions in order to explain ASOA.

This investigation shows that the bottom-up calculated ASOA agrees with observed top-down ASOA within 15%. As highlighted above, this ratio is explained by the co-emissions of IVOCs with BTEX from traditional sources (diesel, gasoline, and other fossil fuel emissions) and VCPs (Fig. 5) along with similar rate constants for these ASOA precursors (Table S12). Thus, the $ASOA/R_{BTEX}$ ratio obtained from Fig. 2 results in accurate predictions of ASOA for the urban areas evaluated here, and this value can be used to better estimate ASOA with chemical transport models (Sect. 4).

## 4. Improved Urban SIMPLE Model Using Multi-Cities to Constrain

### 4.1 Updates to the SIMPLE Model

With the combination of the new dataset, which expands across urban areas on three continents, the SIMPLE parameterization for ASOA (Hodzic and Jimenez, 2011) is updated in the standard GEOS-Chem model to reproduce observed ASOA in Fig. 5a. The parameterization operates as represented by Eq. 9.

$$\text{Emissions} \rightarrow \text{SOAP} \xrightarrow{k \times [OH]} \text{ASOA} \qquad \text{Eq. 9}$$

SOAP represents the lumped precursors of ASOA, k is the reaction rate coefficient with OH ($1.25\times10^{-11}$ $cm^3$ $molecules^{-1}$ $s^{-1}$), and [OH] is the OH concentration in molecules $cm^{-3}$.

SOAP emissions were calculated based on the relationship between ΔSOA/ΔCO and $R_{aromatics}$/ΔCO in Fig. 5a. First, we calculated $R_{aromatics}$/ΔCO (Eq. 10) for each grid cell and time step as follows:

$$\frac{R_{aromatics}}{\Delta CO} = \frac{E_B \times k_B + E_T \times k_T + E_X \times k_X}{E_{CO}} \qquad \text{Eq. 10}$$

Where E and k stand for the emission rate and reaction rate coefficient with OH, respectively, for benzene (B), toluene (T), and xylenes (X). Ethylbenzene was not included in this calculation because its emission was not available in HTAPv2 emission inventory. However, ethylbenzene contributed a minor fraction of the mixing ratio (~ 7%, Table S5) and reactivity (~6%) of the total BTEX across the campaigns. Reaction rate constants used in this study were $1.22\times10^{-12}$, $5.63\times10^{-12}$, and $1.72\times10^{-11}$ $cm^3$ $molec.^{-1}$ $s^{-1}$ for benzene, toluene, and xylene, respectively (Atkinson and Arey, 2003; Atkinson et al., 2006).

Second, $E_{SOAP}/E_{CO}$ can be obtained from the result of Eq. 11, using slope and intercept in Fig. 5a, with a correction factor (F) to consider additional SOA production after 0.5 PA equivalent days, since Fig. 5a shows the comparison at 0.5 PA equivalent days. ¶

$$\frac{E_{SOAP}}{E_{CO}} = \left( Slope \times \frac{R_{aromatics}}{\Delta CO} + Intercept \right) \times F \quad \text{Eq. 11}$$

Where slope is 24.8 and intercept is −1.7 from Fig. 5a. F (Eq. 12) can be calculated as follows:¶

$$F = \frac{ASOA_{t=\infty}}{ASOA_{t=0.5d}} = \frac{SOAP_{t=0}}{SOAP_{t=0} \times (1 - exp(-k \times \Delta t \times [OH]))}, \Delta t = 43200\ s \quad \text{Eq. 12}$$

F was calculated as 1.8 by using [OH] = $1.5 \times 10^6$ molecules $cm^{-3}$, which was used in the definition of 0.5 PA equivalent days for Fig. 5a. ¶

Finally, $E_{SOAP}$ can be computed by multiplying CO emissions ($E_{CO}$) for every grid point and time step in GEOS-Chem by the $E_{SOAP}/E_{CO}$ ratio. ¶

¶

**4.2 Results of Updated SIMPLE Model**

The SIMPLE model was originally designed and tested against the observations collected around Mexico City (Hodzic and Jimenez, 2011). It was then tested against observations collected in Los Angeles (Hayes et al., 2015; Ma et al., 2017). As both data sets have nearly identical ΔSOA/ΔCO and $R_{BTEX}$ (Fig. 24 and Fig. 35), it is not surprising that the SIMPLE model did well in predicting the observed ΔSOA/ΔCO for these two urban regions with consistent parameters. Though the SIMPLE model generally performed better than more explicit models, it generally had lower skill in predicting the observed ASOA in urban regions outside of Mexico City and Los Angeles (Shah et al., 2019; Pai et al., 2020).

This may stem from the original SIMPLE model with constant parameters missing the ability to change the amount and reactivity of the emissions, which are different for the various urban regions, versus the ASOA precursors being emitted proportionally to only CO (Hodzic and Jimenez, 2011; Hayes et al., 2015). For example, in the HTAP emissions inventory, the CO emissions for Seoul, Los Angeles, and Mexico City are all similar (Fig. S8); thus, the original SIMPLE model would suggest similar ΔSOA/ΔCO for all three urban locations. However, as shown in Fig. 2~~4~~ and Fig. 3~~5~~, the ΔSOA/ΔCO is different by nearly a factor of 2. The inclusion of the emissions and reactivity, where $R_{BTEX}$ for Seoul is approximately a factor of 2.5 higher than Los Angeles and Seoul, into the improved SIMPLE model better accounts for the variability in SOA production, as shown in Fig. 2~~5~~. Thus, the inclusion and use of this improved SIMPLE model refines the simplified representation of ASOA in chemical transport models and/or box models.

The "improved" SIMPLE shows higher ASOA compared to the default VBS GEOS-Chem (Fig. 6a,b). In areas strongly impacted by urban emissions (e.g., Europe, East Asia, India, east and west coast US, and regions impacted by Santiago, Chile, Buenos Aires, Argentina, Sao Paulo, Brazil, Durban and Cape Town, South Africa, and Melbourne and Sydney, Australia), the "improved" SIMPLE model predicts up to 14 μg $m^{-3}$ more ASOA, or ~30 to 60 times more ASOA than the default scheme (Fig. 6c,d). As shown in Fig. 1, during intensive measurements, the ASOA composed 17-39% of $PM_1$, with an average contribution of ~25%. The default ASOA scheme in GEOS-Chem greatly underestimates the fractional contribution of ASOA to total $PM_{2.5}$ (<2%; Fig. 6e). The "improved" SIMPLE model greatly improves the predicted fractional contribution, showing that ASOA in the urban regions ranges from 15-30%,

with an average of ~15% for the grid cells corresponding to the urban areas investigated here (Fig. 6f). Thus, the "improved" SIMPLE predicts the fractional contribution of ASOA to total $PM_{2.5}$ far more realistically, compared to observations. As discussed in Sect. 2.3 and Eq. 11, having the model accurately predict the fractional contribution of ASOA to the total PM is very important, as the total $PM_{2.5}$ is derived from satellite-based estimates (van Donkelaar et al., 2015), and the model fractions are then applied to those total $PM_{2.5}$ estimates. The ability for the "improved" SIMPLE model to better represent the ASOA composition provides confidence attributing the ASOA contribution to premature mortality.

## 5. Preliminary Evaluation of Worldwide Premature Deaths Due to ASOA with Updated SIMPLE Parameterization

The improved SIMPLE parameterization is used along with GEOS-Chem to provide an accurate estimation of ASOA formation in urban areas worldwide and provide an ability to obtain realistic simulations of ASOA based on measurement data. We use this model to quantify the attribution of $PM_{2.5}$ ASOA to premature deaths. Analysis up to this point has been for $PM_1$; however, both the chemical transport model and epidemiological studies utilize $PM_{2.5}$. For ASOA, this will not impact the discussion and results here because the mass of OA (typically 80–90%) is dominated by $PM_1$ (e.g., Bae et al., 2006; Seinfeld and Pandis, 2006), and ASOA is formed mostly through condensation of oxidized species, which favors partitioning onto smaller particles (Seinfeld and Pandis, 2006).

The procedure for this analysis is described in Fig. 7 and Sect. 2.35 and S32.6. Briefly, we combine high-resolution satellite-based $PM_{2.5}$ estimates (for exposure) and a chemical

742 transport model (GEOS-Chem, for fractional composition) to estimate ASOA concentrations and
743 various sensitivity analysis (van Donkelaar et al., 2015). We calculated ~3.3 million premature
744 deaths (using the Integrated Exposure-Response, IER, function) are due to long-term exposure of
745 ambient $PM_{2.5}$ (Fig. S97, Table S164), consistent with recent literature (Cohen et al., 2017).

746 The attribution of ASOA $PM_{2.5}$ premature deaths can be calculated one of two ways: (a)
747 marginal method (Silva et al., 2016) or (b) attributable fraction method (Anenberg et al., 2019).
748 For method (a), it is assumed that a fraction of the ASOA is removed, keeping the rest of the
749 $PM_{2.5}$ components approximately constant, and the change in deaths is calculated from the deaths
750 associated with the total concentration less the deaths calculated using the reduced total $PM_{2.5}$
751 concentrations. For method (b), the health impact is attributed to each $PM_{2.5}$ component by
752 multiplying the total deaths by the fractional contribution of each component to total $PM_{2.5}$. For
753 method (a), the deaths attributed to ASOA are ~340,000 people per year (Fig. 8); whereas, for
754 method (b), the deaths are ~370,000 people per year. Both of these are based on the IER response
755 function (Cohen et al., 2017).

756 Additional recent work (Burnett et al., 2018) has suggested less reduction in the
757 premature deaths versus $PM_{2.5}$ concentration relationship at higher $PM_{2.5}$ concentrations, and
758 lower concentration limits for the threshold below which this relationship is negligible, both of
759 which lead to much higher estimates of $PM_{2.5}$ associated premature deaths. This is generally
760 termed the Global Exposure Mortality Model (GEMM). Using the two attribution methods
761 described above (a and b), the ASOA $PM_{2.5}$ premature deaths are estimated to be ~640,000
762 (method a) and ~900,000 (method b) (Fig. S97 and Fig. S120 and Table S175).

Compared to prior studies using chemical transport models to estimate premature deaths associated with ASOA (e.g., Silva et al., 2016; Ridley et al., 2018), which assumed non-volatile POA and "traditional" ASOA precursors, the attribution of premature mortality due to ASOA is over an order of magnitude higher in this study (Fig. 9). This occurs using either the IER and GEMM approach for estimating premature mortality (Fig. 9). For regions with larger populations and more $PM_{2.5}$ pollution, the attribution is between a factor of 40 to 80 higher. This stems from the non-volatile POA and "traditional" ASOA precursors over-estimating POA and under-estimating ASOA compared to observations (Schroder et al., 2018). These offsetting errors will lead to model predicted total OA similar to observations (Ridley et al., 2018; Schroder et al., 2018), yet different conclusions on whether POA versus SOA is more important for reducing $PM_{2.5}$ associated premature mortality. Using a model constrained to day-time atmospheric observations (Fig. 2~~5~~ and Fig. 4~~6~~, see Sect. 4) leads to a more accurate estimation of the contribution of photochemically-produced ASOA to $PM_{2.5}$ associated premature mortality that has not been possible in prior studies. We note that ozone concentrations change little as we change the ASOA simulation (see Sect. S4 ~~in the SI~~ and Fig. S1~~42~~).

A limitation in this study is the lack of sufficient measurements in South and Southeast Asia, Eastern Europe, Africa, and South America (Fig. 1), though these areas account for 44% of the predicted reduction in premature mortality for the world (Table S1~~64~~). However, as highlighted in Table S1~~86~~, these regions likely still consume both transportation fuels and VCPs, although in lower per capita amounts than more industrialized countries. This consumption is expected to lead to the same types of emissions as for the cities studied here, though more field measurements are needed to validate global inventories of VOCs and resulting oxidation

785 products in the developing world. Transportation emissions of VOCs are expected to be more
786 dominant in the developing world due to higher VOC emission factors associated with inefficient
787 combustion engines, such as two-stroke scooters (Platt et al., 2014) and auto-rickshaws (e.g.,
788 Goel and Guttikunda, 2015).

789 Solid fuels are used for residential heating and cooking, which impact the outdoor air
790 quality as well (Hu et al., 2013, 2016; Lacey et al., 2017; Stewart et al., 2020), and which also
791 lead to SOA (Heringa et al., 2011). As discussed in Sect. 3.1, though the majority of the studies
792 evaluated here occurred in spring to summer time, when solid fuel emissions are decreased, two
793 studies occurred during the winter/early spring time, where solid fuel emissions were important
794 (Hu et al., 2013; Schroder et al., 2018). These studies still follow the same relationship between
795 ASOA and $R_{BTEX}$ as the studies that focused on spring/summer time photochemistry. Thus, the
796 limited datasets available indicate that photochemically produced ASOA from solid fuels follow
797 a similar relationship to that from other ASOA sources.

798 Also, solid fuel sources are included in the inventories used in our modeling. For the
799 HTaP emission inventory used here (Janssens-Maenhout et al., 2015), small-scale combustion,
800 which includes heating and cooking (e.g., solid-fuel use), is included in the residential emission
801 sector. Both CO and BTEX are included in this source, and can account for a large fraction of the
802 total emissions where solid-fuel use may be important (Fig. S15). Thus, as CO and BTEX are
803 used in the updated SIMPLE model, and campaigns that observed solid-fuel emissions fall
804 within the trend for all urban areas, the solid-fuel contribution to photochemically-produced
805 ASOA is accounted for (as accurately as allowed by current datasets) in the estimation of ASOA
806 for the attribution to premature mortality.

Note that recent work has observed potential nighttime aqueous chemistry and/or oxidation by nitrate radical from solid fuel emissions to produce ASOA (Kodros et al., 2020). Thus, missing this source of ASOA may lead to an underestimation of total ASOA versus the photochemically-produced ASOA we discuss here, leading to a potential underestimation in the attribution of ASOA to premature mortality. From the studies that investigated "night-time aging" of solid-fuel emissions to form SOA, we predict that the total ASOA may be underestimated by 1 to 3 μg $m^{-3}$ (Kodros et al., 2020). This potential underestimation, though, is less than the current underestimation in ASOA in GEOS-Chem (default versus "Updated" SIMPLE).

~~Also, unlike many of the cities studied here, solid fuels are used for residential heating and cooking, which impact the outdoor air quality as well (Hu et al., 2013, 2016; Lacey et al., 2017; Stewart et al., 2020), and which also lead to SOA (Heringa et al., 2011).~~ Recently, emission factors from Abidjan, Côte d'Ivoire, a developing urban area, showed the dominance of emissions from transportation and solid fuel burning, with BTEX being an important fraction of the total emissions, and that all the emissions were efficient in producing ASOA (Dominutti et al., 2019). Further, investigation of emissions in New Delhi region of India demonstrated the importance of both transportation and solid fuel emissions (Stewart et al., 2020; Wang et al., 2020) while model comparisons with observations show an underestimation of OA compared to observations due to a combination of emissions and OA representation (Jena et al., 2020). Despite emission source differences, SOA is still an important component of $PM_{2.5}$ (e.g., Singh et al., 2019) and thus will impact air quality and premature mortality in developing regions. Admittedly, though, our estimates will be less accurate for these regions.

## 6. Conclusions

In summary, ASOA is an important, though inadequately constrained component of air pollution in megacities and urban areas around the world. This stems from the complexity associated with the numerous precursor emission sources, chemical reactions, and oxidation products that lead to observed ASOA concentrations. We have shown here that the variability in observed ASOA across urban areas is correlated with $R_{BTEX}$, a marker for the co-emissions of IVOC from both transportation and VCP emissions. Global simulations indicate ASOA contributes to a substantial fraction of the premature mortality associated with $PM_{2.5}$. Reductions of the ASOA precursors will reduce the premature deaths associated with $PM_{2.5}$, indicating the importance of identifying and reducing exposure to sources of ASOA. These sources include emissions that are both traditional (transportation) as well as non-traditional emissions of emerging importance (VCPs) to ambient $PM_{2.5}$ concentrations in cities around the world. Further investigation of speciated IVOCs and SVOCs for urban areas around the world along with SOA mass concentration and other photochemical products (e.g., $O_x$, PAN, and HCHO) for other urban areas, especially in South Asia, throughout Africa, and throughout South America, would provide further constraints to improve the SIMPLE model and our understanding of the emission sources and chemistry that leads to the observed SOA and its impact on premature mortality.

**Acknowledgements**

This study was partially supported by grants from NASA NNX15AT96G, NNX16AQ26G, Sloan Foundation 2016-7173, NSF AGS-1822664, EPA STAR 83587701-0, NERC NE/H003510/1, NERC NE/H003177/1, NERC NE/H003223/1, NOAA NA17OAR4320101, NCAS R8/H12/83/037, Natural Science and Engineering Research Council of Canada (NSERC, RGPIN/05002-2014), and the Fonds de Recherche du Québec —Nature et technologies (FRQNT, 2016-PR-192364). This manuscript has not been formally reviewed by EPA. The views expressed in this document are solely those of the authors and do not necessarily reflect those of the Agency. EPA does not endorse any products or commercial services mentioned in this publication. We thank Katherine Travis for useful discussions. We acknowledge B J. Bandy, J. Lee, G. P. Mills, d. D. Montzka, J. Stutz, A. J. Weinheimer E. J. Williams, E. C. Wood, and D. R. Worsnop for use of their data.

**Data Availability**

TexAQS measurements are available at https://esrl.noaa.gov/csl/groups/csl7/measurements/2000TexAQS/LaPorte/DataDownload/ and upon request. NEAQS measurements are available at https://www.esrl.noaa.gov/csl/groups/csl7/measurements/2002NEAQS/. MILAGRO measurements are available at http://doi.org/10.5067/Aircraft/INTEXB/Aerosol-TraceGas. CalNex measurements are available at https://esrl.noaa.gov/csl/groups/csl7/measurements/2010calnex/Ground/DataDownload/. ClearfLo measurements are available at https://catalogue.ceda.ac.uk/uuid/6a5f9eedd68f43348692b3bace3eba45. SEAC$^4$RS measurements are available at http://doi.org/10.5067/Aircraft/SEAC4RS/Aerosol-TraceGas-Cloud. WINTER measurements are available at https://data.eol.ucar.edu/master_lists/generated/winter/. KORUS-AQ measurements are available at http://doi.org/10.5067/Suborbital/KORUSAQ/DATA01. Data from Chinese campaigns are available upon request, and rest of data used were located in papers cited. GEOS-Chem data available upon request. Figures will become accessible at cires1.colorado.edu/jimenez/group_pubs.html.

**Competing Interests**

The authors declare no competing interests.

**Author Contribution**

B.A.N., D.S.J., B.C.M., J.A.dG., and J.L.J designed the experiment and wrote the paper. B.A.N., PC.-J., D.A.D., W.H., J.C.S, J.A., D.R.B., M.R.C., H.C., M.M.C., P.F.D, G.S.D., R.D., F.F, A.F., J.B.G., G.G., J.F.H, T.F.H., P.L.H., J.H., M.H., L.G.H., B.T.J., W.C.K., J.L., I.B.P., J.P., B.R.,

C.E.R., D.R., J.M.R., T.B.R, M.S., J.W., C.W., P.W., G.M.W., D.E.Y., B.Y., J.A.dG., and J.L.J. collected and analyzed the data. D.S.J. and A.H. ran the GEOS-Chem model and B.A.N., D.S.J, and J.L.J. analyzed the model output. B.A.N., P.L.H., J.M.S., and J.L.J. ran and analyzed the 0-D model used for ASOA budget analysis of ambient observations. B.C.M., A.L., M.L., and Q.Z. analyzed and provided the emission inventories used for the 0-D box model. D.S.J., D.K.H., and M.O.N. conducted the ASOA attribution to mortality calculation, and B.A.N., D.S.J., D.K.H., M.O.N., J.A.dG, and J.L.J analyzed the results. All authors reviewed the paper.

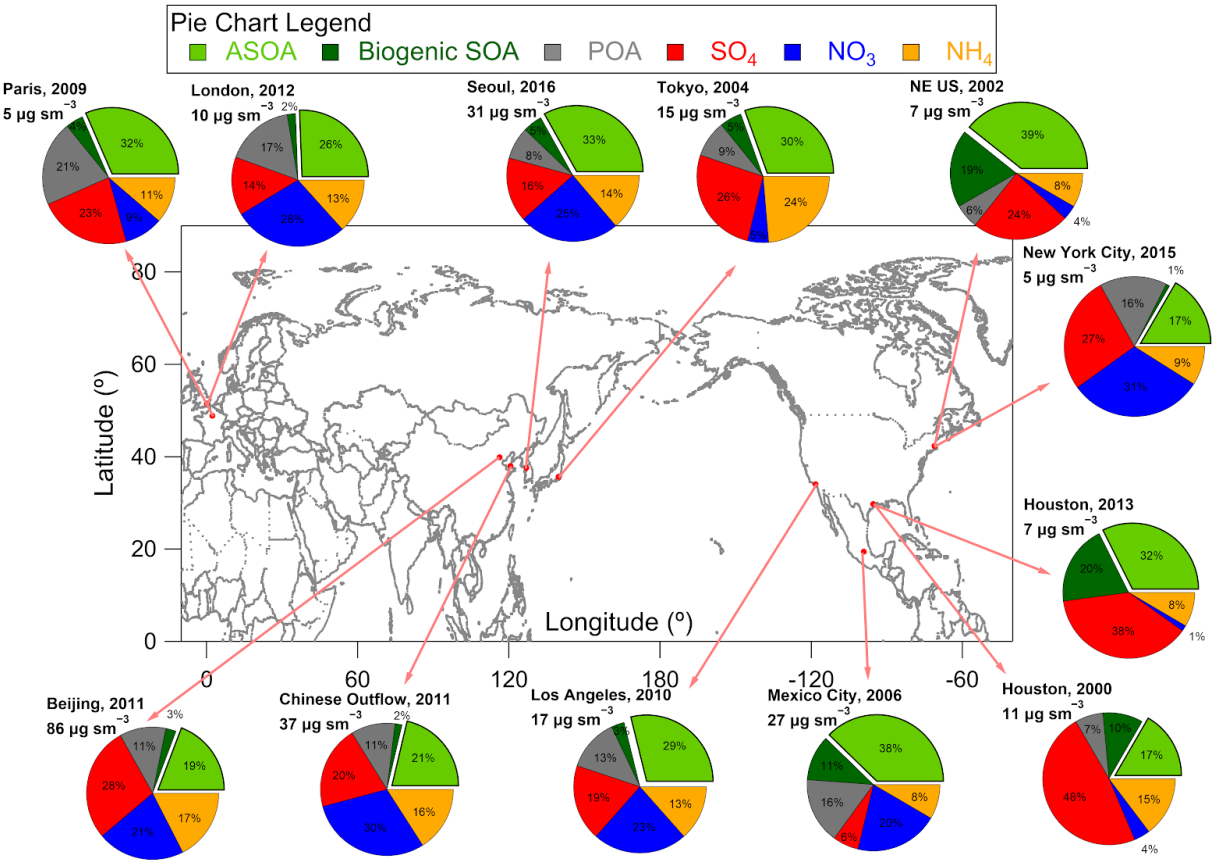


893

894 **Figure 1**. Non-refractory submicron aerosol composition measured in urban and urban outflow
895 regions from field campaigns used in this study, all in units of μg $m^{-3}$, at standard temperature
896 (273 K) and pressure (1013 hPa) ($sm^{-3}$). See Sect. S32 and ~~(GEOS-Chem Section and~~ Table 1~~)~~
897 for further information on measurements, studies, and apportionment of SOA into ASOA and
898 BSOA.

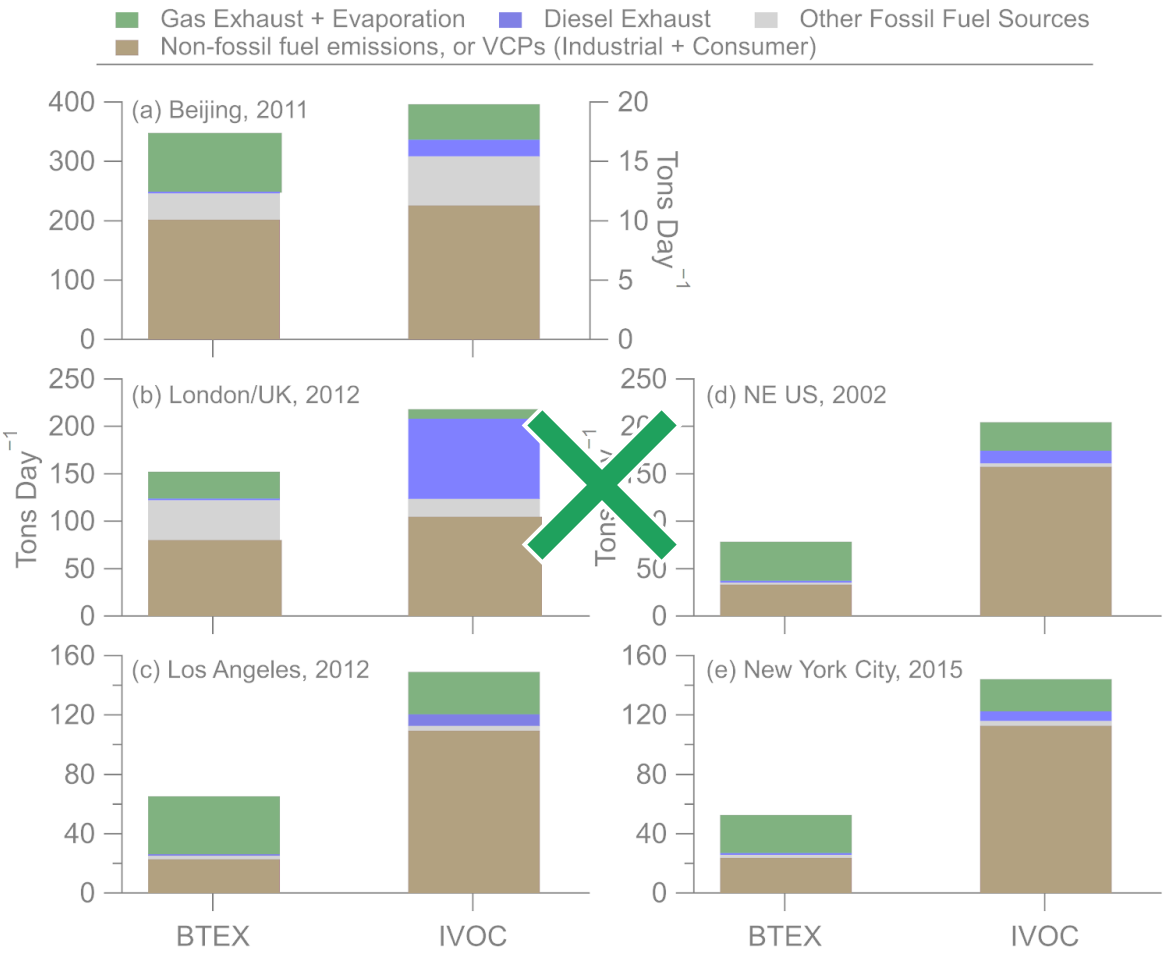


899

900 **Figure 2**. Comparison of BTEX and IVOC sources for (a) Beijing (see SI section about Beijing
901 emission inventory), (b) London (see SI section about London/UK emission inventory), and (c)
902 Los Angeles, (d) Northeast United States, and (e) New York City (see SI section about United
903 States for (c) – (e)). For (a), BTEX is on the left axis and IVOC is on the right axis, due to the
904 small emissions per day for IVOC.

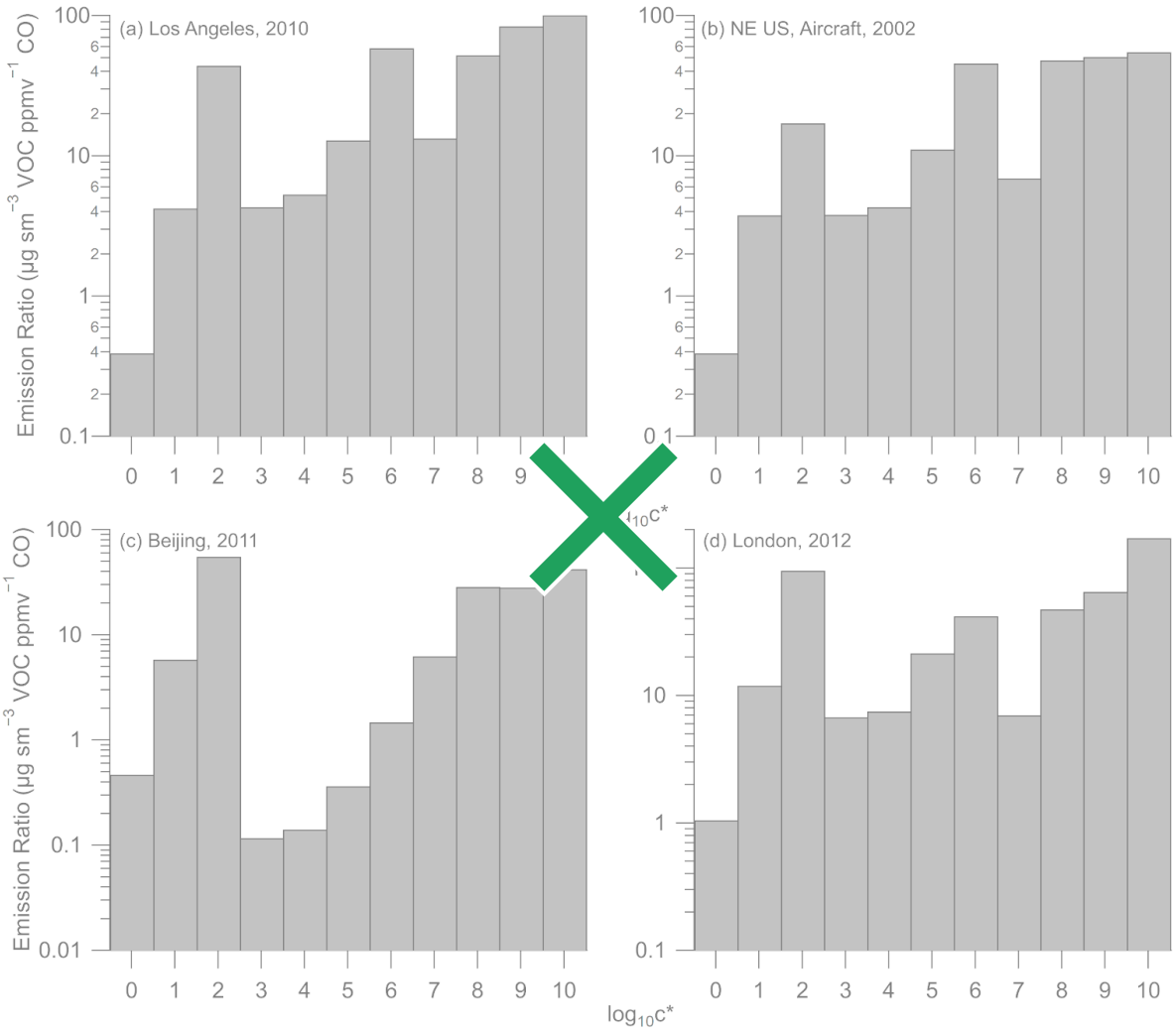


**Figure 3**. Emission ratio versus saturation concentration ($\log_{10}(c^*)$) for (a) Los Angeles, (b) NE US, aircraft, (c) Beijing, and (d) London. The emission ratios for VOCs ($\log_{10}(c^*) \geq 7$) were taken from de Gouw et al. (2017) and Ma et al. (2017) for Los Angeles, Warneke et al. (2007) for NE US, aircraft, and Wang et al. (2014) for Beijing while the VOC emission ratio for London is from Table S6 to Table S8. For VOCs between $\log_{10}(c^*)$ of 3 and 6 (IVOCs), the volatility distribution from McDonald et al. (2018), along with the ratio of IVOC to BTEX from Figure SI-6 and the emission ratio of BTEX (Table S6), were used to determine the emission ratio versus saturation concentration. Finally, for VOCs between $\log_{10}(c^*)$ 0 and 2 (SVOCs), the volatility distributions from Robinson et al. (2007) for non-fossil fuel POA and from Worton et al. (2014) for fossil fuel POA were used to convert the normalized POA mass concentration (Table S9) to VOC emission ratios. Note, the emission ratio versus saturation concentration for New York City, 2015, was similar to (b), as the emissions were similar (Fig. 2) and the BTEX for New York City is the same as NE US (Table S5).

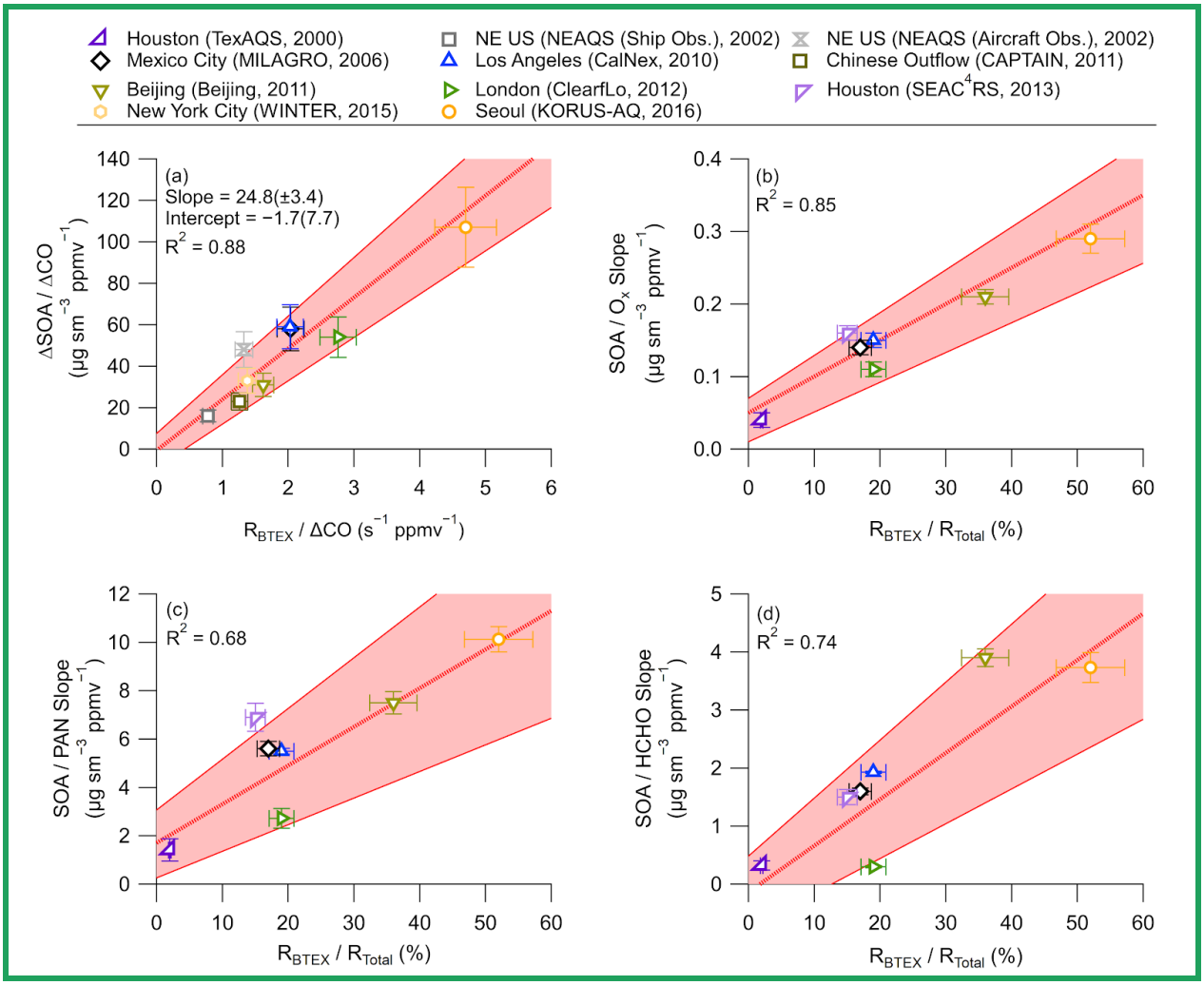


**Figure 2**. (a) Scatter plot of background and dilution corrected ASOA concentrations (ΔASOA/ΔCO at PA = 0.5 equivalent days) versus BTEX emission reactivity ratio ($R_{BTEX}$= $\sum_i [VOC/CO]_i$) for multiple major field campaigns on three continents. Comparison of ASOA versus (b) Ox, (c) PAN, and (d) HCHO slopes versus the ratio of the BTEX/Total emission reactivity, where total is the OH reactivity for the emissions of BTEX + C¬2-3 alkenes + C2-6 alkanes (Table S5 through Table S7), for the campaigns studied here. For all figures, red shading is the ±1σ uncertainty of the slope, and the bars are ±1σ uncertainty of the data (see Sect. S5).

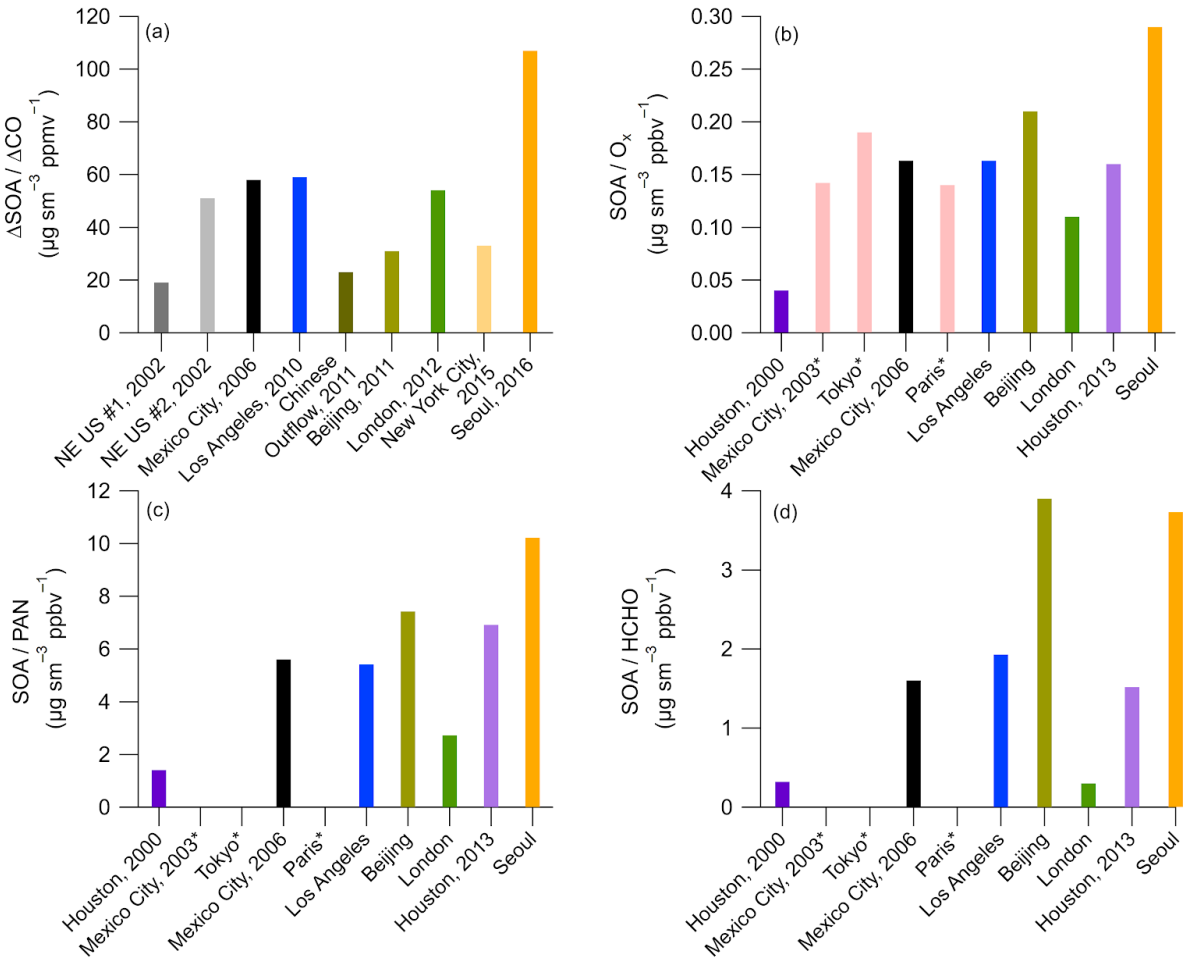


928

929 **Figure 3~~2~~4**. (a) A comparison of the ΔSOA/ΔCO for the urban campaigns on three continents.
930 Comparison of (b) SOA/Ox, (c) SOA/HCHO, and (d) SOA/PAN slopes for the urban areas
931 (Table S4). For (b) through (d), cities marked with * have no HCHO, PAN, or hydrocarbon data.

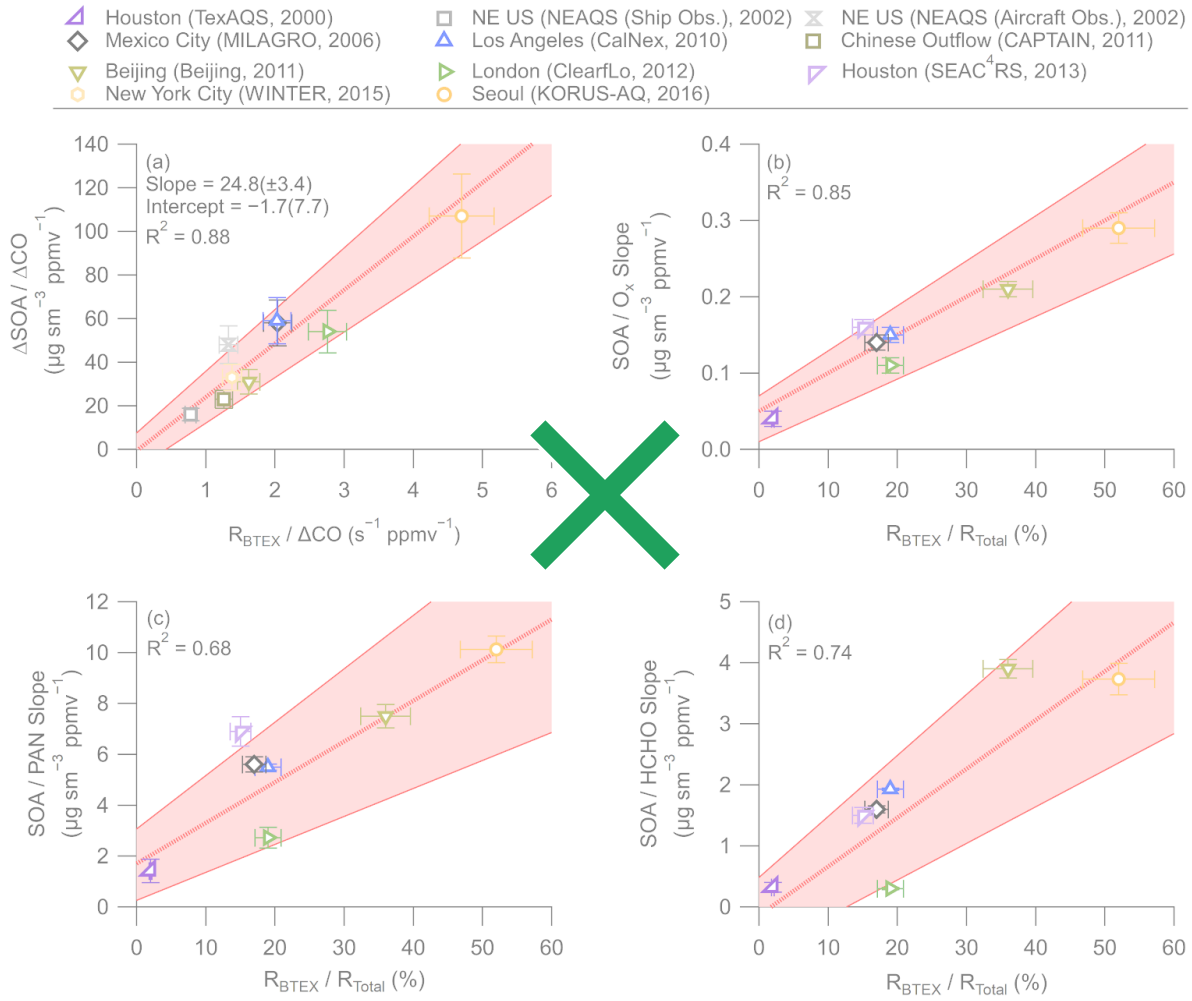


932

933 **Figure 3**5. (a) Scatter plot of background and dilution corrected ASOA concentrations
934 (ΔASOA/ΔCO at PA = 0.5 equivalent days) versus BTEX emission reactivity ratio ($R_{BTEX}$ =
935 $\sum_i [VOC/CO]_i$) for multiple major field campaigns on three continents. Comparison of ASOA
936 versus (b) Ox, (c) PAN, and (d) HCHO slopes versus the ratio of the BTEX/Total emission
937 reactivity, where total is the OH reactivity for the emissions of BTEX + C=2-3 alkenes + C2-6
938 alkanes (Table S5 through Table S7), for the campaigns studied here. For all figures, red shading
939 is the ±1σ uncertainty of the slope, and the bars are ±1σ uncertainty of the data (see Sect. 2.2S5).

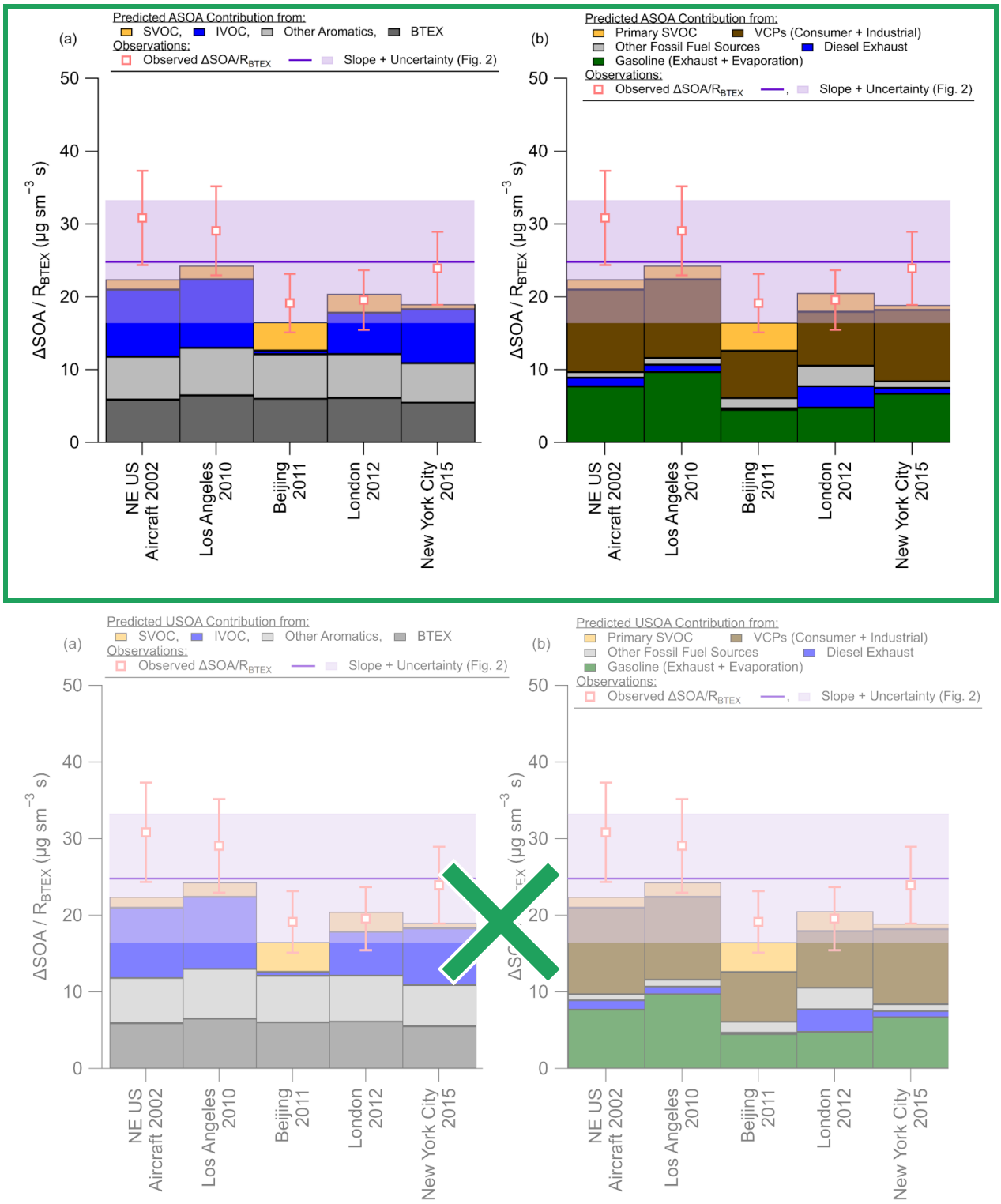


**Figure 46**. (a) Budget analysis for the contribution of the observed $\Delta SOA/R_{BTEX}$ (Fig. 25) for cities with known emissions inventories for different volatility classes (see SI and Fig. 52 and Fig. S63). (b) Same as (a), but for sources of emissions. For (a) and (b), SVOC is the

945 contribution from both vehicle and other (cooking, etc.) sources. See ~~Sect. 2 and~~ SI for
946 information about the emissions, ASOA precursor contribution, error analysis, and discussion
947 about sensitivity of emission inventory IVOC/BTEX ratios for different cities and years in the
948 US.

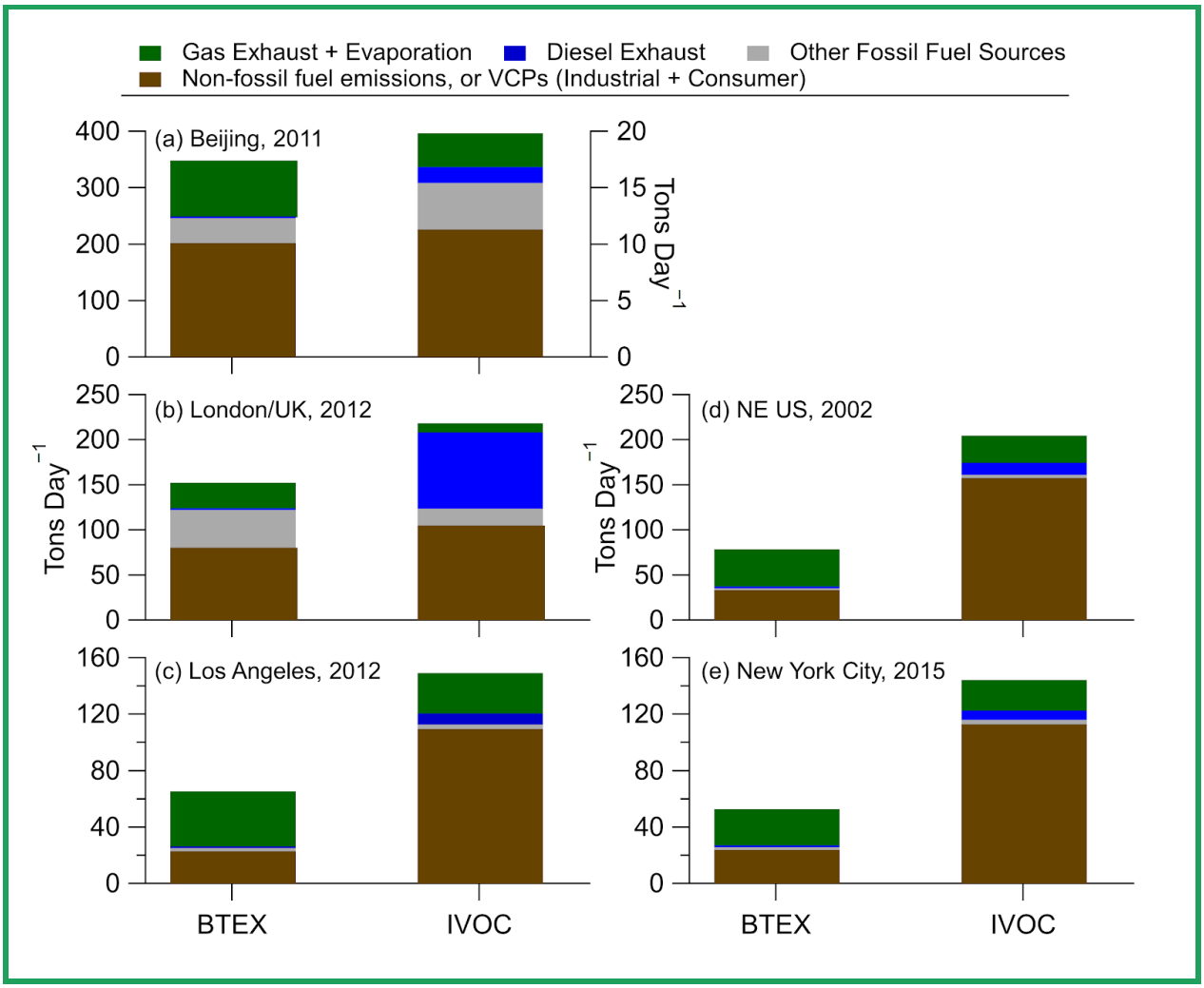


**Figure 5**. Comparison of BTEX and IVOC sources for (a) Beijing (see SI section about Beijing emission inventory), (b) London (see SI section about London/UK emission inventory), and (c) Los Angeles, (d) Northeast United States, and (e) New York City (see SI section about United States for (c) – (e)). For (a), BTEX is on the left axis and IVOC is on the right axis, due to the small emissions per day for IVOC.

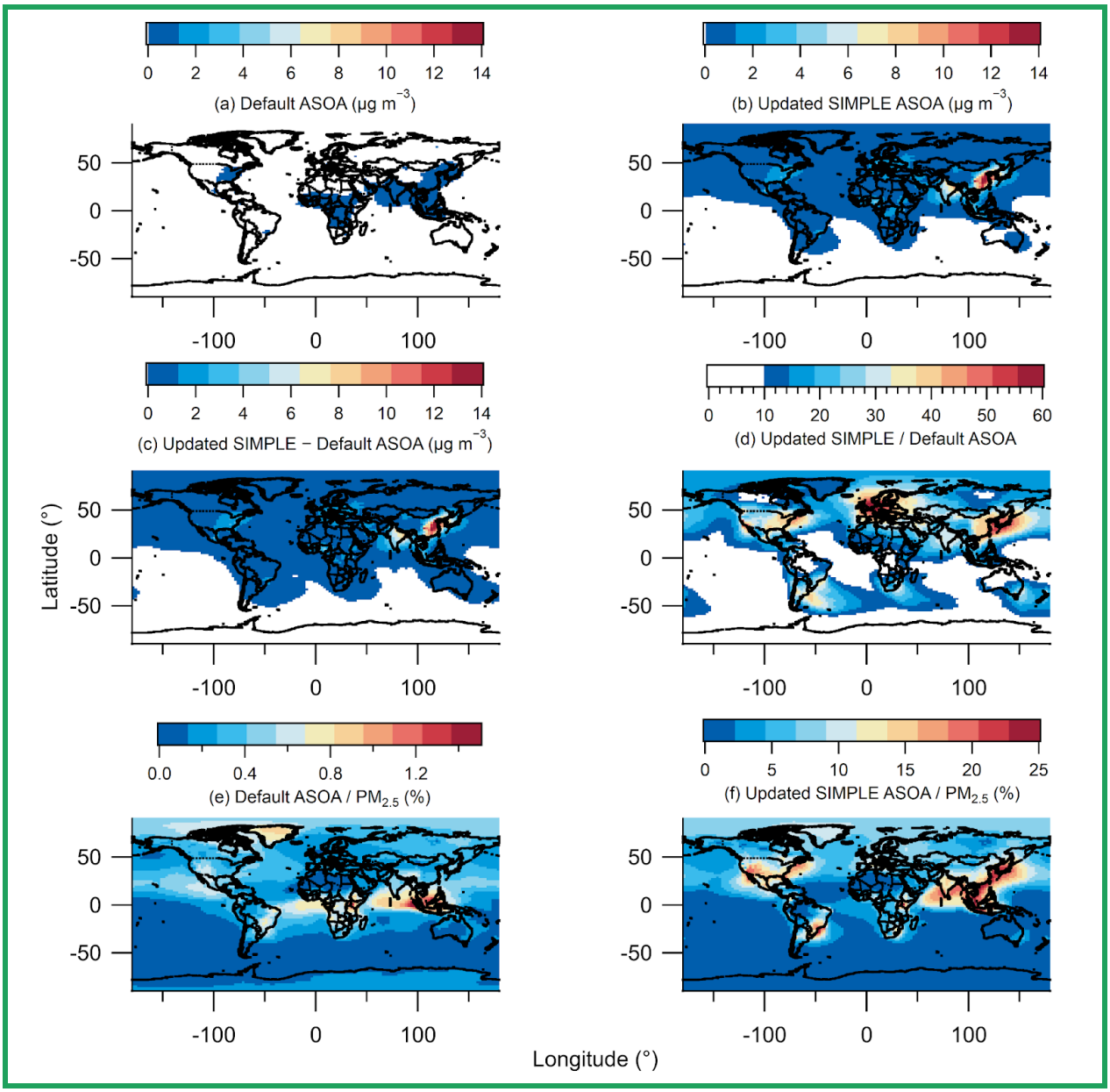


955

956 **Figure 6.** (a) Annual average modeled ASOA using the default VBS. (b) Annual average
957 modeled ASOA using the updated SIMPLE model. (c) Difference between annual average
958 modeled updated SIMPLE and default VBS. (d) Ratio between annual average modeled updated
959 SIMPLE and default VBS. (e) Percent contribution of annual average modeled ASOA using
960 default VBS to total modelled $PM_{2.5}$. (f) Percent contribution of annual average modeled ASOA
961 using updated SIMPLE to total modelled $PM_{2.5}$.

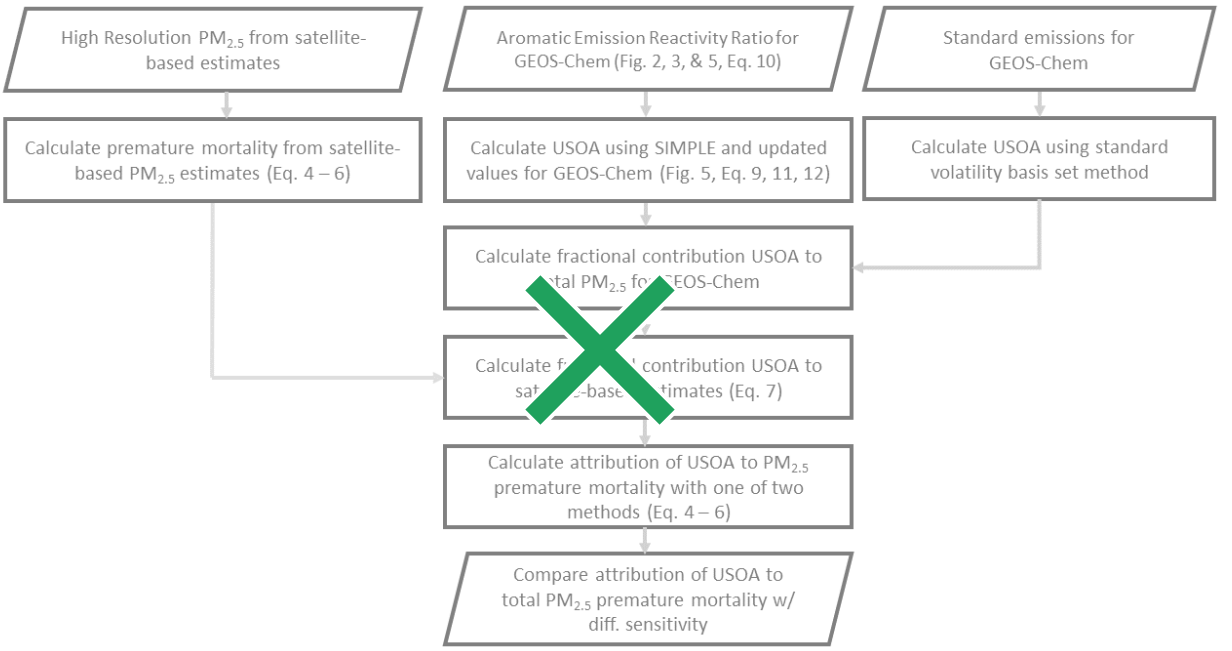


962

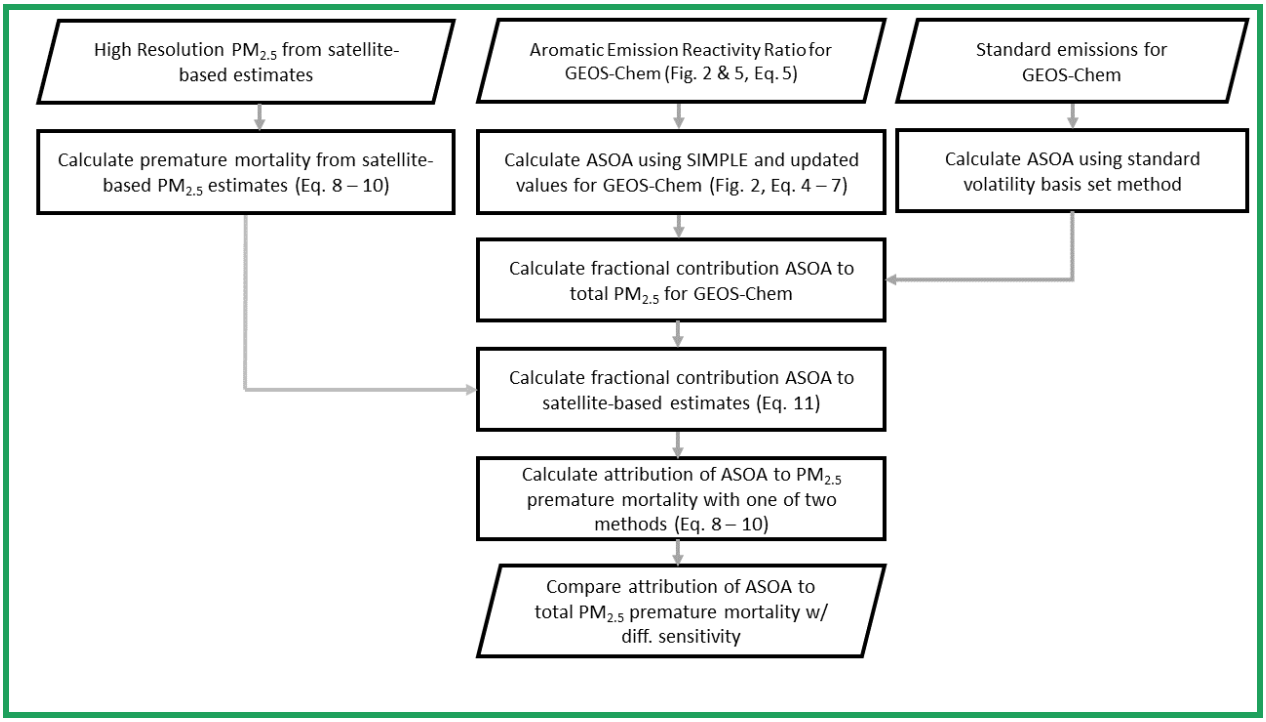


963

964 **Figure 7**. Flowchart describing how observed ASOA production was used to calculate ASOA in
965 GEOS-Chem, and how the satellite-based $PM_{2.5}$ estimates and GEOS-Chem $PM_{2.5}$ speciation was
966 used to estimate the premature mortality and attribution of premature mortality by ASOA. See
967 Sect. 2 and SI for further information about the details in the figure. SIMPLE is described in
968 Eq. ~~49~~ and by Hodzic and Jimenez (2011) and Hayes et al. (2015). The one of two methods
969 mentioned include either the Integrated Exposure-Response (IER) (Burnett et al., 2014) with

970 Global Burden of Disease (GBD) dataset (IHME, 2016) or the new Global Exposure Mortality
971 Model (GEMM) (Burnett et al., 2018) methods. For both IER and GEMM, the marginal method
972 (Silva et al., 2016) or attributable fraction method (Anenberg et al., 2019) are used.

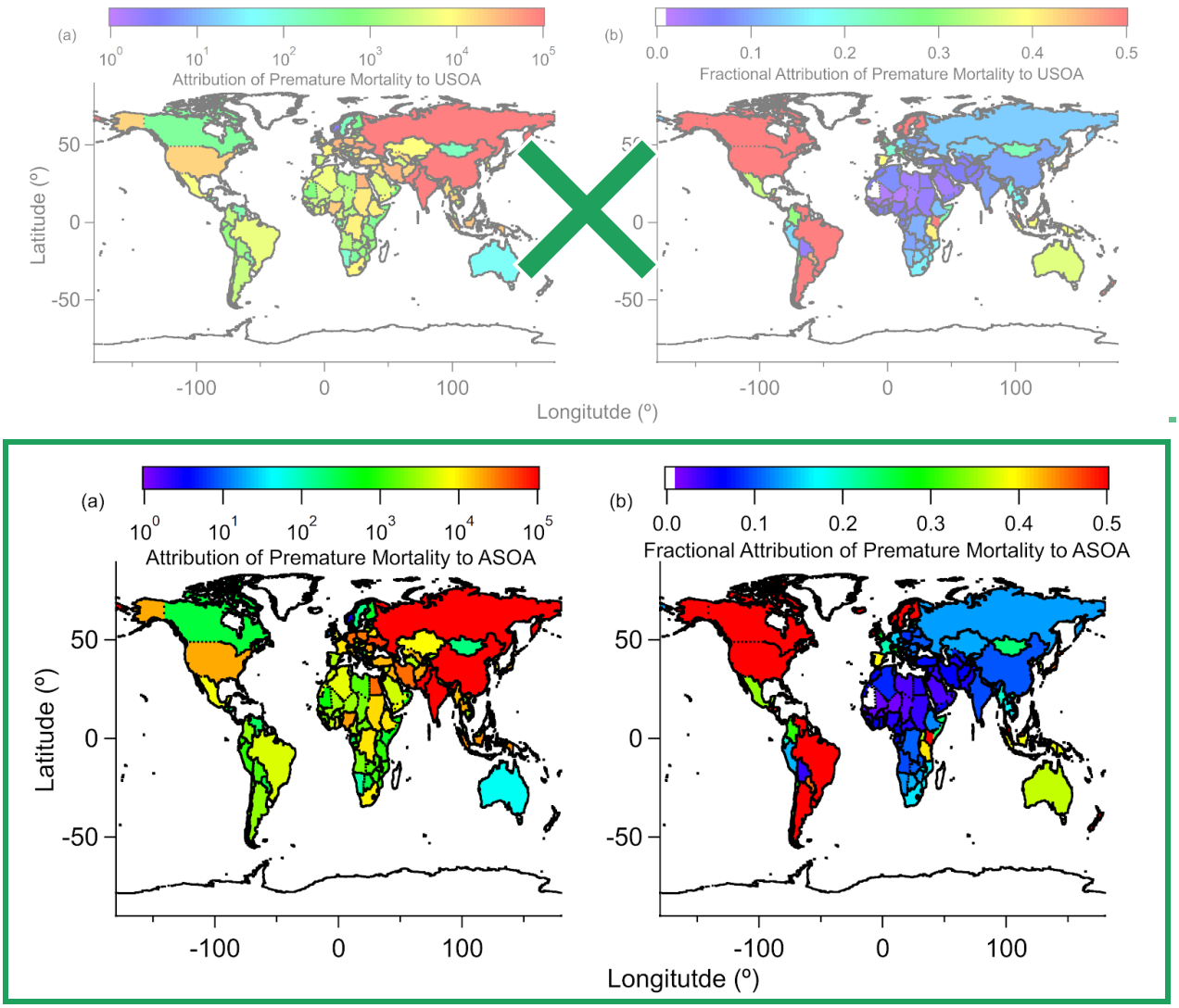


**Figure 8**. Five-year average (a) estimated reduction in $PM_{2.5}$-associated premature deaths, by country, upon removing ASOA from total $PM_{2.5}$, and (b) fractional reduction (reduction $PM_{2.5}$ premature deaths / total $PM_{2.5}$ premature deaths) in $PM_{2.5}$-associated premature deaths, by country, upon removing ASOA from GEOS-Chem. The IER methods are used here. See Fig. S97 and Fig. S120 for results using GEMM. See Fig. S108 for 10×10 $km^2$ area results in comparison with country-level results.

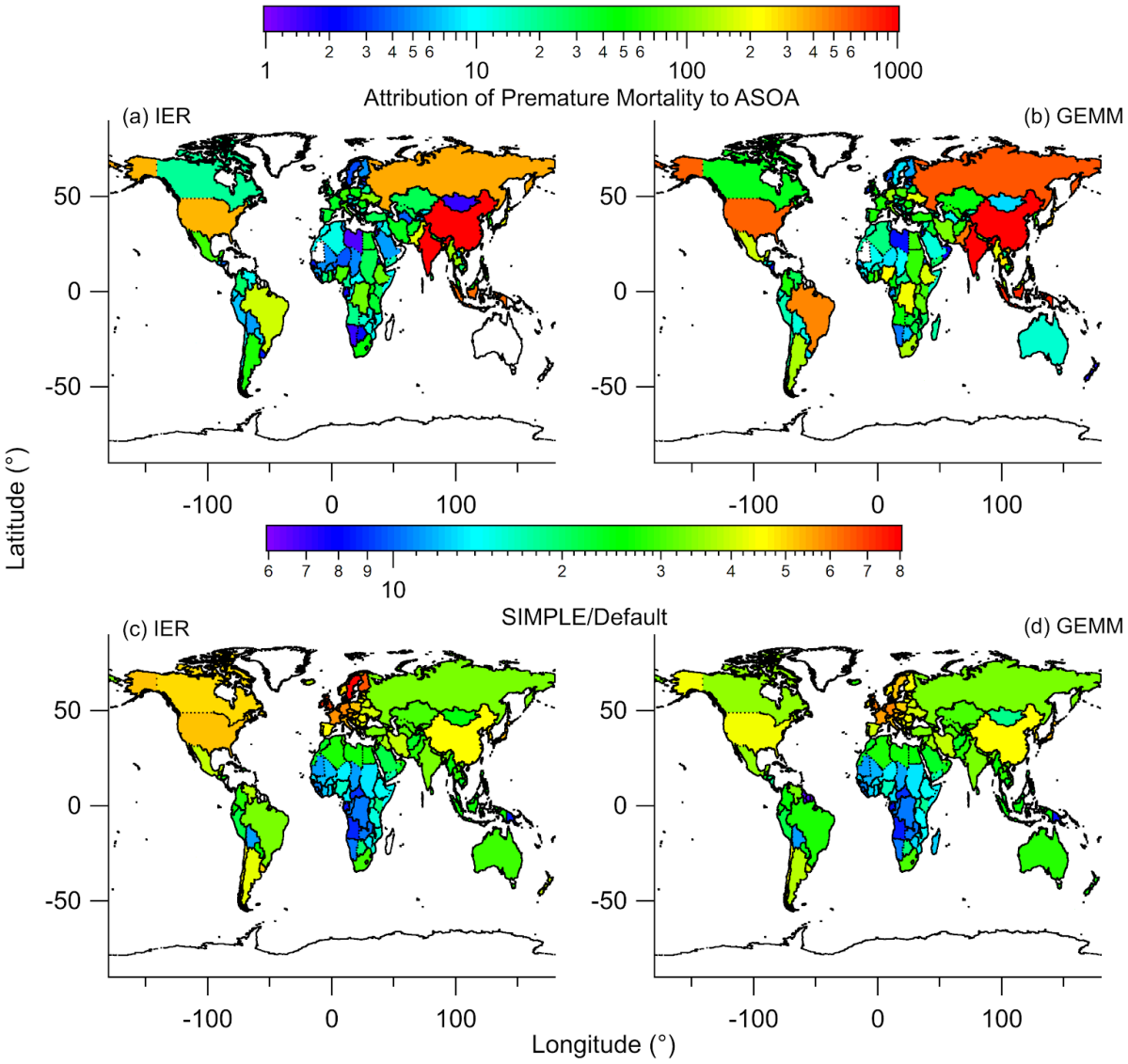


981

982 **Figure 9**. Attribution of premature mortality to ASOA using (a) IER or (b) GEMM, using the
983 non-volatile primary OA and traditional SOA precursors method in prior studies (e.g., Ridley et
984 al., 2018). The increase in attribution of premature mortality to ASOA for the "SIMPLE" model
985 (Fig. 8) versus the non-volatile primary OA and traditional SOA precursor method ("Default"),
986 for (c) IER and (d) GEMM.

Table 1. List of campaigns used here. For values previously reported for those campaigns, they are noted. For Seasons, W = Winter, Sp = Spring, and Su = Summer.

| Location | Field Campaign | Coordinates | | Time Period | Season | Previous Publication/Campaign Overview |
|---|---|---|---|---|---|---|
| | | Long. (°) | Lat. (°) | | | |
| Houston, TX, USA (2000) | TexAQS 2000 | −95.4 | 29.8 | 15/Aug/2000 - 15/Sept/2000 | Su | Jimenez et al. (2009)[a], Wood et al. (2010)[b] |
| Northeast USA (2002) | NEAQS 2002 | −78.1 - −70.5 | 32.8 - 43.1 | 26/July/2002; 29/July/2002 - 10/Aug/2002 | Su | Jimenez et al. (2009)[a], de Gouw and Jimenez (2009)[c], Kleinman et al. (2007)[c] |
| Mexico City, Mexico (2003) | MCMA-2003 | −99.2 | 19.5 | 31/Mar/2003 - 04/May/2003 | Sp | Molina et al. (2007), Herndon et al. (2008)[b] |
| Tokyo, Japan (2004) | | 139.7 | 35.7 | 24/July/2004 - 14/Aug/2004 | Su | Kondo et al. (2008)[a], Miyakawa et al. (2008)[a], Morino et al. (2014)[b] |
| Mexico City, Mexico (2006) | MILAGRO | −99.4 - −98.6 | 19.0 − 19.8 | 04/Mar/2006 - 29/Mar/2006 | Sp | Molina et al. (2010), DeCarlo et al. (2008)[a], Wood et al. (2010)[b], DeCarlo et al. (2010)[c] |
| Paris, France (2009) | MEGAPOLI | 48.9 | 2.4 | 13/July/2009 - 29/July/2009 | Su | Freney et al. (2014)[a], Zhang et al. (2015)[b] |
| Pasadena, CA, USA (2010) | CalNex | −118.1 | 34.1 | 15/May/2010 - 16/June/2010 | Sp | Ryerson et al. (2013), Hayes et al. (2013)[a,b,c] |
| Changdao Island, China (2011) | CAPTAIN | 120.7 | 38.0 | 21/Mar/2011 - 24/Apr/2011 | Sp | Hu et al. (2013)[a,c] |
| Beijing, China (2011) | CareBeijing 2011 | 116.4 | 39.9 | 03/Aug/2011 - 15/Sept/2011 | Su | Hu et al. (2016)[a,b,c] |
| London, UK (2012) | ClearfLo | 0.1 | 51.5 | 22/July/2012 - 18/Aug/2012 | Su | Bohnenstengel et al. (2015) |
| Houston, TX, USA (2013) | SEAC$^4$RS | −96.0 - −94.0 | 29.2 - 30.3 | 01/Aug/2013 - 23/Sept/2013 | Su | Toon et al. (2016) |
| New York City, NY, USA (2015) | WINTER | −74.0 - −69.0 | 39.5 - 42.5 | 07/Feb/2015 | W | Schroder et al. (2018)[a,c] |
| Seoul, South Korea (2016) | KORUS-AQ | 124.6 - 128.0 | 36.8 - 37.6 | 01/May/2016 - 10/June/2016 | Sp | Nault et al. (2018)[a,b,c,d] |

[a]Reference used for $PM_1$ composition. [b]Reference used for $SOA/O_x$ slope. [c]Reference used for $\Delta OA/\Delta CO$ value. [d]Reference used for SOA/HCHO and SOA/PAN slopes

## References


Anenberg, S., Miller, J., Henze, D. and Minjares, R.: A global snapshot of the air pollution-related health impacts of transportation sector emissions in 2010 and 2015, ICCT, Climate & Clean Air Coalition., 2019.

Atkinson, R. and Arey, J.: Atmospheric Degradation of Volatile Organic Compounds, Chem. Rev., 103, 4605–4638, 2003.

Atkinson, R., Baulch, D. L., Cox, R. A., Crowley, J. N., Hampson, R. F., Hynes, R. G., Jenkin, M. E., Rossi, M. J., Troe, J. and IUPAC Subcommittee: Evaluated kinetic and photochemical data for atmospheric chemistry: Volume II - gas phase reactions of organic species, Atmos. Chem. Phys., 6(11), 3625–4055, 2006.

Bae, M.-S., Demerjian, K. L. and Schwab, J. J.: Seasonal estimation of organic mass to organic carbon in PM2.5 at rural and urban locations in New York state, Atmos. Environ., 40(39), 7467–7479, 2006.

Bahreini, R., Ervens, B., Middlebrook, A. M., Warneke, C., de Gouw, J. A., DeCarlo, P. F., Jimenez, J. L., Brock, C. A., Neuman, J. A., Ryerson, T. B., Stark, H., Atlas, E., Brioude, J., Fried, A., Holloway, J. S., Peischl, J., Richter, D., Walega, J., Weibring, P., Wollny, A. G. and Fehsenfeld, F. C.: Organic aerosol formation in urban and industrial plumes near Houston and Dallas, Texas, J. Geophys. Res., 114, 1185, 2009.

Bertram, T. H., Perring, A. E., Wooldridge, P. J., Crounse, J. D., Kwan, A. J., Wennberg, P. O., Scheuer, E., Dibb, J., Avery, M., Sachse, G., Vay, S. A., Crawford, J. H., McNaughton, C. S., Clarke, A., Pickering, K. E., Fuelberg, H., Huey, G., Blake, D. R., Singh, H. B., Hall, S. R., Shetter, R. E., Fried, A., Heikes, B. G. and Cohen, R. C.: Direct Measurements of the Convective Recycling of the Upper Troposphere, Science, 315(5813), 816–820, 2007.

Bey, I., Jacob, D. J., Yantosca, R. M., Logan, J. A., Field, B. D., Fiore, A. M., Li, Q., Liu, H. Y., Mickley, L. J. and Schultz, M. G.: Global modeling of tropospheric chemistry with assimilated meteorology: Model description and evaluation, J. Geophys. Res. D: Atmos., 106(D19), 23073–23095, 2001.

Bohnenstengel, S. I., Belcher, S. E., Aiken, A., Allan, J. D., Allen, G., Bacak, A., Bannan, T. J., Barlow, J. F., Beddows, D. C. S., Bloss, W. J., Booth, A. M., Chemel, C., Coceal, O., Di Marco, C. F., Dubey, M. K., Faloon, K. H., Fleming, Z. L., Furger, M., Gietl, J. K., Graves, R. R., Green, D. C., Grimmond, C. S. B., Halios, C. H., Hamilton, J. F., Harrison, R. M., Heal, M. R., Heard, D. E., Helfter, C., Herndon, S. C., Holmes, R. E., Hopkins, J. R., Jones, A. M., Kelly, F. J., Kotthaus, S., Langford, B., Lee, J. D., Leigh, R. J., Lewis, A. C., Lidster, R. T., Lopez-Hilfiker, F. D., McQuaid, J. B., Mohr, C., Monks, P. S., Nemitz, E., Ng, N. L., Percival, C. J., Prévôt, A. S. H., Ricketts, H. M. A., Sokhi, R., Stone, D., Thornton, J. A., Tremper, A. H., Valach, A. C., Visser, S., Whalley, L. K., Williams, L. R., Xu, L., Young, D. E., Zotter, P., Bohnenstengel, S. I., Belcher, S. E., Aiken, A., Allan, J. D., Allen, G., Bacak, A., Bannan, T. J., Barlow, J. F., Beddows, D. C. S., Bloss, W. J., Booth, A. M., Chemel, C., Coceal, O., Marco, C. F. D., Dubey,

M. K., Faloon, K. H., Fleming, Z. L., Furger, M., Gietl, J. K., Graves, R. R., Green, D. C., Grimmond, C. S. B., Halios, C. H., Hamilton, J. F., Harrison, R. M., Heal, M. R., Heard, D. E., Helfter, C., Herndon, S. C., Holmes, R. E., Hopkins, J. R., Jones, A. M., Kelly, F. J., Kotthaus, S., Langford, B., Lee, J. D., Leigh, R. J., Lewis, A. C., Lidster, R. T., Lopez-Hilfiker, F. D., et al.: Meteorology, Air Quality, and Health in London: The ClearfLo Project, Bull. Am. Meteorol. Soc., 96(5), 779–804, 2015.

Burnett, R., Chen, H., Szyszkowicz, M., Fann, N., Hubbell, B., Pope, C. A., Apte, J. S., Brauer, M., Cohen, A., Weichenthal, S., Coggins, J., Di, Q., Brunekreef, B., Frostad, J., Lim, S. S., Kan, H., Walker, K. D., Thurston, G. D., Hayes, R. B., Lim, C. C., Turner, M. C., Jerrett, M., Krewski, D., Gapstur, S. M., Diver, W. R., Ostro, B., Goldberg, D., Crouse, D. L., Martin, R. V., Peters, P., Pinault, L., Tjepkema, M., van Donkelaar, A., Villeneuve, P. J., Miller, A. B., Yin, P., Zhou, M., Wang, L., Janssen, N. A. H., Marra, M., Atkinson, R. W., Tsang, H., Quoc Thach, T., Cannon, J. B., Allen, R. T., Hart, J. E., Laden, F., Cesaroni, G., Forastiere, F., Weinmayr, G., Jaensch, A., Nagel, G., Concin, H. and Spadaro, J. V.: Global estimates of mortality associated with long-term exposure to outdoor fine particulate matter, Proc. Natl. Acad. Sci. U. S. A., 115(38), 9592–9597, 2018.

Burnett, R. T., Pope, C. A., Ezzati, M., Olives, C., Lim, S. S., Mehta, S., Shin, H. H., Singh, G., Hubbell, B., Brauer, M., Anderson, H. R., Smith, K. R., Balmes, J. R., Bruce, N. G., Kan, H., Laden, F., Prüss-Ustün, A., Turner, M. C., Gapstur, S. M., Diver, W. R. and Cohen, A.: An integrated risk function for estimating the global burden of disease attributable to ambient fine particulate matter exposure, Environ. Health Perspect., 122(4), 397–403, 2014.

CIESIN: Gridded Population of the World (GPW), v4, SEDAC [online] Available from: https://sedac.ciesin.columbia.edu/data/collection/gpw-v4 (Accessed 12 May 2020), 2017.

Coggon, M. M., McDonald, B. C., Vlasenko, A., Veres, P. R., Bernard, F., Koss, A. R., Yuan, B., Gilman, J. B., Peischl, J., Aikin, K. C., DuRant, J., Warneke, C., Li, S.-M. and de Gouw, J. A.: Diurnal Variability and Emission Pattern of Decamethylcyclopentasiloxane ($D_5$) from the Application of Personal Care Products in Two North American Cities, Environ. Sci. Technol., 52(10), 5610–5618, 2018.

Cohen, A. J., Brauer, M., Burnett, R., Anderson, H. R., Frostad, J., Estep, K., Balakrishnan, K., Brunekreef, B., Dandona, L., Dandona, R., Feigin, V., Freedman, G., Hubbell, B., Jobling, A., Kan, H., Knibbs, L., Liu, Y., Martin, R., Morawska, L., Pope, C. A., Shin, H., Straif, K., Shaddick, G., Thomas, M., van Dingenen, R., van Donkelaar, A., Vos, T., Murray, C. J. L. and Forouzanfar, M. H.: Estimates and 25-year trends of the global burden of disease attributable to ambient air pollution: an analysis of data from the Global Burden of Diseases Study 2015, Lancet, 389(10082), 1907–1918, 2017.

DeCarlo, P. F., Dunlea, E. J., Kimmel, J. R., Aiken, A. C., Sueper, D., Crounse, J., Wennberg, P. O., Emmons, L., Shinozuka, Y., Clarke, A., Zhou, J., Tomlinson, J., Collins, D. R., Knapp, D., Weinheimer, A. J., Montzka, D. D., Campos, T. and Jimenez, J. L.: Fast airborne aerosol size and chemistry measurements above Mexico City and Central Mexico during the MILAGRO

campaign, Atmos. Chem. Phys., 8(14), 4027–4048, 2008.

DeCarlo, P. F., Ulbrich, I. M., Crounse, J., de Foy, B., Dunlea, E. J., Aiken, A. C., Knapp, D., Weinheimer, A. J., Campos, T., Wennberg, P. O. and Jimenez, J. L.: Investigation of the sources and processing of organic aerosol over the Central Mexican Plateau from aircraft measurements during MILAGRO, Atmos. Chem. Phys., 10(12), 5257–5280, 2010.

Dominutti, P., Keita, S., Bahino, J., Colomb, A., Liousse, C., Yoboué, V., Galy-Lacaux, C., Morris, E., Bouvier, L., Sauvage, S. and Borbon, A.: Anthropogenic VOCs in Abidjan, southern West Africa: from source quantification to atmospheric impacts, Atmos. Chem. Phys., 19(18), 11721–11741, 2019.

van Donkelaar, A., Martin, R. V., Brauer, M. and Boys, B. L.: Use of Satellite Observations for Long-Term Exposure Assessment of Global Concentrations of Fine Particulate Matter, Environ. Health Perspect., 123(2), 135–143, 2015.

van Donkelaar, A., Martin, R. V., Brauer, M., Hsu, N. C., Kahn, R. A., Levy, R. C., Lyapustin, A., Sayer, A. M. and Winker, D. M.: Global Estimates of Fine Particulate Matter using a Combined Geophysical-Statistical Method with Information from Satellites, Models, and Monitors, Environ. Sci. Technol., 50(7), 3762–3772, 2016.

Duncan Fairlie, T., Jacob, D. J. and Park, R. J.: The impact of transpacific transport of mineral dust in the United States, Atmos. Environ., 41(6), 1251–1266, 2007.

Dzepina, K., Volkamer, R. M., Madronich, S., Tulet, P., Ulbrich, I. M., Zhang, Q., Cappa, C. D., Ziemann, P. J. and Jimenez, J. L.: Evaluation of recently-proposed secondary organic aerosol models for a case study in Mexico City, Atmos. Chem. Phys., 9(15), 5681–5709, 2009.

EMEP/EEA: EMEP/EEA Air Pollutant Emission Inventory Guidebook 2016, EEA, Luxembourg., 2016.

Ensberg, J. J., Hayes, P. L., Jimenez, J. L., Gilman, J. B., Kuster, W. C., de Gouw, J. A., Holloway, J. S., Gordon, T. D., Jathar, S., Robinson, A. L. and Seinfeld, J. H.: Emission factor ratios, SOA mass yields, and the impact of vehicular emissions on SOA formation, Atmos. Chem. Phys., 14(5), 2383–2397, 2014.

Freney, E. J., Sellegri, K., Canonaco, F., Colomb, A., Borbon, A., Michoud, V., Crumeyrolle, S., Amarouche, N., Bourianne, T., Gomes, L., Prevot, A. S. H., Beekmann, M. and Schwarzenböeck, A.: Characterizing the impact of urban emissions on regional aerosol particles: Airborne measurements during the MEGAPOLI experiment, Atmos. Chem. Phys., 14(3), 1397–1412, 2014.

Gentner, D. R., Isaacman, G., Worton, D. R., Chan, A. W. H., Dallmann, T. R., Davis, L., Liu, S., Day, D. A., Russell, L. M., Wilson, K. R., Weber, R., Guha, A., Harley, R. A. and Goldstein, A. H.: Elucidating secondary organic aerosol from diesel and gasoline vehicles through detailed characterization of organic carbon emissions, Proc. Natl. Acad. Sci. U. S. A., 109(45),

18318–18323, 2012.

Goel, R. and Guttikunda, S. K.: Evolution of on-road vehicle exhaust emissions in Delhi, Atmos. Environ., 105, 78–90, 2015.

de Gouw, J. A. and Jimenez, J. L.: Organic Aerosols in the Earth's Atmosphere, Environ. Sci. Technol., 43(20), 7614–7618, 2009.

de Gouw, J. A., Middlebrook, A. M., Warneke, C., Goldan, P. D., Kuster, W. C., Roberts, J. M., Fehsenfeld, F. C., Worsnop, D. R., Canagaratna, M. R., Pszenny, A. A. P., Keene, W. C., Marchewka, M., Bertman, S. B. and Bates, T. S.: Budget of organic carbon in a polluted atmosphere: Results from the New England Air Quality Study in 2002, J. Geophys. Res. D: Atmos., 110(16), 1–22, 2005.

de Gouw, J. A., Gilman, J. B., Kim, S.-W., Lerner, B. M., Isaacman-VanWertz, G., McDonald, B. C., Warneke, C., Kuster, W. C., Lefer, B. L., Griffith, S. M., Dusanter, S., Stevens, P. S. and Stutz, J.: Chemistry of Volatile Organic Compounds in the Los Angeles basin: Nighttime Removal of Alkenes and Determination of Emission Ratios, J. Geophys. Res.: Atmos., 122(21), 11,843–11,861, 2017.

Grieshop, A. P., Logue, J. M., Donahue, N. M. and Robinson, A. L.: Laboratory investigation of photochemical oxidation of organic aerosol from wood fires 1: measurement and simulation of organic aerosol evolution, Atmos. Chem. Phys., 9(4), 1263–1277, 2009.

Hallquist, M., Wenger, J. C., Baltensperger, U., Rudich, Y., Simpson, D., Claeys, M., Dommen, J., Donahue, N. M., George, C., Goldstein, A. H., Hamilton, J. F., Herrmann, H., Hoffmann, T., Iinuma, Y., Jang, M., Jenkin, M. E., Jimenez, J. L., Kiendler-Scharr, A., Maenhaut, W., McFiggans, G., Mentel, T. F., Monod, A., Prévôt, A. S. H., Seinfeld, J. H., Surratt, J. D., Szmigielski, R. and Wildt, J.: The formation, properties and impact of secondary organic aerosol: current and emerging issues, Atmos. Chem. Phys., 9(14), 5155–5236, 2009.

Hayes, P. L., Ortega, A. M., Cubison, M. J., Froyd, K. D., Zhao, Y., Cliff, S. S., Hu, W. W., Toohey, D. W., Flynn, J. H., Lefer, B. L., Grossberg, N., Alvarez, S., Rappenglück, B., Taylor, J. W., Allan, J. D., Holloway, J. S., Gilman, J. B., Kuster, W. C., de Gouw, J. A., Massoli, P., Zhang, X., Liu, J., Weber, R. J., Corrigan, A. L., Russell, L. M., Isaacman, G., Worton, D. R., Kreisberg, N. M., Goldstein, A. H., Thalman, R., Waxman, E. M., Volkamer, R., Lin, Y. H., Surratt, J. D., Kleindienst, T. E., Offenberg, J. H., Dusanter, S., Griffith, S., Stevens, P. S., Brioude, J., Angevine, W. M. and Jimenez, J. L.: Organic aerosol composition and sources in Pasadena, California, during the 2010 CalNex campaign, J. Geophys. Res. D: Atmos., 118(16), 9233–9257, 2013.

Hayes, P. L., Carlton, A. G., Baker, K. R., Ahmadov, R., Washenfelder, R. A., Alvarez, S., Rappenglück, B., Gilman, J. B., Kuster, W. C., de Gouw, J. A., Zotter, P., Prévôt, A. S. H., Szidat, S., Kleindienst, T. E., Ma, P. K. and Jimenez, J. L.: Modeling the formation and aging of secondary organic aerosols in Los Angeles during CalNex 2010, Atmos. Chem. Phys., 15(10),

5773–5801, 2015.

Heringa, M. F., DeCarlo, P. F., Chirico, R., Tritscher, T., Dommen, J., Weingartner, E., Richter, R., Wehrle, G., Prévôt, A. S. H. and Baltensperger, U.: Investigations of primary and secondary particulate matter of different wood combustion appliances with a high-resolution time-of-flight aerosol mass spectrometer, Atmos. Chem. Phys., 11(12), 5945–5957, 2011.

Herndon, S. C., Onasch, T. B., Wood, E. C., Kroll, J. H., Canagaratna, M. R., Jayne, J. T., Zavala, M. A., Knighton, W. B., Mazzoleni, C., Dubey, M. K., Ulbrich, I. M., Jimenez, J. L., Seila, R., de Gouw, J. A., de Foy, B., Fast, J., Molina, L. T., Kolb, C. E. and Worsnop, D. R.: Correlation of secondary organic aerosol with odd oxygen in Mexico City, Geophys. Res. Lett., 35(15), L15804, 2008.

Hodzic, A. and Jimenez, J. L.: Modeling anthropogenically controlled secondary organic aerosols in a megacity: A simplified framework for global and climate models, Geosci. Model Dev., 4(4), 901–917, 2011.

Hodzic, A., Jimenez, J. L., Madronich, S., Aiken, A. C., Bessagnet, B., Curci, G., Fast, J., Lamarque, J.-F., Onasch, T. B., Roux, G., Schauer, J. J., Stone, E. A. and Ulbrich, I. M.: Modeling organic aerosols during MILAGRO: importance of biogenic secondary organic aerosols, Atmos. Chem. Phys., 9(18), 6949–6981, 2009.

Hodzic, A., Jimenez, J. L., Prévôt, A. S. H., Szidat, S., Fast, J. D. and Madronich, S.: Can 3-D models explain the observed fractions of fossil and non-fossil carbon in and near Mexico City?, Atmos. Chem. Phys., 10(22), 10997–11016, 2010a.

Hodzic, A., Jimenez, J. L., Madronich, S., Canagaratna, M. R., DeCarlo, P. F., Kleinman, L. and Fast, J.: Modeling organic aerosols in a megacity: potential contribution of semi-volatile and intermediate volatility primary organic compounds to secondary organic aerosol formation, Atmos. Chem. Phys., 10(12), 5491–5514, 2010b.

Hu, W., Hu, M., Hu, W., Jimenez, J. L., Yuan, B., Chen, W., Wang, M., Wu, Y., Chen, C., Wang, Z., Peng, J., Zeng, L. and Shao, M.: Chemical composition, sources, and aging process of submicron aerosols in Beijing: Contrast between summer and winter, J. Geophys. Res. D: Atmos., 121(4), 1955–1977, 2016.

Hu, W. W., Hu, M., Yuan, B., Jimenez, J. L., Tang, Q., Peng, J. F., Hu, W., Shao, M., Wang, M., Zeng, L. M., Wu, Y. S., Gong, Z. H., Huang, X. F. and He, L. Y.: Insights on organic aerosol aging and the influence of coal combustion at a regional receptor site of central eastern China, Atmos. Chem. Phys., 13(19), 10095–10112, 2013.

IHME: Global Burden of Disease Study 2015 (GBD 2015) Data Resources, GHDx [online] Available from: http://ghdx.healthdata.org/gbd-2015 (Accessed 2019), 2016.

Jaeglé, L., Quinn, P. K., Bates, T. S., Alexander, B. and Lin, J.-T.: Global distribution of sea salt aerosols: new constraints from in situ and remote sensing observations, Atmos. Chem. Phys.,

11(7), 3137–3157, 2011.

Janssen, R. H. H., Tsimpidi, A. P., Karydis, V. A., Pozzer, A., Lelieveld, J., Crippa, M., Prévôt, A. S. H., Ait-Helal, W., Borbon, A., Sauvage, S. and Locoge, N.: Influence of local production and vertical transport on the organic aerosol budget over Paris, J. Geophys. Res. D: Atmos., 122(15), 8276–8296, 2017.

Janssens-Maenhout, G., Crippa, M., Guizzardi, D., Dentener, F., Muntean, M., Pouliot, G., Keating, T., Zhang, Q., Kurokawa, J., Wankmüller, R., Denier van der Gon, H., Kuenen, J. J. P., Klimont, Z., Frost, G., Darras, S., Koffi, B. and Li, M.: HTAP_v2.2: a mosaic of regional and global emission grid maps for 2008 and 2010 to study hemispheric transport of air pollution, Atmos. Chem. Phys., 15(19), 11411–11432, 2015.

Jathar, S. H., Gordon, T. D., Hennigan, C. J., Pye, H. O. T., Pouliot, G., Adams, P. J., Donahue, N. M. and Robinson, A. L.: Unspeciated organic emissions from combustion sources and their influence on the secondary organic aerosol budget in the United States, Proc. Natl. Acad. Sci. U. S. A., 111(29), 10473–10478, 2014.

Jena, C., Ghude, S. D., Kulkarni, R., Debnath, S., Kumar, R., Soni, V. K., Acharja, P., Kulkarni, S. H., Khare, M., Kaginalkar, A. J., Chate, D. M., Ali, K., Nanjundiah, R. S. and Rajeevan, M. N.: Evaluating the sensitivity of fine particulate matter ($PM_{2.5}$) simulations to chemical mechanism in Delhi, Atmos. Chem. Phys. Discuss., doi:10.5194/acp-2020-673, 2020.

Jimenez, J. L., Canagaratna, M. R., Donahue, N. M., Prevot, A. S. H., Zhang, Q., Kroll, J. H., DeCarlo, P. F., Allan, J. D., Coe, H., Ng, N. L., Aiken, A. C., Docherty, K. S., Ulbrich, I. M., Grieshop, A. P., Robinson, A. L., Duplissy, J., Smith, J. D., Wilson, K. R., Lanz, V. A., Hueglin, C., Sun, Y. L., Tian, J., Laaksonen, A., Raatikainen, T., Rautiainen, J., Vaattovaara, P., Ehn, M., Kulmala, M., Tomlinson, J. M., Collins, D. R., Cubison, M. J., Dunlea, E. J., Huffman, J. A., Onasch, T. B., Alfarra, M. R., Williams, P. I., Bower, K., Kondo, Y., Schneider, J., Drewnick, F., Borrmann, S., Weimer, S., Demerjian, K., Salcedo, D., Cottrell, L., Griffin, R., Takami, A., Miyoshi, T., Hatakeyama, S., Shimono, A., Sun, J. Y., Zhang, Y. M., Dzepina, K., Kimmel, J. R., Sueper, D., Jayne, J. T., Herndon, S. C., Trimborn, A. M., Williams, L. R., Wood, E. C., Middlebrook, A. M., Kolb, C. E., Baltensperger, U. and Worsnop, D. R.: Evolution of organic aerosols in the atmosphere, Science, 326(5959), 1525–1529, 2009.

Khare, P. and Gentner, D. R.: Considering the future of anthropogenic gas-phase organic compound emissions and the increasing influence of non-combustion sources on urban air quality, Atmos. Chem. Phys., 18(8), 5391–5413, 2018.

Kleinman, L. I., Daum, P. H., Lee, Y.-N., Senum, G. I., Springston, S. R., Wang, J., Berkowitz, C., Hubbe, J., Zaveri, R. A., Brechtel, F. J., Jayne, J., Onasch, T. B. and Worsnop, D.: Aircraft observations of aerosol composition and ageing in New England and Mid-Atlantic States during the summer 2002 New England Air Quality Study field campaign, J. Geophys. Res. D: Atmos., 112(D9), D09310, 2007.

Kondo, Y., Morino, Y., Fukuda, M., Kanaya, Y., Miyazaki, Y., Takegawa, N., Tanimoto, H.,

McKenzie, R., Johnston, P., Blake, D. R., Murayama, T. and Koike, M.: Formation and transport of oxidized reactive nitrogen, ozone, and secondary organic aerosol in Tokyo, J. Geophys. Res. D: Atmos., 113(D21), D21310, 2008.

Koo, B., Knipping, E. and Yarwood, G.: 1.5-Dimensional volatility basis set approach for modeling organic aerosol in CAMx and CMAQ, Atmos. Environ., 95, 158–164, 2014.

Krewski, D., Jerrett, M., Burnett, R. T., Ma, R., Hughes, E., Shi, Y., Turner, M. C., Arden, C., Thurston, G., Calle, E. E., Thun, M. J., Beckerman, B., Deluca, P., Finkelstein, N., Ito, K., Moore, D. K., Newbold, K. B., Ramsay, T., Ross, Z., Shin, H. and Tempalski, B.: Extended Follow-Up and Spatial Analysis of the American Cancer Society Study Linking Particulate Air Pollution and Mortality Number 140 May 2009 PRESS VERSION., 2009.

Kuwata, M., Zorn, S. R. and Martin, S. T.: Using Elemental Ratios to Predict the Density of Organic Material Composed of Carbon, Hydrogen, and Oxygen, Environ. Sci. Technol., 46(2), 787–794, 2012.

Lacey, F. G., Henze, D. K., Lee, C. J., van Donkelaar, A. and Martin, R. V.: Transient climate and ambient health impacts due to national solid fuel cookstove emissions, Proc. Natl. Acad. Sci. U. S. A., 114(6), 1269–1274, 2017.

Landrigan, P. J., Fuller, R., Acosta, N. J. R., Adeyi, O., Arnold, R., Basu, N., Baldé, A. B., Bertollini, R., Bose-O'Reilly, S., Boufford, J. I., Breysse, P. N., Chiles, T., Mahidol, C., Coll-Seck, A. M., Cropper, M. L., Fobil, J., Fuster, V., Greenstone, M., Haines, A., Hanrahan, D., Hunter, D., Khare, M., Krupnick, A., Lanphear, B., Lohani, B., Martin, K., Mathiasen, K. V., McTeer, M. A., Murray, C. J. L., Ndahimananjara, J. D., Perera, F., Potočnik, J., Preker, A. S., Ramesh, J., Rockström, J., Salinas, C., Samson, L. D., Sandilya, K., Sly, P. D., Smith, K. R., Steiner, A., Stewart, R. B., Suk, W. A., van Schayck, O. C. P., Yadama, G. N., Yumkella, K. and Zhong, M.: The Lancet Commission on pollution and health, Lancet, 391(10119), 462–512, 2018.

Lelieveld, J., Evans, J. S., Fnais, M., Giannadaki, D. and Pozzer, A.: The contribution of outdoor air pollution sources to premature mortality on a global scale, Nature, 525(7569), 367–371, 2015.

Liao, J., Hanisco, T. F., Wolfe, G. M., St. Clair, J., Jimenez, J. L., Campuzano-Jost, P., Nault, B. A., Fried, A., Marais, E. A., Gonzalez Abad, G., Chance, K., Jethva, H. T., Ryerson, T. B., Warneke, C. and Wisthaler, A.: Towards a satellite formaldehyde – in situ hybrid estimate for organic aerosol abundance, Atmos. Chem. Phys., 19(5), 2765–2785, 2019.

Li, M., Liu, H., Geng, G., Hong, C., Liu, F., Song, Y., Tong, D., Zheng, B., Cui, H., Man, H., Zhang, Q. and He, K.: Anthropogenic emission inventories in China: a review, Natl Sci Rev, 4(6), 834–866, 2017.

Li, M., Zhang, Q., Zheng, B., Tong, D., Lei, Y., Liu, F., Chaopeng, H., Kang, S., Yan, L., Zhang, Y., Bo, Y., Su, H., Cheng, Y. and He, K.: Persistent growth of anthropogenic non-methane volatile organic compound (NMVOC) emissions in China during 1990-2017: drivers, speciation

and ozone formation potential, Atmos. Chem. Phys., 19, 8897–8913, 2019.

Liu, F., Zhang, Q., Tong, D., Zheng, B., Li, M., Huo, H. and He, K. B.: High-resolution inventory of technologies, activities, and emissions of coal-fired power plants in China from 1990 to 2010, Atmos. Chem. Phys., 15(23), 13299–13317, 2015.

Lu, Q., Zhao, Y. and Robinson, A. L.: Comprehensive organic emission profiles for gasoline, diesel, and gas-turbine engines including intermediate and semi-volatile organic compound emissions, Atmos. Chem. Phys., 18, 17637–17654, 2018.

Ma, P. K., Zhao, Y., Robinson, A. L., Worton, D. R., Goldstein, A. H., Ortega, A. M., Jimenez, J. L., Zotter, P., Prévôt, A. S. H., Szidat, S. and Hayes, P. L.: Evaluating the impact of new observational constraints on P-S/IVOC emissions, multi-generation oxidation, and chamber wall losses on SOA modeling for Los Angeles, CA, Atmos. Chem. Phys., 17(15), 9237–9259, 2017.

Marais, E. A., Jacob, D. J., Jimenez, J. L., Campuzano-Jost, P., Day, D. A., Hu, W., Krechmer, J., Zhu, L., Kim, P. S., Miller, C. C., Fisher, J. A., Travis, K., Yu, K., Hanisco, T. F., Wolfe, G. M., Arkinson, H. L., Pye, H. O. T., Froyd, K. D., Liao, J. and McNeill, V. F.: Aqueous-phase mechanism for secondary organic aerosol formation from isoprene: application to the southeast United States and co-benefit of $SO_2$ emission controls, Atmos. Chem. Phys., 16(3), 1603–1618, 2016.

McDonald, B. C., de Gouw, J. A., Gilman, J. B., Jathar, S. H., Akherati, A., Cappa, C. D., Jimenez, J. L., Lee-Taylor, J., Hayes, P. L., McKeen, S. A., Cui, Y. Y., Kim, S.-W., Gentner, D. R., Isaacman-VanWertz, G., Goldstein, A. H., Harley, R. A., Frost, G. J., Roberts, J. M., Ryerson, T. B. and Trainer, M.: Volatile chemical products emerging as largest petrochemical source of urban organic emissions, Science, 359(6377), 760–764, 2018.

Miyakawa, T., Takegawa, N. and Kondo, Y.: Photochemical evolution of submicron aerosol chemical composition in the Tokyo megacity region in summer, J. Geophys. Res. D: Atmos., 113(D14), D14304, 2008.

Molina, L. T., Kolb, C. E., de Foy, B., Lamb, B. K., Brune, W. H., Jimenez, J. L., Ramos-Villegas, R., Sarmiento, J., Paramo-Figueroa, V. H., Cardenas, B., Gutierrez-Avedoy, V. and Molina, M. J.: Air quality in North America's most populous city – overview of the MCMA-2003 campaign, Atmos. Chem. Phys., 7(10), 2447–2473, 2007.

Molina, L. T., Madronich, S., Gaffney, J. S., Apel, E., de Foy, B., Fast, J., Ferrare, R., Herndon, S., Jimenez, J. L., Lamb, B., Osornio-Vargas, A. R., Russell, P., Schauer, J. J., Stevens, P. S., Volkamer, R. and Zavala, M.: An overview of the MILAGRO 2006 Campaign: Mexico City emissions and their transport and transformation, Atmos. Chem. Phys., 10(18), 8697–8760, 2010.

Morino, Y., Tanabe, K., Sato, K. and Ohara, T.: Secondary organic aerosol model intercomparison based on secondary organic aerosol to odd oxygen ratio in Tokyo, J. Geophys. Res.: Atmos., 119(23), 13,489–13,505, 2014.

Nault, B. A., Campuzano-Jost, P., Day, D. A., Schroder, J. C., Anderson, B., Beyersdorf, A. J., Blake, D. R., Brune, W. H., Choi, Y., Corr, C. A., de Gouw, J. A., Dibb, J., DiGangi, J. P., Diskin, G. S., Fried, A., Huey, L. G., Kim, M. J., Knote, C. J., Lamb, K. D., Lee, T., Park, T., Pusede, S. E., Scheuer, E., Thornhill, K. L., Woo, J.-H. and Jimenez, J. L.: Secondary Organic Aerosol Production from Local Emissions Dominates the Organic Aerosol Budget over Seoul, South Korea, during KORUS-AQ, Atmos. Chem. Phys., 18, 17769–17800, 2018.

Pai, S. J., Heald, C. L., Pierce, J. R., Farina, S. C., Marais, E. A., Jimenez, J. L., Campuzano-Jost, P., Nault, B. A., Middlebrook, A. M., Coe, H., Shilling, J. E., Bahreini, R., Dingle, J. H. and Vu, K.: An evaluation of global organic aerosol schemes using airborne observations, Atmos. Chem. Phys., 20(5), 2637–2665, 2020.

Pankow, J. F. and Asher, W. E.: SIMPOL.1: a simple group contribution method for predicting vapor pressures and enthalpies of vaporization of multifunctional organic compounds, Atmos. Chem. Phys., 8(10), 2773–2796, 2008.

Park, R. J., Jacob, D. J., Palmer, P. I., Clarke, A. D., Weber, R. J., Zondlo, M. A., Eisele, F. L., Bandy, A. R., Thornton, D. C., Sachse, G. W. and Bond, T. C.: Export efficiency of black carbon aerosol in continental outflow: Global implications, J. Geophys. Res. D: Atmos., 110(D11), D11205, 2005.

Park, R. J., Jacob, D. J., Kumar, N. and Yantosca, R. M.: Regional visibility statistics in the United States: Natural and transboundary pollution influences, and implications for the Regional Haze Rule, Atmos. Environ., 40(28), 5405–5423, 2006.

Parrish, D. D., Kuster, W. C., Shao, M., Yokouchi, Y., Kondo, Y., Goldan, P. D., de Gouw, J. A., Koike, M. and Shirai, T.: Comparison of air pollutant emissions among mega-cities, Atmos. Environ., 43(40), 6435–6441, 2009.

Peng, Z. and Jimenez, J. L.: KinSim: A Research-Grade, User-Friendly, Visual Kinetics Simulator for Chemical-Kinetics and Environmental-Chemistry Teaching, J. Chem. Educ., 96(4), 806–811, 2019.

Platt, S. M., Haddad, I. E., Pieber, S. M., Huang, R.-J., Zardini, A. A., Clairotte, M., Suarez-Bertoa, R., Barmet, P., Pfaffenberger, L., Wolf, R., Slowik, J. G., Fuller, S. J., Kalberer, M., Chirico, R., Dommen, J., Astorga, C., Zimmermann, R., Marchand, N., Hellebust, S., Temime-Roussel, B., Baltensperger, U. and Prévôt, A. S. H.: Two-stroke scooters are a dominant source of air pollution in many cities, Nat. Commun., 5(1), 3749, 2014.

Pollack, I. B., Ryerson, T. B., Trainer, M., Neuman, J. A., Roberts, J. M. and Parrish, D. D.: Trends in ozone, its precursors, and related secondary oxidation products in Los Angeles, California: A synthesis of measurements from 1960 to 2010, J. Geophys. Res. D: Atmos., 118(11), 5893–5911, 2013.

Punger, E. M. and West, J. J.: The effect of grid resolution on estimates of the burden of ozone and fine particulate matter on premature mortality in the USA, Air Qual. Atmos. Health, 6(3),

563–573, 2013.

Pye, H. O. T. and Seinfeld, J. H.: A global perspective on aerosol from low-volatility organic compounds, Atmos. Chem. Phys., 10, 4377–4401, 2010.

Ridley, D. A., Heald, C. L., Ridley, K. J. and Kroll, J. H.: Causes and consequences of decreasing atmospheric organic aerosol in the United States, Proc. Natl. Acad. Sci. U. S. A., 115(2), 290–295, 2018.

Robinson, A. L., Donahue, N. M., Shrivastava, M. K., Weitkamp, E. A., Sage, A. M., Grieshop, A. P., Lane, T. E., Pierce, J. R. and Pandis, S. N.: Rethinking Organic Aerosols: Semivolatile Emissions and Photochemical Aging, Science, 315(5816), 1259–1262, 2007.

Rumble, J. R., Ed.: CRC Handbook of Chemistry and Physics, 100th Edition, 2019 - 2020, Taylor & Francis Group., 2019.

Ryerson, T. B., Andrews, A. E., Angevine, W. M., Bates, T. S., Brock, C. A., Cairns, B., Cohen, R. C., Cooper, O. R., de Gouw, J. A., Fehsenfeld, F. C., Ferrare, R. A., Fischer, M. L., Flagan, R. C., Goldstein, A. H., Hair, J. W., Hardesty, R. M., Hostetler, C. A., Jimenez, J. L., Langford, A. O., McCauley, E., McKeen, S. A., Molina, L. T., Nenes, A., Oltmans, S. J., Parrish, D. D., Pederson, J. R., Pierce, R. B., Prather, K., Quinn, P. K., Seinfeld, J. H., Senff, C. J., Sorooshian, A., Stutz, J., Surratt, J. D., Trainer, M., Volkamer, R., Williams, E. J. and Wofsy, S. C.: The 2010 California Research at the Nexus of Air Quality and Climate Change (CalNex) field study, J. Geophys. Res. D: Atmos., 118(11), 5830–5866, 2013.

Sacks, J., Buckley, B., Alexis, N., Angrish, M., Beardslee, R., Benson, A., Brown, J., Buckley, B., Campen, M., Chan, E., Coffman, E., Davis, A., Dutton, S. J., Eftim, S., Gandy, J., Hemming, B. L., Hines, E., Holliday, K., Kerminen, V.-M., Kiomourtzoglou, M.-A., Kirrane, E., Kotchmar, D., Koturbash, I., Kulmala, M., Lassiter, M., Limaye, V., Ljungman, P., Long, T., Luben, T., Malm, W., McDonald, J. F., McDow, S., Mickley, L., Mikati, I., Mulholland, J., Nichols, J., Patel, M. M., Pinder, R., Pinto, J. P., Rappazzo, K., Richomond-Bryant, J., Rosa, M., Russell, A., Schichtel, B., Stewart, M., Stanek, L. W., Turner, M., Van Winkle, L., Wagner, J., Weaver, Christopher, Wellenius, G., Whitsel, E., Yeckel, C., Zanobetti, A. and Zhang, M.: Integrated Science Assessment (ISA) for Particulate Matter (Final Report, Dec 2019), Environmental Protection Agency. [online] Available from: https://cfpub.epa.gov/ncea/isa/recordisplay.cfm?deid=347534 (Accessed 20 October 2020), 2019.

Schroder, J. C., Campuzano-Jost, P., Day, D. A., Shah, V., Larson, K., Sommers, J. M., Sullivan, A. P., Campos, T., Reeves, J. M., Hills, A., Hornbrook, R. S., Blake, N. J., Scheuer, E., Guo, H., Fibiger, D. L., McDuffie, E. E., Hayes, P. L., Weber, R. J., Dibb, J. E., Apel, E. C., Jaeglé, L., Brown, S. S., Thronton, J. A. and Jimenez, J. L.: Sources and Secondary Production of Organic Aerosols in the Northeastern US during WINTER, J. Geophys. Res. D: Atmos., doi:10.1029/2018JD028475, 2018.

Seinfeld, J. H. and Pandis, S. N.: Atmospheric Chemistry and Physics: From Air Pollution to

Climate Change, Second., John Wiley & Sons, Inc., Hoboken, NJ USA., 2006.

Shaddick, G., Thomas, M. L., Amini, H., Broday, D., Cohen, A., Frostad, J., Green, A., Gumy, S., Liu, Y., Martin, R. V., Pruss-Ustun, A., Simpson, D., van Donkelaar, A. and Brauer, M.: Data Integration for the Assessment of Population Exposure to Ambient Air Pollution for Global Burden of Disease Assessment, Environ. Sci. Technol., 52(16), 9069–9078, 2018.

Shah, V., Jaeglé, L., Thornton, J. A., Lopez-Hilfiker, F. D., Lee, B. H., Schroder, J. C., Campuzano-Jost, P., Jimenez, J. L., Guo, H., Sullivan, A. P., Weber, R. J., Green, J. R., Fiddler, M. N., Bililign, S., Campos, T. L., Stell, M., Weinheimer, A. J., Montzka, D. D. and Brown, S. S.: Chemical feedbacks weaken the wintertime response of particulate sulfate and nitrate to emissions reductions over the eastern United States, Proc. Natl. Acad. Sci. U. S. A., 115(32), 8110–8115, 2018.

Shah, V., Jaeglé, L., Jimenez, J. L., Schroder, J. C., Campuzano-Jost, P., Campos, T. L., Reeves, J. M., Stell, M., Brown, S. S., Lee, B. H., Lopez-Hilfiker, F. D. and Thornton, J. A.: Widespread Pollution from Secondary Sources of Organic Aerosols during Winter in the Northeastern United States, Geophys. Res. Lett., doi:10.1029/2018GL081530, 2019.

Shrivastava, M., Cappa, C. D., Fan, J., Goldstein, A. H., Guenther, A. B., Jimenez, J. L., Kuang, C., Laskin, A., Martin, S. T., Ng, N. L., Petaja, T., Pierce, J. R., Rasch, P. J., Roldin, P., Seinfeld, J. H., Shilling, J., Smith, J. N., Thornton, J. A., Volkamer, R., Wang, J., Worsnop, D. R., Zaveri, R. A., Zelenyuk, A. and Zhang, Q.: Recent advances in understanding secondary organic aerosol: Implications for global climate forcing, Rev. Geophys., 55(2), 509–559, 2017.

Silva, R. A., Adelman, Z., Fry, M. M. and West, J. J.: The Impact of Individual Anthropogenic Emissions Sectors on the Global Burden of Human Mortality due to Ambient Air Pollution, Environ. Health Perspect., 124(11), 1776–1784, 2016.

Singh, A., Satish, R. V. and Rastogi, N.: Characteristics and sources of fine organic aerosol over a big semi-arid urban city of western India using HR-ToF-AMS, Atmos. Environ., 208, 103–112, 2019.

Stewart, G. J., Nelson, B. S., Acton, W. J. F., Vaughan, A. R., Farren, N. J., Hopkins, J. R., Ward, M. W., Swift, S. J., Arya, R., Mondal, A., Jangirh, R., Ahlawat, S., Yadav, L., Sharma, S. K., Yunus, S. S. M., Hewitt, C. N., Nemitz, E., Mullinger, N., Gadi, R., Sahu, L. K., Tripathi, N., Rickard, A. R., Lee, J. D., Mandal, T. K. and Hamilton, J. F.: Emissions of intermediate-volatility and semi-volatile organic compounds from domestic fuels used in Delhi, India, Atmos. Chem. Phys. Discuss., doi:10.5194/acp-2020-860, 2020.

The International GEOS-Chem User Community: geoschem/geos-chem: GEOS-Chem 12.0.0 release, , doi:10.5281/ZENODO.1343547, 2018.

Toon, O. B., Maring, H., Dibb, J., Ferrare, R., Jacob, D. J., Jensen, E. J., Luo, Z. J., Mace, G. G., Pan, L. L., Pfister, L., Rosenlof, K. H., Redemann, J., Reid, J. S., Singh, H. B., Thompson, A. M., Yokelson, R., Minnis, P., Chen, G., Jucks, K. W. and Pszenny, A.: Planning, implementation,

and scientific goals of the Studies of Emissions and Atmospheric Composition, Clouds and Climate Coupling by Regional Surveys (SEAC$^4$RS) field mission, J. Geophys. Res. D: Atmos., 121(9), 4967–5009, 2016.

Tsimpidi, A. P., Karydis, V. A., Zavala, M., Lei, W., Molina, L., Ulbrich, I. M., Jimenez, J. L. and Pandis, S. N.: Evaluation of the volatility basis-set approach for the simulation of organic aerosol formation in the Mexico City metropolitan area, Atmos. Chem. Phys., 10(2), 525–546, 2010.

Vaden, T. D., Imre, D., Beránek, J., Shrivastava, M. and Zelenyuk, A.: Evaporation kinetics and phase of laboratory and ambient secondary organic aerosol, Proc. Natl. Acad. Sci. U. S. A., 108(6), 2190–2195, 2011.

Wang, L., Slowik, J. G., Tripathi, N., Bhattu, D., Rai, P., Kumar, V., Vats, P., Satish, R., Baltensperger, U., Ganguly, D., Rastogi, N., Sahu, L. K., Tripathi, S. N. and Prévôt, A. S. H.: Source characterization of volatile organic compounds measured by proton-transfer-reaction time-of-flight mass spectrometers in Delhi, India, Atmos. Chem. Phys., 20(16), 9753–9770, 2020.

Wang, M., Shao, M., Chen, W., Yuan, B., Lu, S., Zhang, Q., Zeng, L. and Wang, Q.: A temporally and spatially resolved validation of emission inventories by measurements of ambient volatile organic compounds in Beijing, China, Atmos. Chem. Phys., 14(12), 5871–5891, 2014.

Wang, Y. Q., Zhang, X. Y., Sun, J. Y., Zhang, X. C., Che, H. Z. and Li, Y.: Spatial and temporal variations of the concentrations of $PM_{10}$, $PM_{2.5}$ and $PM_1$ in China, Atmos. Chem. Phys., 15, 13585–13598, 2015.

Warneke, C., McKeen, S. A., de Gouw, J. A., Goldan, P. D., Kuster, W. C., Holloway, J. S., Williams, E. J., Lerner, B. M., Parrish, D. D., Trainer, M., Fehsenfeld, F. C., Kato, S., Atlas, E. L., Baker, A. and Blake, D. R.: Determination of urban volatile organic compound emission ratios and comparison with an emissions database, J. Geophys. Res. D: Atmos., 112(D10), doi:10.1029/2006JD007930, 2007.

Warneke, C., de Gouw, J. A., Holloway, J. S., Peischl, J., Ryerson, T. B., Atlas, E., Blake, D., Trainer, M. and Parrish, D. D.: Multiyear trends in volatile organic compounds in Los Angeles, California: Five decades of decreasing emissions, J. Geophys. Res. D: Atmos., 117(D21), D00V17, 2012.

Wood, E. C., Canagaratna, M. R., Herndon, S. C., Onasch, T. B., Kolb, C. E., Worsnop, D. R., Kroll, J. H., Knighton, W. B., Seila, R., Zavala, M., Molina, L. T., Decarlo, P. F., Jimenez, J. L., Weinheimer, A. J., Knapp, D. J., Jobson, B. T., Stutz, J., Kuster, W. C. and Williams, E. J.: Investigation of the correlation between odd oxygen and secondary organic aerosol in Mexico City and Houston, Atmos. Chem. Phys., 10(18), 8947–8968, 2010.

Worton, D. R., Isaacman, G., Gentner, D. R., Dallmann, T. R., Chan, A. W. H., Ruehl, C., Kirchstetter, T. W., Wilson, K. R., Harley, R. A. and Goldstein, A. H.: Lubricating Oil Dominates Primary Organic Aerosol Emissions from Motor Vehicles, Environ. Sci. Technol., 48(7),

3698–3706, 2014.

Zhang, Q., Alfarra, M. R., Worsnop, D. R., James, D., Coe, H., Canagaratna, M. R. and Jimenez, J. L.: Deconvolution and Quantification of Hydrocarbon-like and Oxygenated Organic Aerosols Based on Aerosol Mass Spectrometry Deconvolution and Quantification of Hydrocarbon-like and Oxygenated Organic Aerosols Based on Aerosol Mass Spectrometry, Environ. Sci. Technol., 39(13), 4938–4952, 2005.

Zhang, Q., Streets, D. G., Carmichael, G. R., He, K. B., Huo, H., Kannari, A., Klimont, Z., Park, I. S., Reddy, S., Fu, J. S., Chen, D., Duan, L., Lei, Y., Wang, L. T. and Yao, Z. L.: Asian emissions in 2006 for the NASA INTEX-B mission, Atmos. Chem. Phys., 9(14), 5131–5153, 2009.

Zhang, Q. J., Beekmann, M., Freney, E., Sellegri, K., Pichon, J. M., Schwarzenboeck, A., Colomb, A., Bourrianne, T., Michoud, V. and Borbon, A.: Formation of secondary organic aerosol in the Paris pollution plume and its impact on surrounding regions, Atmos. Chem. Phys., 15(24), 13973–13992, 2015.

Zhao, Y., Hennigan, C. J., May, A. A., Daniel, S., Gouw, J. A. D., Gilman, J. B., Kuster, W. C. and Robinson, A. L.: Intermediate-Volatility Organic Compounds: A Large Source of Secondary Organic Aerosol, Environ. Sci. Technol, 48(23), 13743–13750, 2014.

Zhao, Y., Saleh, R., Saliba, G., Presto, A. A., Gordon, T. D., Drozd, G. T., Goldstein, A. H., Donahue, N. M. and Robinson, A. L.: Reducing secondary organic aerosol formation from gasoline vehicle exhaust, Proc. Natl. Acad. Sci. U. S. A., 114(27), 6984–6989, 2017.

Zheng, B., Huo, H., Zhang, Q., Yao, Z. L., Wang, X. T., Yang, X. F., Liu, H. and He, K. B.: High-resolution mapping of vehicle emissions in China in 2008, Atmos. Chem. Phys., 14(18), 9787–9805, 2014.

Zheng, B., Tong, D., Li, M., Liu, F., Hong, C., Geng, G., Li, H., Li, X., Peng, L., Qi, J., Yan, L., Zhang, Y., Zhao, H., Zheng, Y., He, K. and Zhang, Q.: Trends in China's anthropogenic emissions since 2010 as the consequence of clean air actions, Atmos. Chem. Phys., 18(19), 14095–14111, 2018.

**Supplemental Information for:**

# Anthropogenic Secondary Organic Aerosols Contribute Substantially to Air Pollution Mortality

Benjamin A. Nault et al.

Correspondence: Jose L. Jimenez (jose.jimenez@colorado.edu)

## S1 Emission Inventories for Various Urban Areas around the World

All BTEX (benzene, toluene, ethylbenzene, and xylenes) and non-BTEX aromatic emissions are shown in Table S5 (BTEX) or Table S8 (non-BTEX aromatics). The emission ratios are derived from ambient measurements utilizing photochemical aging techniques (Nault et al., 2018).

Details of the emission inventories for cities in the US, for Beijing, and for London/UK used here to estimate the IVOC:BTEX emission ratio (Fig. 5) and thus the IVOC emissions can be found below. Briefly, emissions for the US are based on McDonald et al. (2018), for China on the Multi-resolution Emission Inventory for China (MEIC) (Zhang et al., 2009; Zheng et al., 2014, 2018; Liu et al., 2015; Li et al., 2017, 2019), and for the UK on the National Atmospheric Emissions Inventory (NAEI) (EMEP/EEA, 2016). The IVOC:BTEX emission ratio from inventories are multiplied with the observed BTEX, either reported value from studies (NE US aircraft (Warneke et al. 2007), Los Angeles (de Gouw et al. 2017), Beijing (Wang et al. 2014), and New York City (Warneke et al. 2007)) or estimated from Eq. 3 (London), measured in urban air to estimate IVOCs emitted in each region (Table S5), including North America, Europe, and Asia. This ensures IVOC emissions used in our calculations properly reflect differences in mixtures of emission sources (e.g., mobile sources versus VCPs) that vary by continent for each field campaign. Additionally, we rely on inventories for estimating atmospheric abundances of IVOCs because it has been challenging to measure the full range of IVOC precursors that are emitted into urban air due to many of the IVOCs from VCPs being oxygenated VOCs. These compounds are challenging to measure using traditional instrumentation (e.g., gas chromatography-mass spectrometry), leading to potential underestimation of the IVOC emission

ratios (Zhao et al., 2014, 2017; Lu et al., 2018). The bottom-up IVOC:BTEX ratios for the US, Beijing, and UK are described in greater detail below. IVOC emissions are classified based on their vapor pressure (effective saturation concentration: $10^3 < C^* < 10^6$ μg $m^{-3}$), with the vapor pressure estimated by the SIMPOL.1 model (Pankow and Asher, 2008). The ASOA yields and rate constants for IVOC oxidation were parameterized with data from n-tridecane and n-pentadecane for gasoline and diesel emissions, respectively (Jathar et al. 2014), and for VCPs, the yields and rate constants for IVOC oxidation were parameterized with data from n-tetradecane (McDonald et al. 2018).

Similar to IVOCs, the ability to measure the full range of SVOCs emitted into urban air is challenging. Therefore, we estimate SVOC emission ratios relative to POA mass concentrations (Table S9), as described by Ma et al. (2017). For the hydrocarbon-like portion, we used the volatility distribution from Worton et al. (2014) to estimate SVOC, as this is associated with fossil fuel emissions from transportation (Zhang et al., 2005). For the other POA, we used the volatility distribution from Robinson et al. (2007), as this POA is typically cooking primary aerosol. These profiles were selected to be consistent with Ma et al. (2017).

To estimate the SVOC mass concentration in equilibrium with the POA (Table S9) in each bin, the POA mass concentration is first multiplied by the fraction of POA measured in each bin from literature. This yields the concentration of POA for that specific volatility bin. Then the total POA + SVOC concentration for that bin is obtained divided by the amount of material found in the particle phase for that bin for the average temperature (~298 K) and OA mass concentration (~10 μg $m^{-3}$). Then, the gas-phase SVOC concentration is calculated by

multiplying the total concentration by the gas-phase fraction. Thus, e.g., SVOC in the C* = 100 μg $m^{-3}$ bin, ~91% of the SVOC mass will be found in the gas-phase.

Fig. S6 shows the calculated emission ratio versus saturation concentration (c*) for the cities with emission inventories. The saturation concentration for SVOC was determined as part of the estimation procedure discussed above. For IVOC, the emission ratios for the different sources (gasoline, diesel, other fossil fuel sources, and VCP emissions) were split into the volatility bins, as in McDonald et al. (2018). Finally, for BTEX and non-BTEX aromatics, and other VOC emission ratios (see Fig. S6 for references for the other VOC emission ratios), CRC (Rumble, 2019) or SIMPOL.1 (Pankow and Asher, 2008) (for estimating vapor pressures not in CRC) was used to estimate the saturation concentrations.

## ~~Section~~ S1.1 US Emission Inventories

*Anthropogenic VOC emissions*

The US emissions of VOCs is based on a mass balance estimate of the petrochemical industry reported by McDonald et al. (2018). Briefly, fuel sales and chemical product use are estimated from publicly available reports on energy use, chemical production, economic surveys, and freight shipments. Mobile source emission factors are from prior work quantifying both on-road and off-road engines (McDonald et al., 2013, 2015). Evaporative sources of transportation fuels are considered in addition to tailpipe exhaust (Pierson et al., 1999). VCP emission factors are based on literature values, including from the indoor environment, and reported in McDonald et al. (2018). Other fossil energy sources of VOCs, such as from oil refineries and industry, are taken from official inventories reported by the California Air

Resources Board (CARB, 2013) or US Environmental Protection Agency (NEI, 2015). McDonald et al. (2018) reported fossil-VOC emissions for the Los Angeles basin in the year 2010.

*Speciation of VOC emissions*

The total VOC emissions are speciated to estimate BTEX and IVOC emissions from petrochemical VOC sources. Briefly, gasoline and diesel exhaust, gasoline fuel, and headspace vapors are based on profiles reported in the literature from the Caldecott Tunnel (Gentner et al., 2012, 2013). Speciation profiles of VCPs are based on California Air Resources Board surveys of architectural coatings (Davis, 2007) and consumer products (CCPR, 2015). Other industrial solvent uses and point/area source emissions are from the EPA SPECIATE (v4.4) database (EPA, 2014).

*Extrapolating IVOC/BTEX ratios from 2010 Los Angeles to other field campaigns*

In the ASOA mass closure estimation, three separate field campaigns are utilized from the US: NEAQS 2002 (Boston/New York City), CalNex 2010 (Los Angeles), and WINTER 2015 (New York City outflow). These field campaigns span two megacities (Los Angeles and New York City), ~one decade, and two seasons (summer versus winter). Here, we discuss how each of these variables could affect the IVOC/BTEX emissions ratio. We focus the discussion on mobile sources and VCPs because these are the dominant contributors to BTEX and IVOCs.

The IVOC/BTEX emissions ratio could be affected by the population density of a city. It is well-established that per capita transportation fuel use decreases with increasing population

density (Gately et al., 2015), whereas VCP usage is expected to scale with population. Relative to Los Angeles, the per capita fuel use in New York City is ~2 times lower (Gately et al., 2015), resulting in lower on-road transportation VOC emissions relative to VCPs. Because aromatics are mainly found in gasoline, whereas the IVOCs have a higher contribution from VCPs, the IVOC/BTEX ratio is expected to be higher in New York City than Los Angeles.

To assess impacts of annual trends on the IVOC/BTEX ratio, we utilize long-term trend analyses of mobile source VOC emissions in Los Angeles (McDonald et al., 2013, 2015; Hassler et al., 2016). The main effect is that on-road gasoline emissions have decreased with time, both from the tailpipe of vehicles (McDonald et al., 2013) and of gasoline-related VOCs in ambient air measurements (Warneke et al., 2012). We utilize the EPA Trends Report to scale VOC emissions for other anthropogenic sectors, including VCPs and industrial sources (https://www.epa.gov/air-emissions-inventories/air-pollutant-emissions-trends-data). The EPA Trends Report suggests that VCP (or solvent) emissions decreased by ~30% between 2002 and 2010, including efforts to reduce the VOC content of architectural coatings (Matheson, 2002). After 2010, the emissions have been slightly increasing, likely due to population growth. Because both mobile sources and VCP emissions are decreasing with time, the IVOC/BTEX emissions ratio is not significantly altered.

Lastly, the effects of seasonality influence on-road transportation emissions through: (i) increased VOC emissions in winter relative to summer from cold-starting engines, and (ii) lower evaporative emissions due to colder ambient temperatures. We estimate that exhaust emissions from passenger vehicles increases by ~50% due to higher cold-start emissions in winter relative to summer based on the EPA MOVES model (MOVES, 2015). Evaporated gasoline and

headspace vapors are known to exhibit a temperature-dependence (Rubin et al., 2006), and estimated to be ~20% and ~80% lower, respectively, based on typical wintertime temperatures of New York City relative to summertime Los Angeles. Due to compensating factors between cold-start engines and evaporated fuels, the IVOC/BTEX emissions are not significantly affected by seasonality.

Overall, when taking into account differences in population density between Los Angeles and New York City, trends of mobile source and VCP emissions over time, and seasonality, the IVOC/BTEX emission ratios range between ~2.3 to 2.7, which is a relatively small range. This sensitivity analysis helps explain why the enhancement observed in SOA scales with BTEX levels in the urban atmosphere.

## ~~Section~~ S1.2 Beijing Emission Inventory

*Anthropogenic VOC emissions*

The total VOC emissions of Beijing were developed following the bottom-up framework of the Multi-resolution Emission Inventory for China (MEIC) model (available at http://www.meicmodel.org), based on a technology-based methodology. The details of activity rates, emission factors, technology distribution, and control measures configured in the MEIC model are summarized in a series of papers (Zhang et al., 2009; Zheng et al., 2014, 2018; Liu et al., 2015; Li et al., 2017, 2019).

In the MEIC model, a detailed four-level source classification system, representing sector, fuel/product, technology/solvent type, and end-of-pipe pollutant abatement facilities, was established by including over 700 emitting sources for each province. All anthropogenic sources,

including power plants, industrial sources, volatile chemical products, fossil fuel burning in residential stoves, transportation were all considered.

Power plants are treated as point sources in the MEIC model. The VOC emissions were derived from the China coal-fired Power Plant Emissions Database (CPED, (Liu et al., 2015)), which is developed based on information of each unit on fuel type, fuel quality, combustion technology, etc.

Volatile chemical products are comprised of solvent use applied for architecture, vehicles, wood, and other industrial purposes, glue use, printing, pesticide use, and domestic solvent use. The market share of waterborne and solvent-based paint is further taken into account for each source category. For the on-road transportation sector, the improved emissions developed by Zheng et al. (2014) were integrated into the framework of MEIC, which estimated the vehicle population and emission factors at a county level. Both the VOC emissions in running mode and evaporation were considered. Emission standards covering pre-Euro I and Euro I to Euro V in Beijing were applied for each vehicle type (Zheng et al., 2018; Li et al., 2019). Regarding oxygenated volatile organic compounds (OVOCs), the emission factors for on-road vehicles were corrected, as current emission factors are only for non-methane hydrocarbons (NMHC). Correction ratios of 1.32, 1.08, 1.10, and 1.06 were applied for heavy-duty and light-duty diesel vehicles, and heavy-duty and light-duty gasoline vehicles, respectively, to the original values to comply with the follow-up speciation for the total VOC, following the method of Li et al. (2014, 2019).

*Speciation of VOC emissions*

Emissions by individual chemical species were developed based on the profile-assignment approach (Li et al., 2014, 2019). First, a "composite" profile database for China was established by integrating the local profiles and supplementing it with the SPECIATE v4.5 database for absent sources ((Simon et al., 2010), available at: https://www.epa.gov/air-emissions-modeling/speciate-version-45-through-40). The detailed procedure for developing the composite profile database is illustrated in Li et al. (2014). In brief, for sources where there are significant differences in technology or legislation between China and western countries, only local profiles are used; otherwise, all candidate profiles are included for further compilation in the composite profile database. Local profiles covering most of the important sources were gathered and reviewed, including biofuel combustion, coal combustion, asphalt production, oil production, refinery, paint use, gasoline evaporation, gasoline vehicle exhaust, diesel vehicles, and so on, as detailed illustrated in Li et al. (2019).

Then, profiles for all combustion-related sources, including fossil fuel combustion in power plants, industry, residential, and transportation sectors were reviewed, and incomplete profiles that were absent from the OVOC fractions were corrected by appending the component of "OVOC" with fractions derived from the "complete" profiles for the same source. After OVOC correction, all "candidate" profiles were averaged by species to establish the composite profile database. Finally, the composite profile to each source was assigned by setting up the source linkage between the profile database and the inventory. Emissions by individual chemical species for each source were then further developed.

**~~Section~~ S1.3 London/United Kingdom Emission Inventory**

*Anthropogenic VOC emissions*

The National Atmospheric Emissions Inventory (NAEI) estimates UK emissions of VOCs from anthropogenic sources following methods in the EMEP/EEA Emissions Inventory Guidebook (EMEP/EEA, 2016) for submission under the revised EU Directive 2016/2284/EU on National Emissions Ceilings (NECD), available at: https://eur-lex.europa.eu/legal-content/EN/TXT/PDF/?uri=CELEX:32016L2284&from=EN, and the United Nations Economic Commission for Europe (UNECE) Convention on Long-Range Transboundary Air Pollution (CLRTAP), available at: http://www.ceip.at/ms/ceip_home1/ceip_home/reporting_instructions/reporting_programme/. The NECD and CLRTAP define those VOC sources to be included and excluded from the national inventory (for example, emissions of NMVOCs from biogenic sources are not included). The Guidebook provides estimation methodologies and default emission factors for each source category, although countries can use country-specific emission factors where these are deemed relevant. The NAEI currently covers organic emissions from around 400 individual source categories, with a large contribution from a diverse range of industrial processes and solvents, but with very few individually dominant sources. The inventory then speciates emissions into ~650 individual compounds, or groups of compounds. Groupings of organics, for example, expressed as 'sum of all C14 compounds,' make up a substantial fraction of IVOC emissions, rather than being reported as individual compounds.

Emissions from the use of solvents and other volatile chemicals in industry and in consumer products, fuel production and distribution, food and drink manufacture and other non-combustion industrial processes accounted for 72% of all UK NMVOC emissions in 2017,

according to the NAEI. Both the solvent and industrial process sectors cover a diverse range of emission source categories: the NAEI identifies 136 separate categories across the two sectors

For the road transport sector, the NAEI reports exhaust emissions of NMVOCs and its emissions from evaporative losses of fuel vapor from petrol vehicles. Emissions from re-fueling at filling stations are reported separately under the fugitive emissions from the fuel distribution sector. The method used for road transport in the NAEI follows the method in the European COPERT 5 model and described in the EMEP/EEA Emissions Inventory Guidebook. The method uses average speed-related emission factors for hot exhaust emissions of total hydrocarbons for detailed vehicle categories (vehicle type, weight and/or engine size) and Euro standards for petrol cars, diesel cars, petrol and diesel light goods vehicles, rigid and articulated HGVs, buses and coaches, and mopeds and motorcycles, and combines these with detailed traffic and fleet activity data derived from information provided by DfT. Separate estimates are made of methane emissions for each vehicle type and subtracted from the THC emissions to derive the NMVOC emissions.

Evaporative emissions from vehicles are estimated in the NAEI, using the Guidebook method for three different processes: diurnal losses, hot soak, and running losses. Emissions are dependent on ambient temperature and fuel vapor pressure and different factors are provided for vehicles with and without carbon canisters for evaporative emission controls. All vehicles from Euro 1 onwards are fitted with these devices; so, evaporative emission have been decreasing from the early 1990s with the penetration of these vehicles in the fleet. The method also takes into account the reduction in Reid Vapour Petrol of petrol sold in the UK since 2000, as required

for compliance with the EU Fuel Quality Directive 98/70/EC, amended by Directive 2009/30/EC.

*Speciation of VOC emissions*

The NAEI is considered to adequately reflect annual real world emissions of BTEX (see, for example, eddy covariance flux comparisons in London by Langford et al. (2010) and Vaughn et al. (2017)); so, those values are taken directly from the NAEI and used here. IVOCs, and particularly long chain hydrocarbons, are included in many cases in the inventory as groups, but their emissions are known to be significantly underestimated when compared against field observations. We use the observations of Dunmore et al. (2015), made in wintertime central London in 2012, as guide to uprate NAEI emissions for IVOC species based on the estimated discrepancies between inventory and field observation reported for each carbon number above C10. This leads to some significant multipliers being applied to the inventory values, sometimes of the order 60 to 70. We assume that the same multipliers apply to all sources, since field data does not provide any means to attribute different factors to road transport IVOCs compared with IVOCs from VCP sources.

Since the NAEI represents a reporting of emissions for the purposes of compliance with international treaties, some fraction of those emissions are not released on the mainland UK. For this paper, offshore BTEX and IVOC emissions, arising for example from offshore oil and gas activity, aircraft in cruise, or shipping and emissions associated with overseas Crown Dependencies are removed from the UK total, since they play no part in determining the

chemical environment of London. The annual NAEI totals are then divided equally to give a daily national emission.

## S2 ASOA Budget Analysis of Ambient Observations

To calculate the ASOA budget, we used the observed BTEX (Table S5) and non-BTEX aromatic (Table S8) emission ratios, the emission inventories for IVOC (see above), and estimated SVOCs from the primary OA emissions (see above). The methods to calculate ASOA from emissions have been described in detail elsewhere (Hayes et al., 2015; Ma et al., 2017; Schroder et al., 2018), and are briefly described here. All calculations described were conducted with the KinSim v4.02 chemical kinetics simulator (Peng and Jimenez, 2019) within Igor Pro 7 (Lake Oswego, Oregon), and are summarized in Fig. S7. A typical average particle diameter for urban environments of ~200 nm (Seinfeld and Pandis, 2006) is used to estimate the condensational sink term for the partitioning of gas-to-particle, although condensation is always fast compared to the experiment timescales. Further, we assume an average 250 g $mol^{-1}$ molar mass for OA and an average SOA density of 1.4 g $cm^{-3}$ (Vaden et al., 2011; Kuwata et al., 2012). Finally, all models are initialized with the campaign specific OA background (typically ~2 µg $sm^{-3}$) and POA (Table S9) for partitioning of gases to the particle phase, and ran at the average temperature for the campaign.

For the modeled VOCs (BTEX and non-BTEX aromatics), each species undergoes temperature-dependent OH oxidation (Table S12), forming four SVOCs that partition between gas- and particle-phase, using updated SOA yields that account for wall loss (Ma et al., 2017). For IVOCs, the emission weighted SOA yields and rate constants from the "Zhao" option (Zhao

et al., 2014) of Ma et al. (2017) are used, and the products are apportioned into three SVOC bins and one low-volatility organic compound (LVOC) bin (Fig. S7). Finally, SVOCs undergo photooxidation at a rate of $4\times10^{-11}$ $cm^3$ $molecules^{-1}$ $s^{-1}$ (Dzepina et al., 2009; Hodzic et al., 2010b; Tsimpidi et al., 2010; Hodzic and Jimenez, 2011; Hayes et al., 2015; Ma et al., 2017; Schroder et al., 2018), producing one product per oxidation step, with yields from Robinson et al. (2007) for cooking and other SVOCs and yields from Worton et al. (2014) for fossil fuel related SVOCs, as recommended by Ma et al. (2017). The products from SVOC and IVOC oxidation are allowed to further oxidize, as highlighted in Fig. S7 and described in prior studies (Hayes et al., 2015; Ma et al., 2017; Schroder et al., 2018). Generally, each product reacts at a rate of $4\times10^{-11}$ $cm^3$ $molecules^{-1}$ $s^{-1}$ to produce some product at one volatility bin lower, adding one oxygen to the compound for each oxidation (Dzepina et al., 2009; Tsimpidi et al., 2010; Hodzic and Jimenez, 2011; Hayes et al., 2015; Ma et al., 2017; Schroder et al., 2018). An update includes fragmentation for a fraction of the molecules that are oxidized, as described in Schroder et al. (2018) and Koo et al. (2014). As shown in Fig. S7, fragmentation of the compound occurs as it is oxidized and goes down one volatility bin. For further oxidation of SVOCs from the oxidation of primary IVOCs, one oxygen is added and 0.25 carbon is removed per step, leading to an increase in mass of 1.03 (instead of 1.07) per oxidation step (Koo et al., 2014; Schroder et al., 2018). For further oxidation of products from primary SVOC emissions, one oxygen is added and 0.5 carbon is removed per step, leading to a decrease in mass of 1% (instead of 1.07) per oxidation step (Koo et al. 2014; Schroder et al. 2018).

## S3 GEOS-Chem Modeling

The model used in this study is GEOS-Chem v12.0.0 (Bey et al., 2001; The International GEOS-Chem User Community, 2018). This model is used for the following calculations: (1) ASOA apportionment (Fig. 1), (2) apportionment of ASOA to total PM2.5 for premature mortality calculations (Worldwide Premature Deaths Due to ASOA), and (3) sensitivity analysis for ASOA production and emissions on premature mortality calculations. GEOS-Chem is operated at 2°×2.5° horizontal resolution. Goddard Earth Observing System – Forward Processing (GEOS-FP) assimilated data from the NASA Global Modeling and Assimilation Office (GMAO) were used for input meteorological fields. The model was run for 2013 to 2018 to take into account interannual variability of meteorological impacts onto $PM_{2.5}$ (therefore, averaging $PM_{2.5}$ over variations in meteorology). However, the HTAPv2 emission inventory, which was used for anthropogenic emissions (Janssens-Maenhout et al., 2015), was kept constant for the 5 years. Analysis of the HTAP emissions, compared to other emission inventories, generally showed the highest correlation with observations ($R^2$ = 0.54), versus the other inventories (CEDS $R^2$ = 0.26, MACCity $R^2$ = 0.00, and RETROv2 $R^2$ = 0.04), leading to the selection of this emission inventory. GEOS-Chem simulates gas and aerosol chemistry with ~700 chemical reactions. GEOS-Chem calculates the following $PM_{2.5}$ species: sulfate, ammonium, nitrate (Park et al., 2006); black carbon and POA (Park et al., 2005); SOA (Pye and Seinfeld, 2010; Marais et al., 2016); sea salt (accumulation mode only (Jaeglé et al., 2011)); and, dust (Duncan Fairlie et al., 2007).

**S3.1 Biogenic SOA**

For monoterpene and sesquiterpene SOAs, we used the default complex SOA scheme (without semi-volatile POA) using the two-product model framework (Pye and Seinfeld, 2010). This scheme calculates initial oxidation of VOCs with OH, $O_3$, and $NO_3$, and resulting products are assigned to four different gas-phase semi-volatile species (TSOA0–3) based on volatilities ($c^* = 0.1, 1, 10, 100$ μg $m^{-3}$). Aerosol and gas species fractions are calculated online using the partitioning theory, and all are removed by dry and wet deposition processes.

For isoprene SOA, we used the explicit isoprene chemistry developed by Marais et al. (2016). All the isoprene-derived gas-phase products, including isoprene peroxy radical, ISOPOOH, IEPOX, glyoxal, and methylglyoxal, are explicitly simulated. Irreversible heterogeneous uptake of precursors to aqueous aerosols are further calculated using online aerosol pH and surface area.

GEOS-Chem was used to estimate the relative fractions of the measured SOA in our studies between anthropogenic and biogenic (isoprene and monoterpene) sources (Fig. 1). Extensive research has been conducted to evaluate and improve the models performance in predicting BSOA, as summarized in Table S3. Though these evaluations mainly occurred in the southeast US, a recent study has also included more global observations to compare with GEOS-Chem (Pai et al., 2020). Generally, GEOS-Chem appears to overestimate biogenically derived SOA; however, the model predicted SOA is typically within the uncertainty of the AMS (Table S3). The overestimation, though, would suggest that the fraction of urban SOA may be under-predicted by this method, whereas the BSOA may be over-predicted. Therefore, in urban regions, the amount of SOA from biogenic sources may be lower, especially after the rapid SOA enhancements (within 12 to 24 equivalent photochemical hours that have been observed around

the world (Nault et al., 2018)). Typically the BSOA is present as a regional background and subtracted for the analyses used in this work, which focus on strong urban plumes on top of that background (Hayes et al., 2013, 2015).

### S3.2 Default GEOS-Chem Sensitivity to ASOA Simulations

For the sensitivity calculation using the "traditional" ASOA precursors, we used the two-product model framework (Pye and Seinfeld, 2010). Benzene, toluene, and xylene are oxidized with OH and converted to peroxy radicals. These peroxy radicals react with $HO_2$ or NO, resulting in non-volatile ASOA ($HO_2$ pathway, ASOAN species in GEOS-Chem) or semi-volatile ASOA tracers (NO pathway, ASOA1-3 in GEOS-Chem). As is the case for monoterpene and sesquiterpene SOA above, GEOS-Chem calculates online partitioning and dry/wet deposition processes for semi-volatile ASOA tracers. Other conditions including mortality calculation are kept the same as the base simulation above.

¶

## S4 Ozone Sensitivity to ASOA Simulations

A potential issue in the attribution of premature mortality to AOSA is that reducing emissions that lead to ASOA is that this may impact ozone concentrations. A sensitivity analysis was conducted, where the ASOA emissions were reduced by 20% (Fig. S14). In general, there is a less than 1% reduction in total ozone concentration in the boundary layer. This is due to the fact that the most important AVOCs that contribute to ozone formation are light alkenes (e.g., ethylene and propylene, Fig. 2), which are not ASOA precursors. Though the reaction rate

constant of the ASOA precursors is generally high (Table S12), the concentration of the precursors is low and they thus account for a low percentage of the total ozone production potential (Table S5 through Table S9). For example, the measured OH reactivity (Sect. 3) for two different urban regions was between 15 to 25 $s^{-1}$ (Griffith et al., 2016; Whalley et al., 2016) while the OH reactivity for the ASOA precursors for the same region was between 2 to 4 $s^{-1}$. The small contribution to the OH reactivity is in line to the minimal impact to the ozone concentration observed in Fig. S14.

## S5 Error Analysis of Observations

The errors that will be discussed here are in reference to Fig. 2 and Fig. 4 and Table S4 either come from the 1σ uncertainty in the slopes (the SOA versus $O_x$, HCHO, or PAN values) or propagation of uncertainty in observations. For SOA, we estimate the 1σ uncertainty of ~15%, which is lower than the typical 1σ uncertainty of the AMS (Bahreini et al., 2009) due to the careful calibrations and excellent intercomparisons in the various campaigns (see Table 1 for references for the AMS comparisons). For ΔCO, the largest uncertainty is associated with the CO background (Hayes et al., 2013; Nault et al., 2018), and is estimated to be ~10% at 0.5 photochemical equivalent days (Hayes et al., 2013). The uncertainty in the emission ratios is ~10% (Wang et al., 2014; de Gouw et al., 2017); though, it may be higher for the values calculated here (see above) due to the uncertainty in CO background, rate constants, and photochemical age. Therefore, for Fig. 2a, the uncertainty in the y-values is 18% and the uncertainty in the x-values is 10%. For Fig. 4, the uncertainty in the measurement is 21%.

Another potential source of uncertainty may stem from the fit of the data in Fig. 2a, as the data point from Seoul (KORUS-AQ) could be impacting the fit due to the difference in its value compared to the other locations. Statistical analysis for the influence of the data from Seoul on the figure was conducted, including a T-test, Cook's Distance test, and Difference in Fits test (Table S11). All three statistical tests show that the data from Seoul (and all the data in general) is not overly influencing the reported slope.

A further potential source of uncertainty in this analysis is the calculated VOC emission ratios for the studies that did not have ratios published previously (Houston 2000, London, Houston 2013, and Seoul). To investigate how well Eq. 3 does in estimating the VOC emission ratios, a comparison of the estimated VOC emission ratios versus previously published ratios for two different cities, Mexico City (Apel et al., 2010; Bon et al., 2011) and Los Angeles (de Gouw et al., 2017) was made (Table S10). Also, for Mexico City, two locations, an urban and a suburban site, were compared both against each other (Apel et al., 2010; Bon et al., 2011) and the calculated values from Eq. 3.

First, as shown in Table S10, even for the same location (suburban Mexico City), different values in the emission ratio, especially for the alkanes, can be observed, by as much as a factor of 7. This can be partially explained by differences in how the emission ratios were determined. For both Apel et al. (2010) and Bon et al. (2011), the authors took the slope of VOCs versus CO and used different regression techniques and different time periods. Comparing their technique with ours, we generally estimate VOC emission ratios within 50% of the reported values, and the estimation improves for shorter lived compounds (e.g., aromatics). However, de Gouw et al. (2017) more carefully took chemistry into consideration for any potential losses of

399 the VOCs prior to observation to determine emission ratios, similar to this study. We believe the
400 comparison with de Gouw et al. (2017) provides a more useful comparison in the method
401 presented here. We find, at most, a 30% difference in the emission ratios, with an average
402 difference of 4±15% for all compounds. Thus, from this analysis, we conclude that (1) there is
403 large variability in VOC emission ratios across urban areas around the world, which has been
404 highlighted in other studies (Warneke et al., 2007), and (2) the method that considers losses of
405 VOCs is the more accurate procedure to estimate VOC emissions and leads to the best
406 reproducibility across studies and lowest uncertainty (< 30%, ~4% on average).

## Supporting Information Tables

**Table S1.** List of instruments whose observations are used in this study. In some cases ΔSOA/ΔCO (Table S4), SOA versus $O_x$ slope (Table S4), or VOC emission ratios (Table S5 through Table S8) had already been reported, and, in those cases, we use the previous literature reports in our analyses.

| Location | SOA | $O_x$ | HCHO | PAN | VOCs | CO |
|---|---|---|---|---|---|---|
| Houston, TX, USA (2000) | Q-AMS[a] | CL & UV Absortpion[b] | DOAS[c] | GC-ECD[d] | GC-FID, GC-MS[e] | Infrared Absortion[f] |
| Mexico City, Mexico (2006) | HR-ToF-AMS[g] | CL[h] | TDLAS[i] | CIMS[j] | WAS[k] | UV RF[l] |
| Los Angeles, CA, USA (2010) | HR-ToF-AMS[g] | CL & UV Absorption[m] | Average of DOAS[c] & Hantzsch Reaction[n] | GC-ECD[d] | GC-MS[o] | UV RF[l] |
| Beijing, China (2011) | HR-ToF-AMS[g] | CL & UV Absorption[p] | PTR-MS[q] | GC-ECD[r] | GC-FID[s] | IR Absorption[p] |
| London, UK (2012) | C-ToF-AMS[t] | CL & UV Absorption[u] | Hantzsch Reaction[n] | GC-ECD[v] | GC-FID & GC×GC-FID[w] | UV RF[l] |
| Houston, TX, USA (2013) | HR-ToF-AMS[g] | CL[x] | Average of LIF[y] & CAMS[z] | CIMS[j] | WAS[k] | DACOM[aa] |
| Seoul, South Korea (2016) | HR-ToF-AMS[g] | CL[h] | CAMS[z] | CIMS[j] | WAS[k] | DACOM[aa] |

[a]Quadrupole Aerosol Mass Spectrometer (Q-AMS) (Jayne et al., 2000)
[b]Chemiluminescence (CL) and UV Absorption (Williams et al., 1997)
[c]Differential Optical Absorption Spectrometry (DOAS) (Stutz and Platt, 1996, 1997)
[d]Gas chromatography-electron capture detector (GC-ECD) (Williams et al., 2000; Roberts et al., 2002)
[e]Gas chromatography-flame ionization detector (GC-FID) and gas chromatography mass spectrometer (Roberts et al., 2001)
[f]TECO Model 48s IR gas-filter
[g]High Resolution Time-of-Flight Aerosol Mass Spectrometer (HR-ToF-AMS) (DeCarlo et al., 2006)
[h]Chemiluminescence (CL) and UV Absorption (Weinheimer et al., 1994)
[i]Tunable diode laser absorption spectroscopic (TDLAS) measurements (Fried et al., 2003)
[j]Chemical ionization mass spectrometer (CIMS) (Huey L Tanner D Slusher D Dibb J Arimoto R Chen G Davis D Buhr M Nowak J Mauldin R Eisele F, 2004; Slusher et al., 2004; Kim et al., 2007)
[k]Whole air sample, followed by analysis with GC-FID and/or GC-MS (Blake et al., 2003)
[l]UV Resonance Fluorescence (RF) (Gerbig et al., 1999)

[m]Chemiluminescence (CL) and UV Absorption (Hayes et al., 2013)
[n]Hantzsch reaction (Cárdenas et al., 2000)
[o]Gas chromatograph mass spectrometer (Gilman et al., 2010)
[p]Chemiluminescence (CL), UV Absorption, and IR Absorption (Hu et al., 2016)
[q]Proton transfer reaction mass spectrometer (PTR-MS) (Warneke et al., 2011)
[r]Gas chromatography electron capture detector (GC-ECD) (Zhang et al., 2017)
[s]Gas chromatography flame ionization detector (GC-FID) (Wang et al., 2014)
[t]Compact Time-of-Flight Aerosol Mass Spectrometer (C-ToF-AMS) (Drewnick et al., 2005)
[u]Chemiluminescence (CL) and UV Absorption (Whalley et al., 2016)
[v]Gas chromatography electron capture detector (GC-ECD) (Whalley et al., 2016)
[w]Gas chromatography flame ionization detector (GC-FID) (Dunmore et al., 2015)
[x]Chemiluminescence (CL) (Ryerson et al., 1999; Pollack et al., 2010)
[y]Laser induced fluorescence (LIF) (Cazorla et al., 2015)
[z]Compact Atmospheric Multi-species Spectrometer (CAMS) difference frequency absorption spectrometer (Weibring et al., 2010)
[aa]Tunable diode laser absorption spectroscopy (Sachse et al., 1987)

**Table S2.** Concentrations of $PM_1$ components shown in Fig. 1. References for the measurements can be found in Table 1.

| Dataset Location | Average Concentration (μg $sm^{-3}$) of submicron aerosol under standard temperature and pressure | | | | |
|---|---|---|---|---|---|
| | **SOA** | **HOA** | **$SO_4$** | **$NO_3$** | **$NH_4$** |
| Houston, TX, USA (2000) | 2.7 | 0.7 | 4.9 | 0.4 | 1.5 |
| Northeast USA (2002) | 4.9 | 0.5 | 2.0 | 0.3 | 0.7 |
| Tokyo, Japan (2004) | 6.0 | 1.5 | 4.4 | 0.9 | 4.0 |
| Mexico City, Mexico (2006) | 11.2 | 4.8 | 1.9 | 6.0 | 2.5 |
| Paris, France (2009) | 1.9 | 1.1 | 1.2 | 0.5 | 0.6 |
| Los Angeles, CA, USA (2010) | 5.0 | 2.0 | 2.9 | 3.6 | 2.1 |
| Changdao Island, China (2011) | 9.4 | 4.4 | 8.3 | 12.2 | 6.5 |
| Beijing, China (2011) | 17.1 | 8.9 | 22.0 | 16.8 | 13.7 |
| London, UK (2012) | 2.7 | 1.6 | 1.4 | 2.7 | 1.3 |
| Houston, TX, USA (2013) | 3.7 | 0.0 | 2.7 | 0.1 | 0.6 |
| New York City, NY, USA (2015) | 0.8 | 0.7 | 1.2 | 1.4 | 0.4 |
| Seoul, South Korea (2016) | 11.9 | 1.3 | 5.0 | 7.9 | 4.4 |

**Table S3.** Table summarizing the results of recent GEOS-Chem performance evaluations for modeling BSOA.

| Study | Observed Data | Species | Details |
|---|---|---|---|
| Fisher et al. (2016)[a] | SEAC$^4$RS, below 1 km (spatial pattern), below 500 m (bias) | Isoprene | Spatial patterns well captured, and biases are +34% for isoprene and +3% for monoterpenes |
| | | Monoterpene | |
| | | Organic Nitrates from Isoprene | Spatial patterns well captured, and biases are -0.6% for first- and -35% for second-generation isoprene nitrates |
| | SEAC$^4$RS, 0 - 4 km vertical profiles | Isoprene | Agreed well but GEOS-Chem somewhat overestimated observed concentrations near 1km |
| | | Monoterpene | |
| | | HCHO | |
| | | Organic Nitrates from Isoprene | Agreed within measurement uncertainties |
| | SOAS, at the surface | Isoprene | Underestimated isoprene and monoterpenes (-28% and -54%), but overestimated first- and second- generation isoprene nitrates (+85% and +43%) |
| | | Monoterpene | |
| | | HCHO | |
| | | Organic Nitrates from Isoprene | |
| Travis et al. (2016) | SEAC$^4$RS, 0 - 12 km | First Generation from Isoprene Nitrates | Good agreement for ISOPOOH and ISOPN, underestimation of HPALDs by a factor of two |
| | | ISOPOOH | |
| | | HPALDS | |
| Marais et al. (2016) | SOAS, at the surface | IEPOX-SOA | Good agreement for isoprene derived aerosols, mean concentrations were almost the same |
| | | ISOPOOH-SOA | |
| | SEAC$^4$RS, below 2 km (spatial pattern) | IEPOX-SOA | Spatial patterns well captured |

[a]This study decreased isoprene emissions by 15% and doubled monoterpene emissions of MEGANv2.1.

**Table S3 cont.**

| Study | Observed Data | Species | Details |
|---|---|---|---|
| Kaiser et al. (2018)[a] | SEAC$^4$RS | Isoprene | All were overestimated, except for first generation isoprene nitrates |
| | | HCHO | |
| | | ISOPOOH | |
| | | MVK + MACR | |
| | | First Generation Isoprene Nitrates | |
| Pai et al. (2020) | 15 airborne campaigns (SEAC$^4$RS, GoAmazon, SENEX, OP3, etc.) | OA under biognic dominant conditions | Slight overestimation, but generally very similar in magnitude |

[a]NEI $NO_x$ emissions other than power plants decreased by 60%, soil $NO_x$ emissions were reduced by 50% across the Midwestern US. With the decrease of $NO_x$ emissions, ISOPOOH concentrations were increased in GEOS-Chem.

**Table S4**. Dilution-corrected SOA concentrations at 0.5 equivalent days and slopes of SOA versus $O_x$, HCHO, and PAN used in Fig. 2 and Fig. 3. References for the values can be found either in Table 1 or found in Fig. S2 through Fig. S4. Uncertainty is 1σ, and either represents propagation in uncertainty in measurements (see Sect. S5) for ΔSOA/ΔCO or uncertainty in slopes for SOA versus the three photochemical species.

| Dataset Location | ΔSOA/ΔCO at 0.5 eq. days | SOA vs. $O_x$ Slopes | SOA vs. HCHO Slopes | SOA vs. PAN Slopes |
|---|---|---|---|---|
| Houston, TX, USA (2000) | | 0.04±0.01[a] | 0.32±0.08 | 1.41±0.46 |
| Northeast USA (2002) | 16±3[b]<br>48±9[c] | | | |
| Mexico City, Mexico (2003) | | 0.14±0.01[a] | | |
| Tokyo, Japan (2004) | | 0.19±0.01[a] | | |
| Mexico City, Mexico (2006) | 58±10 | 0.16±0.01 | 1.60±0.06 | 5.60±0.30 |
| Paris, France (2009) | | 0.14±0.01[a] | | |
| Pasadena, CA, USA (2010) | 59±11 | 0.16±0.01 | 1.93±0.02 | 5.41±0.12 |
| Changdao Island, China (2011) | 23±4 | | | |
| Beijing, China (2011) | 31±6 | 0.21±0.01 | 3.90±0.15 | 7.42±0.46 |
| London, UK (2012) | 54±10 | 0.13±0.01 | 0.36±0.02 | 3.37±0.41 |
| Houston, TX, USA (2013) | | 0.16±0.01 | 1.52±0.13 | 6.92±0.58 |
| New York City, NY, USA (2015) | 33±6 | | | |
| Seoul, South Korea (2016) | 107±19 | 0.29±0.02 | 3.73±0.26 | 10.13±0.52 |

[a]Missing reported uncertainty; therefore, assuming ±0.01, as that is typical for other campaigns [b]From de Gouw et al. (2005). [c]From Kleinman et al. (2007).

**Table S5**. Emission ratios of BTEX aromatics used in this study. If no reference is listed, then the emission ratio was calculated using Eq. 3.

| Dataset Location | Emission Ratios (ppbv aromatic/ppmv CO) | | | | | References |
|---|---|---|---|---|---|---|
| | Benzene | Toluene | Ethylbenzene | m+p-xylene | o-xylene | |
| Houston, TX, USA (2000) | 2.6 | 3.5 | 0.6 | 2.8 | 0.8 | |
| NE USA, Ship (2002) | 0.9 | 2.0 | 0.2 | 0.6 | 0.3 | Baker et al. (2008) |
| NE USA, Aircraft (2002) | 0.8 | 2.9 | 0.4 | 1.2 | 0.5 | Warneke et al. (2007) |
| Mexico City, Mexico (2006) | 0.9 | 7.5 | 0.9 | 1.1 | 0.4 | Apel et al. (2010) |
| Los Angeles, CA, USA (2010) | 1.3 | 3.4 | 0.6 | 2.1 | 0.8 | de Gouw et al. (2017) |
| Changdao Island, China (2011) | 2.3 | 1.9 | 0.5 | 1.3 | 0.4 | Yuan et al. (2013) |
| Beijing, China (2011) | 1.2 | 2.4 | 1.0 | 1.6 | 0.6 | Wang et al. (2014) |
| London, UK (2012) | 1.8 | 6.3 | 1.2 | 2.2 | 1.1 | |
| Houston, TX, USA (2013) | 2.3 | 3.0 | 0.6 | 3.9 | 1.2 | |
| New York City, NY, USA (2015) | 0.8 | 2.9 | 0.4 | 1.2 | 0.5 | Warneke et al. (2007)[a] |
| Seoul, South Korea (2016) | 1.1 | 13.1 | 2.4 | 3.3 | 2.3 | |

[a]Using the emissions from Warneke et al. (2007) instead of Schroder et al. (2018) as Schroder et al. found significant uncertainty in the emissions calculated from observations.

**Table S6**. Emission ratios of alkanes used in this study. If no reference is listed, then the emission ratio was calculated using Eq. 3.

| Dataset Location | Emission Ratios (ppbv alkane/ppmv CO) | | | | | | | References |
|---|---|---|---|---|---|---|---|---|
| | Ethane | Propane | n-Butane | i-Butane | n-Pentane | i-Pentane | n-Hexane | |
| Houston, TX, USA (2000) | 40.9 | 24.3 | 9.0 | 14.7 | 3.1 | 10.0 | 3.1 | |
| NE USA, Ship (2002) | 8.3 | 2.3 | 1.8 | 1.3 | 1.0 | 2.8 | 0.9 | Baker et al. (2008) |
| NE USA, Aircraft (2002) | 9.9 | 9.0 | 2.4 | 1.3 | 2.0 | 5.4 | 0.6 | Warneke et al. (2007) |
| Mexico City, Mexico (2006) | 7.4 | 41.5 | 15.1 | 4.8 | 2.1 | 2.7 | 1.5 | Apel et al. (2010) |
| Los Angeles, CA, USA (2010) | 16.5 | 13.4 | 5.0 | 3.2 | 3.4 | 8.7 | 1.4 | de Gouw et al. (2017) |
| Changdao Island, China (2011) | 7.7 | 4.5 | 2.5 | 1.2 | 1.0 | 1.5 | 0.5 | Yuan et al. (2013) |
| Beijing, China (2011) | 4.3 | 3.9 | 2.5 | 2.5 | 1.2 | 2.0 | 0.6 | Wang et al. (2014) |
| London, UK (2012) | 33.0 | 17.8 | 17.3 | 8.4 | 4.6 | 11.3 | 1.3 | |
| Houston, TX, USA (2013) | 86.5 | 37.3 | 14.6 | 10.6 | 7.0 | 10.5 | 3.0 | |
| Seoul, South Korea (2016) | 16.1 | 0.4 | 6.0 | 3.4 | 3.1 | 3.7 | 1.7 | |

**Table S7**. Emission ratios of alkenes used in this study. If no reference is listed, then the emission ratio was calculated using Eq. 3.

| Dataset Location | Emission Ratios (ppbv alkene/ppmv CO) | | References |
|---|---|---|---|
| | Ethene | Propene | |
| Houston, TX, USA (2000) | 24.4 | 28.4 | |
| NE USA, Ship (2002) | 4.4 | 1.1 | Baker et al. (2008) |
| NE USA, Aircraft (2002) | 4.9 | 1.4 | Warneke et al. (2007) |
| Mexico City, Mexico (2006) | 8.4 | 2.6 | Apel et al. (2010) |
| Los Angeles, CA, USA (2010) | 11.2 | 4.1 | de Gouw et al. (2017) |
| Changdao Island, China (2011) | 5.3 | 1.4 | Yuan et al. (2013) |
| Beijing, China (2011) | 4.4 | 1.4 | Wang et al. (2014) |
| London, UK ()2012) | 10.3 | 6.2 | |
| Houston, TX, USA (2013) | 12.0 | 15.8 | |
| Seoul, South Korea (2016) | 5.4 | 2.1 | |

**Table S8**. Emission ratios of non-BTEX aromatics used in this study. If no reference is listed, then the emission ratio was calculated using Eq. 3.

| Dataset Location | Emission Ratios (ppbv aromatic/ppmv CO) | | | References |
|---|---|---|---|---|
| | Trimethylbenzenes | Ethyltoluenes | Propylbenzene | |
| NE USA, Aircraft (2002) | 0.71 | 0.58 | 0.14 | Warneke et al. (2007) |
| Los Angeles, CA, USA (2010) | 1.47 | 0.56 | 0.13 | de Gouw et al.(2017) |
| Beijing, China (2011) | 0.57 | 0.41 | 0.09 | Wang et al. (2014) |
| London, UK (2012) | 0.49 | 0.23 | 0.58 | |
| New York City, NY, USA (2015) | 0.71 | 0.58 | 0.14 | Warneke et al. (2007) |

**Table S9**. Normalized mass concentration of primary organic aerosol (POA/CO) measured in various campaigns, used to determine SVOC emission ratios.

| Dataset Location | Normalized Mass Concentration (μg $sm^{-3}$ $ppmv^{-1}$) | | References |
|---|---|---|---|
| | HOA/CO | Other POA/CO | |
| NE USA (2002) | 12.2 | - | de Gouw et al. (2005) |
| Los Angeles, CA, USA (2010) | 5.3 | 7.7 | Hayes et al. (2013) |
| Beijing, China (2011) | 6.1 | 9.9 | Hu et al. (2016) |
| London, UK (2012) | 17.9 | 14.1 | Young et al. (2015) |
| New York City, NY, USA (2015) | 5.6 | 14.4 | Schroder et al. (2018) |

**Table S10.** Comparison of estimated VOC emission ratios from two studies from Mexico City (Apel et al. 2010; Bon et al. 2011), one study from Los Angeles (de Gouw et al. 2017), and this study.

| VOC Ratio | Apel et al. (2010) Downtown MC | This Study | Apel et al. (2010) Suburbs MC | Bon et al. (2011) Outskirt MC | This Study | de Gouw et al. (2017) LA | This Study |
|---|---|---|---|---|---|---|---|
| Ethane | 7.4 | 8.2 | 3.0 | 21.5 | 8.2 | 16.5 | 18.9 |
| Propane | 41.5 | 36.9 | 49.3 | 61.7 | 38.4 | 13.4 | 14.0 |
| n-Butane | 15.1 | 14.9 | 15.3 | 21.7 | 14.1 | 5.0 | 5.7 |
| i-Butane | 4.8 | 4.8 | 5.3 | 7.2 | 4.9 | 3.2 | 3.5 |
| n-Pentane | 2.1 | 2.9 | 2.1 | 2.5 | 2.1 | 3.4 | 3.4 |
| i-Pentane | 2.7 | 3.6 | 3.2 | 3.3 | 3.1 | 8.7 | 7.8 |
| n-Hexane | 1.5 | 1.9 | 1.3 | 1.5 | 1.2 | 1.4 | 1.7 |
| Ethene | 8.4 | 6.1 | 7.9 | 7.0 | 7.1 | 11.2 | 9.6 |
| Propene | 2.6 | 1.3 | 2.9 | 3.0 | 1.6 | 4.1 | 3.9 |
| Benzene | 0.9 | 1.0 | 1.2 | 1.2 | 1.3 | 1.3 | 1.4 |
| Toluene | 7.5 | 9.2 | 5.2 | 4.2 | 4.1 | 3.4 | 3.0 |
| Ethylbenzene | 0.9 | 0.8 | 0.4 | 4.3* | 0.4 | 0.6 | 0.6 |
| m+p-Xylene | 1.1 | 0.7 | 0.5 | No Data | 0.4 | 2.1 | 1.9 |
| o-Xylene | 0.4 | 0.2 | 0.2 | No Data | 0.2 | 0.8 | 0.7 |
| Trimethylbenzenes | No Data | No Data | No Data | No Data | No Data | 1.6 | 1.1 |
| Ethyltoluenes | No Data | No Data | No Data | No Data | No Data | 0.6 | 0.4 |
| Propylbenzene | No Data | No Data | No Data | No Data | No Data | 0.1 | 0.1 |

*In Bon et al. (2011), they reported the sum of C8 aromatics, which is the sum of ethylbenzene and xylenes

**Table S110**. Statistical analysis of the data used in Fig. 2 to determine if any point is influencing the slope, using the T-test, Cook's Distance test, and Difference in Fits test. For the T-test, the point is influential if the t value is < 0.05 while for the Cook's Distance and Difference in Fits test, the point is influential if the value is > 1.~~**Sensitivity analysis of slopes and R2 by removing one city each. All slopes are statistically similar at the 95% confidence interval.**~~

| ~~**Dataset Location**~~ | ~~**Slope (μg sm$^{-3}$ s)**~~ | ~~**$R^2$**~~ |
|---|---|---|
| ~~All~~ | ~~24.8±3.4~~ | ~~0.88~~ |
| ~~Without Seoul~~ | ~~34.0±10.5~~ | ~~0.64~~ |
| ~~Without NYC~~ | ~~24.8±3.8~~ | ~~0.8~~ |
| ~~Without London~~ | ~~24.2±3.4~~ | ~~0.90~~ |
| ~~Without Beijing~~ | ~~24.2±3.5~~ | ~~0.89~~ |
| ~~Without Chinese Outflow~~ | ~~24.0±3.6~~ | ~~0.88~~ |
| ~~Without LA~~ | ~~24.2±3.3~~ | ~~0.90~~ |
| ~~Without Mexico City~~ | ~~24.2±3.4~~ | ~~0.90~~ |
| ~~Without NE US Aircraft~~ | ~~24.8±2.9~~ | ~~0.92~~ |
| ~~Without NE US, Boat~~ | ~~24.2±4.0~~ | ~~0.86~~ |

| Campaign | T-test | Cook's Distance | Difference in Fits |
|---|---|---|---|
| NE US Ship | 0.63 | 0.06 | -0.29 |
| NE US Aircraft | 0.12 | 0.27 | 0.73 |
| Mexico City | 0.39 | 0.06 | 0.33 |
| Los Angeles | 0.32 | 0.08 | 0.38 |
| Changdao Island, China | 0.41 | 0.09 | -0.38 |
| Beijing | 0.42 | 0.06 | -0.32 |
| London | 0.31 | 0.13 | -0.48 |
| NYC | 0.90 | 0.00 | -0.05 |
| Seoul | 0.99 | 0.00 | 0.01 |

494 **Table S11-2**. Rate constants used throughout this study.

| Compound | Rate Constant ($cm^3$ $molec.^{-1}$ $s^{-1}$) | References |
|---|---|---|
| *Alkanes* | | |
| Ethane | $6.9\times10^{-12}\times\exp(-1000/T)$ | Atkinson et al. (2006) |
| Propane | $7.6\times10^{-12}\times\exp(-585/T)$ | Atkinson et al. (2006) |
| n-Butane | $9.8\times10^{-12}\times\exp(-425/T)$ | Atkinson et al. (2006) |
| i-Butane | $1.17\times10^{-17}\times T^2\times\exp(213/T)$ | Atkinson and Arey (2003) |
| n-Pentane | $2.52\times10^{-17}\times T^2\times\exp(158/T)$ | Atkinson and Arey (2003) |
| i-Pentane | $3.6\times10^{-12}$ | Atkinson and Arey (2003) |
| n-Hexane | $2.54\times10^{-14}\times T\times\exp(-112/T)$ | Atkinson and Arey (2003) |
| *Alkenes* | | |
| Ethene | $7.84\times10^{-12,a}$ | Atkinson et al. (2006) |
| Propene | $2.86\times10^{-11,a}$ | Atkinson et al. (2006) |
| *Aromatics* | | |
| Benzene | $2.3\times10^{-12}\times\exp(-190/T)$ | Atkinson et al. (2006) |
| Toluene | $1.8\times10^{-12}\times\exp(340/T)$ | Atkinson et al. (2006) |
| Ethylbenzene | $7\times10^{-12}$ | Atkinson and Arey (2003) |
| m+p-xylene | $1.87\times10^{-11,b}$ | Atkinson and Arey (2003) |
| o-xylene | $1.36\times10^{-11}$ | Atkinson and Arey (2003) |
| Trimethylbenzenes | $2.73\times10^{-12}\times\exp(730/T)$ | Bohn and Zetzsch (2012) |
| Ethyltoluenes | $1.2\times10^{-11}$ | Atkinson and Arey (2003) |
| Propylbenzene | $5.8\times10^{-12}$ | Atkinson and Arey (2003) |
| *S/IVOCs* | | |
| IVOCs C* = 4 - 6 | $2\times10^{-11}$ | Jathar et al. (2014)<br>McDonald et al. (2018) |
| IVOCs C* = 3 | $3\times10^{-11}$ | |
| SVOCs & "aging" | $4\times10^{-11}$ | Tsimpidi et al. (2010) |
| *$NO_x$/$NO_y$* | | |
| OH + $NO_2$ | $1.23\times10^{-11,a}$ | Mollner et al. (2010) |

[a]Showing the rate constant at 298 K, 1013 hPa. However, for this study, we used the temperature and pressure dependent formulation listed in each respective reference.
[b]This is the average of m-xylene and p-xylene rate constants.

498 **Table 13.** Parameters for VOC, IVOC, and SVOC aerosol yields. The yields are taken from Ma
499 et al. (2017).

| Compound | Stoichiometric SOA yield High-NOx, 298 K (µg $m^{-3}$) | | | | |
|---|---|---|---|---|---|
| | 0.1 | 1 | 10 | 100 | 1000 |
| Benzene<br>Toluene<br>Ethyltoluene<br>Propylbenzenes | N/A | 0.276 | 0.002 | 0.431 | 0.202 |
| Xylenes<br>Trimethylbenzenes | N/A | 0.310 | 0.000 | 0.420 | 0.209 |
| IVOC C* = 6 | 0.007 | 0.090 | 0.206 | 0.350 | 0.00 |
| IVOC C* = 5 | 0.0498 | 0.0814 | 0.456 | 0.278 | 0.00 |
| IVOC C* = 4 | 0.053 | 0.103 | 0.464 | 0.266 | 0.00 |
| IVOC C* = 3 | 0.064 | 0.0914 | 0.562 | 0.209 | 0.00 |
| HOA C* = 2 | N/A | N/A | 0.28 | N/A | N/A |
| HOA C* = 1 | N/A | 0.18 | N/A | N/A | N/A |
| HOA C* = 0 | 0.12 | N/A | N/A | N/A | N/A |
| COA C* = 2 | N/A | N/A | 0.1881 | N/A | N/A |
| COA C* = 1 | N/A | 0.1188 | N/A | N/A | N/A |
| COA C* = 0 | 0.0594 | N/A | N/A | N/A | N/A |

500

**Table S142**. Table of GBD parameters, which is the mean of the draw values (see associated file) from the IHME website: http://ghdx.healthdata.org/record/global-burden-disease-study-2010-gbd-2010-ambient-air-pollution-risk-model-1990-2010.

| Parameter | IHD | Stroke | COPD | LC | ALRI |
|---|---|---|---|---|---|
| $\alpha$ | 1.4273 | 1.2641 | 15.224 | 114.74 | 2.2023 |
| $\beta$ | 0.04764 | 0.00722 | 0.00095 | 0.000141 | 0.000284 |
| $\rho$ | 0.376 | 1.314 | 0.684 | 0.741 | 1.183 |
| $PM_{2.5,Threshold}$ | 7.462 | 7.387 | 7.374 | 7.380 | 7.283 |

**Table S153**. Table of GEMM parameters. The GEMM parameters are from Burnett et al. (2018), with the Chinese male cohort.

| Cause of Death | Age Range (years) | θ | Standard Error θ | α | μ | π |
|---|---|---|---|---|---|---|
| NCD + LRI | >25 | 0.1430 | 0.01807 | 1.6 | 15.5 | 36.8 |
| | 27.5 | 0.1585 | 0.01477 | 1.6 | 15.5 | 36.8 |
| | 32.5 | 0.1577 | 0.01470 | 1.6 | 15.5 | 36.8 |
| | 37.5 | 0.1570 | 0.01463 | 1.6 | 15.5 | 36.8 |
| | 42.5 | 0.1558 | 0.01450 | 1.6 | 15.5 | 36.8 |
| | 47.5 | 0.1532 | 0.01425 | 1.6 | 15.5 | 36.8 |
| | 52.5 | 0.1499 | 0.01394 | 1.6 | 15.5 | 36.8 |
| | 57.5 | 0.1462 | 0.01361 | 1.6 | 15.5 | 36.8 |
| | 62.5 | 0.1421 | 0.01325 | 1.6 | 15.5 | 36.8 |
| | 67.5 | 0.1374 | 0.01284 | 1.6 | 15.5 | 36.8 |
| | 72.5 | 0.1319 | 0.01234 | 1.6 | 15.5 | 36.8 |
| | 77.5 | 0.1253 | 0.01174 | 1.6 | 15.5 | 36.8 |
| | 85 | 0.1141 | 0.01071 | 1.6 | 15.5 | 36.8 |
| IHD | >25 | 0.2969 | 0.01787 | 1.9 | 12 | 40.2 |
| | 27.5 | 0.5070 | 0.02458 | 1.9 | 12 | 40.2 |
| | 32.5 | 0.4762 | 0.02309 | 1.9 | 12 | 40.2 |
| | 37.5 | 0.4455 | 0.02160 | 1.9 | 12 | 40.2 |
| | 42.5 | 0.4148 | 0.02011 | 1.9 | 12 | 40.2 |
| | 47.5 | 0.3841 | 0.01862 | 1.9 | 12 | 40.2 |
| | 52.5 | 0.3533 | 0.01713 | 1.9 | 12 | 40.2 |
| | 57.5 | 0.3226 | 0.01564 | 1.9 | 12 | 40.2 |
| | 62.5 | 0.2919 | 0.01415 | 1.9 | 12 | 40.2 |

509 **Table 153 cont.**

| Cause of Death | Age Range (years) | θ | Standard Error θ | α | μ | π |
|---|---|---|---|---|---|---|
| IHD | 67.5 | 0.2612 | 0.01266 | 1.9 | 12 | 40.2 |
| | 72.5 | 0.2304 | 0.01117 | 1.9 | 12 | 40.2 |
| | 77.5 | 0.1997 | 0.00968 | 1.9 | 12 | 40.2 |
| | 85 | 0.1536 | 0.00745 | 1.9 | 12 | 40.2 |
| Stroke | >25 | 0.2720 | 0.07697 | 6.2 | 16.7 | 23.7 |
| | 27.5 | 0.4513 | 0.11919 | 6.2 | 16.7 | 23.7 |
| | 32.5 | 0.4240 | 0.11197 | 6.2 | 16.7 | 23.7 |
| | 37.5 | 0.3966 | 0.10475 | 6.2 | 16.7 | 23.7 |
| | 42.5 | 0.3693 | 0.09752 | 6.2 | 16.7 | 23.7 |
| | 47.5 | 0.3419 | 0.09030 | 6.2 | 16.7 | 23.7 |
| | 52.5 | 0.3146 | 0.08307 | 6.2 | 16.7 | 23.7 |
| | 57.5 | 0.2872 | 0.07585 | 6.2 | 16.7 | 23.7 |
| | 62.5 | 0.2598 | 0.06863 | 6.2 | 16.7 | 23.7 |
| | 67.5 | 0.2325 | 0.06190 | 6.2 | 16.7 | 23.7 |
| | 72.5 | 0.2051 | 0.05418 | 6.2 | 16.7 | 23.7 |
| | 77.5 | 0.1778 | 0.04695 | 6.2 | 16.7 | 23.7 |
| | 85 | 0.1368 | 0.03611 | 6.2 | 16.7 | 23.7 |
| COPD | >25 | 0.2510 | 0.06762 | 6.5 | 2.5 | 3.2 |
| Lung Cancer | >25 | 0.2942 | 0.06147 | 6.2 | 9.3 | 29.8 |
| LRI | >25 | 0.4468 | 0.11735 | 6.4 | 5.7 | 8.4 |

510

**Table S164**. Calculated premature mortality from PM with all aerosol (base mortality) and removing ASOA, using the IER method.

| Location[a] | Base Mortality | Mortality reduced due to removing ASOA | Percent mortality reduced due to removing ASOA |
|---|---|---|---|
| North America | 43,408 | 18,479 | 43% |
| Central America | 11,808 | 3,395 | 29% |
| South America | 31,214 | 10,100 | 32% |
| Africa | 258,294 | 14,869 | 6% |
| Western Europe | 305,754 | 31,880 | 10% |
| Eastern Europe | 195,749 | 16,003 | 8% |
| South Asia | 938,967 | 75,085 | 8% |
| Southeastern Asia | 135,433 | 31,886 | 24% |
| East Asia | 1,315,720 | 122,190 | 9% |
| Oceania | 95 | 27 | 28% |
| Rest of the World | 72,385 | 13,337 | 18% |
| Total | 3,308,957 | 337,224 | 10% |

[a]Locations defined by:
http://themasites.pbl.nl/tridion/en/themasites/_disabled_image/background/regions/index-2.html

**Table S175**. Calculated premature mortality from PM with all aerosol (base mortality) and removing ASOA, using the GEMM method.

| Location[a] | Base Mortality | Mortality reduced due to removing ASOA | Percent mortality reduced due to removing ASOA |
|---|---|---|---|
| North America | 178,793 | 24,892 | 14% |
| Central America | 58,516 | 7,298 | 12% |
| South America | 145,395 | 22,372 | 15% |
| Africa | 765,946 | 34,528 | 5% |
| Western Europe | 768,991 | 50,427 | 7% |
| Eastern Europe | 465,341 | 25,552 | 5% |
| South Asia | 2,285,903 | 166,228 | 7% |
| Southeastern Asia | 347,191 | 50,802 | 15% |
| East Asia | 2,487,349 | 220,264 | 9% |
| Oceania | 3,375 | 428 | 13% |
| Rest of the World | 269,769 | 35,051 | 13% |
| Total | 7,776,570 | 638,219 | 8% |

[a]Locations defined by:
http://themasites.pbl.nl/tridion/en/themasites/_disabled_image/background/regions/index-2.html

**Table S186**. List of total final consumption, in millions of tonnes of oil equivalent, of oil products and oil, for each organization. Total final consumption includes imports, and does not include exports (IEA, 2019).

| Organization | Industry | Transportation | Non-Energy |
|---|---|---|---|
| World | 307 | 2533 | 645 |
| OECD | 89 | 1147 | 326 |
| Africa | 18.4 | 115.4 | 7.9 |
| Non-OECD | 28.3 | 135 | 20 |
| Middle East | 33.5 | 126.3 | 47.5 |
| Non-OECD Europe and Eurasia | 35 | 101 | 53 |

**Supplemental figures for this study**

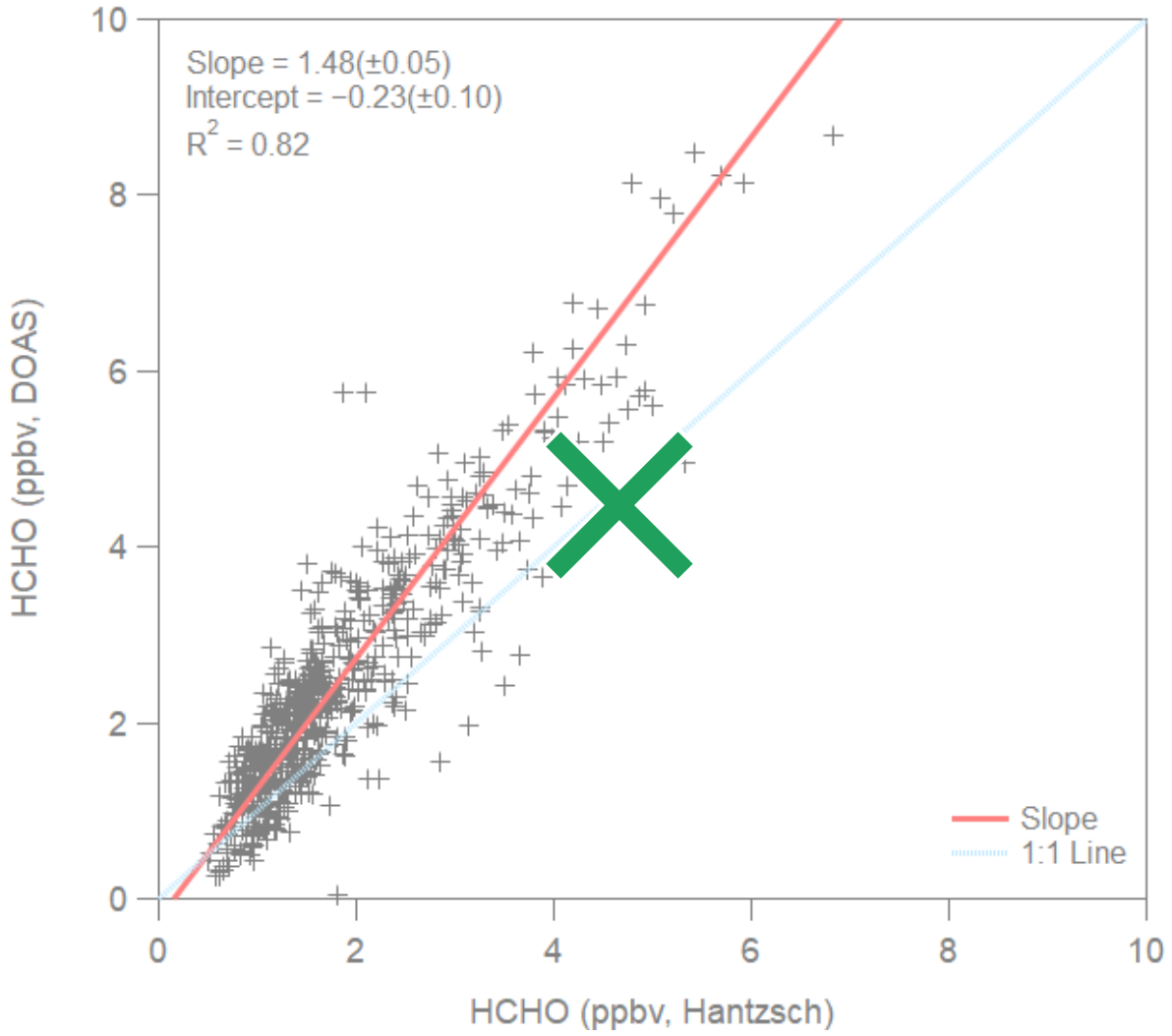


**Figure S1**. Comparison of HCHO measured by the DOAS (Stutz and Platt, 1996, 1997) and Hantzsch reaction (Cárdenas et al., 2000) methods during the CalNex 2010 study in Pasadena, CA, ground site (Ryerson et al., 2013).

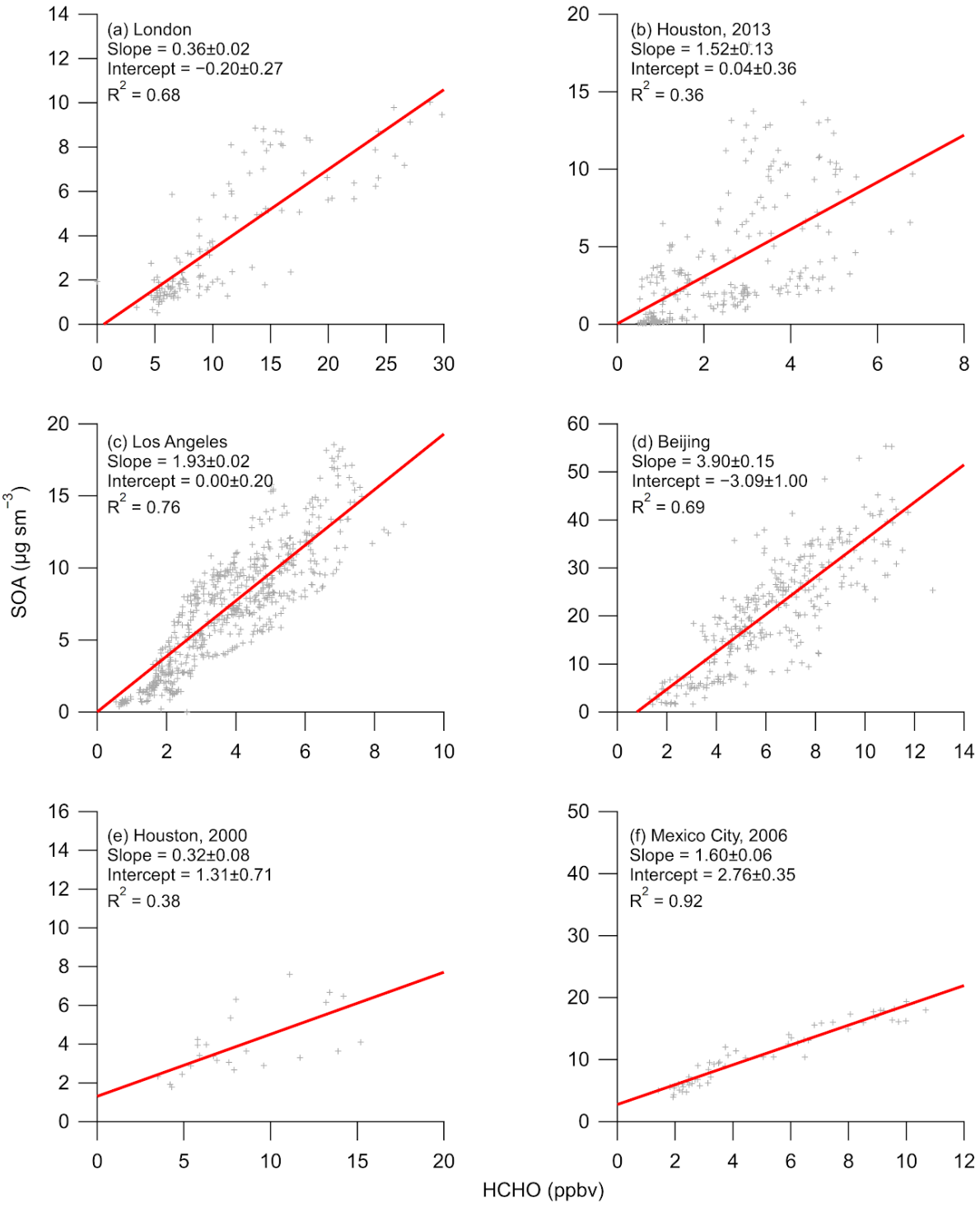


530

531 **Figure S12**. Regression plot of SOA versus HCHO from different campaigns around the world
532 that have not been previously published. Note, for (c), HCHO is 1.24×Hantzsch HCHO, to
533 account for the differences between the two HCHO measurements during CalNex. Note, for (a),
534 SOA is 0.5×OA, estimated from Young et al. (2015), and for (f), SOA is 0.8×OA, estimated from
535 DeCarlo et al. (2010).

536

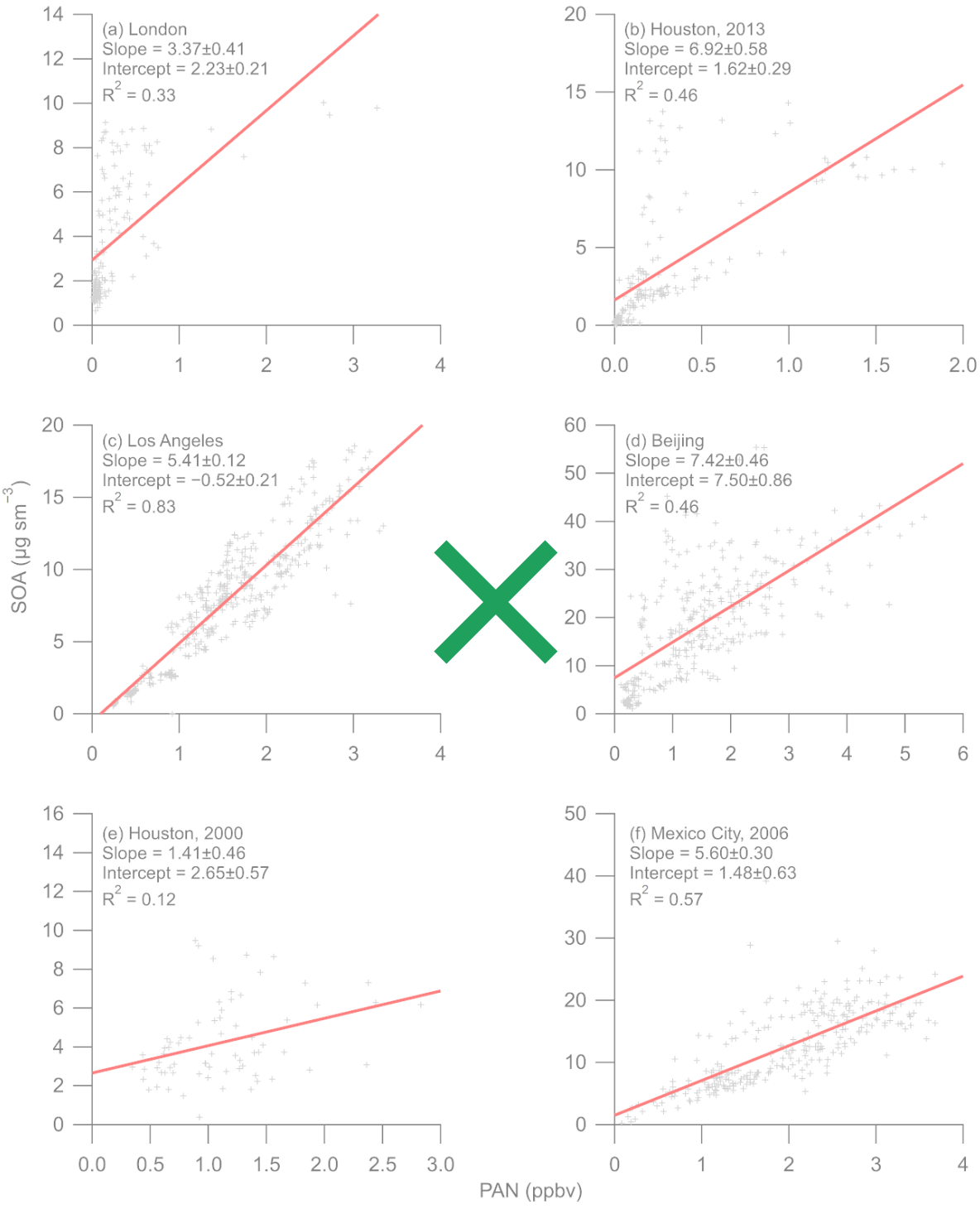
(a) London
Slope = 3.37±0.41
Intercept = 2.23±0.21
R2 = 0.33
(b) Houston, 2013
Slope = 6.92±0.58
Intercept = 1.62±0.29
R2 = 0.46
(c) Los Angeles
Slope = 5.41±0.12
Intercept = −0.52±0.21
R2 = 0.83
(d) Beijing
Slope = 7.42±0.46
Intercept = 7.50±0.86
R2 = 0.46
(e) Houston, 2000
Slope = 1.41±0.46
Intercept = 2.65±0.57
R2 = 0.12
(f) Mexico City, 2006
Slope = 5.60±0.30
Intercept = 1.48±0.63
R2 = 0.57
SOA (μg sm-3)
PAN (ppbv)

537

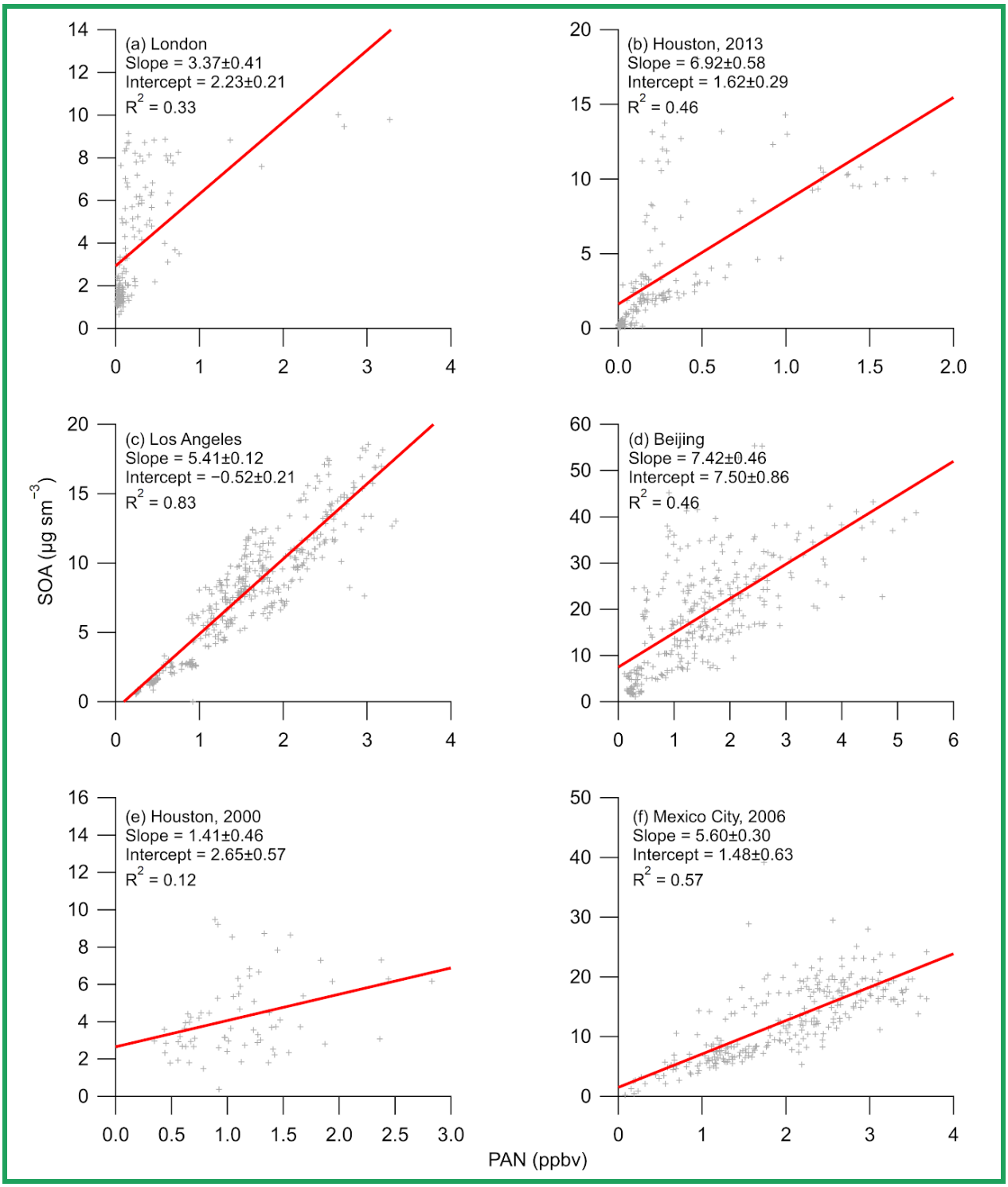


538

539 **Figure S23**. Regression plot of SOA versus PAN from different campaigns around the world that
540 have not been previously published. Note, for (a), SOA is 0.5×OA, estimated from Young et al.
541 (2015), and for (f), SOA is 0.8×OA, estimated from DeCarlo et al. (2010).

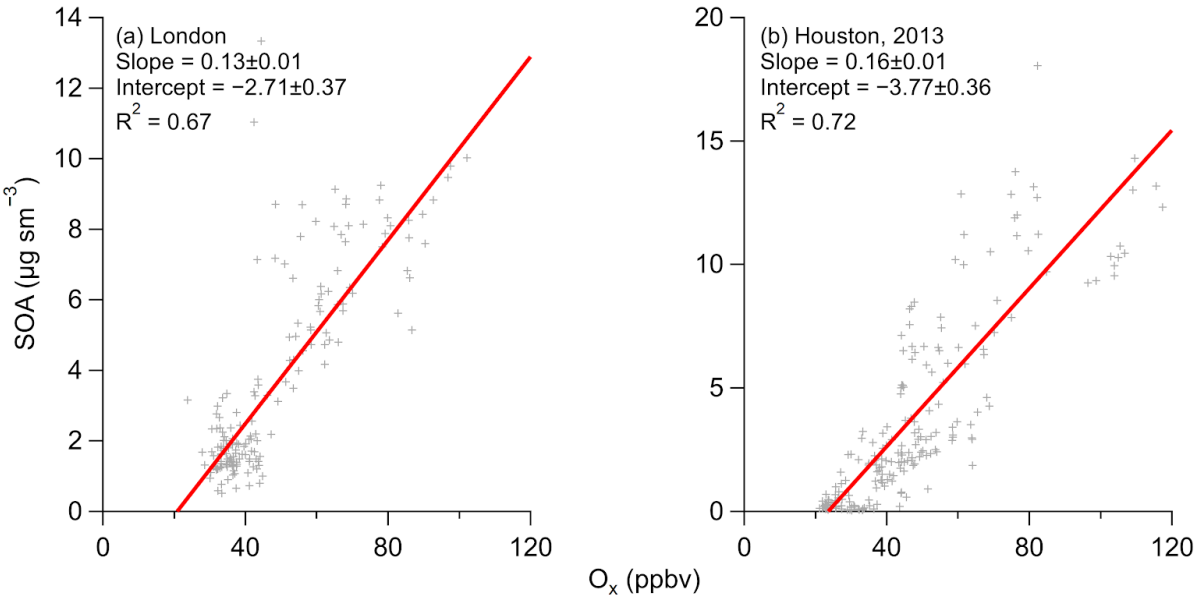


**Figure S34**. Regression plot of SOA versus Ox from different campaigns around the world that have not been previously published. Note, for (a), SOA is 0.5×OA, estimated from Young et al. (2015).

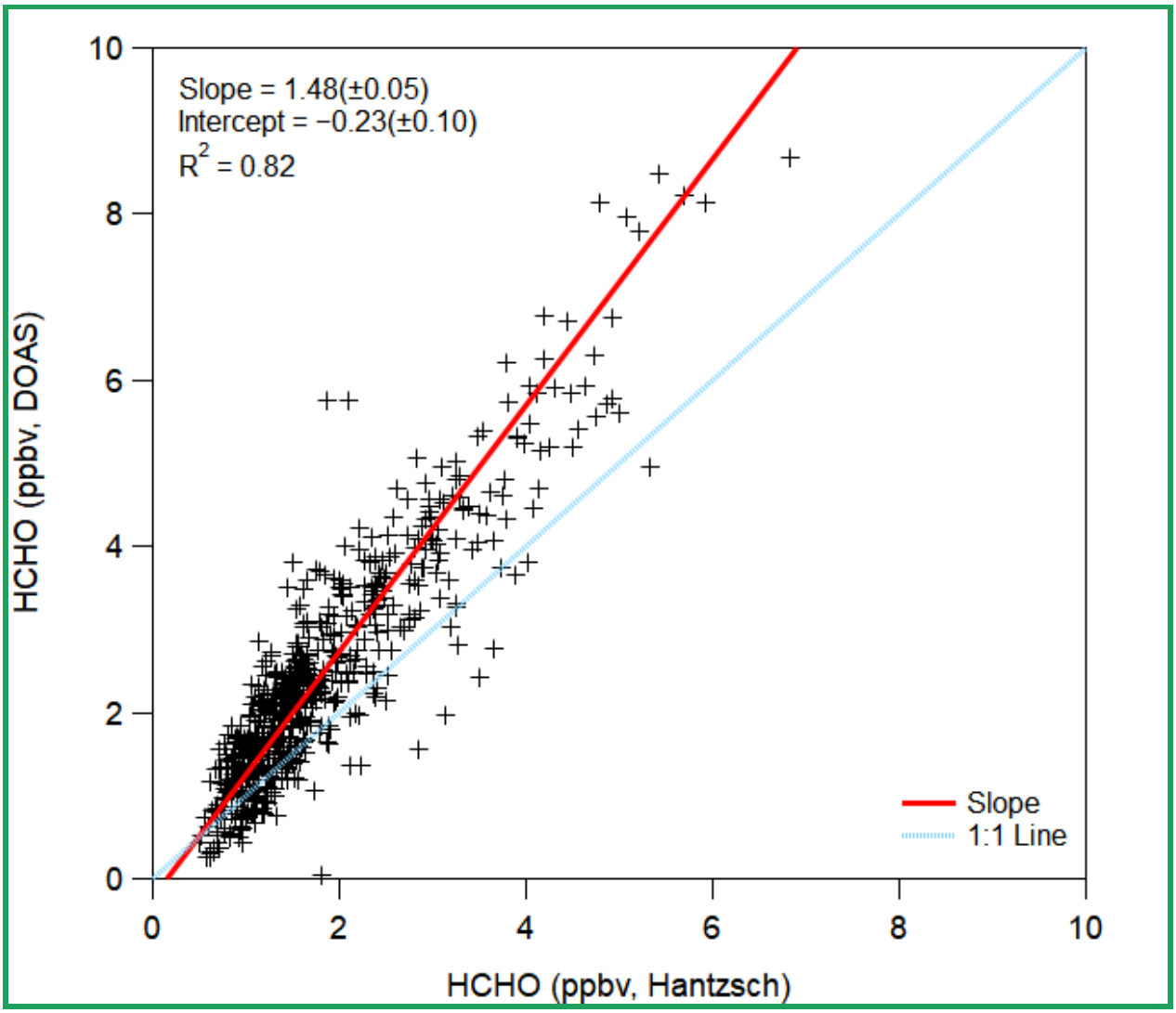


547

548 **Figure S4**. Comparison of HCHO measured by the DOAS (Stutz and Platt, 1996, 1997) and
549 Hantzsch reaction (Cárdenas et al., 2000) methods during the CalNex 2010 study in Pasadena,
550 CA, ground site (Ryerson et al., 2013).

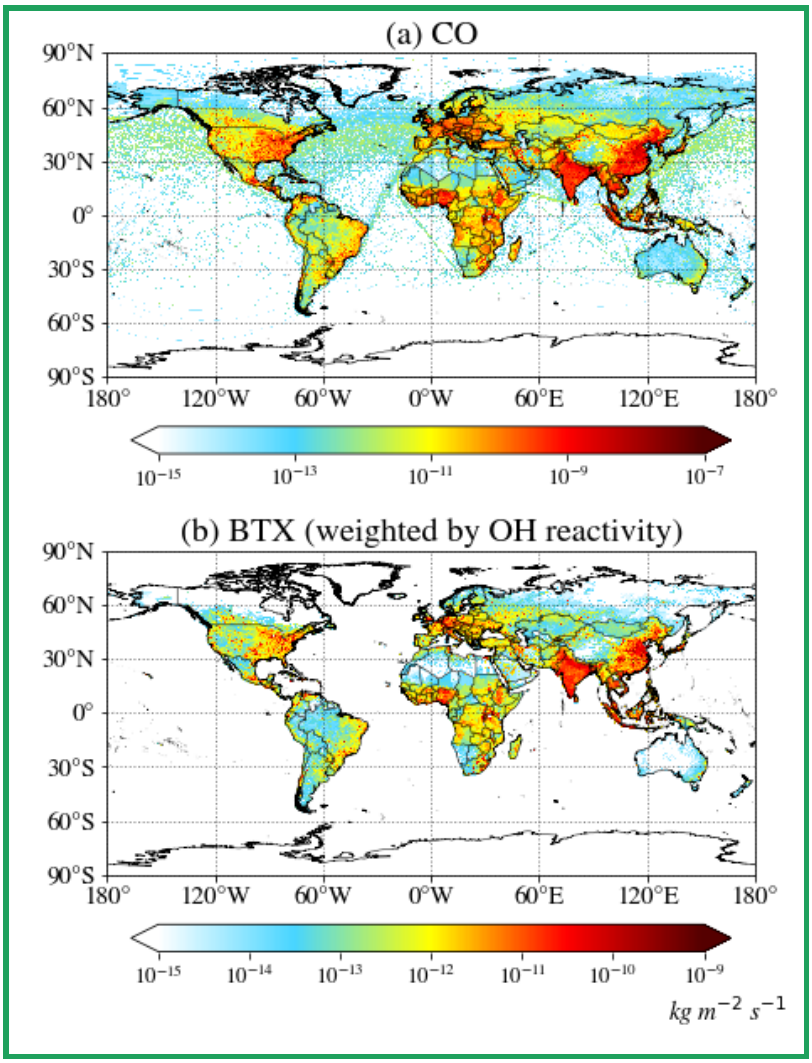


551

552 **Figure S5.** (a) Annually average CO emissions from HTaP. (b) Annually average benzene,
553 toluene, and xylenes (BTX) emissions, weighted by their OH reaction rate

554 ( $E_{weight} = N \frac{\sum_i E_i k_{OH,i}}{\sum_i k_{OH,i}}$, $i = B, T, X$ ; N=3).

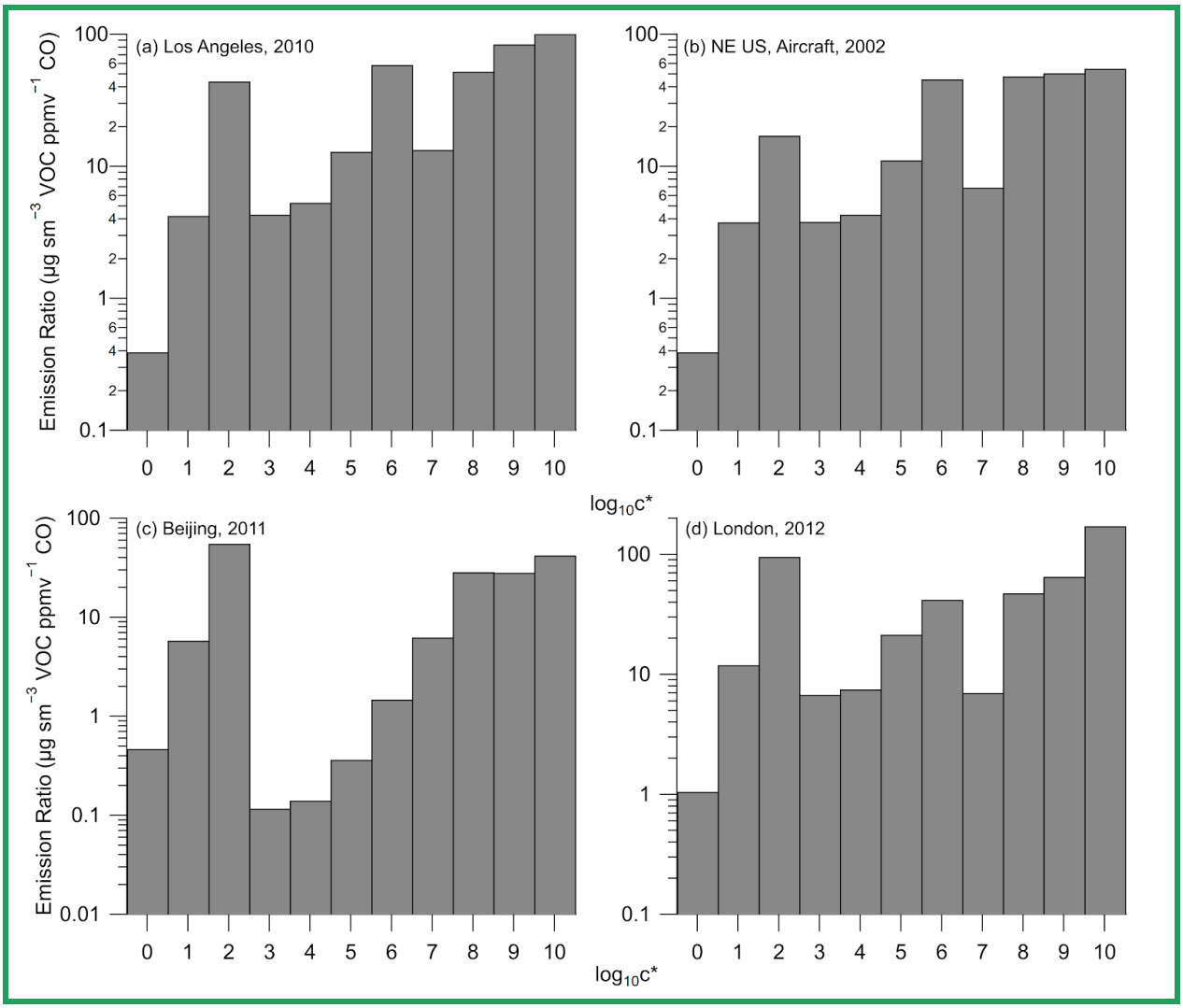


**Figure S6.** Emission ratio versus saturation concentration ($\log_{10}(c^*)$) for (a) Los Angeles, (b) NE US, aircraft, (c) Beijing, and (d) London. The emission ratios for VOCs ($\log_{10}(c^*) \geq 7$) were taken from de Gouw et al. (2017) and Ma et al. (2017) for Los Angeles, Warneke et al. (2007) for NE US, aircraft, and Wang et al. (2014) for Beijing while the VOC emission ratio for London is from Table S6 to Table S8. For VOCs between $\log_{10}(c^*)$ of 3 and 6 (IVOCs), the volatility distribution from McDonald et al. (2018), along with the ratio of IVOC to BTEX from Figure SI-6 and the emission ratio of BTEX (Table S6), were used to determine the emission ratio versus saturation concentration. Finally, for VOCs between $\log_{10}(c^*)$ 0 and 2 (SVOCs), the volatility distributions from Robinson et al. (2007) for non-fossil fuel POA and from Worton et al. (2014) for fossil fuel POA were used to convert the normalized POA mass concentration (Table S9) to VOC emission ratios. Note, the emission ratio versus saturation concentration for New York City, 2015, was similar to (b), as the emissions were similar (Fig. 5) and the BTEX for New York City is the same as NE US (Table S5).

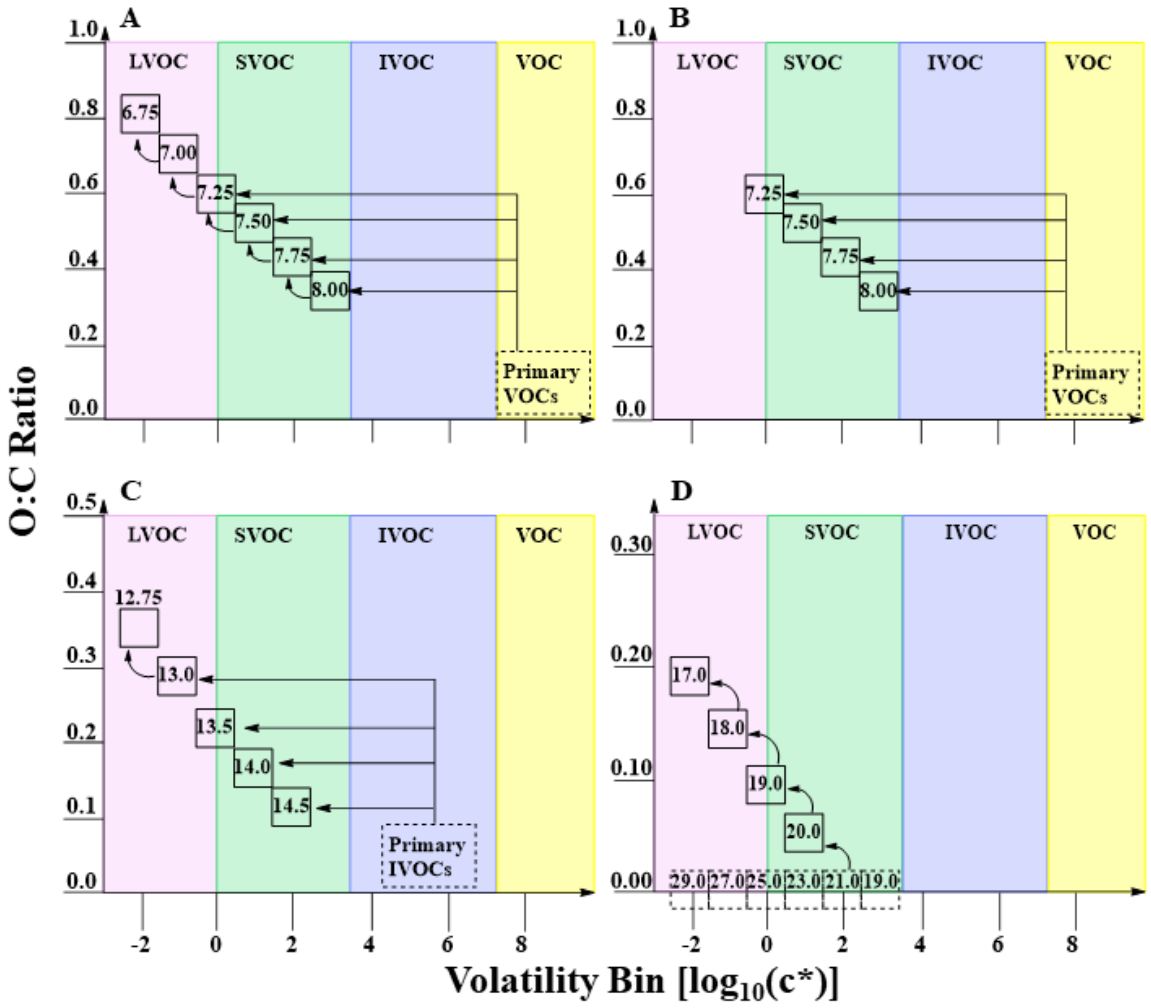


**Figure S75**. 2-D VBS space defined by oxygen to carbon (O:C) ratio and saturation concentration [$\log_{10}$(c*)] for different oxidation mechanisms and primary sources of OA precursors. Dashed boxes represent primary emissions, while the full boxes represent the secondary oxidation products. (A) and (B) represent different parameterizations for treating traditional anthropogenic and biogenic sources of SOA. Both parameterizations depict the oxidation of an 8-carbon precursor VOC. (A) represents the TSI, or aging, parameterization; (B) represents the MA, or wall-loss corrected, parameterization. (C) Represents the initial oxidation and aging pathway of P-IVOCs following the ZHAO parameterization. It should be noted that the carbon number corresponds to first generation aging and subsequent oxidation results in a 0.25 reduction in carbon number. (D) Represents the decadal aging of SVOCs by hydroxyl radicals. In (D), the full aging pathway of only the C21 species is depicted as an example, though all primary species are allowed to age until the $\log_{10}$(c*) = -2 bin. All emitted P-SVOC species undergo the same decadal aging scheme which begins from the saturation concentration bin of the emitted species.

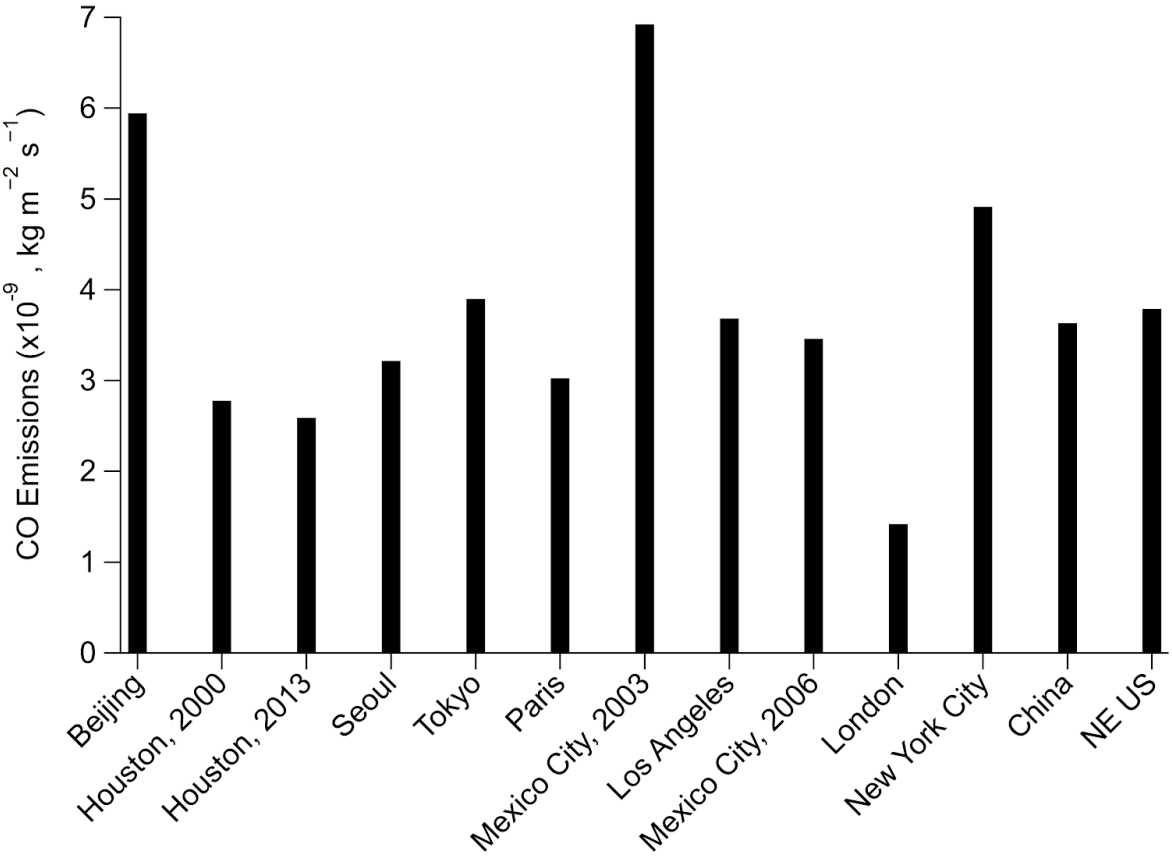


584

585 **Figure S~~86~~**. CO emissions for the cities investigated here from HTAP (Janssens-Maenhout et al.,
586 2015).

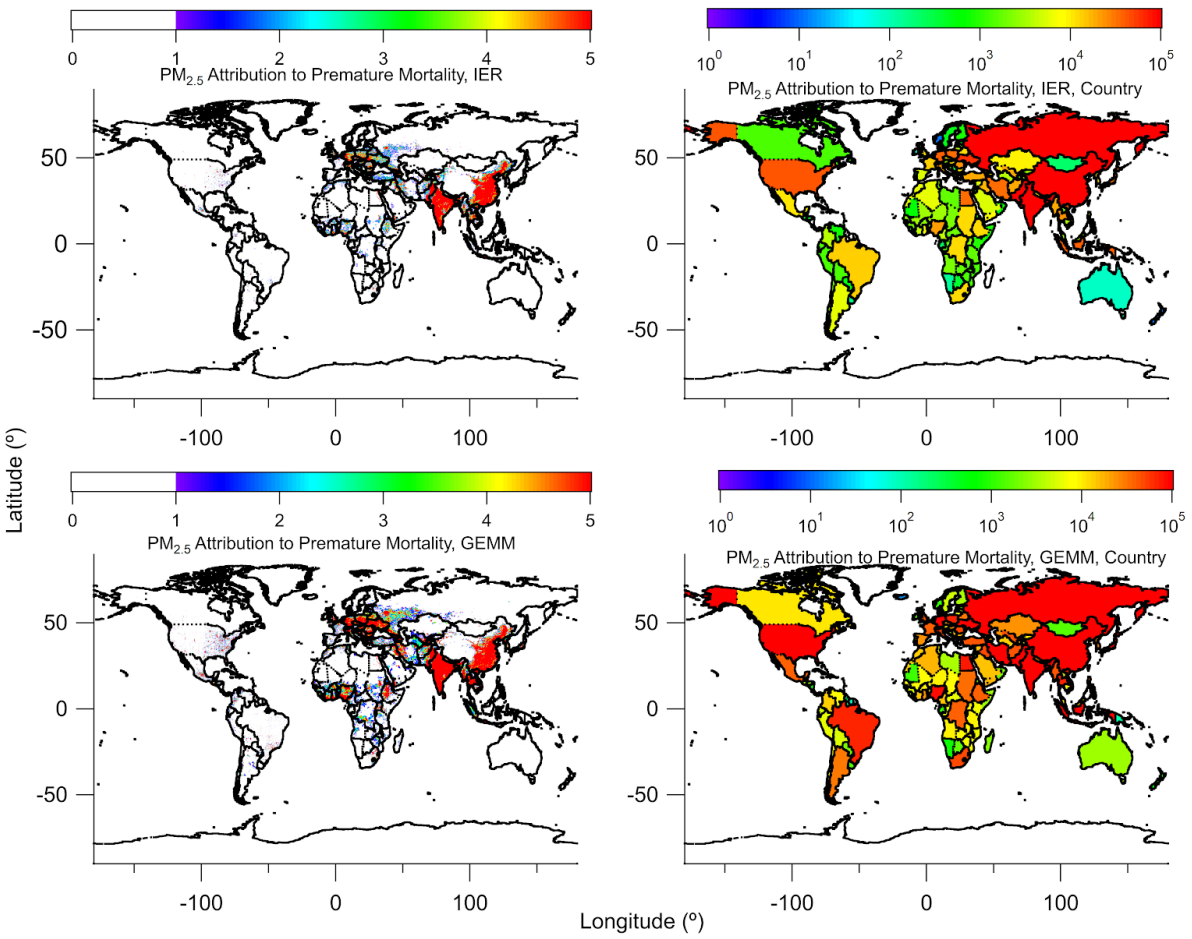


587

588 **Figure S97**. (top) Total deaths associated to $PM_{2.5}$ (left) per 10×10 $km^2$ area and (right) summed
589 up for each country, using the Integrated Exposure-Response (IER) method (Burnett et al.,
590 2014). These values are derived from satellite. (bottom) Same as above, but using the Global
591 Exposure Mortality Model (GEMM) (Burnett et al., 2018) for $PM_{2.5}$ per 10×10 $km^2$ area (left)
592 and summed up for each country (right). Premature mortality was determined with $PM_{2.5}$ derived
593 by the methods described in van Donkelaar (2015), which includes satellite and ground-based
594 observations of aerosol.

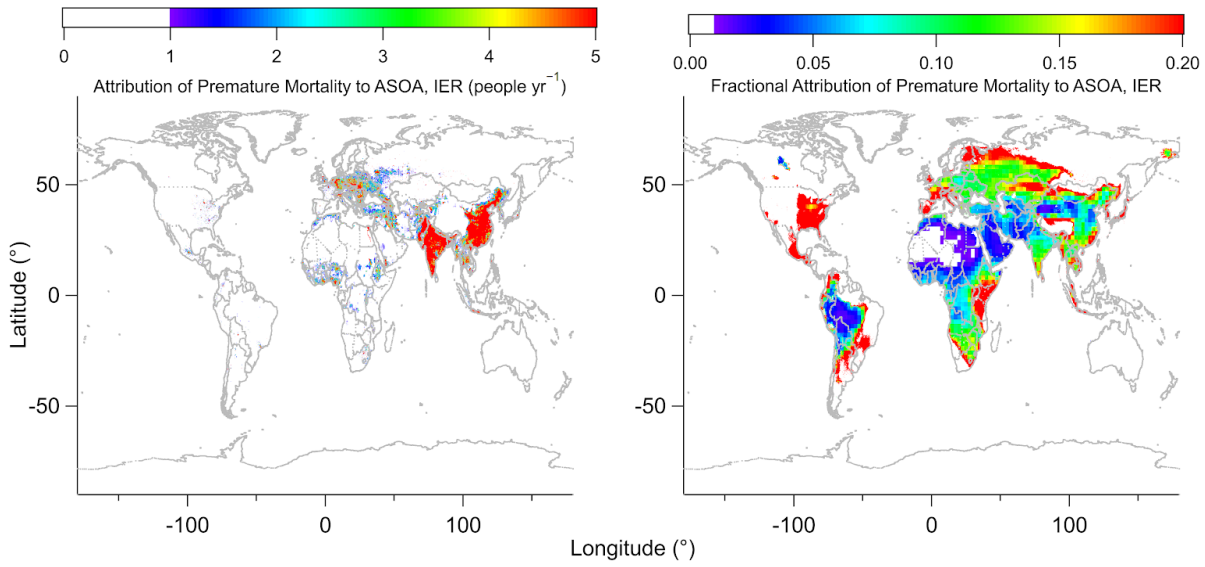


595

596 **Figure S108**. Same as Fig. 8, where top are the results per 10×10 km$^2$ area for the attribution of
597 premature mortality to ASOA (people yr$^{-1}$, left) and fractional attribution of premature mortality
598 to ASOA for one year (right) by the IER method. See Fig. 8 for per country comparison.

599

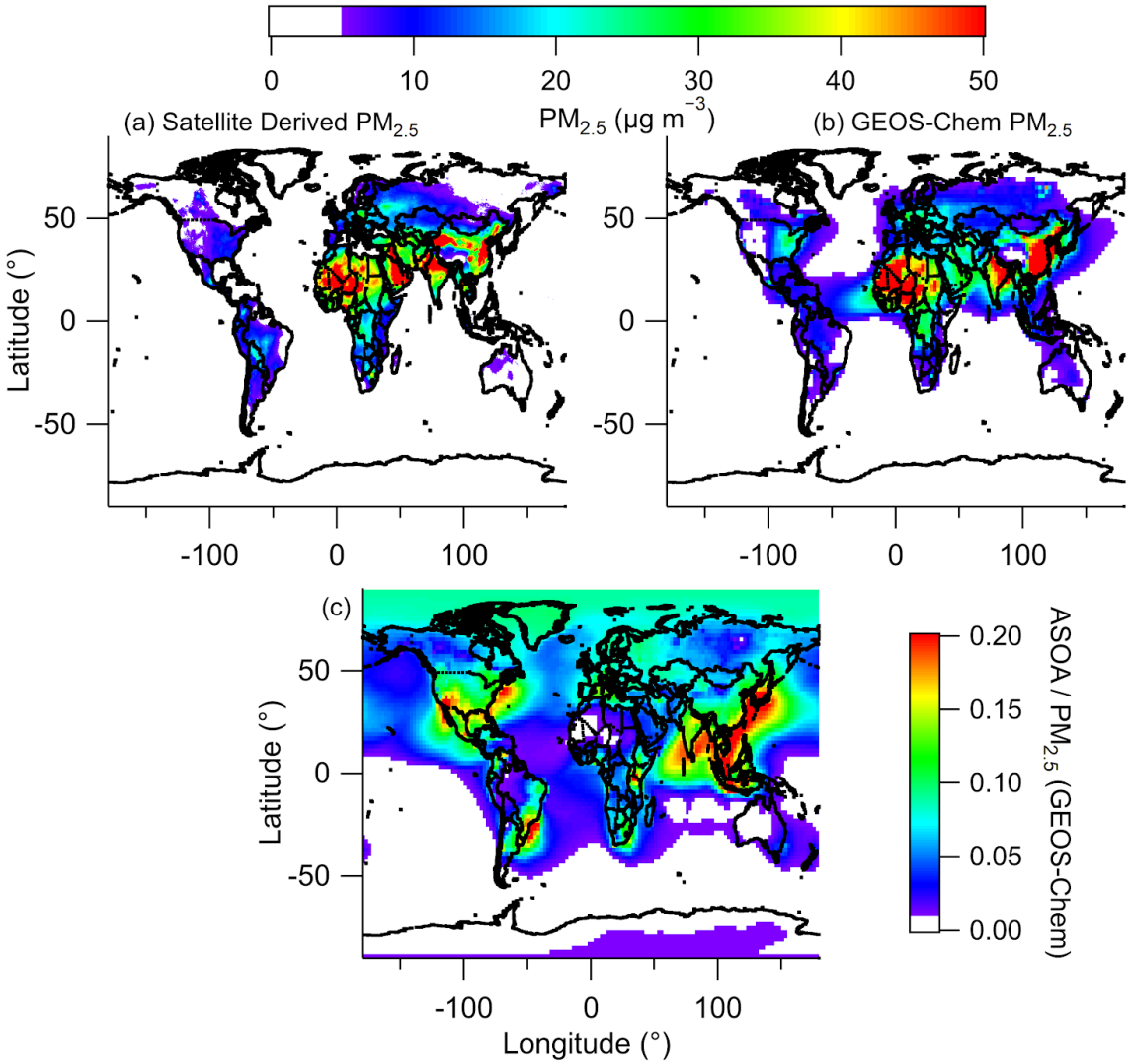


600 **Figure S119**. Comparison of satellite retrieved $PM_{2.5}$ (upper left) versus modeled $PM_{2.5}$ (upper
601 right). (Bottom) Fractional contribution of ASOA to total modeled $PM_{2.5}$.

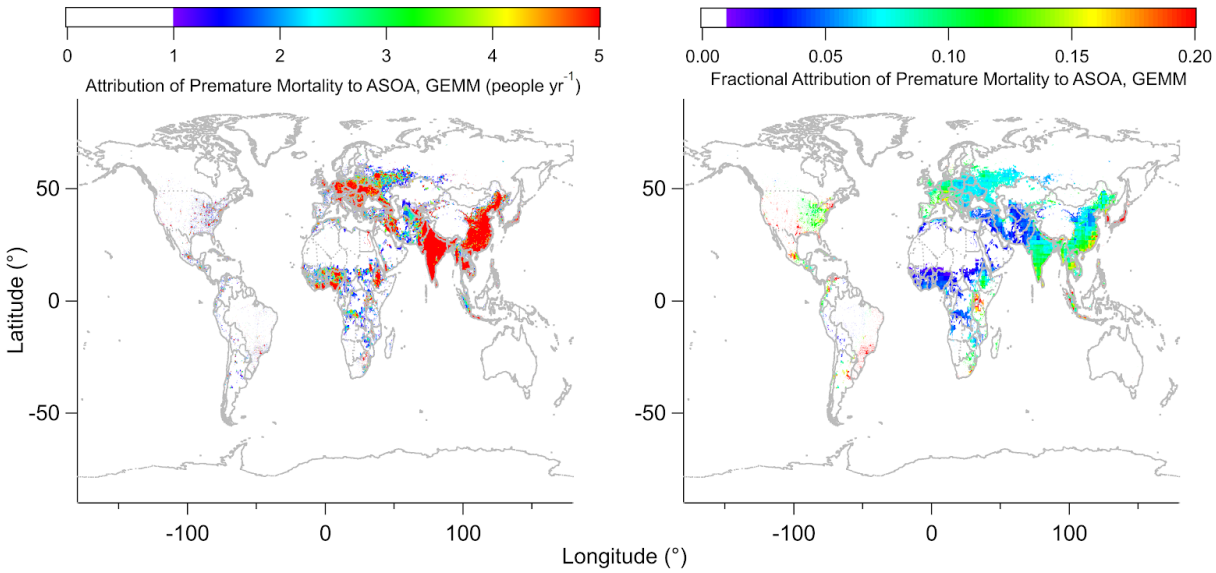


602

603 **Figure S120**. Same as Fig. S10, but using the GEMM from Burnett et al. (2018). (top). (Left)
604 Attribution of premature mortality to ASOA per 10×10 $km^2$ area (people $yr^{-1}$) and (Right)
605 fractional attribution of preamture mortality to ASOA per $10\times10^2$ km for one year.

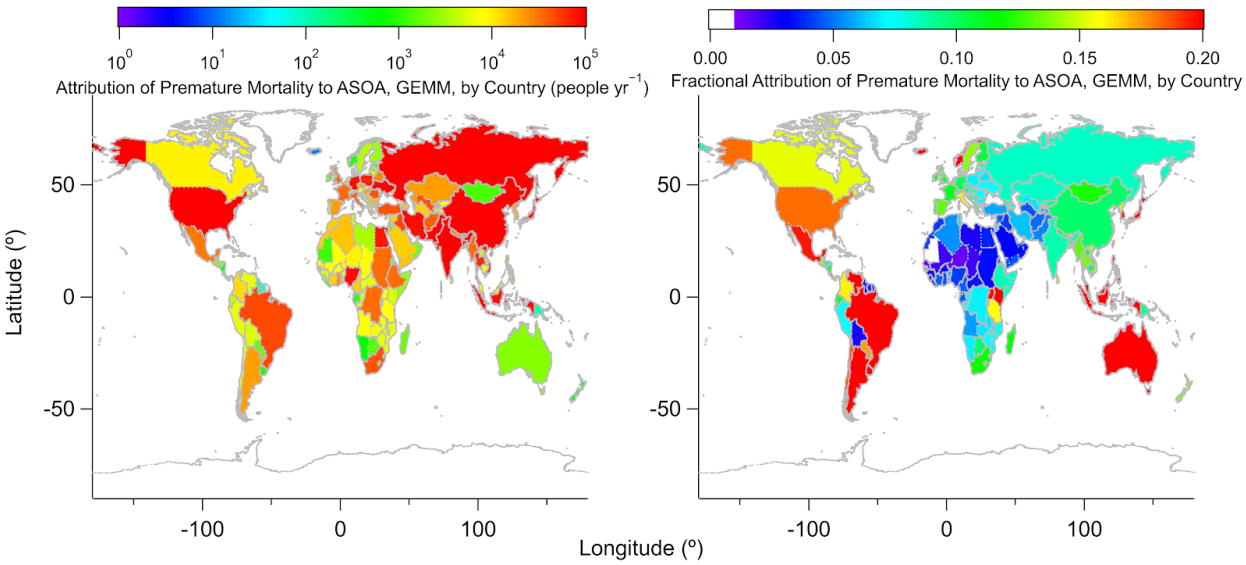


606

607 **Figure S131**. Same as Fig. S12 but summed up for each country for the (left) attribution of
608 premature mortality to ASOA (people yr$^{-1}$) and (right) the fractional attribution of premature
609 mortality to ASOA for one year.

610

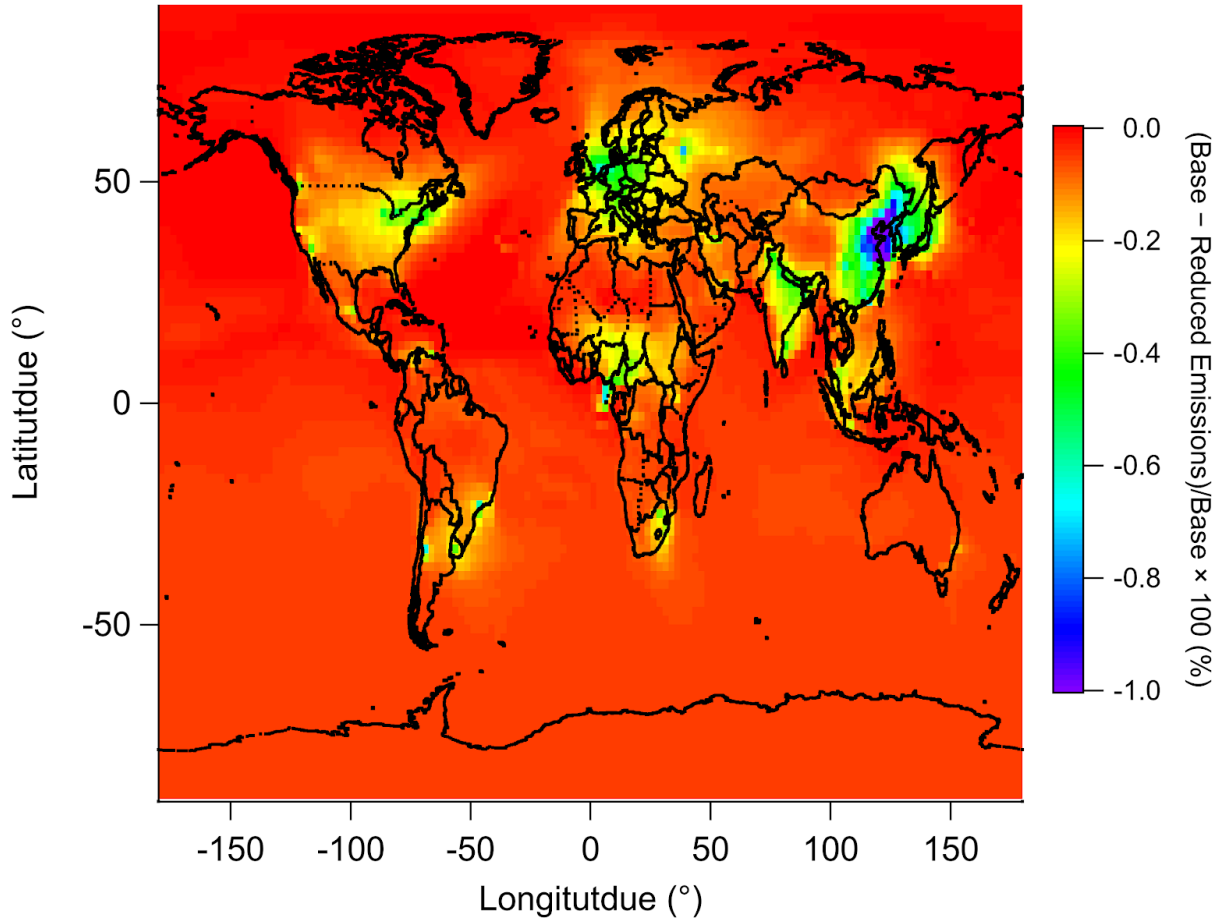


**Figure S142**. Comparison for surface level ozone upon reducing SOA precursors by 20%.

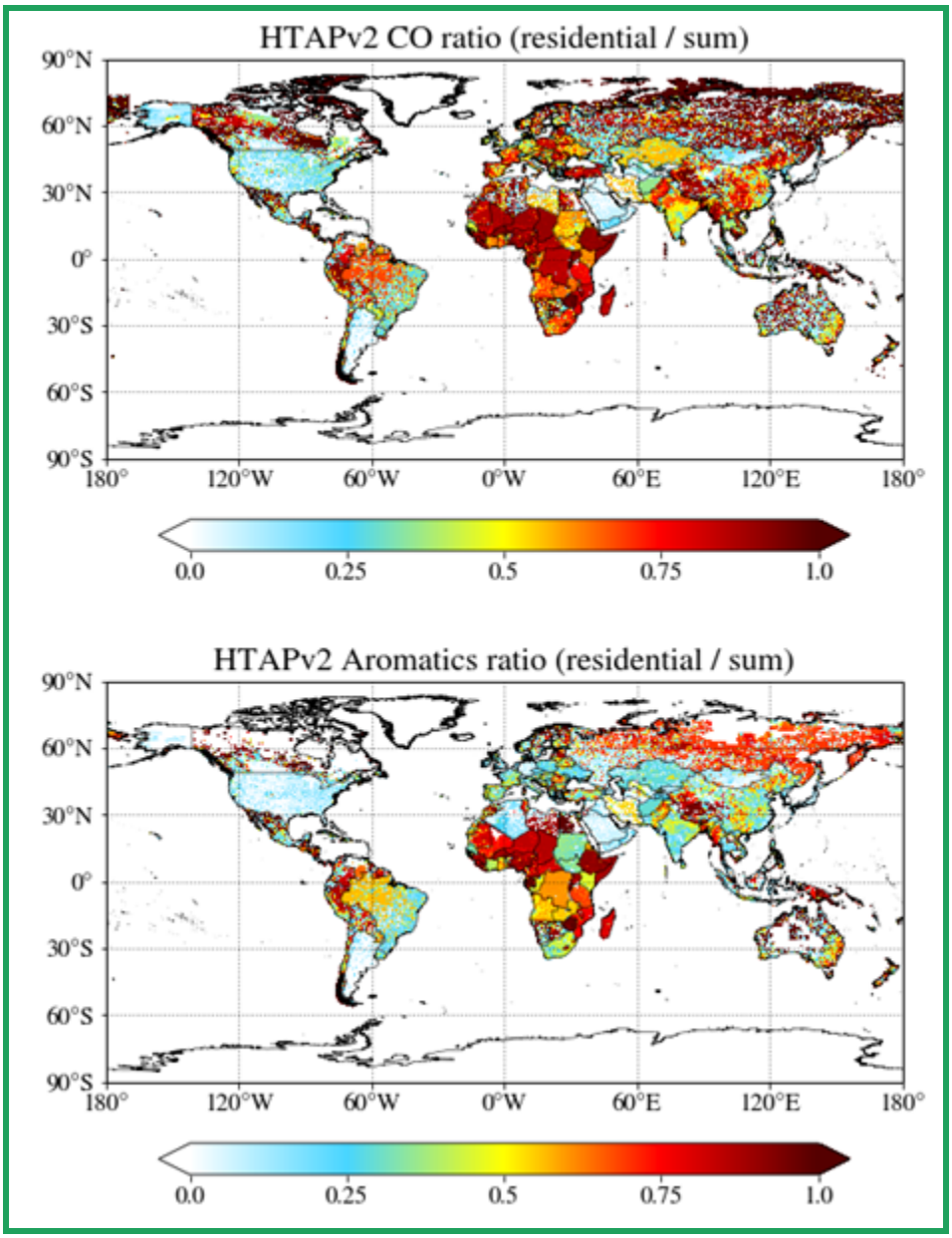


613

614 **Figure S15.** (top) Fractional contribution of CO emissions from residential sources to total
615 emission sources from HTaP. (bottom) Fractional contribution of BTEX emissions from
616 residential sources to total emission sources from HTaP. Residential sources include small-scale
617 combustion, such as heating and cooking, which may include solid-fuel emissions.

## References


Apel, E. C., Emmons, L. K., Karl, T., Flocke, F., Hills, a. J., Madronich, S., Lee-Taylor, J., Fried, A., Weibring, P., Walega, J., Richter, D., Tie, X., Mauldin, L., Campos, T., Weinheimer, A., Knapp, D., Sive, B., Kleinman, L., Springston, S., Zaveri, R., Ortega, J., Voss, P., Blake, D., Baker, A., Warneke, C., Welsh-Bon, D., de Gouw, J., Zheng, J., Zhang, R., Rudolph, J., Junkermann, W. and Riemer, D. D.: Chemical evolution of volatile organic compounds in the outflow of the Mexico City Metropolitan area, Atmos. Chem. Phys., 10(5), 2353–2375, 2010.

Atkinson, R. and Arey, J.: Atmospheric Degradation of Volatile Organic Compounds, Chem. Rev., 103, 4605–4638, 2003.

Atkinson, R., Baulch, D. L., Cox, R. A., Crowley, J. N., Hampson, R. F., Hynes, R. G., Jenkin, M. E., Rossi, M. J., Troe, J. and IUPAC Subcommittee: Evaluated kinetic and photochemical data for atmospheric chemistry: Volume II - gas phase reactions of organic species, Atmos. Chem. Phys., 6(11), 3625–4055, 2006.

Baker, A. K., Beyersdorf, A. J., Doezema, L. A., Katzenstein, A., Meinardi, S., Simpson, I. J., Blake, D. R. and Sherwood Rowland, F.: Measurements of nonmethane hydrocarbons in 28 United States cities, Atmos. Environ., 42(1), 170–182, 2008.

Blake, N. J., Blake, D. R., Simpson, I. J., Meinardi, S., Swanson, A. L., Lopez, J. P., Katzenstein, A. S., Barletta, B., Shirai, T., Atlas, E., Sachse, G., Avery, M., Vay, S., Fuelberg, H. E., Kiley, C. M., Kita, K. and Rowland, F. S.: NMHCs and halocarbons in Asian continental outflow during the Transport and Chemical Evolution over the Pacific (TRACE-P) Field Campaign: Comparison with PEM-West B, Journal of Geophysical Research-Atmospheres, 108(D20), 8806, 2003.

Bohn, B. and Zetzsch, C.: Kinetics and mechanism of the reaction of OH with the trimethylbenzenes – experimental evidence for the formation of adduct isomers, Phys. Chem. Chem. Phys., 14(40), 13933, 2012.

Burnett, R., Chen, H., Szyszkowicz, M., Fann, N., Hubbell, B., Pope, C. A., Apte, J. S., Brauer, M., Cohen, A., Weichenthal, S., Coggins, J., Di, Q., Brunekreef, B., Frostad, J., Lim, S. S., Kan, H., Walker, K. D., Thurston, G. D., Hayes, R. B., Lim, C. C., Turner, M. C., Jerrett, M., Krewski, D., Gapstur, S. M., Diver, W. R., Ostro, B., Goldberg, D., Crouse, D. L., Martin, R. V., Peters, P., Pinault, L., Tjepkema, M., van Donkelaar, A., Villeneuve, P. J., Miller, A. B., Yin, P., Zhou, M., Wang, L., Janssen, N. A. H., Marra, M., Atkinson, R. W., Tsang, H., Quoc Thach, T., Cannon, J. B., Allen, R. T., Hart, J. E., Laden, F., Cesaroni, G., Forastiere, F., Weinmayr, G., Jaensch, A., Nagel, G., Concin, H. and Spadaro, J. V.: Global estimates of mortality associated with long-term exposure to outdoor fine particulate matter, Proc. Natl. Acad. Sci. U. S. A., 115(38), 9592–9597, 2018.

Burnett, R. T., Pope, C. A., Ezzati, M., Olives, C., Lim, S. S., Mehta, S., Shin, H. H., Singh, G., Hubbell, B., Brauer, M., Anderson, H. R., Smith, K. R., Balmes, J. R., Bruce, N. G., Kan, H., Laden, F., Prüss-Ustün, A., Turner, M. C., Gapstur, S. M., Diver, W. R. and Cohen, A.: An integrated risk function for estimating the global burden of disease attributable to ambient fine

particulate matter exposure, Environ. Health Perspect., 122(4), 397–403, 2014.

CARB: CEPAM: 2013 Almanac - Standard Emissions Tool, [online] Available from: https://www.arb.ca.gov/app/emsinv/fcemssumcat2013.php, 2013.

Cárdenas, L. M., Brassington, D. J., Allan, B. J., Coe, H., Alicke, B., Platt, U., Wilson, K. M., Plane, J. M. C. and Penkett, S. A.: Intercomparison of Formaldehyde Measurements in Clean and Polluted Atmospheres, J. Atmos. Chem., 37(1), 53–80, 2000.

Cazorla, M., Wolfe, G. M., Bailey, S. A., Swanson, A. K., Arkinson, H. L. and Hanisco, T. F.: A new airborne laser-induced fluorescence instrument for in situ detection of formaldehyde throughout the troposphere and lower stratosphere, Atmos. Meas. Tech., 8(2), 541–552, 2015.

CCPR: The California Consumer Products Regulation., 2015.

Davis, M. S.: 2005 Architectural Coatings Survey Final Report, CARB., 2007.

DeCarlo, P. F., Kimmel, J. R., Trimborn, A., Northway, M. J., Jayne, J. T., Aiken, A. C., Gonin, M., Fuhrer, K., Horvath, T., Docherty, K. S., Worsnop, D. R. and Jimenez, J. L.: Field-deployable, high-resolution, time-of-flight aerosol mass spectrometer, Anal. Chem., 78(24), 8281–8289, 2006.

DeCarlo, P. F., Ulbrich, I. M., Crounse, J., de Foy, B., Dunlea, E. J., Aiken, A. C., Knapp, D., Weinheimer, A. J., Campos, T., Wennberg, P. O. and Jimenez, J. L.: Investigation of the sources and processing of organic aerosol over the Central Mexican Plateau from aircraft measurements during MILAGRO, Atmos. Chem. Phys., 10(12), 5257–5280, 2010.

van Donkelaar, A., Martin, R. V., Brauer, M., Hsu, N. C., Kahn, R. A., Levy, R. C., Lyapustin, A., Sayer, A. M. and Winker, D. M.: Global Estimates of Fine Particulate Matter using a Combined Geophysical-Statistical Method with Information from Satellites, Models, and Monitors, Environ. Sci. Technol., 50(7), 3762–3772, 2016.

Drewnick, F., Hings, S. S., DeCarlo, P., Jayne, J. T., Gonin, M., Fuhrer, K., Weimer, S., Jimenez, J. L., Demerjian, K. L., Borrmann, S. and Worsnop, D. R.: A New Time-of-Flight Aerosol Mass Spectrometer (TOF-AMS)—Instrument Description and First Field Deployment, Aerosol Sci. Technol., 39(7), 637–658, 2005.

Dunmore, R. E., Hopkins, J. R., Lidster, R. T., Lee, J. D., Evans, M. J., Rickard, A. R., Lewis, A. C. and Hamilton, J. F.: Diesel-related hydrocarbons can dominate gas phase reactive carbon in megacities, Atmos. Chem. Phys., 15, 9983–9996, 2015.

EMEP/EEA: EMEP/EEA Air Pollutant Emission Inventory Guidebook 2016, EEA, Luxembourg., 2016.

EPA: SPECIATE v4.4, US Environmental Protection Agency., 2014.

Fisher, J. A., Jacob, D. J., Travis, K. R., Kim, P. S., Marais, E. A., Miller, C. C., Yu, K., Zhu, L.,

690 Yantosca, R. M., Sulprizio, M. P., Mao, J., Wennberg, P. O., Crounse, J. D., Teng, A. P., Nguyen,
691 T. B., Clair, J. M. S., Cohen, R. C., Romer, P., Nault, B. A., Wooldridge, P. J., Jimenez, J. L.,
692 Campuzano-Jost, P., Day, D. A., Hu, W., Shepson, P. B., Xiong, F., Blake, D. R., Goldstein, A.
693 H., Misztal, P. K., Hanisco, T. F., Wolfe, G. M., Ryerson, T. B., Wisthaler, A. and Mikoviny, T.:
694 Organic nitrate chemistry and its implications for nitrogen budgets in an isoprene- and
695 monoterpene-rich atmosphere: Constraints from aircraft (SEAC$^4$RS) and ground-based (SOAS)
696 observations in the Southeast US, Atmos. Chem. Phys., 16(9), doi:10.5194/acp-16-5969-2016,
697 2016.

698 Fried, A., Crawford, J., Olson, J., Walega, J., Potter, W., Wert, B., Jordan, C., Anderson, B.,
699 Shetter, R., Lefer, B., Blake, D., Blake, N., Meinardi, S., Heikes, B., O'Sullivan, D., Snow, J.,
700 Fuelberg, H., Kiley, C. M., Sandholm, S., Tan, D., Sachse, G., Singh, H., Faloona, I., Harward,
701 C. N. and Carmichael, G. R.: Airborne tunable diode laser measurements of formaldehyde during
702 TRACE-P: Distributions and box model comparisons, J. Geophys. Res. D: Atmos., 108(D20),
703 8798, 2003.

704 Gately, C. K., Hutyra, L. R. and Wing, I. S.: Cities, traffic, and $CO_2$: A multidecadal assessment
705 of trends, drivers, and scaling relationships, Proc. Natl. Acad. Sci. U. S. A., 112(16), 4999–5004,
706 2015.

707 Gentner, D. R., Isaacman, G., Worton, D. R., Chan, A. W. H., Dallmann, T. R., Davis, L., Liu, S.,
708 Day, D. A., Russell, L. M., Wilson, K. R., Weber, R., Guha, A., Harley, R. A. and Goldstein, A.
709 H.: Elucidating secondary organic aerosol from diesel and gasoline vehicles through detailed
710 characterization of organic carbon emissions, Proc. Natl. Acad. Sci. U. S. A., 109(45),
711 18318–18323, 2012.

712 Gentner, D. R., Worton, D. R., Isaacman, G., Davis, L. C., Dallmann, T. R., Wood, E. C.,
713 Herndon, S. C., Goldstein, A. H. and Harley, R. A.: Chemical Composition of Gas-Phase
714 Organic Carbon Emissions from Motor Vehicles and Implications for Ozone Production,
715 Environ. Sci. Technol., 47(20), 11837–11848, 2013.

716 Gerbig, C., Schmitgen, S., Kley, D., Volz-Thomas, A., Dewey, K. and Haaks, D.: An improved
717 fast-response vacuum-UV resonance fluorescence CO instrument, J. Geophys. Res. D: Atmos.,
718 104(D1), 1699–1704, 1999.

719 Gilman, J. B., Burkhart, J. F., Lerner, B. M., Williams, E. J., Kuster, W. C., Goldan, P. D.,
720 Murphy, P. C., Warneke, C., Fowler, C., Montzka, S. A., Miller, B. R., Miller, L., Oltmans, S. J.,
721 Ryerson, T. B., Cooper, O. R., Stohl, A. and de Gouw, J. A.: Ozone variability and halogen
722 oxidation within the Arctic and sub-Arctic springtime boundary layer, Atmos. Chem. Phys.,
723 10(21), 10223–10236, 2010.

724 de Gouw, J. A., Middlebrook, A. M., Warneke, C., Goldan, P. D., Kuster, W. C., Roberts, J. M.,
725 Fehsenfeld, F. C., Worsnop, D. R., Canagaratna, M. R., Pszenny, A. A. P., Keene, W. C.,
726 Marchewka, M., Bertman, S. B. and Bates, T. S.: Budget of organic carbon in a polluted
727 atmosphere: Results from the New England Air Quality Study in 2002, J. Geophys. Res. D:

Atmos., 110(16), 1–22, 2005.

de Gouw, J. A., Gilman, J. B., Kim, S.-W., Lerner, B. M., Isaacman-VanWertz, G., McDonald, B. C., Warneke, C., Kuster, W. C., Lefer, B. L., Griffith, S. M., Dusanter, S., Stevens, P. S. and Stutz, J.: Chemistry of Volatile Organic Compounds in the Los Angeles basin: Nighttime Removal of Alkenes and Determination of Emission Ratios, J. Geophys. Res.: Atmos., 122(21), 11,843–11,861, 2017.

Griffith, S. M., Hansen, R. F., Dusanter, S., Michoud, V., Gilman, J. B., Kuster, W. C., Veres, P. R., Graus, M., Gouw, J. A., Roberts, J., Young, C., Washenfelder, R., Brown, S. S., Thalman, R., Waxman, E., Volkamer, R., Tsai, C., Stutz, J., Flynn, J. H., Grossberg, N., Lefer, B., Alvarez, S. L., Rappenglueck, B., Mielke, L. H., Osthoff, H. D. and Stevens, P. S.: Measurements of hydroxyl and hydroperoxy radicals during CalNex-LA: Model comparisons and radical budgets, J. Geophys. Res. D: Atmos., 121(8), 4211–4232, 2016.

Hassler, B., McDonald, B. C., Frost, G. J., Borbon, A., Carslaw, D. C., Civerolo, K., Granier, C., Monks, P. S., Monks, S., Parrish, D. D., Pollack, I. B., Rosenlof, K. H., Ryerson, T. B., von Schneidemesser, E. and Trainer, M.: Analysis of long-term observations of $NO_x$ and CO in megacities and application to constraining emissions inventories, Geophys. Res. Lett., 43(18), 9920–9930, 2016.

Hayes, P. L., Ortega, A. M., Cubison, M. J., Froyd, K. D., Zhao, Y., Cliff, S. S., Hu, W. W., Toohey, D. W., Flynn, J. H., Lefer, B. L., Grossberg, N., Alvarez, S., Rappenglück, B., Taylor, J. W., Allan, J. D., Holloway, J. S., Gilman, J. B., Kuster, W. C., de Gouw, J. A., Massoli, P., Zhang, X., Liu, J., Weber, R. J., Corrigan, A. L., Russell, L. M., Isaacman, G., Worton, D. R., Kreisberg, N. M., Goldstein, A. H., Thalman, R., Waxman, E. M., Volkamer, R., Lin, Y. H., Surratt, J. D., Kleindienst, T. E., Offenberg, J. H., Dusanter, S., Griffith, S., Stevens, P. S., Brioude, J., Angevine, W. M. and Jimenez, J. L.: Organic aerosol composition and sources in Pasadena, California, during the 2010 CalNex campaign, J. Geophys. Res. D: Atmos., 118(16), 9233–9257, 2013.

Huey L Tanner D Slusher D Dibb J Arimoto R Chen G Davis D Buhr M Nowak J Mauldin R Eisele F, K. E.: CIMS measurements of HNO3 and SO2 at the South Pole during ISCAT 2000, Atmos. Environ., 38(32), 5411–5421, 2004.

Hu, W., Hu, M., Hu, W., Jimenez, J. L., Yuan, B., Chen, W., Wang, M., Wu, Y., Chen, C., Wang, Z., Peng, J., Zeng, L. and Shao, M.: Chemical composition, sources, and aging process of submicron aerosols in Beijing: Contrast between summer and winter, J. Geophys. Res. D: Atmos., 121(4), 1955–1977, 2016.

IEA: World energy balances, IEA World Energy Statistics and Balances, doi:10.1787/data-00521-en, 2019.

Janssens-Maenhout, G., Crippa, M., Guizzardi, D., Dentener, F., Muntean, M., Pouliot, G., Keating, T., Zhang, Q., Kurokawa, J., Wankmüller, R., Denier van der Gon, H., Kuenen, J. J. P., Klimont, Z., Frost, G., Darras, S., Koffi, B. and Li, M.: HTAP_v2.2: a mosaic of regional and

global emission grid maps for 2008 and 2010 to study hemispheric transport of air pollution, Atmos. Chem. Phys., 15(19), 11411–11432, 2015.

Jayne, J. T., Leard, D. C., Zhang, X. F., Davidovits, P., Smith, K. A., Kolb, C. E. and Worsnop, D. R.: Development of an aerosol mass spectrometer for size and composition analysis of submicron particles, Aerosol Sci. Technol., 33(1-2), 49–70, 2000.

Kaiser, J., Jacob, D. J., Zhu, L., Travis, K. R., Fisher, J. A., González Abad, G., Zhang, L., Zhang, X., Fried, A., Crounse, J. D., St. Clair, J. M. and Wisthaler, A.: High-resolution inversion of OMI formaldehyde columns to quantify isoprene emission on ecosystem-relevant scales: application to the southeast US, Atmos. Chem. Phys., 18(8), 5483–5497, 2018.

Kim, S., Huey, L. G., Stickel, R. E., Tanner, D. J., Crawford, J. H., Olson, J. R., Chen, G., Brune, W. H., Ren, X., Lesher, R., Wooldridge, P. J., Bertram, T. H., Perring, A., Cohen, R. C., Lefer, B. L., Shetter, R. E., Avery, M., Diskin, G. and Sokolik, I.: Measurement of $HO_2NO_2$ in the free troposphere during the Intercontinental Chemical Transport Experiment–North America 2004, J. Geophys. Res. D: Atmos., 112, D12S01, 2007.

Kleinman, L. I., Daum, P. H., Lee, Y.-N., Senum, G. I., Springston, S. R., Wang, J., Berkowitz, C., Hubbe, J., Zaveri, R. A., Brechtel, F. J., Jayne, J., Onasch, T. B. and Worsnop, D.: Aircraft observations of aerosol composition and ageing in New England and Mid-Atlantic States during the summer 2002 New England Air Quality Study field campaign, J. Geophys. Res. D: Atmos., 112(D9), D09310, 2007.

Langford, B., Nemitz, E., House, E., Phillips, G. J., Famulari, D., Davison, B., Hopkins, J. R., Lewis, A. C. and Hewitt, C. N.: Fluxes and concentrations of volatile organic compounds above central London, UK, Atmos. Chem. Phys., 10(2), 627–645, 2010.

Li, M., Zhang, Q., Streets, D. G., He, K. B., Cheng, Y. F., Emmons, L. K., Huo, H., Kang, S. C., Lu, Z., Shao, M., Su, H., Yu, X. and Zhang, Y.: Mapping Asian anthropogenic emissions of non-methane volatile organic compounds to multiple chemical mechanisms, Atmos. Chem. Phys., 14(11), 5617–5638, 2014.

Li, M., Liu, H., Geng, G., Hong, C., Liu, F., Song, Y., Tong, D., Zheng, B., Cui, H., Man, H., Zhang, Q. and He, K.: Anthropogenic emission inventories in China: a review, Natl Sci Rev, 4(6), 834–866, 2017.

Li, M., Zhang, Q., Zheng, B., Tong, D., Lei, Y., Liu, F., Chaopeng, H., Kang, S., Yan, L., Zhang, Y., Bo, Y., Su, H., Cheng, Y. and He, K.: Persistent growth of anthropogenic non-methane volatile organic compound (NMVOC) emissions in China during 1990-2017: drivers, speciation and ozone formation potential, Atmos. Chem. Phys., 19, 8897–8913, 2019.

Liu, F., Zhang, Q., Tong, D., Zheng, B., Li, M., Huo, H. and He, K. B.: High-resolution inventory of technologies, activities, and emissions of coal-fired power plants in China from 1990 to 2010, Atmos. Chem. Phys., 15(23), 13299–13317, 2015.

Marais, E. A., Jacob, D. J., Jimenez, J. L., Campuzano-Jost, P., Day, D. A., Hu, W., Krechmer, J.,

Zhu, L., Kim, P. S., Miller, C. C., Fisher, J. A., Travis, K., Yu, K., Hanisco, T. F., Wolfe, G. M., Arkinson, H. L., Pye, H. O. T., Froyd, K. D., Liao, J. and McNeill, V. F.: Aqueous-phase mechanism for secondary organic aerosol formation from isoprene: application to the southeast United States and co-benefit of $SO_2$ emission controls, Atmos. Chem. Phys., 16(3), 1603–1618, 2016.

Matheson, R. R.: 20th- to 21st-Century Technological Challenges in Soft Coatings, Science, 297(5583), 976–979, 2002.

McDonald, B. C., Gentner, D. R., Goldstein, A. H. and Harley, R. A.: Long-Term Trends in Motor Vehicle Emissions in U.S. Urban Areas, Environ. Sci. Technol., 47(17), 10022–10031, 2013.

McDonald, B. C., Goldstein, A. H. and Harley, R. A.: Long-Term Trends in California Mobile Source Emissions and Ambient Concentrations of Black Carbon and Organic Aerosol, Environ. Sci. Technol., 49(8), 5178–5188, 2015.

McDonald, B. C., de Gouw, J. A., Gilman, J. B., Jathar, S. H., Akherati, A., Cappa, C. D., Jimenez, J. L., Lee-Taylor, J., Hayes, P. L., McKeen, S. A., Cui, Y. Y., Kim, S.-W., Gentner, D. R., Isaacman-VanWertz, G., Goldstein, A. H., Harley, R. A., Frost, G. J., Roberts, J. M., Ryerson, T. B. and Trainer, M.: Volatile chemical products emerging as largest petrochemical source of urban organic emissions, Science, 359(6377), 760–764, 2018.

Mollner, A. K., Valluvadasan, S., Feng, L., Sprague, M. K., Okumura, M., Milligan, D. B., Bloss, W. J., Sander, S. P., Martien, P. T., Harley, R. A., McCoy, A. B. and Carter, W. P. L.: Rate of Gas Phase Association of Hydroxyl Radical and Nitrogen Dioxide, Science, 330(6004), 646–649, 2010.

MOVES: MOVES2014a User Guide., 2015.

NEI: National Emissions Inventory (NEI) 2011, version 1, Research Triangle Park., 2015.

Pai, S. J., Heald, C. L., Pierce, J. R., Farina, S. C., Marais, E. A., Jimenez, J. L., Campuzano-Jost, P., Nault, B. A., Middlebrook, A. M., Coe, H., Shilling, J. E., Bahreini, R., Dingle, J. H. and Vu, K.: An evaluation of global organic aerosol schemes using airborne observations, Atmos. Chem. Phys., 20(5), 2637–2665, 2020.

Pierson, W. R., Schorran, D. E., Fujita, E. M., Sagebiel, J. C., Lawson, D. R. and Tanner, R. L.: Assessment of Nontailpipe Hydrocarbon Emissions from Motor Vehicles, J. Air Waste Manage. Assoc., 49(5), 498–519, 1999.

Pollack, I. B., Lerner, B. M. and Ryerson, T. B.: Evaluation of ultraviolet light-emitting diodes for detection of atmospheric $NO_2$ by photolysis - chemiluminescence, J. Atmos. Chem., 65(2-3), 111–125, 2010.

Roberts, J. M., Stroud, C. A., Jobson, B. T., Trainer, M., Hereid, D., Williams, E., Fehsenfeld, F., Brune, W., Martinez, M. and Harder, H.: Application of a sequential reaction model to PANs and

aldehyde measurements in two urban areas, Geophys. Res. Lett., 28(24), 4583–4586, 2001.

Roberts, J. M., Flocke, F., Stroud, C. A., Hereid, D., Williams, E., Fehsenfeld, F., Brune, W., Martinez, M. and Harder, H.: Ground-based measurements of peroxycarboxylic nitric anhydrides (PANs) during the 1999 Southern Oxidants Study Nashville Intensive, J. Geophys. Res. D: Atmos., 107(D21), 4554, 2002.

Rubin, J. I., Kean, A. J., Harley, R. A., Millet, D. B. and Goldstein, A. H.: Temperature dependence of volatile organic compound evaporative emissions from motor vehicles, J. Geophys. Res. D: Atmos., 111(D3), D03305, 2006.

Ryerson, T. B., Huey, L. G., Knapp, K., Neuman, J. A., Parrish, D. D., Sueper, D. T. and Fehsenfeld, F. C.: Design and initial characterization of an inlet for gas-phase $NO_y$ measurements from aircraft, J. Geophys. Res. D: Atmos., 104(D5), 5483–5492, 1999.

Ryerson, T. B., Andrews, A. E., Angevine, W. M., Bates, T. S., Brock, C. A., Cairns, B., Cohen, R. C., Cooper, O. R., de Gouw, J. A., Fehsenfeld, F. C., Ferrare, R. A., Fischer, M. L., Flagan, R. C., Goldstein, A. H., Hair, J. W., Hardesty, R. M., Hostetler, C. A., Jimenez, J. L., Langford, A. O., McCauley, E., McKeen, S. A., Molina, L. T., Nenes, A., Oltmans, S. J., Parrish, D. D., Pederson, J. R., Pierce, R. B., Prather, K., Quinn, P. K., Seinfeld, J. H., Senff, C. J., Sorooshian, A., Stutz, J., Surratt, J. D., Trainer, M., Volkamer, R., Williams, E. J. and Wofsy, S. C.: The 2010 California Research at the Nexus of Air Quality and Climate Change (CalNex) field study, J. Geophys. Res. D: Atmos., 118(11), 5830–5866, 2013.

Sachse, G. W., Hill, G. F., Wade, L. O. and Perry, M. G.: Fast-Response, High-Precision Carbon Monoxide Sensor using a Tunable Diode Laser Absorption Technique, J. Geophys. Res.: Atmos., 92(D2), 2071–2081, 1987.

Schroder, J. C., Campuzano-Jost, P., Day, D. A., Shah, V., Larson, K., Sommers, J. M., Sullivan, A. P., Campos, T., Reeves, J. M., Hills, A., Hornbrook, R. S., Blake, N. J., Scheuer, E., Guo, H., Fibiger, D. L., McDuffie, E. E., Hayes, P. L., Weber, R. J., Dibb, J. E., Apel, E. C., Jaeglé, L., Brown, S. S., Thronton, J. A. and Jimenez, J. L.: Sources and Secondary Production of Organic Aerosols in the Northeastern US during WINTER, J. Geophys. Res. D: Atmos., doi:10.1029/2018JD028475, 2018.

Simon, H., Beck, L., Bhave, P. V., Divita, F., Hsu, Y., Luecken, D., Mobley, J. D., Pouliot, G. A., Reff, A., Sarwar, G. and Strum, M.: The development and uses of EPA's SPECIATE database, Atmos. Pollut. Res., 1(4), 196–206, 2010.

Slusher, D. L., Huey, L. G., Tanner, D. J., Flocke, F. M. and Roberts, J. M.: A thermal dissociation-chemical ionization mass spectrometry (TD-CIMS) technique for the simultaneous measurement of peroxyacyl nitrates and dinitrogen pentoxide, J. Geophys. Res.: Atmos., 109(D19), D19315–D19315, 2004.

Stutz, J. and Platt, U.: Numerical analysis and estimation of the statistical error of differential optical absorption spectroscopy measurements with least-squares methods, Appl. Opt., 35(30),

6041, 1996.

Stutz, J. and Platt, U.: Improving long-path differential optical absorption spectroscopy with a quartz-fiber mode mixer, Appl. Opt., 36(6), 1105, 1997.

Travis, K. R., Jacob, D. J., Fisher, J. A., Kim, P. S., Marais, E. A., Zhu, L., Yu, K., Miller, C. C., Yantosca, R. M., Sulprizio, M. P., Thompson, A. M., Wennberg, P. O., Crounse, J. D., St. Clair, J. M., Cohen, R. C., Laughner, J. L., Dibb, J. E., Hall, S. R., Ullmann, K., Wolfe, G. M., Pollack, I. B., Peischl, J., Neuman, J. A. and Zhou, X.: Why do models overestimate surface ozone in the Southeast United States?, Atmos. Chem. Phys., 16(21), 13561–13577, 2016.

Vaughan, A. R., Lee, J. D., Shaw, M. D., Misztal, P. K., Metzger, S., Vieno, M., Davison, B., Karl, T. G., Carpenter, L. J., Lewis, A. C., Purvis, R. M., Goldstein, A. H. and Hewitt, C. N.: VOC emission rates over London and South East England obtained by airborne eddy covariance, Faraday Discuss., 200(0), 599–620, 2017.

Wang, M., Shao, M., Chen, W., Yuan, B., Lu, S., Zhang, Q., Zeng, L. and Wang, Q.: A temporally and spatially resolved validation of emission inventories by measurements of ambient volatile organic compounds in Beijing, China, Atmos. Chem. Phys., 14(12), 5871–5891, 2014.

Warneke, C., McKeen, S. A., de Gouw, J. A., Goldan, P. D., Kuster, W. C., Holloway, J. S., Williams, E. J., Lerner, B. M., Parrish, D. D., Trainer, M., Fehsenfeld, F. C., Kato, S., Atlas, E. L., Baker, A. and Blake, D. R.: Determination of urban volatile organic compound emission ratios and comparison with an emissions database, J. Geophys. Res. D: Atmos., 112(D10), doi:10.1029/2006JD007930, 2007.

Warneke, C., Veres, P., Holloway, J. S., Stutz, J., Tsai, C., Alvarez, S., Rappenglueck, B., Fehsenfeld, F. C., Graus, M., Gilman, J. B. and de Gouw, J. A.: Airborne formaldehyde measurements using PTR-MS: calibration, humidity dependence, inter-comparison and initial results, Atmos. Meas. Tech., 4(10), 2345–2358, 2011.

Warneke, C., de Gouw, J. A., Holloway, J. S., Peischl, J., Ryerson, T. B., Atlas, E., Blake, D., Trainer, M. and Parrish, D. D.: Multiyear trends in volatile organic compounds in Los Angeles, California: Five decades of decreasing emissions, J. Geophys. Res. D: Atmos., 117(D21), D00V17, 2012.

Weibring, P., Richter, D., Walega, J. G., Rippe, L. and Fried, A.: Difference frequency generation spectrometer for simultaneous multispecies detection, Opt. Express, 18(26), 27670, 2010.

Weinheimer, A. J., Walega, J. G., Ridley, B. A., Gary, B. L., Blake, D. R., Blake, N. J., Rowland, F. S., Sachse, G. W., Anderson, B. E. and Collins, J. E.: Meridional distributions of $NO_x$ , $NO_y$ , and other species in the lower stratosphere and upper troposphere during AASE II, Geophys. Res. Lett., 21(23), 2583–2586, 1994.

Whalley, L. K., Stone, D., Bandy, B., Dunmore, R., Hamilton, J. F., Hopkins, J., Lee, J. D., Lewis, A. C. and Heard, D. E.: Atmospheric OH reactivity in central London: observations, model predictions and estimates of in situ ozone production, Atmos. Chem. Phys., 16(4),

2109–2122, 2016.

Williams, E. J., Roberts, J. M., Baumann, K., Bertman, S. B., Buhr, S., Norton, R. B. and Fehsenfeld, F. C.: Variations in $NO_y$ composition at Idaho Hill, Colorado, J. Geophys. Res. D: Atmos., 102(D5), 6297–6314, 1997.

Williams, J., Roberts, J. M., Bertman, S. B., Stroud, C. A., Fehsenfeld, F. C., Baumann, K., Buhr, M. P., Knapp, K., Murphy, P. C., Nowick, M. and Williams, E. J.: A method for the airborne measurement of PAN, PPN, and MPAN, J. Geophys. Res. D: Atmos., 105(D23), 28943–28960, 2000.

Young, D. E., Allan, J. D., Williams, P. I., Green, D. C., Flynn, M. J., Harrison, R. M., Yin, J., Gallagher, M. W. and Coe, H.: Investigating the annual behaviour of submicron secondary inorganic and organic aerosols in London, Atmos. Chem. Phys., 15, 6351–6366, 2015.

Yuan, B., Hu, W. W., Shao, M., Wang, M., Chen, W. T., Lu, S. H., Zeng, L. M. and Hu, M.: VOC emissions, evolutions and contributions to SOA formation at a receptor site in eastern China, Atmos. Chem. Phys., 13(17), 8815–8832, 2013.

Zhang, Q., Streets, D. G., Carmichael, G. R., He, K. B., Huo, H., Kannari, A., Klimont, Z., Park, I. S., Reddy, S., Fu, J. S., Chen, D., Duan, L., Lei, Y., Wang, L. T. and Yao, Z. L.: Asian emissions in 2006 for the NASA INTEX-B mission, Atmos. Chem. Phys., 9(14), 5131–5153, 2009.

Zheng, B., Huo, H., Zhang, Q., Yao, Z. L., Wang, X. T., Yang, X. F., Liu, H. and He, K. B.: High-resolution mapping of vehicle emissions in China in 2008, Atmos. Chem. Phys., 14(18), 9787–9805, 2014.

Zheng, B., Tong, D., Li, M., Liu, F., Hong, C., Geng, G., Li, H., Li, X., Peng, L., Qi, J., Yan, L., Zhang, Y., Zhao, H., Zheng, Y., He, K. and Zhang, Q.: Trends in China's anthropogenic emissions since 2010 as the consequence of clean air actions, Atmos. Chem. Phys., 18(19), 14095–14111, 2018.